THE SIMULTANEOUS ELECTRODEPOSITION OF LEAD AND LEAD DIOXIDE

A thesis submitted to the Council of National Academic Awards in partial fulfilment for the degree of

Doctor of Philosophy

by

P. Lydon B.Sc., M.Sc.

City of London Polytechnic
Central House

PART I

Department of Metallurgy and Materials
Sir John Cass School of Science and Technology
City of London Polytechnic
Whitechapel High Street
London, E1 7PF

DECLARATION

I, the undersigned PATRICK LYDON hereby declare that the work contained in this thesis has not been submitted before or elsewhere for an academic qualification and that I have not been, during my registration with the CNAA for the Ph.D candidature, registered with any other academic or professional institution as a candidate.

Signed.....

CONTENTS

ACKNOWLEDGEMENTS

The author wishes to thank his supervisor Professor L L Shreir for his advice, guidance and encouragement throughout this work.

Thanks are also due to The Royal Armnaments Research and Development Establishment (RARDE) for their financial assistance under contract AT/2111/021 Mat/R and for the use of their Auger spectrophotometer. In particular the author wishes to express his appreciation to Messrs J F Smith and J Queay of RARDE for the advice and interest they have shown in this project and to Mr J Winn for his assistance with the Auger spectrophotometer studies.

The author also gratefully acknowledges the help and co-operation given by Mr G Bowman of the Ionic Plating Company and Dr's J Dawson and G Sussex of the University of Manchester Institute of Science and Technology, for the use of their impedance analyser.

Thanks are also due to the members of staff and research students at the Department of Metallurgy and Materials, Sir John Cass College of Science and Technology, The City of London Polytechnic, especially the technical staff, for their friendly assistance and advice. The author would also like to express his special thanks to Mr P Cook for his assistance with the scanning electron microscope and X-ray diffractometer studies and Mr B Sanderson for his assistance with the colorimetric analysis.

Finally the author gratefully acknowledges the help, advice and encouragement of his colleagues David Wood, John Boran and John Skulczuk, his employers Roxby Engineering International Ltd for the use of their word processor and last but by no means least all the typists who have struggled with his handwriting, especially Sandra Le Quesne, Teresa Reynolds (his sister), Megan Evans, Mary Haynes, Margaret Cumming, Renee Jackson and Jackie Turner without whose invaluable help the final manuscript would not have been produced.

ABSTRACT

The simultaneous electrodeposition of both Pb and PbO_2 from $Pb(NO_3)_2$ solutions onto a Ni substrate has been investigated with particular reference to the influence of different organic addition agents on the nature of the Pb and PbO_2 deposit, the porosity of the Pb deposit and the current efficiency for deposition.

Plating solutions for Pb based on $Pb(NO_3)_2$ that operate at room temperature and up to 50°C have been developed which produce Pb deposits with properties almost equivalent to those from conventional $Pb(BF_4)_2$ plating solutions. The effect of certain additives in modifying the adhesion and grain size of PbO_2 deposits has also been reported.

Pb and PbO_2 deposits prepared by electrodeposition from $Pb(NO_3)_2$ solutions containing selected organic addition agents were evaluated for use as the active materials in the $Pb/HBF_4/PbO_2$ primary battery. Tests have confirmed that the Pb and PbO_2 deposits produced by simultaneous electrodeposition from a $Pb(NO_3)_2$ solution containing selected addition agents were not as effective in terms of discharge properties, when compared to the PbO_2 and Pb deposited separately from conventional plating solutions. However, Pb and PbO_2 deposited simultaneously, satisfied the requirements of the active material used in the $Pb/HBF_4/PbO_2$ battery.

The continuing problem of the varying degrees of adhesion of electrodeposited PbO_2 onto etched Ni foils with no significant variation in composition was investigated. The adhesion of PbO_2 to etched Ni200 foil was found to be good, whilst that to Ni270 was proved to be poor. Certain physical and electrochemical properties of foils that exhibitied both 'good' and 'bad' adhesion of PbO_2 were investigated, in order to ascertain the cause of the adhesion problem.

A number of possible reasons for the poor adhesion of PbO_2 to certain batches of Ni foil have been examined and a probable explanation for the adhesion failures has been proposed.

The kinetics and mechanism of Pb deposition from $Pb(NO_3)_2$ solutions and the effect of selected organic addition agents on this process have been studied using the rotating disc, pulse potentiostatic and electrochemical impedance techniques. The diffusion coefficent for Pb^{2+} ions, near the reversible potential has been determined and the effect of certain organic additions agents on the values for the Pb diffusion coefficent have been reported. Other electrochemical parameters for Pb deposition from $Pb(NO_3)_2$ solutions, namely the exchange current density and double layer capacitance have also been determined.

A method for calculating the theoretical voltage rise time for the $Pb/HBF_4/PbO_2$ battery has been examined. This work has provided an explanation of the improved voltage rise time obtained by heat-treatment of electrodeposited PbO_2. To supplement these studies the anodic dissolution of Pb and cathodic reduction of PbO_2 in 48% HBF_4 together with the thermal decomposition of PbO_2 were also investigated.

The influence of pH, selected inorganic anions and organic complexing agents on the passivity of Ni in KNO_3 solutions has been studied. This work supplements the relatively scant amount of information available in the literature on this subject and provides information on the effect of possible additives to the $Pb(NO_3)_2$ plating solutions, on the passivity of Ni in such solutions.

INTRODUCTION

Batteries can be designed and constructed from a range of materials and used for a wide variety of applications. In certain applications particularly military ones the batteries are designed and constructed for a particular use with the active materials and method of construction selected so that the desired operating parameters can be achieved.

For a number of years now one type of battery system has been used to operate proximity fuses in different types of artillery shells and rockets, namely the lead/lead dioxide/fluoroboric acid battery. These miniature fuse batteries are produced from thin nickel sheets plated with lead and lead dioxide so as to reduce the size of the battery to a minimum. This involves two separate operations in different plating solutions.

(a) The cathodic deposition of Pb

(b) The anodic deposition of PbO_2

The electrodeposition of PbO_2 is normally carried out in a solution of a lead salt that gives a high activity of Pb^{2+} e.g lead nitrate or acetate. It has been established that the former gives a deposit that is predominantly β PbO_2 (136) whereas that deposited from the latter is predominantly α PbO_2(135).

In the UK the nitrate bath is preferred. However in the USA although the nitrate bath is used initially to produce the majority of the deposit, it is then given a thin overlay of the electrochemically more active α -PbO_2 from the acetate bath in order to reduce the voltage rise time.

These baths are not suitable, however, for the electrodeposition of Pb, which deposit as dendrites of very large grain size, giving incomplete coverage of the substrate. In addition these deposits are relatively non-adherent since they grow preferentially in a direction perpendicular to the substrate. For these reasons the electrodeposition of Pb is in practice carried out using soluble lead salts with an inorganic complexing agent such as lead fluoroborate $Pb(BF_4)_2$, lead fluorosilicate $PbSiF_6$ and lead sulphamate $Pb(NH_2SO_3)_2$. With these baths addition agents are invariably used to give smoother deposits of Pb since non adherent deposits are produced at high current densities. Another objectionable feature of these baths is that they are strongly acidic and could not be used for the anodic deposition of PbO_2 onto Ni since the Ni would not remain passive in such an electrolyte.

The aim of the present study was to formulate a plating solution that would be suitable for the simultaneous electrodeposition of Pb at the cathode and PbO_2 at the anode onto substrates of nickel foil and produce deposits that would meet the requirements of a fuse battery.

This could be achieved by one of two possibilities:

(a) Modification of the lead nitrate bath so that it produced reasonably good Pb deposits or

(b) Modification of the lead fluoroborate bath or a similar lead plating solution so that it produced electrochemically active PbO_2 on a nickel foil substrate.

In both cases the modifications to the plating solution must ensure no detrimental effect is obtained on either deposit.

In view of the fact that the PbO_2 deposit is the more vital component of the battery, since it determines the time in which the maximum cell voltage is reached once the battery is activated. It was decided to concentrate on modifications that could be carried out to the $Pb(NO_3)_2$ bath.

There were a number of possible approaches to the problem of modifying the bath so that it gave fine grained, compact, coherent and adherent Pb deposits without affecting the properties of the anodically deposited PbO_2 but the obvious choice was the use of organic addition agents that are usually effective at low concentrations. The desirable requirements are :

1) The anodic and cathodic efficiencies are not significantly affected.

2) The electrochemical properties and adhesion of PbO_2 to the nickel are not affected.

3) The organic addition agents are stable when subjected to conditions of cathodic reduction and anodic oxidation.

In view of the vast number and diversity of addition agents used in commercial plating baths an extensive literature survey was made to select those that appeared to be the most promising, particular consideration was given to those already used in Pb and Pb alloy deposition.

Once suitable addition agents were identified the deposition parameters of the $Pb(NO_3)_2$ solution were adjusted to achieve the optimum deposit properties.

The current efficiency for deposition, porosity, adhesion and morphology of both Pb and PbO_2 deposits were investigated, as well as the discharge properites of Pb and PbO_2 deposits obtained from a simultaneous plating solution and compared to those of deposits from conventional plating solutions. The mechanism of addition agent action in $Pb(NO_3)_2$ solutions was investigated in some detail to aid the understanding of the Pb deposition process, with particular attention paid to the stability of selected organic addition agents.

The adhesion of PbO_2 to certain batches of nickel sheet was also found to be poor when compared to that of others with no significant difference in composition of the nickel foil. This recurring problem of PbO_2 adhesion onto nickel was studied to try and identify the factors

responsible for the poor adhesion and thus decrease the high reject rate of electrodeposited PbO_2 onto Ni sheet obtained in the commercial production of battery plate material. As part of this work an investigation into the passivity of nickel in nitrate solutions was also undertaken.

1 LITERATURE SURVEY

1.1 The electrochemical applications of lead

The largest single use for lead in Western Europe and Japan is in storage batteries. Barak (1) reports that in 1973 the total consumption of lead in the USA, Canada, Western Europe and Japan was some 3M tons of which 35% was used in the production of storage batteries. However, more recent figures for the total amount of lead used in 1980 show the total world consumption of lead to be only 2.67M tons, whilst the total amount used in lead-acid batteries is 1.29M tons representing some 48% of the total usage. The figures for lead usage in the UK during 1980 were obtained from the World Metal Bureau Statistics with the end uses of lead listed in Table 1 which shows the many different applications of lead, with the percentage of lead used in storage batteries 32.3% of the total.

Table 1 - Applications of Pb in UK in 1980

UK Principal End Uses	Tonnage (Thousands of tons)
Batteries (metal)	49.3
Batteries (oxide)	49.3
Cables	21.7
Tetraethyl	63.3
Other oxides and compounds	18.6
White Lead	0.9
Shot	6.5
Sheet, foil and pipe	51.0
Collapsible tubes	1.4
Other rolled and extruded products	0.4
Alloys	21.6
Miscellaneous	21.5
Total	305.5

As can be seen from the above Table there are a number of different applications for lead, with storage batteries representing the major electrochemical application.

However, lead is used in a large number of other electrochemical applications, an account of which is given by Barak (1).

Apart from its use in batteries lead anodes are used in the production of organo-lead compounds, the most common one being lead tetraethyl, the anti-knock additive in petrol, whilst PbO_2 electrodeposited onto various metals such as Pt, Ni or Ti is used as an anode in the manufacture of certain chemicals, e.g chlorates, perchlorates, bromates, iodates.

Lead cathodes can be used for a variety of reduction reactions and are particularly favoured because of their high hydrogen overvoltage. Lead alloys have also been used as anodes in electrometallurgy since the 1920's and are used in the form of Pb-1Ag for electroprecipitation of Cu and Zn, whilst Pb-6Sb is used as an anode in Cr plating. Lead alloys, such as Pb-1-2%Ag and Pb-1Ag-6Sb are used as impressed current anodes in cathodic protection and this also applies to Pb containing Pt microelectrodes, whilst the electrochemical refining of lead accounts for some 12% of the total quantity of refined lead. Lead and lead alloy electrodeposits have a wide variety of uses, which will be discussed later.

The present study is directly related to the lead acid primary battery, for which only a small quantity of lead is used annually. However, when one refers to the lead acid battery one automatically thinks of the lead acid storage battery. It is therefore considered appropriate to outline it's mode of operation before embarking on a more detailed account of the lead acid primary battery.

1.1.1 The lead acid storage battery

This battery was first invented by Plante (2) as early as 1859, who showed that if a current from an external source is passed between two lead electrodes immersed in a sulphuric acid electrolyte, the surface of the anode is oxidised to PbO_2 whilst that of the cathode is reduced to spongy Pb. These

reactions are reversible so that when the electrodes are connected together by means of an external circuit, the PbO_2 is reduced to $PbSO_4$ whilst the Pb is oxidised to $PbSO_4$. The overall equilibrium may be represented as follows :

$$Pb + PbO_2 + 2H_2SO_4 \rightleftharpoons 2PbSO_4 + 2H_2O$$

$$E_o = 2.041V \text{ at } 25^oC$$

The original Plante cell consists of spirally wound positive and negative plates with an interposed separator, all of which is housed in a cylindrical container filled with dilute H_2SO_4. Because of the planar nature of the electrodes, the true surface area is not sufficient to give adequate electrical power. Plante therefore had to activate his plates by repeated cycling and discharge, which transformed the lead surfaces into porous active masses (a process known as forming).

In 1881 Faure took out a patent (3) to produce lead acid storage batteries by a different method, the basic principle of which is still in use today. He applied a powdered mixture of lead oxides, mixed with sulphuric acid in the form of a "paste" to the plates, which were immersed in dilute H_2SO_4. By passing current in only one direction it was possible to convert the lower oxides to PbO_2 at the anode and to spongy Pb at the cathode.

The present-day SLI (starting, lighting and ignition) battery is of the Faure type, housing 6 cells connected in series to give a nominal e.m.f of 12V. The outer casing of the battery is constructed of hard rubber or polypropylene, with the interior partioned into 6 compartments housing the plates in a series of interconnected individual cells. The plates themselves are formed from Pb-Sb alloy grids, which facilitiates adhesion of the paste. The Pb-Sb alloy has been used for a number of years because of :

1) The poor mechanial strength of Pb causes it to facture in the pressing operation or during general handling.

2) The better adhesion of the paste to lead alloys than to pure lead.

3) Difficulty of casting the intricate shapes of thin grids with pure lead.

4) Poor corrosion resistance of lead due to grain recrystallisation at room temperature.

The paste consists of mixtures of the lower oxides of lead mixed with H_2SO_4 spread onto perforated paper. This is then placed either side of the grid, pressed on, and then allowed to dry at room temperature in the case of the negative and at 40^oC in the case of the positive plates.

The paste itself is 65-85% lead oxide with the remainder metallic lead, and is prepared by heating lead particles in air at a controlled flow rate. The dust is then mixed with H_2SO_4 to produce the paste.

The cured plates are placed in forming tanks containing H_2SO_4 of specific gravity 1.02 and a current passed. The positive plates are then converted to PbO_2 and the negative to spongy Pb. The plates are then assembled into the cell, separated by means of porous PVC separators and a connection made to each plate by Pb-Sb alloy straps.

The major drawback of the Faure battery is that in the completion of the recharging process large quantities of hydrogen and oxygen are evolved, necessitating the addition of water to replace the lost electrolyte. The reason for most of the gas evolution is the presence of grid alloying elements, e.g Sb which have lower hydrogen overvoltages than pure lead.

The introduction of new alloying elements for grid manufacture has helped alleviate this problem to produce maintenance free lead acid batteries examples being Pb/Sb ternary alloys, Pb/Ca, Pb/Sn/Se or dispersion-strengthed lead

Additives termed expanders, may also be added to the paste to give improved cycle life, increased capacity at high c.d and low temperature. The most commonly used ones are lignosulphonates or inorganic ones such as $BaSO_4$ or $SrSO_4$. H_3PO_4 may also be added to the battery electrolyte to increase the cycle life, minimise paste shedding and decrease the amount of anode gassing by increasing the oxygen overvoltage on PbO_2.

1.1.2 Primary batteries

The term 'Primary battery' refers to batteries where the products of the reaction are soluble, and although some degree of reversibility is inherent in the cell reaction. They are unsuitable for recharging.

Typical examples of such systems are :

1) The Daniel Cell, which consists of a Cu cathode immersed in a saturated $CuSO_4$ solution that is separated from a Zn electrode in a $ZnSO_4$ solution by a porous membrane.

2) The Leclanche dry cell, e.m.f 1.5V which comprises of a cylindrical Zn anode, surrounded by a paste of NH_4Cl $ZnCl_2$ and starch with a central C/MnO_2 cathode.

Other common primary cells are the Mallory-Ruben zinc and mercury/mercuric oxide in an alkaline electrolyte battery and the silver-zinc alkaline battery. The lead/lead dioxide/ fluoroboric acid battery system is a primary cell, and although it has not gained widespread use it has important applications as a reserve battery. In view of its importance to the present work a brief summary of reserve batteries followed by a more detailed account of the $Pb/HBF_4/PbO_2$ cell, will now be given.

1.1.3 Reserve primary batteries

The term reserve primary battery refers to electrochemical power supplies which are designed, manufactured and stored in a form which ensures complete inertness until a specific action is taken by the user or by an activating device. The main benefits of such a system are :

1 Unlimited shelf life when properly packed, compared to the conventional primary cells where "self corrosion" of the active material limits shelf life.

2 High rates of discharge over a wide temperature range.

3 A large degree of freedom in battery design, since these batteries are either purpose built or permit unconventional design.

4 Fast activation i.e time taken for the battery system to be energised or to reach its full working e.m.f.

There are three basic types of reserve batteries, classification of which is based on the system used to activate the battery i.e whether by gas, heat or liquid. Such a broad classification permits the use of a wide number of electrochemical systems under each example.

The mode of activation may be manual, e.g. simple immersion in the electrolyte or automatic, where the initiating action results from a condition of use. The linear acceleration resulting from a projectile firing causing puncture of an ampoule containing the electrolyte and allowing ingress of the electrolyte into the cell being one such example. Reserve batteries, also require a volume in which to store the electrolyte this means replacing increased shelf life for energy density with the batteries operating at some 25% of the energy density of a conventional battery.

1.1.3.1 Gas activated

Gas activated reserve batteries have not reached any significant level of development and are not widely used. In principle they operate by the interaction of a gas and a salt to produce a working electrolyte.

Two basic chemical systems have been developed :

1 NH_3 vapour diffusing throughout the active structure where it is absorbed by salts to produce an ammoniacal solution. The solutions contain various thiocyanates such as KSCN, LiSCN or NH_4SCN, which provide good low temperature electrolytes. The anode material is Pb, Mg or Zn used in combination with a PbO_2 or heavy metal sulphide cathode. Single cell combinations are capable or producing 1.5 to 2.5V. These systems may be deactivated by removing the ammonia under vaccum.

2 The second type of system involves the use of reactive vapours which produce an electrolyte by chemical reaction with a second consitituent located within the cell. One combination is water vapour reacting with an acid anhydride, e.g P_2O_5 to produce phosphoric acid. A more practical system is the reaction of HF with H_3BO_3 to produce a fluoroboric acid electrolyte. This electrolyte may be used with a Pb anode and PbO_2 cathode.

1.1.3.2 Heat activated

Thermal batteries are a unique form of reserve battery, since all the active materials are present in the cell and not stored separately. Activation is accomplished by the combustion of an integrally located heat source, followed by the transport of heat to the cell element. Hence no material transport is required. Such devices have (a) very long shelf life (b) operate over a wide temperature range (c) ruggedness (d) quick activation and (e) are easily miniaturised.

These units are often short lived (a few minutes) and exhibit an upper limit of energy of 60 to 120 kilowatt hours. Their applications are largely in the military field or for emergency short duration alarms.

Such cells invariably use anodes of Mg or Ca in a sheet or clad form with up to 1 V per cell being produced by Ca anodes at a high discharge rate. The practical electrolytes are normally eutectic mixtures of lithium and potassium halides, with the cathode being any reducible compound that is thermally stable at operating temperatures of 300 to 600°C. The cell voltage, and operating c.d is largely dependent on the choice of reactant. This can range from 1 to 3V or more per cell at current densities of a few amps per cm^2. Acceptable cathodic reactants are :

1 Soluble ions such as chromates or heavy metal cations

2 Metallic oxides e.g FeO, W_2O_3 and V_2O_5 in the form of a filled organic paper.

Several designs of cells have been produced, but the basic design consists of the structural element with all the active materials being arranged to give layer units.

1.1.3.3 Liquid activated

This classification covers the widest type of reserve batteries and includes those activated by water, alkali, acid or more recently lithium primary batteries activated by a non-aqueous electrolyte.

1.1.3.3.1 Alkali activated

Alkaline primary reserve batteries are dominated by the high-rate, high-energy density Ag_2O/KOH/Zn system used in auxillary missile power and weapon systems. The system is normally applied to situations requiring more than a few kilowatts or in situations demanding very high current, i.e tens or even hundreds of amps.

Generally these devices activate in a fraction of a second, may be operated over a wide temperature range, and have high electrical stability, with e.m.f's rarely exceeding a nominal 28V per device.

The prime anodic material is Zn, but Cd may also be used although it is more costly and has a lower discharge rate. The use of KOH as an electrolyte is universal. The choice of the higher oxide of silver AgO or the lower oxide Ag_2O, is important since the battery is required to survive high temperature storage. Degradation of the higher oxide affects the capacity and discharge, but build up of the oxygen pressure may affect the filling mechanism as the materials are stored under vacuum. Consequently, it is not unusual to accept the lower voltage of 1.6V to 1.8V per cell and lower capacity obtained with Ag_2O, to gain reliablity and meet shelf storage requirements.

The majority of alkali reserve cells are automatically activated by some external force, usually electrical though a few are manually activated.

1.1.3.3.2 Water activated

This type of battery has application in radio sounders for a variety of sea-associated emergencies, lighting, signal beacons, markers and in various military uses such as torpedos.

These devices have a life time of hours and are usually maintained under load when activated. They do have the disadvantage, however, that they often produce electrical noise due to chemical side reactions that can occur, although the heat generated from them does help make possible low-temperature operation.

The energy density of these batteries is particularly high since only the active materials are involved and there is no stored electrolyte.

There are two different chemical systems which may be used each involving a magnesium anode and a water electrolyte, with sea water being preferred because of its high conductivity. The activation time for a battery when sea water is used is only a few seconds, whilst that for fresh water may be a few minutes.

The cathode material may be either AgCl or CuCl, AgCl having a slightly higher cell voltage, i.e 1.3V compared to 1.2V, for CuCl, improved high-rate and low-temperature performance and a high electrical conductivity. The reason for the selection of CuCl, is where the cost has to be kept to a minimum.

The design of these cells may take several forms with the simplest being a simple cell, wound structure with a sandwich relationship of cathode/separator/anode.

1.1.3.3.3 Non aqueous electrolytes

This type of classification covers the most recent advances in reserve-battery technology, notably the development of systems using Li anodes. A number of primary Li systems have been developed commercially namely Li/SO_2, Li/(CF)n - (lithium/polycarbon monofluoride), Li/MnO_2, Li/I_2P_2VP, (lithium iodide/poly-2-vinyl pyridine), Li/Ag_2CrO_4, Li/V_2O_5, $Li/SOCl_2$.

The last two are the most widely used systems, with the $SOCl_2$ system having much better discharge properties than the V_2O_5 system. Detailed explanations of the $Li/SOCl_2$ system are given by Ravid (4) and Dey and Hamilton (6). The $Li/SOCl_2$ system utilises Li as the

anode with $SOCl_2$ as the cathodic reactant and supporting electrolyte, and the half cell reactions are :

Anode: $4\ Li \longrightarrow 4\ Li^+ + 4e$

Cathode: $2SOCl_2 + 4e \longrightarrow S + 4Cl^- + SO_2$

Overall reaction: $4Li + 2SOCl_2 \longrightarrow 4\ LiCl + SO_2 + S$

The SO_2 evolved dissolves in the electrolyte and does not generate any gas pressure.

Activation of these cells is by deformation of the cell case bottom causing a shattering of the glass ampoule storing the $SOCl_2$, which is then released and absorbed into the Teflon-bonded, porous-carbon cathode. All the batteries are hermetically sealed to prevent the lithium reacting with moisture in the air and have a shelf life of 15 years.

Voltage rise on activation is almost instantaneous and at a low c.d of 0.01 Adm^{-2} an e.m.f of 3V is reached within 200 ms at $-40^{o}C$, whilst at higher c.ds (5 Adm^{-2}) 2V is reached within 5 s at this temperature. The practical operating range of the $SOCl_2$ electrolyte is large - $55^{o}C$ to + $70^{o}C$ with the electrical conductivity only decreasing slightly with temperature. The open circuit voltage is 3.7 volts. In reserve applications because the battery is unactivated, it does not have a protective layer of LiCl and may therefore be discharged at relatively high pulse loads up to 5 Adm^{-2}.

The uses of these systems are mainly as military power sources for electronic fuses in mines, bombs, artillery shells and rockets where only one off power sources are required, but non-military applications such as personal-emergency locators or power sources for medical instruments do exist. The advantage of these systems is that they operate at a high degree of reliability in adverse conditions, even after prolonged inactive storage.

1.1.3.3.4 Acid activated batteries

The most widely used reserve battery is the system ($Pb/HBF_4/PbO_2$), although other chemical systems are used. The anodes may be electrodeposited Pb or sheet Pb, Cd or Zn with the electrolyte chosen to yield only soluble reaction products such as fluorosilicic, perchloric or fluoroboric acids. The cathodes are normally PbO_2 electroplated onto nickel, or nickel-plated mild steel. These systems are amenable to miniaturised designs and are capable of withstanding extreme environmental conditions with a good electrical stability and an activation time of less than 1s. The disadvantage of these systems is that they rarely have a practical operating life of more than a few minutes and units capable of a few hundred watt minutes are unusual.

1.1.4 The $Pb/HBF_4/PbO_2$ primary battery

Introduction

The main difference between the lead acid primary and secondary batteries lies in the solubility of their reaction products and the size and construction of the battery. Whereas $PbSO_4$ formed in the secondary battery is insoluble, the $Pb(ClO_4)_2$, $Pb(BF_4)_2$ or $Pb(SiF_6)$ formed in primary batteries is freely soluble and after some time the individual half-cell reactions result in complete dissolution of the Pb and PbO_2.

Primary lead acid batteries have the advantage that they are often smaller and lighter than the secondary battery and are capable of discharge at high rates over a wide range of temperature, without the evolution of gas (17).

However, they do have certain disadvantages, most of which have been mentioned previously, but the major one is their very limited shelf life when activated. This is not because of the reaction of the active solids i.e Pb or PbO_2 with the HBF_4,

but because of acid attack on the substrate material through the pores in the electrodeposited PbO_2. A decrease in the initial capacity by about 1% min^{-1} has been reported by MacDonald (5), therefore these batteries have to be used within a short time after activation. This problem is alleviated by physically separating the electrolyte and bringing it into contact with cell materials only when needed.

The electrolyte most widely used in the lead acid primary battery is fluoroboric acid (HBF_4) although perchloric ($HClO_4$) and fluorosilicic (H_2SiF_6) acids are sometimes used.

The lead anode may be in the form of lead deposited onto nickel, nickel plated mild steel or simply lead foil which may contain 0.08% Ca (1) to give it the required rigidity.

The PbO_2 cathode is produced by anodic oxidation of Pb^{2+} ions using an inert substrate, normally nickel sheet or nickel-plated mild steel, although other types of cathode construction may sometimes be used.

Kilduff and Horsey (7) describe the construction of "bonded PbO_2" electrodes, which consist of a steel substrate coated with a conductive material which is in turn overlaid with a coating of PbO_2 in a resin matrix.

Any noble metal would provide a conducting interface for the PbO_2 layer but silver is preferred. This is applied to the steel either by plating or by application of a water-based resinous coating which is made conducting by a dispersion of Ag flake or by highly conductive carbon black. This coating is applied to the substrate but remains uncured until after the application of the top coat, which contains 90% by weight of electrochemicaly prepared β-PbO_2 of small particle size, dispersed in an epoxy polyamide resin. The coating is cured by heating up to 70°C.

A more detailed explanation of the construction of such electrodes and recent developments in this field is given by Paulson (8).

Casson and Kelly (10) use a novel design of PbO_2 electrode where the PbO_2 is in a granular form and is packed so as to be in contact with a current collector. The material is packed in a polystryrene container with a lid, with a perforated terylene gauze liner around the internal diameter and on the base. Three layers of PbO_2 particles, of size 0.5 to 2.0mm, are laid in the container interspaced with carbonised braid, coiled through the structure.

The advantages of bonded PbO_2 electrodes are that their activated stand time may be increased quite significantly when compared to batteries based on electrodeposited β-PbO_2. MacDonald (5) has demonstrated that bonded electrodes do not show any appreciable self-discharge until 48 hours after activated standing at room temperature, compared to only 6 min for electrodeposited β-PbO_2. In fact at temperatures of $-50^{o}C$, he reports no significant self-discharge of bonded electrodes after 4 months activated standing.

Electrodeposited β-PbO_2 plates also have a limited discharge capability owing to the fact that there is a limit to the thickness of PbO_2 which may be deposited . This is due to brittleness of the PbO_2 and its poor adhesion to the electrode substrate. On the other hand, bonded PbO_2 electrodes may be produced with slightly thicker coatings and hence increased power density. The process used at present by the Ministry of Defence to produce $Pb/HBF_4/PbO_2$ battery plate material is that described by Smith (9), using Pb and PbO_2, electro-deposited onto nickel sheet.

1.1.4.1 Commercial production of $Pb/HBF_4/PbO_2$ battery plate

Nickel sheet of thickness 125 μm manufactured to BS 3073 NA11 is used as the substrate material for both Pb and PbO_2 deposition. The nickel sheet is first cut into plates of 150 x 220 mm, with a tag on the longer side of the strip to make electrical connection, and then vapour degreased in trichloroethylene. The plates are held, two at a time in a PVC jig and separated by a silicone rubber gasket. This enables deposition of Pb to be carried out on one side of the plate only, and for the subsequent plating operation i.e PbO_2 deposition, the sheets are reversed, so that deposition is again confined to one side. This gives a Ni sheet with Pb on one side and PbO_2 on the other, which is termed a "bipolar electrode".

The exact plating operation after the sheets have been fitted into the jig is as follows :

1 Cathodic degreasing at 5 Adm^{-2} in a solution containing

NaOH	50 gl^{-1}
Na_2CO_3	50 gl^{-1}
Na_2SO_4	10 gl^{-1}

2 Rinse in tap water

3 Anodic etch in 30% H_2SO_4 at 2.7 Adm^{-2} at 50°C for 10 min.

4 Rinse in demineralised water

5 Deposit lead at 2.7 Adm^{-2} at 30°C for 15 min from a solution of

$Pb(BF_4)_2$	230 gl^{-1}
HBF_4	22 gl^{-1}
H_3BO_3	12 gl^{-1}
Gelatin	0.2 gl^{-1}

6 Remove plates under demineralised water, rinse and dry in hot air.

7 Refit into jigs with plated side inwards and repeat stages 1,2, 3 ,4.

8 Deposit lead dioxide from a $Pb(NO_3)_2$ solution containing 360 gl^{-1} $Pb(NO_3)_2$ at 2 Adm^{-2} at 50°C for 15 mins.

9 Rinse plates under deionised water, remove from jig and dry under hot air.

1.1.4.2 Design and construction of the $Pb/HBF_4/PbO_2$ fuse battery

Electronic proximity fuses for artillery shells, bombs, rockets and motors were developed to give an increase in the effectiveness of the projectile. However to function properly they had to have a self-contained power source, namely a reserve battery.

The first successful fuse batteries used carbon and Zn electrodes with a chromic acid electrolyte, but were soon replaced with the $Pb/HBF_4/PbO_2$ battery, which used bipolar electrodes stacked in a voltaic pile with separators. This construction has not changed much over the years. The bipolar battery plate is punched out to the required dimensions from the large sheets produced by the process outlined above. These are then stacked in a voltaic pile with absorbent separators between each plate spaced about 0.18 mm apart. The electrolyte is stored separately in a frangible ampoule, which is mounted above

a rupturing surface on a flexible disc, rigid enough to keep the ampoule away from the surface during normal handling but flexible enough to allow the ampoule to collide with the rupturing surface on impact. The initiating action which causes the rupturing of the ampoule is the acceleration of the shell when fired. As aritllery shells experience forces of 1,500 to 80,000g the ampoule must be designed to fracture only when these forces are exerted. A more detailed account of the activation system used in certain fuse batteries is given by Casson and Kelly (10).

Polyethylene ampoules are quite often used because they are unattacked by HBF_4. They have a localised thin section which is designed to rupture during activation. The electrolyte once released is distributed into the cells, by centrifugal force created by the spinning projectile. The electrolyte then enters via orifices which are located further from the axis of rotation than any other part of the battery, so that all the electrolyte will flow into the cells. Once the electrolyte has entered the cells they are activated.

The spacers absorb the electrolyte and help remove it from the cell orifice, which helps to prevent short circuits in the cell and to therefore eliminate battery noise. The introduction of the electrolyte into the battery and different types of battery design are discussed in the patent literature (11). Turril and Kirchberger (12) give a detailed account of the construction of a cheap fuse battery used by the US Army, and an account of different types of fuse batteries is also given by Barron (13) who describes their construction and end uses.

MacDonald (14) also outlines the characteristics of a typical fuse battery, the specifications of which are given below.

Number of cells	14
Minimum Voltage	15V
Current	0.03 A
Discharge duration	20 secs
Temperature range	$-40^{o}C$ to $+ 60^{o}C$
Activation time	0.4 sec
Battery volume	2.5cc
Weight	4g

The above specifications are in fact often exceeded to a significant degree. No published data could be found for the design characteristics of fuse batteries used by the British Army.

In nearly all the batteries the choice of storage ampoule materials was invariably copper. Barron (13) states this is because copper is preferred by the US Army, since it is easily worked, not too expensive and resists HBF_4.

The ampoule material normally used by the British Army is polyethylene. Though Barron (13) expresses doubt as to its use because of wide variations in physical strength and permability with temperature.

1.1.4.3 Pb/PbO_2 reserve battery electrolyte

Fluoroboric acid is suitable for reserve batteries because of its wide liquidus range, ready availability, good conductivity and high solubility for lead, some 36.5 wt% Pb^{2+} at $20^{o}C$ or 380 gl^{-1} as $Pb(BF_4)_2$ (15). However other electrolytes are also suitable for use in Pb/PbO_2 primary batteries namely perchloric or fluorosilicic acids. Perchloric acid is not often used because of the dangers of handling, since it is a powerful oxidising agent and has been known to ignite organic material. Fluorosilic acid is unsuitable for low temperature applications since it freezes at below $-32^{o}C$.

The fluoroboric acid used in the battery is concentrated HBF_4 (48% aqueous solution) containing 2.5% H_3BO_3. The H_3BO_3 is added to prevent hydrolysis of the borofluoride ion to fluorides and hydroxy borofluoride ($BF_3(OH)^-$), which is detrimental since it could result in passivation of the lead anode by insoluble lead salts.

The liquidus range of HBF_4 is 208°C, since it freezes at -78°C and decomposes at 130°C. The conductivity ranges from 0.61 ohm^{-1} cm^{-1} at 23°C to 0.06 ohm^{-1} cm^{-1} at -60°C.

1.1.5 Discharge properties of the Pb/PbO_2 primary battery

Bushrod and Hampson (16) have studied the discharge properties of the Pb/PbO_2 primary battery in HBF_4 and H_2SiF_6 and to some extent $HClO_4$ using electrodeposited PbO_2 cathodes and Pb foil anodes. They conclude that discharge is terminated by the formation of a passive film of reaction products at high current densities and that the greater the acid concentration, the lower the solubility of the passivating reaction products. However, dilute electrolytes also reduce the extent of discharge because of their high resistivity.

They also found that increased separation of battery electrodes improves their capacity, since this allows easier access to the electrolyte and freer convection thus delaying the onset of passivation. When all these factors are taken into account there appeared to be a concentration maximum at which the optimum capacity is reached.

With fluorosilicic acid high-current drain results in the passivation of the electrode and therefore this electrolyte is not suitable for high current drain situations. Table 2 below, shows some of the discharge properties of the various acids, for battery plate with a electrode spacing of 0.34 cm (16).

TABLE 2

Discharge properties of the various electrolytes used in the lead acid primary battery

Current Amps	Fluoroboric acid			Fluorosilicic acid			Perchloric acid		
	Ah	Volts	Conc mole l^{-1}	Ah	V	Conc mole l^{-1}	Ah	V	Conc %
15	2.40	1.52	6.7	2.35	1.63	4.05	3.4	1.70	55%
20	1.85	1.51	6.75	1.90	1.57	3.60	2.9	1.66	
30	1.55	1.44	5.7	1.00	1.48	2.93	2.34	1.56	

From Table 2 it would appear that $HClO_4$ would be the best choice, with discharge current densities up to 50 Adm^{-2} being technically feasible. However, the safety aspects with regard to its handling often preclude its use although Bagshaw (18) does give an account of a $Pb/HClO_4/PbO_2$ reserve battery used in torpedoes. Fluoroboric acid has no marked advantages over fluorosilicic acid and the overall cell reaction for the former is :

$$Pb + PbO_2 + 4HBF_4 \rightleftharpoons 2\ Pb(BF_4)_2 + 2H_2O$$

$$E^0 = 1.86V \text{ at } 25^oC$$

MacDonald showed that c.d's of up to 5 Adm^{-2} do not appear to affect the coulombic efficiency for reduction of electro-deposited PbO_2 whilst above this value the coulombic efficiency decays reaching a value of 16% at 20 Adm^{-2}. At low temperatures the coulombic efficiency is affected by the internal resistance of the cell whilst at high temperature self-discharge occurs. The reason for the poor coulombic efficiency is that the PbO_2 because of its poor

mechanical strength, may become detached from the electrode whilst at high c.d's passivation occurs. Pulse currents of up to 30 Adm^{-2} are feasible for this system. The U.S Army bases its design characteristics on a current load of 3.1 Adm^{-2} (13) for the $Pb/HBF_4/PbO_2$ battery.

The values for the exchange c.d (i_o) for the reduction of PbO_2 have been reported by MacDonald (5) in HBF_4 as 10^{-5} Acm^{-2}, whilst Hampson (19) reports the value as 10^{-4} Acm^{-2}. No values could be found for the exchange c.d for Pb dissolution in HBF_4 but Haruyama (20) reports a value of 0.3 Acm^{-2} for its dissolution in 1M $HClO_4$.

1.1.6 The 'activation time' for $Pb/HBF_4/PbO_2$ batteries

The activation time of a battery refers to the time taken for the battery to reach a given operating voltage once the electrolyte is added to the system. In the case of the $Pb/HBF_4/PbO_2$ system the activation time has been found to be dependent on the nature of the PbO_2 electrode but independent of the Pb electrode. It is also markedly dependent on temperature and only becomes of practical important at low temperatures.

The battery plate material produced by RARDE must conform to Specification AP3/91/71 Issue 2, Items 7.2 and 7.3 which states that at a temperature of $-33^{o}C$ the cell e.m.f must exceed 1.22 V within 100 ms after activation.

Smith (9) has studied in some detail the phenomenon of activation and concluded that the pH of the lead nitrate solution from which the β-PbO_2 deposits are obtained, and the subsequent heat treatment afforded to these deposits, has significant effects on the activation or voltage rise time of these batteries. He obtained batches of β-PbO_2 electro-

deposited onto nickel from solutions containing 360 gl^{-1} of $Pb(NO_3)_2$, pH of 3.9 and 3.2. Another batch prepared from a solution of pH 3.9 was then heat-treated at 250°C for half an hour inducing a compressive stress of some 147 MN m^{-2} into the deposit. The mean voltages at selected times after activation were then determined and the results are shown in Table 3.

TABLE 3

Voltage rise times as a result of various pretreatments to PbO_2 electrodeposits

Sample	Cell voltage (volts) at a given time after activation in 48% HBF_4 and -32°C				
	50ms	60ms	120ms	500ms	2mins
PbO_2 prepared at pH 3.9	1.226	1.235	1.255	1.288	1.4
PbO_2 prepared at pH 3.2	1.135	1.141	1.167	1.231	1.338
PbO_2 prepared at pH 3.9 then heated to 250°C for half an hour	1.321	1.326	1.330	1.337	1.400

The heat treatment of the electrodeposited β-PbO_2 increased the cell e.m.f of the $Pb/HBF_4/PbO_2$ battery by 0.1V, 500 ms after activation (9, 21). However, heat treatment of the PbO_2 battery plate is not used at present in commercial plate manufacturer.

The method used by the US Army to decrease the activation times for their $Pb/HBF_4/PbO_2$ batteries was first developed by Darland (22) and it is now quite common in US battery plate manufacture. This is the application of a thin overlay coating of α-PbO_2 deposited from a Pb acetate bath onto the β-PbO_2; this overlay of α-PbO_2 on β-PbO_2 must be used since the high internal stresses in the former make it impossible to plate thick, adherent coatings.

The higher activity of the α-PbO_2 is attributed to its greater surface area when compared to β-PbO_2, and this is considered to contribute to the shorter activation time. Also α-PbO_2 is reported to show higher e.m.f's than β-PbO_2 in HBF_4, i.e 0.1V at 25°C and 0.21V at -40°C when compared to the values for β-PbO_2 at the same temperature (23).

Kilduff and Horsey (7) report that in the manufacture of battery plates in the USA the total thickness of β-PbO_2 is 188 microns and that of the α-PbO_2 overlay as 63 microns. The disadvantages of using the α-PbO_2 overlay according to Smith (9) are the corrosion problems associated with the residual acetic acid in the coating and the decrease in potential which occurs once the overlay is consumed. The latter may even cause noise in the battery, and for these reasons overlay coatings are not used by RARDE in the production of reserve energisers. Investigations have been carried out by Sinclair (24) into the effect of the purity of HBF_4 on the activation time of the $Pb/HBF_4/PbO_2$ battery. He reported that the concentrations of Cl^- and SO_4^{2-} ions in HBF_4 were critical since they caused temporary or partial passivation of the anode by $PbCl_2$ or $PbSO_4$, above 0.035 mol dm^{-3} in the case of Cl^- and 0.11 mol cm^{-3} in the case of SO_4^{2-}. A lack of H_3BO_3 which would result in an increased F concentration because of hydrolysis of the BF_4^- had a detrimental effect on activation time. However, in the concentration range 0.04 to 0.05 mol dm^{-3} H_3BO_3 in HBF_4, no detrimental effect was observed.

1.1.7 The adhesion of PbO_2 on battery plate material

The adhesion of β-PbO_2 to the inert supporting substrate is very important, and poorly adherent coatings are undesirable, since small particles of PbO_2 may become detached from the nickel plate causing short circuits in the battery owing to the small electrode spacing. This detachment may also reduce the effective coulombic efficiency. The PbO_2-Ni electrode plate itself is die cut after manufacture and poorly adherent coatings of β-PbO_2 will tend to flake off exposing the Ni during the cutting operations, thus making the plate unsuitable for use.

Poorly adherent coatings may also give poor voltage-rise times. The maintenance of a good standard of adhesion has been continual problem in the production of reserve energisers.

A large amount of the research effort undertaken in this work has been conducted into this particular problem and the problem of adhesion merits discussion in a separate section (see Section 1.4).

1.1.8 $Pb/HBF_4/PbO_2$ secondary battery

The discussion so far has centered on the $Pb/HBF_4/PbO_2$ primary battery, which does in fact possess some degree of reversibility depending upon the nature of the PbO_2 electrode. For example, in the case of the tripolar sheet electrodes with electrodeposited PbO_2 on nickel, recharging of this battery would be impossible. The nickel anode would dissolve in the HBF_4 and would not remain an inert substrate for PbO_2 deposition. However, if an inert electrode such as carbon is used as a supporting electrode for PbO_2, this would remain inert on charging and PbO_2 would be redeposited from the solution of $Pb(BF_4)_2$ in HBF_4, whilst at the cathode Pb would also be redeposited. Work on the development of a secondary $Pb/HBF_4/PbO_2$ battery has only been investigated to

any significant extent by Beck (25, 26). He used Pb anodes with thin graphite-filled polypropylene electrodes containing PbO_2 as the cathode. He claims a life of 2000 cycles to partial discharge with the first 200-300 cycles at full discharge.

The limitation of the cycle life is due to the one-sided accumulation of active masses as a result of a difference in the current efficiencies for the different half cell processes. The reason for the interest in the secondary $Pb/HBF_4/PbO_2$ batteries is that they have a number of possible advantages over the $Pb/H_2SO_4/PbO_2$ storage battery. The latter has a poor active mass utilisation, and a limiting power density especially at low temperatures.

The theoretical energy density (E_s) for the $Pb/H_2SO_4/PbO_2$ system is 170 Whr kg^{-1} nevertheless the energy density actually attained in practice is only in the range of 22-23 Wh kg^{-1}. The E_s theoretical for the $Pb/HBF_4/PbO_2$ battery is low in comparison 107 Whr kg^{-1}, but because of increased active mass utilisation practical energy densities of 35-40 Wh kg^{-1} may be obtained, making this system appear a viable proposition.

1.2 Lead Plating

1.2.1 History of lead plating

De Roullz (27, 29) in 1840 was one of the first to electroplate lead, from a solution containing 5 gl^{-1} PbO and 50 gl^{-1} NaOH, and early American electroplaters (30) reported the production of lead electrodeposits from low concentration $Pb(CH_3COO)_2$ and $Pb(NO_3)_2$ solutions, at low c.ds. However, the first person to formulate a practical plating solution was Leuchs (31) in 1886 who used solutions of either

$Pb(BF_4)_2$ or $PbSiF_6$. Nevertheless, it was Betts (32) in 1901 who first patented the use of a fluorosilicate solution similar to that described by Leuchs and later patented a fluoroborate solution containing gelatin as an addition agent (33).

The fluorosilicic acid process developed by Betts was used successfullly for refining Pb containing impurities and precious metals, and produced very high purity metal (99.999%). The process is unique in that it removes practically all the bismuth from the impure anodes and this metal along with others is deposited in the anode slime. The Betts process is particularly applicable to refining lead with a high bismuth content, and the method represents some 12% or 450,000 tonnes of the total world refining capacity (1). The fluoroborate process although used in electrorefining Pb is more commonly used in the electrowinning of Pb and in industrial Pb plating.

Lead may be satisfactorily deposited from a wide variety of aqueous solutions, organic electrolytes and molten salts and a number of good references now exist that cover quite adequately the types and uses of electrolytes for lead plating (25).

1.2.2 The applications of lead electrodeposits

Lead has excellent corrosion resistance in certain acids notably H_2SO_4 and H_3PO_4 which is due to the formation of protective films, whilst in other environments the high hydrogen overvoltage contributes to the slow rates of corrosion. Electroplating of Pb is used because of the good corrosion resistance of the metal and the ability of plating to produce thin smooth Pb coatings. Thus the main uses of electrodeposited coatings of Pb are for protection rather than decoration e.g in the lining of chemical apparatus, brine refrigeration tanks, pipe fittings, barrel plating of nuts and bolts and as coatings for copper strip used for connections to lead acid accumulators.

The principal tonnage usage of Pb is when deposited as an alloy coating. Alloyed with Sn for use on printed circuit boards, or as an electrodeposited bearing alloy such as Pb-Sn, Pb-Sn-Cu, Pb-Sb or Pb-In. In the production of terne plate a Pb-Sn alloy coating containing 8-12% Sn deposited on mild steel. This material has excellent corrosion resistance and formability and has a widespread use in the motor industry in the production of petrol tanks. Seth (24) covers some of the less common applications of Pb electrodeposits.

1.2.3 The mechanical properties of electrodeposited Pb

The hardness of lead deposits has been measured and is reported to lie in the range 3 to 20 VHN (35). These values include the value of 3 VHN for annealed lead and 20 VHN for lead deposited from proprietary brush plating solutions, though more typical values lie in the range of 4 VHN (36, 37) to 7 or 8 VHN (38, 39).

Typical values for other mechanical properties of lead electrodeposits are tensile strength 1.39 to 1.57 $kgmm^{-2}$, elongation 50 to 53% and density 11.34 gcm^{-3} (40). The fatigue strength of steel is reported (41) to be only slightly affected by lead electrodeposits as compared to the decrease caused by those of nickel or chromium.

The internal stress of electrodeposited lead is almost zero (42) though a compressive stress of 2.8 $kgmm^{-2}$ is obtained for lead electrodeposited from a perchlorate bath (43,44) and a compressive stress of 0.02 $kgmm^{-2}$ is quoted for lead electrodeposited to a thickness of 10 µm from an acetate bath. This changes to a tensile stress of 0.01 $kgmm^{-2}$ at a thickness of 12.5 µm (45). The values of the internal stress in lead deposits are low in comparison to other electrodeposited coatings, and for example, Ni has a value of 4.2 to 45.5 $kgmm^{-2}$ and Cr 35 to 175 $kgmm^{-2}$ (44). Values for the resistivity of electrodeposited Pb are quoted by Safranek and Layer (46) as 20 to 22.9 micro ohm cm.

1.2.4 Lead plating solutions

1.2.4.1 Lead fluoroborate

The $Pb(BF_4)_2$ plating solution is prepared by reacting basic lead carbonate 2 $Pb(OH)_2$ $PbCO_3$ with fluoroboric acid, which is prepare by the addition of HF to H_3 BO_3.

$$4HF + H_3BO_3 \rightleftharpoons HBF_4 + 3H_2O$$

In practice some free H_3BO_3 is left in the HBF_4 to prevent hydrolysis, since this would cause the precipation of insoluble lead salts from the $Pb(BF_4)_2$ solution. The presence of free boric acid has no effect on the nature of the lead electrodeposit and its concentration is maintained at 6 to 30 gl^{-1}. Excess HBF_4 is also present in the concentration range of 6 to 70 gl^{-1} to improve conductivity and give finer-grained deposits.

The composition of a typical $Pb(BF_4)_2$ plating solution depends on the type of deposit required and for low thicknesses produced at low c.ds Lowenheim (47) recommends bath No.1 (see Table 4) whilst for barrel or still plating in which heavier deposits are required bath No.2 is recommended.

TABLE 4

Typical composition of $Pb(BF_4)_2$ plating solutions

Component	Bath No 1 Concentration gl^{-1}	Bath No 2 Concentration gl^{-1}
Pb as $Pb(BF_4)_2$	120	240
Free HBF_4	30	60
Excess H_3BO_3	13.3	26.6
Gelatin	0.2	0.2

Gelatin is added to $Pb(BF_4)_2$ plating solutions to prevent dendritic growth and improve deposit morphology, and is the most commonly used addition agent for this purpose. Other addition agents have been suggested, and these will be considered subsequently. The commercial operating characteristics of a $Pb(BF_4)_2$ bath are as follows :

Temperature		25-40°C
Cathode current density	Bath No 1	0.5 to 5 Adm^{-2}
		average of 2 Adm^{-2}
	Bath No 2	0.5 to 7 Adm^{-2}
		average 3 Adm^{-2}
Operating pH		1 to 1.5
Throwing power		8-9% (Haring-Blum Cell)
Anode current density		1-3 Adm^{-2}

The solution is easy to control since both anode and cathode current efficiencies are 100%, the only loss of lead being due to drag-out. Slight agitation of the bath is necessary to prevent striatification of the lead deposits which is usually accomplished by slight cathode movement. $Pb(BF_4)_2$ solutions also have excellent throwing power and are one of the most conductive plating solutions. Safranek (46) reports that an increase in the rate of agitation gives increased rates of deposition and with a solution flow of 1.25 m sec^{-1} or greater, c.ds of 160 Adm^{-2} corresponding to deposition rates of 100 μm min^{-1} are possible from a solution containing 2.5M $Pb(BF_4)_2$. Graham and Pinkerton (48) have also studied high speed deposition of Pb from fluoroborates and claim limiting c.ds of up to 337 Adm^{-2} at a cathode velocity of 0.75 m sec^{-1} with average plating c.ds of 107 Adm^{-2} from a bath containing 470 gl^{-1} $Pb(BF_4)_2$ + 45 gl^{-1} free HBF_4 and 45 gl^{-1} H_3BO_3, the operating temperature being 65°C.

Investigations into the properties and hardening of electroformed Pb deposited from fluoroborate solutions have been conducted by Dini and Helms (38, 49). Dispersion strengthening of electrodeposited Pb by the codeposition of fine particles of TiO_2 or $BaSO_4$ from $Pb(BF_4)_2$ solutions has also been studied by Wiesner et al (50).

Lead electrodeposition from fluoroborate solutions is of particular interest in the production of $Pb/HBF_4/PbO_2$ reserve batteries of the bipolar type, since this solution is used for electrodepositing Pb onto one side of the substrate electrode to form the battery negative. In the batteries produced in the UK the lead plating solution used is that described by Smith (9) namely, 230 gl^{-1} $Pb(BF_4)_2$, 22 gl^{-1} free HBF_4 and 12 gl^{-1} free H_3BO_3 with 0.2 gl^{-1} gelatin, deposition being carried out at 2.7 Adm^{-2} and at 30°C.

1.2.4.2 Lead fluorosilicate

Fluorosilicic acid is prepared by the action of HF on SiO_2

$$6HF + SiO_2 \rightleftharpoons H_2SiF_6 + 2H_2O$$

The fluorosilicic acid so produced is then treated with PbO to form $PbSiF_6$.

$$PbO + H_2SiF_6 \rightleftharpoons PbSiF_6 + H_2O$$

Only a small quantity of excess fluorosilicic acid (3 to 5%) is tolerated in solution since it is unstable and the decomposition products may cause precipitation of insoluble lead salts. Boric acid is sometimes added to plating solutions to prevent hydrolysis of the H_2SiF_6 to SiO_2. The bath is usually

operated at 35 to 40°C with a total lead content of 75 to 180 gl^{-1} as PbO, and gelatin is again the most widely used addition agent although others have been reported.

Lowenheim (47) outlines the operating characteristics of a typical fluorosilicate solution as follows:

Temperature	35-40°C
Cathode c.d	0.5 - 8 Adm^{-2}
Anode c.d	0.5 - 3 Adm^{-2}
Cathode and anode current efficiencies	100%

Barak (1) however reports cathode efficiencies of 93 to 95% from a fluorosilicate solution.

The composition of two fluorosilicate baths are given as :

Component	Betts (51) concentration gl^{-1}	Reeve (52) concentration gl^{-1}
Pb	75	180
Total fluorosilicate	150	140
Animal Glue	0.2	5.4

The fluorosilicate bath is widely used for electrorefining lead, but it is not as good as the fluoroborate bath for producing protective lead coatings because they are not so finely grained or dense. It has the further disadvantage that it is necessary to give an undercoat of copper before plating steel with lead and is more susceptible to decomposition, though it is less expensive than the fluoroborate bath.

1.2.4.3 Lead sulphamate baths

This bath consists of a solution of $Pb(NH_2SO_3)_2$, with sufficient excess of sulphamic acid NH_2SO_3H to give a pH of 1.5. The $Pb(NH_2SO_3)_2$ is prepared from the reaction of PbO with NH_2SO_3H.

$$PbO + 2\ NH_2SO_3H \rightleftharpoons Pb(NH_2SO_3)_2 + H_2O$$

This solution is fairly stable, though if the pH is too low or the temperature too high hydrolysis to ammonium bisulphate can occur resulting in the precipitation $PbSO_4$. The solution is usually made concentrated enough to provide for operation over a wide range of current densities and the normal Pb concentration lies between 100 and 165 gl^{-1} at pH 1.5. The composition of some sulphamate baths is given below :

	DuPont(53)	Piontelli (54)	Mathers (55)
$Pb(NH_2SO_3)_2$ (Pb as metal)	140 gl^{-1}	80 gl^{-1}	54 gl^{-1}
Free NH_2SO_3H acid	not given	100 gl^{-1}	50 gl^{-1}
pH	1.5		1-1.5

The plating solution used by DuPont (53) was the first sulphamate bath to be used commercially for Pb deposition whilst Piontelli's (54) solution is used in the electrorefining of lead.

Sulphamates have the advantage over fluoroborate and fluorosilicate in electrorefining since HF is not necessary in electrolyte preparation. Furthermore, since silver and other impurities such as bismuth, copper and antimony have very low solubilities in NH_2SO_3H, they precipitate as anode slimes.

The $Pb(NH_2SO_3)_2$ plating solutions have other advantages over fluorosilicate plating solutions in that sulphamic acid is easy to store, $Pb(NH_2SO_3)_2$ has a higher solubility, corrosion of the impure anodes is more regular than in the Betts process and less electrolyte is lost in the anode slime. However, the operating c.d for the sulphamic acid refining process is low at 1 to 1.2 Adm^{-2} at a Pb concentration of 80 gl^{-1}.

The operating characteristics of the sulphamate solutions quoted by Lowenheim (47) are; cathode c.d 0.5-4 Adm^{-2}, temperature 24 to 50°C, throwing power 0% as determined by the Haring Blum Cell, with cathode and anode current efficiencies of 100%. Levin at al (56) discuss the use of a high concentration sulphamate solution containing 250 gl^{-1} $Pb(NH_2SO_3)_2$, 50 gl^{-1} NH_2SO_3H and 0.2 to 0.5 gl^{-1} bisphenol as an addition agent. This bath operates at a cathode current efficiency of 97% in the c.d range 2 to 5 Adm^{-2}.

The choice of addition agents for use in sulphamate baths has been studied by Mathers and Forney (55) and an account of their work as well as a detailed survey of sulphamate plating solutions, is given by Shenoi (57). They concluded that a combination of addition agents gave best results, an example being β-napthol $0.7gl^{-1}$ + $7gl^{-1}$ gelatin. Recent work on lead deposition from sulphamate solutions by Samel and Gabe (307) proposes a solution of 108 gl^{-1} Pb, 100 gl^{-1} NH_2SO_3H with gelatin as the addition agent. The solution is operated at 1.2 to 3.5 Adm^{-2} and at 55°C.

1.2.4.4 Lead pyrophosphate

Solutions of lead pyrophosphate have been little used for lead deposition although they have found favour in the electro-deposition of lead-tin alloys (58, 59) as well as in the deposition of more difficult or novel alloys such as Fe-W, Fe-Zn, Zn or Mo alloys (59).

The pyrophosphate baths for the electrodeposition of Pb-Sn alloys were developed as a result of the early work on the electrodeposition of tin (60, 61) and lead (62,63). Sree (64) reports the preparation of a lead pyrophosphate bath by the addition of an alkaline pyrophosphate to lead nitrate. The potassium salt $K_4P_2O_7$ was used, the concentration of which was maintained at 78 gl^{-1}. The $Pb(NO_3)_2$ concentration was 33.2 gl^{-1}, and the working pH was 8.9, adjusted by either the addition of HCl or KOH. Deposition of Pb without treeing may be carried out without the use of addition agents. However, a number of addition agents were investigated and of these gelatin was found to be most suitable, the optimum concentration being 1 gl^{-1}. Increase in the addition agent concentration causes a decrease in the limiting current density for Pb deposition which for the above solution is 3.5 Adm^{-2} at 60°C.

The deposits obtained by Sree (64) were finer grained than those from acid baths such as BF_4^- or $NH_2SO_3^-$ with satisfactory almost pore-free coatings obtained at a thickness of 12 μm and above.

Vaid and Rama Char (65, 66) studied Pb deposition from a Pb pyrophosphate solution based on $Na_4P_2O_7$ and $Pb(NO_3)_2$ and the solution composition they regarded as optimum was 15.5gl^{-1} $Pb(NO_3)_2$ + 52gl^{-1} $Na_4P_2O_7$. The cathode current efficiencies for this solution maintained at 60°C and pH 9.5 with cathode rotation of 1200 rpm were in the range 95 to 100% depending on the c.d and the limiting c.d for deposition of Pb was found to increase with lead concentration; for $Pb(NO_3)_2$ and $Na_4P_2O_7$ concentrations of 20.7 gl^{-1} and 70 gl^{-1} respectively it was 5.1 Adm^{-2}. A slightly higher solution pH is required when using the potassium pyrophosphate salt, since at lower pH's, decomposition of the solution may occur.

1.2.4.5 Lead tripolyphosphate

Izbekova (67) et al have discussed the deposition of Pb from solutions containing the tripolyphosphate ion $(P_3O_{10})^{5-}$. The addition of these tripolyphosphate salts to a solution of Pb salts produces complexes of the type $[Pb(P_3O_{10})_n]^{(5n-)-}$ and investigations by Izbekova have shown that a bath suitable for Pb deposition consists of 0.3 to 0.4M $Na_5P_3O_{10}$ (110 to 147 gl^{-1}, 26 gl^{-1} $Pb(CH_3COO)_2$, 0.1 to 0.3 gl^{-1} gelatin and 0.05M Triton B (a proprietary form of ethylenediaminetetraacetic acid). Plating is carried out at 50 to 60°C with a cathode c.d of 0.8 Adm^{-2} and a low anode c.d of 0.15 Adm^{-2} is necessary to prevent passivation of the soluble Pb anode; cathode current efficiencies of 70-100% were reported.

The plating solution operates at too low a c.d and Pb concentration to warrant anything more than academic interest.

1.2.4.6 Lead cyanide

The use of the lead cyanide bath for the deposition of lead is quoted by Walker and Thorley, (68) though no details as to the exact composition of this electrolyte or its operating conditions were given. The bath consists essentially of lead cynaide in an alkaline solution containing an excess alkali metal cyanide. A problem with this electrolyte is that it absorbs CO_2 from the atmosphere, which causes insoluble Pb salts to precipitate with consequent roughness of the deposit.

The addition of KOH to this electrolyte alleviates this problem since it absorbs the CO_2, forming bicarbonates and carbonates, which form soluble Pb salts and it also increases the conductivity of the electrolyte.

1.2.4.7 Lead phenol sulphonate

Gatos and Mathers (69) have studied in detail the deposition of lead from phenol sulphonate solutions, claiming that these solutions have advantages over the more commonly used fluoroborate and fluorosilicate solutions because of their less hazardous nature and easier handling. The plating solution is prepared by the reaction of phenol sulphonic acid with lead carbonate. The solution is then filtered to remove any insoluble lead sulphate which may be formed and diluted with water to give an optiumum plating solution of 40 gl^{-1} lead and 70 gl^{-1} free phenol sulphonic acid. Plating can then be carried out at room temperature at the recommended cathode c.d of 2.8 Adm^{-2} but unsatisfactory deposits are obtained from this solution unless suitable addition agents are used. Gatos and Mathers made a detailed study of possible addition agents which included investigating some 150 different combinations, and their results showed that combinations of addition agents gave much improved results compared to individual addition agents. The most effective addition agent combination was 20 ml l^{-1} p-cresol, 2 gl^{-1} goulac (a lignosulphonate) and 1 gl^{-1} aloin. Mathers also quotes references to Pb electrodeposition from other organo-lead salts namely, ethylbenzene sulphonate (70) and toluolsulphonate (71).

1.2.4.8 Lead gluconate

Von Fraunhoffer (25) reports a bath for the deposition of lead from lead gluconate using a solution first proposed by Uenc and Okubo (72).

The composition of this bath is 200 gl^{-1}, $2PbCO_3Pb(OH)_2$, 100 gl^{-1} sodium gluconate $CH_2(OH)[CH(OH)]_4COONa$ and 100 gl^{-1} sodium hydroxide, with additions of 0.2 gl^{-1} glue and 0.5 ml l^{-1} Turkey red oil. The bath operates at 70°C at a c.d of 5 Adm^{-2} with a current efficiency of 99% and is reported to have a better throwing power than the fluoroborate or silicofluoride baths.

1.2.4.9 Lead acetate

Loveland (73) uses an electrolyte containing 200 gl^{-1} $Pb(CH_3COO)_2$, 100 gl^{-1} $Na(CH_3COO)_2$, 15 gl^{-1} CH_3COOH with 4 gl^{-1} gelatin, 5 gl^{-1} sucrose + 5 gl^{-1} 2 naphthol-6 sulphonic acid as addition agents. The effective plating range of this solution is from 5.4 to 16.1 Adm^{-2} at an operating temperature of 70°C, with both anode and cathode current efficiencies of 100%. The bath is non-corrosive and can be used for plating lead directly onto steel, and with agitation deposition may be carried out at the upper end of the c.d plating range. It is recommended that prior to deposition and after suitable pre-treatment the articles to be plated should be immersed in 8 to 12% CH_3COOH at 70°C.

A bath based on lead acetate, ammonium acetate and sodium sulphate that forms a lead sulphate complex has been reported by Machu et al (74). This is claimed to have a greater grain refining effect than addition agents such as gelatin and p-cresol, and fine grained deposits are obtained at thicknesses of 10 to 12 µm. Mixtures of 80 gl^{-1} $Pb(CH_3)COO)_2$ and 100 gl^{-1} polyethylenepolyamine produce a "complexed electrolyte" which has been reported to reproduce fine grained compact electrodeposits up to 500 µm thick (75). This bath can be operated at 18-25°C and c.ds of up to 2 Adm^{-2}.

1.2.4.10 Lead perchlorate

There have been reports in the literature on the deposition of lead from perchlorate electrolytes (76-79), which are characterised by their very low pH levels, but apart from their use in coating bearing surfaces there appears to have been very little commercial or technical development of these baths. Henri (79) discusses a perchlorate bath suitable for plating Pb onto Al. The bath consists of 82.5 gl^{-1} $Pb(ClO_4)_2$, 20 gl^{-1} $HClO_4$ with 0.5 ml l^{-1} of oil of cloves as the addition agent.

1.2.4.11 Lead plumbite

There are various references on the electrodeposition of Pb from alkaline solutions (80,81), indeed it was from such a solution that the first recorded lead electrodeposits were obtained (29). Alkaline lead baths are usually based on sodium plumbite solutions prepared by saturating sodium hydroxide solutions with lead oxide. Seth (82) reports an alkaline lead bath that gives fine-grained electrodeposits at nearly 100% cathode efficiency, the composition of which is 0.6M Pb, 2.5-5M NaOH, 0.9-1.2M glycerine, with gelatin or β-napthol used as addition agents, the concentrations of which were not specified. The cathode c.d is in the range of 0.5-1 Adm^{-2}, whilst the anode c.d is 2 Adm^{-2} at 15°C and 7 Adm^{-2} at 60°C. Glycerine increases the solubility of lead from 0.2M to 0.6M in NaOH and also improves the structure of the deposit. A similar alkaline lead bath is described by Kudryavstev (83), which has the composition 0.4-0.5M Pb (as plumbite), 3.5-4.5M NaOH and 50-65 ml^{-1} glycerol, the use of an addition agent is not reported.

1.2.4.12 Lead nitrate

Lead nitrate is one of the cheapest and most abundant lead compounds, yet it is not normally used for electrodeposition of Pb, since it gives characteristic dendritic deposits, i.e Pb trees. The first really detailed study on the electrodeposition of lead from lead nitrate was made by Mathers in 1915 (84), though the production of electrodeposits from this solution has been reported as early as 1885. In view of the importance of the deposition of Pb from $Pb(NO_3)_2$ to the present studies a detailed account of the research effort into the development of $Pb(NO_3)_2$ plating solutions will be given.

There exists in the literature very few papers on this subject, most of the interest in lead electrodeposition from $Pb(NO_3)_2$ solutions being devoted to fundamental studies on electrodeposition from $Pb(NO_3)_2$ solutions, rather than the development of practical plating solutions.

Deposition of lead from a $Pb(NO_3)_2$ bath produces loose non-adherent crystals on the cathode. However, Mathers (84) managed to produce smooth coherent electrodeposits of lead from $Pb(NO_3)_2$ solutions containing certain addition agents. The composition he found most effective was 100 gl^{-1} $Pb(NO_3)_2$ 25 to 50 gl^{-1} CH_3COOH, 40 gl^{-1} $NaNO_3$ and 10 gl^{-1}, of the residue from the extraction of araco aloes, as the addition agent. This bath was operated at room temperature with a cathode c.d of 0.4 Adm^{-2} at a cathode efficiency of 99-98% and an anode efficiency of 100%. The operating life was only 6 weeks after which time the deposits became spongy and non-adherent, presumably because of the degradation of the addition agents. In his search for a suitable addition agent Mathers studied various additives few of which were simple chemicals, and examples of these additions included, saponin, benzoin, eucalyptas, rostrata, manna, lycopdium, formaldehyde, oil of cloves, licorice extract, β-nitroso napthol and phloridizin. The deposits obtained from $Pb(NO_3)_2$ solutions using licorice extract and phloridizin were in fact smooth but degradation of these addition agents soon occured and unsatisfactory deposits were obtained.

No further work on the deposition of lead from a nitrate electrolyte to obtain acceptable lead electrodeposits was reported until 1957 when Gristan and Shun (85) patented a bath consisting of up to 39 gl^{-1} $Pb(NO_3)_2$, 20 gl^{-1} HNO_3 and a proprietary surface active agent. In order to obtain acceptable electrodeposits it was necessary to apply a high c.d for the first few seconds, then to allow deposition to occur at a low c.d. The protective nature of the lead electrodeposit was improved by a chromate passivating treatment. Gritsan et al (86) later patented another $Pb(NO_3)_2$ bath which can be used at room temperature with a cathode c.d range of 0.43 to 0.86 A dm^{-2} to give dense compact deposits of lead. The composition of the bath is 30-35 gl^{-1} $Pb(NO_3)_2$, 20 gl^{-1} HNO_3 and

5.15 gl^{-1} of an addition agent which is the condensation product of naphthalene disulphonic acid with formalin or petroleum sulphonic acid.

Udupa et al (87) have studied the production of Pb-Cu alloys by electrodeposition from a nitrate electrolyte following the earlier work of Skirstymonskaya (88). Udupa discovered that an alloy of Pb-Cu was formed when the additive cetyltrimethyl ammonium bromide was added to a solution of $Pb(NO_3)_2$. The proportion of Pb in the alloy increased with concentration of this addition agent.

Skirstymonskaya's (88) plating solution contained 300 gl^{-1} $Pb(NO_3)_2$, 12 gl^{-1} $Cu(NO_3)_2 3H_2O$, 50 gl^{-1} KNO_3, 10 gl^{-1} NH_4Cl, 20 gl^{-1} tartaric acid and 5ml l^{-1} HNO_3. He also investigated various addition agents but did not find these had any significant effect on the resultant deposit.

1.2.5 Addition agents for use in lead electrodeposition

The use of addition agents for Pb plating solutions is mainly to suppress the production of dendrites, produce fine grained compact deposits, and also in some cases to improve the throwing power of the solution. Some of the addition agents used in Pb electrodeposition have already been mentioned in the preceding discussion on individual plating solutions, with gelatin being the one that has attained the most widespread use.

However, since a major part of the research effort has been devoted to this topic, it is relevant at this stage to summarise the literature on addition agents that are or may be used in lead alloy plating. The first systematic evaluation of the effect of certain addition agents on the polarisation of Pb was made by Renich (89), then later by Loshkarev (90). Kir'yakov (91, 92) studied the effect of certain additives on the polarisation characteristics of Pb in sulphamate solutions, and found that aniline, phenol and resorcinol gave the best electrodeposits.

Nevertheless, the most extensive evaluation of addition agents for use in the high speed deposition of Pb from $Pb(BF_4)_2$ solutions was carried out by Graham and Pinkerton (93), who investigated over 220 possible addition agents. Their method of assessment of each addition agent from a particular bath was confined to visual and microscope examination (x40) of the deposit's appearance for fineness of grain and absence of treeing. They also measured the 'limiting current densities' (l.c.d.) i.e. the highest c.d. at which smooth deposits were produced, and considered that the higher the 'l.c.d.' the more effective the addition agent at a specified rotational speed. In a previous paper Graham and Pinkerton (94) outlined a method of assessing addition agent action by quantitative measurements of the porosity of the deposits obtained from a fluoroborate bath, but only the 9 best addition agents were evaluated in this way.

Of the 220 addition agents evaluated using the techniques described above, 26 were selected for further study and of these only a few were considered effective. These were hydroquinone, 1-amino-4-hydroxy anthraquinone, 6-amino-1-naphthol-3-sulphonic acid, 1,4 naphthoquinone and Norlig MC (a lignin sulphonic acid). The best results were obtained with hydroquinone at a concentration of 10 gl^{-1} and 1-naphthol-4-sulphonic acid at a concentration of 0.2 gl^{-1}. Other authors recommend a number of different addition agents for deposition from $Pb(BF_4)_2$ solutions, and these include gelatin (95, 96), hydroquinone (82), peptone + resorcinol (97), aloin + dibenzene sulphonamide (82),pyridine or quinoline derivatives + polyethylene adducts (47). Wiesner et al (98) have used some of the addition agents suggested by Graham and Pinkerton, namely quinhydrone, (quinone + hydroquinone) but found they gave striated deposits, and as a consequence searched for other suitable additives and discovered that 1 gl^{-1} coumarin + 2 gl^{-1} lignin sulphonic acid gave the best results. Lowenheim (47) has also reported that the addition of peptone and resorcinol to fluoroborate solutions prevented striation of the deposit.

Rajagopal (99) in a recent study on addition agent action in a $Pb(BF_4)_2$ solution suggests a new addition agent based on the polyethoxyether series of general formula $(ROCH_2CH_2)_nOH$, which it is claimed gives smooth, fine grained deposits where R = $(CH_3)_3C\ CH_2C\ (CH_3)_2$ and n is 5 to 30.

Rajagopal also outlines a number of $Pb(BF_4)_2$ solutions containing different additives.

One of the earliest recorded uses of polyethers as addition agents is in the deposition of lead from sulphonate and fluoroborate solutions (100). The polyethers in this patent claim have the general formula.

$$R_1X[(R_20)n\ (R_30)n^1]n^2R_4$$

Where X = oxygen, NH, or sulphur

R_1,R_4 are hydrogen, hydroxyl, or a monovalent organic radical

R_2,R_3 are bivalent organic radicals, and

n, n^1, n^2 are integers

The compounds are water soluble and are produced by reacting polyethylene oxide with a suitable monohydric or dihydric alcohol, mono or dicarboxylic acid, acetal or phenol. The best results are obtained from polyethylene oxides which have carbo-cyclic substituents such as naphthol or para-hydroxy-diphenyl. Commercially produced polyethylene oxides having an aliphatic substituted group are sold under the trade name of "Carbowax", whilst cyclic substituted polyalkylene oxides are sold under the trade names of "Tween"; however, nap polyethylene additives appear to be the most successful.

The use of alkyl and alkyl aryl polyethers, alcohols and polyethylene glycols for deposition from both sulphamate and

fluoroborate solutions has also been reported (100). Anthraquinone sulphonates (101), nictotine (102) and polycyclic sulphonamides may also be used in fluoroborate solutions, whilst gelatin (82), lignosulphonates and polyethoxy polypropylene oxides (103, 104) have been used for $PbSiF_6$ baths. Smyers (105) has described a $PbSiF_6$ bath containing naturally occurring addition agents namely chestnut extract, goulac (a lignin sulphonate) and tannic acid. Mathers (106) used a combination of aloin and goulac for lead deposition from such a solution, though these additives are claimed to give an inferior performance when compared to those quoted by Smyers.

For deposition from $Pb(NH_2SO_3)_2$ solutions the usual additives have been used as well as glue and double phenols (100) and cetyltrimethylammonium bromide (CETB) (107). In the deposition of Pb from alkaline solutions (108) quaternary ammonium compounds (109) and hydroxybenzenes (110) have been used with Rochelle salts also added to improve anode corrosion.

Loveland (73) describes a $Pb(CH_3COO)_2$ plating solution containing gelatin together with a water soluble aromatic sulphonic acid and sucrose as addition agents. He quotes examples of a number of possible sulphonic acids all of which are napthalene derivatives, e.g. 2-naphthol-6-sulphonic acid, 1 naphthol-4-sulphonic acid, amino naphthalene disulphonic acids and naphtholene-1,5-disulphonic acid. Vaid and Rama Char using phenol sulphonate solutions obtained satisfactory deposits with glycerol, goulac, β-naphthol, phenol, resorcinol and diphenyl sulphone additions, but found the best combination was p-cresol and aloin.

1.2.5.1 Addition agents for Sn and Sn-Pb deposition

Unlike lead there has been a lot of interest in the production of bright Sn or Sn-Pb alloy coatings from acid baths, and considerable research effort has been devoted to investigating

addition agents for use in these electrolytes. Some of these additives have proved successful in such solutions and are often effective in lead plating solutions, and for this reason a survey of some of the common and not so common additives employed in acid Pb-Sn baths is relevant. Dohi (111) in his studies on the electrodeposition of bright Pb-Sn alloys from solutions of Sn and Pb cresol or phenol sulphonates used addition agents that are the reaction products of aliphatic aldehydes with aromatic primary amines, e.g. acetaldehyde with o-toludine and acetaldehyde coupled with a surface active agent consisting of nonylphenol reacted with ethylene oxide.

Nevertheless, Rosenberg (112) describes the deposition of bright Sn and Sn-Pb alloys from the more conventional fluoroborate based solutions using an additive which includes an emulsified naphthalene monocarboxldehyde (emulsified to make it soluble) with or without a substituted olefin of general formula

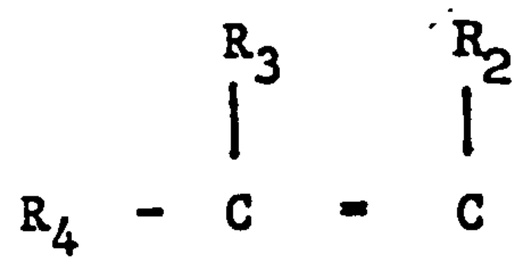

Where R_1, represents carboxy, carboxamido, alkali carboxylate ammonium carboxylate, amine carboxylate or alkali carboxylate

R_2, R_3, R_4 represents hydrogen, methyl or lower alkyl

Other polyether surfactants can be employed including the nitrogen containing aliphatic polyethers.

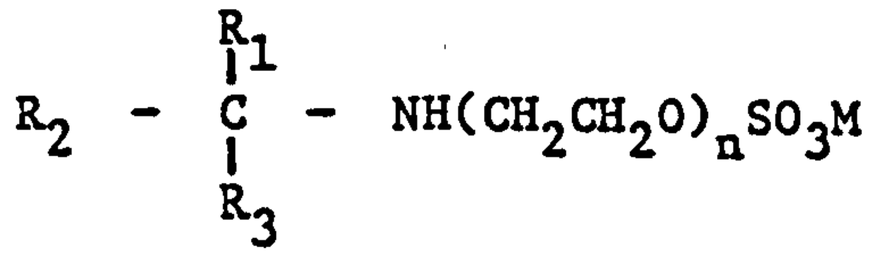

Where R_1, R_2, R_3 are straight or branch-chained alkyl groups containing 3 to 15 carbon atoms

n is an integer from 5 to 20

M is a cation either H^+, Na^+, K^+ or NH_4^+

The aryl hydroxy compounds used are either substituted napthols or phenols, e.g. α-naphthol, β-naphthol, 1,1 bis - 2 - naphthol, 2,4,6 trichlorophenol or p p' dihydroxy diphenyl sulphone. A similar bath to that proposed by Passal (114) was a mixture of polyoxylated surfactant in combination with a lower aliphatic and aromatic aldehyde (115).

A Sn/Pb plating solution that consists of a combination of primary and secondary brightening agents is given by The Philips Co Limited (80). The primary addition agent is of the type

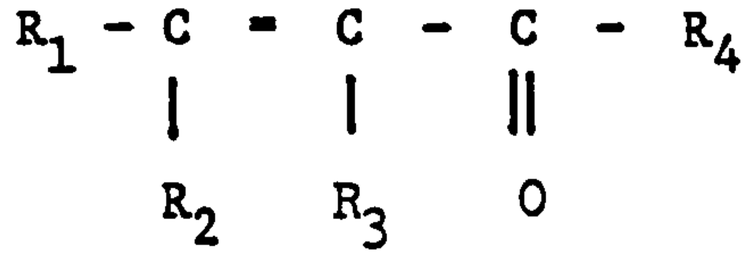

where R_1, R_2, R_4 represents an hydrogen, aliphatic, heterocyclic or aromatic group, and R_3 represents a hydrogen, alkyl group, or esterified carboxyl group.

The secondary brightening agent may be chosen from an acryloyl-containing compound, e.g. formalin, and furthermore it may also consist of one of the following compounds; N - vinylcarbazide, N - vinylpryrolidone, tetrahydrofuran or allylglycidyl ether. The addition of large quantities of polyoxy alkylene surfactant, an example being "Hostapal (V)", is necessary for the proper functioning of this system.

As a rule acid tin baths are composed of multicomponent systems with combinations of aldehydes, ketones, imidazoline surfactants, non-ionic surfactants and amines, and a combination of these additives often has a synergistic effect.

Hsa (113) uses as a brightening system for Sn - Pb plating a combination of 5 gl^{-1} non-ionic polyoxylated surfactant + 4 gl^{-1} of a lower aliphatic aldehyde. (n = 1 to 4) + 2 gl^{-1} of an amine (not specified) + 0.25 gl^{-1} aromatic aldehyde; this bath may even contain other additives, of which gelatin is the most widely used. Another type of additive system for Sn-Pb plating is given by Passal (114) who uses gelatin or high proteose peptones. However, the system he proposes consists of at least one polyether surfactant plus at least one aryl hydroxy compound, the concentration of the former being 4 gl^{-1} whilst that of the latter is 0.5 to 1 gl^{-1}. The preferred wetting agent, which is sold under the trade name of "Tergitol", is a polyalkoxylated alkylphenol.

$$R \quad -O(CH_2CH_2O)n \quad H$$

Where R is an alkyl group of 5 to 15 carbon atoms, (preferably nonyl), and n = 14 to 16.

Other polyether surfactants can be employed including the nitrogen containing aliphatic polyethers (115).

A terne plating solution has also been patented using nicotine and β-naphthol, and it is claimed that these additives result in an improved deposit appearance.

The aforementioned list of organic addition agents indicates the wide diversification of chemicals which may be successfully employed as lead or lead-alloy addition agents. The list given here is by no means complete, especially with regard to the Sn/Pb plating additives, though all the addition agents which have attained any important significance are mentioned.

1.2.6 Anodes and auxillary equipment in lead plating

For Pb plating soluble anodes of high purity Pb are almost invariably employed, and these must be free from impurities such as Sb, Cu or Ag, though small quantities of Bi,Sn or Zn are not thought to be harmful. Sb, Cu and Ag are particularly undesirable since they cause the formation of anode slime which subsequently enters the plating solution and may lead to roughening of the deposit. Improved anode performance is claimed by the addition of 0.01 to 0.1% PbO_2 to these anodes (116). Anodes used in Pb/Sn plating are of approximately the same composition as that of the desired deposit.

The anode efficiency in acid baths is almost 100%, although the efficiency in alkaline baths may be considerably less than 100% (117).

The size and shape of the anode is dependent on the object being plated but it should be thick enough to avoid overheating and any throwing power problems due to an irregular cathode.

Films formed on lead anodes may be removed by treatment with an alkaline solution containing gluconic acid (118), and it is advised that anodes are bagged using either nylon, terylene, diamyl or dacron. The acid plating solutions are stored in either vinyl or rubber lined steel tanks, while alkaline solutions can be used in rubber lined steel or even steel tanks, without any coating.

The pre-treatment processes prior to plating are dependent on the metal to be plated, which if acid is used, must be thoroughly washed so as to avoid contamination of the solution and precipitation of insoluble lead salts.

1.2.7 Testing of lead electrodeposits

For normal purposes the thickness of the electrodeposits is in the range of 6 to 22 μm and quite often a flash of copper is applied to a steel substrate before lead plating, since this is claimed to give good adhesion of the Pb deposit and improved corrosion protection. This is only carried out in the case of thick coatings of Pb since with thin coatings, this may lead to accelerated attack of the underlying steel (47).

A number of specifications exist on the required thickness of Pb electrodeposits to give protection, which are dependent on the environment in which the object is exposed (119, 120, 121). Lowenheim (47) has quoted a value of 125 μm as the necessary thickness required to ensure corrosion protection in severe corrosive environments.

The measurement of thickness of lead coatings can be achieved by simple weight gain measurements, the BNF jet test for which Seth (34) gives the solution composition or the non-destructive Beta-scope method. The latter device measures the β-rays emitted when the electrodeposited Pb coating is subjected to a suitable excitation, and compares this readout with that for a deposit of known thickness giving a direct readout in μm.

The adhesion of lead to nickel is particularly important for the $Pb/HBF_4/PbO_2$ primary battery. After deposition of Pb the composite Pb/Ni anodes are tested for adhesion by applying an adhesive tape to the surface of the deposit and then peeling it away and observing the amount, if any, of Pb

remaining on the tape. Details of this test are given in Ministry of Defence Specification AP3/5 Spec 91/71 Issue 2 Item 7.1. Apart from testing of electrodeposited Pb anodes for use in the $Pb/HBF_4/PbO_2$ primary batteries no other references in the literature have been found on the adhesion of electrodeposited lead. The porosity of electrodeposited Pb has been investigated more than its adhesion, and since porosity measurements of electrodeposited Pb have been used in the present study as a method of assessing addition agent action, it will be covered separately in the next section.

The internal stress, hardness, ductility and resistivity of electrodeposited Pb has already been discussed in Section (1.2.3) and the methods of determining these properties are given in the references in this section.

1.2.8 The porosity of lead electrodeposits

The many methods that are available for porosity determinations on electrodeposited coatings are summarised by Clarke (122), who states that they may be classified into:

1 Pore detection tests that actually make pore sites visible for inspection and counting

2 Porosity index tests that provide a direct numerical measure of porosity

The former type of test, in which the plated surface is exposed to a fluid (liquid or gas) that penetrates the pores and corrodes the substrate exposed, is the more common. The corrosion product exudes from out of the pores and in the simplest test is assessed visually. A print of the pore pattern can be made by absorbing the corrosion product on moist paper pressed against the surface. This test may be further improved by placing a metal cathode against the paper and making the substrate plus coating the anode to aid substrate dissolution; a process which is known as electrography.

A solution of NaCl + dimethylglyoxime has been used as an electrographic method to determine the porosity of gold on nickel (123), the dimethylglyoxime forming a bright red complex with the nickel. Other tests such as the nitric acid, SO_2 and H_2S tests which produce visible corrosion products, are also described by Clarke (124), but these are primarily of use in measuring the porosity of gold electrodeposits on copper,. nickel and silver.

Graham and Pinkerton (94) in their work on the porosity of lead electrodeposits on steel used a method first described by MacNaughton (125), details of which are given in the Appendix of Graham's paper. The method involves placing an absorbent paper soaked in a ferricyanide solution onto the surface of the lead electrodeposit. After a fixed period of time the paper is detached, dried, and the spots on the paper (produced by the iron from the substrate dissolving through pores in the coating to react with the ferricyanide solution) were counted at 20 x magnification. Typical values for the porosity of the additive free bath at $26^{o}C$ obtained by Graham and Pinkerton were given as 0.22 (1.65) pores per cm^2, and for the same bath but with 10 gl^{-1} hydroquinone the values were 0.022 (0.2) pores per cm^2. The figures inside and outside the brackets indicate the pores of diameter less than and greater than 0.5mm, respectively. Seth (34) gives the composition of a test solution for use in porosity determination on electrodeposited lead as 60 gl^{-1} NaCl + 10 gl^{-1} potassium ferrocyanide + 10 gl^{-1} potassium ferricyanide.

Clarke (122) outlines porosity index tests based on electrochemical methods. The measurement of corrosion potential has been shown by certain workers to be a measure of the porosity of electrodeposits (126, 127). This relies on the fact that the coating is often the cathode whilst the substrate is the anode. The corrosion potential of this bimetallic system, may then be used to compute the area of the exposed substrate from a knowledge of the free corrosion potential of the pure metals.

Nevertheless, Clarke (128) has reservations on the applicability of this method. He suggests an electrochemical method of determining the "porosity index" from measurement of the pore resistance. This technique involves the application of a small but increasing potential above the rest potential and measuring the resultant current flow. A linear relationship between current and voltage was obtained under these circumstance, and dV/di was taken as the pore resistance.

No quantitative method of this type was found in the literature for the measurement of the porosity of lead coatings on nickel. Since one of the major objectives of the present study was to evaluate the effect of selected addition agents on improving the surface coverage of electrodeposited Pb on Ni it was necessary to develop a quick yet quantitative method, similar to that used by Clarke. The enviroment was selected so that the Pb coating remained passive when a potential was applied whilst the Ni substrate was active. The choice of enviroment and experimental method is covered in greater detail in Section 2.1.2.

The use of the MacNaughton method (125) adopted by Graham and Pinkerton was considered to be too time consuming and not chosen for further study, especially as modifications were necessary for it to be used successfully with a nickel substrate.

1.3 Lead dioxide (PbO_2)

Lead dioxide PbO_2 is polymorphous and exists in one of two different crystalline modifications, a rhombic form (α-PbO_2) and a tetragonal form (β -PbO_2) or as a mixture of both. It has good electrical conductivity, and is mechanically strong when electrodeposited onto a suitable electrode support. It is corrosion resistant and largely free from chemical attack in solutions containing anions such as Cl^-, Br^-, I^-, ClO_3^-, ClO_4^-, SO_4^{2-}, NO_3^-, CO_3^{2-} and $CH_3CO_2^{2-}$.

PbO_2 electrodeposited onto a suitable substrate such as Ti, Ni or C has found widespread use as a cheap inert anode. These have been used successfully in a range of electrochemical processes including, the electrolysis of NaCl solutions to produce Cl_2, the electrochemical oxidation of iodic acid (HIO_3) to periodic acid (HIO_4), sodium chlorate ($NaClO_3$) to yield sodium perchlorate ($NaClO_4$), and as positive electrodes in reserve batteries (see Section 1.1). However the major electrochemical and tonnage application of PbO_2 is when used as the positive electrode material in the lead acid storage battery (see Section 1.1.1).

PbO_2 also has a limited number of chemical applications as an oxidising agent in the manufacture of chemicals, dyes, matches and pyrotechnics. It is used in considerable quantities as a curing agent for liquid sulphide polymers and in high voltage lightning arresters (129).

1.3.1 Preparation of PbO_2

The two crystalline modifications of PbO_2 can be prepared by either chemical or electrochemical means.

1.3.1.1 Chemical preparation

α-PbO_2

Precipitates of α-PbO_2 may be obtained by the addition of the powerful oxidant ammonium persulphate to solutions containing $Pb(CH_3COO)_2$ and NH_4OH (130), although Bagshaw (131) reports that the product obtained in this way is not crystalline. The method Bagshaw (131) recommends for the production of α-PbO_2 is to heat yellow PbO with $NaClO_3$ to 340°C for 10 mins. The remaining traces of Pb(II) are then removed by washing with 3M HNO_3, and the residual α-PbO_2 is then washed and dried.

1.3.1.2 β-PbO_2

The hydrolysis of 100g of Pb(IV) tetra-acetate dissolved in 2 litres of acetic acid is used to produce β-PbO_2 (130), and this is achieved by the dropwise addition of distilled water to the solution, over a period of 6h with some crystal seeds of β-PbO_2 added to aid nucleation. The precipitate obtained is filtered and then washed to remove any traces of impurity. Another method invloves boiling red lead (Pb_3O_4) in nitric acid, which removes the divalent PbO and leaves β-PbO_2 (132).

1.3.1.3 Commercial production of chemically prepared PbO_2

PbO_2 is produced commercially by the oxidation with chlorine of Pb_3O_4 dissolved in an alkaline solution although other less economical methods may be used, which include the extraction of PbO_2 from Pb_3O_4 by nitric acid or the oxidation of soluble lead salts with chlorine, bromine, hydrogen peroxide or any other strong oxidising agent (129). This results in a mixture of α and β-PbO_2.

1.3.2 Electrochemical preparation of PbO_2

In general, β-PbO_2 is produced electrolytically from acid solutions and α-PbO_2 from alkaline solutions.

1.3.2.1 α-PbO_2

The electrolysis of a saturated solution of $Pb(CH_3COO)_2$ dissolved in a supporting electrolyte of 6.5M ammonium acetate and 1.5M NH_4OH at a current density of 0.5 Adm^{-2} is reported to produce α-PbO_2 (133, 135).

Bode and Voss (133) and Ikari et al (136) have also obtained α-PbO_2 by the electrolysis of a 0.03M sodium plumbate solution prepared from 10 gl^{-1} $Pb(NO_3)_2$ and 25 gl^{-1} NaOH, whilst Dobson (137) has electrodeposited it from a 2M NaOH solution saturated with PbO at a c.d. between 0.08 and 0.16 Adm^{-2}.

1.3.2.2 β-PbO_2

This has been obtained by the electrolysis of acidified $Pb(NO_3)_2$ solutions of various concentrations. Ikari et al (136) electrodeposited β-PbO_2 from a solution of 0.03M $Pb(NO_3)_2$ and 2.5M HNO_3 at a c.d. of 0.3 to 0.5 Adm^{-2}, whilst Spahrbier (138) used 0.7M $Pb(NO_3)_2$ and 2M HNO_3 electrolysed at 0.5 to 1 Adm^{-2}. Chartier (134) used a solution of 0.5M $Pb(NO_3)_2$ with 1M HNO_3. Bagshaw (131), however, used a $Pb(ClO_4)_2$ solution produced from a solution containing 1.8M β-PbO dissolved in 3M $HClO_4$, which was electrolysed at 0.25 Adm^{-2}. Mindt in his work on electrical properties of β-PbO_2 also used a $Pb(ClO_4)_2$ solution to obtain his specimens.

1.3.3 Internal stress of electrodeposited α and β-PbO_2

It has been known for a long time that metallic and non-metallic crystals formed as a result of electrocrystallisation are often in a state of stress. The internal stresses that are developed may vary considerably from highly tensile to highly compressive, and are markedly affected by the nature of the deposit, the deposition conditions and the use of additives.

There have been attempts in the literature to explain the origin of these internal stresses (139) but at present there is no adequate theory to explain the relationship between the

magnitude of stress in various electrodeposits and the conditions of their formation.

Evans (140) states that where the deposited lattice does not match the substrate lattice this lack of epitaxy cannot simply be the sole cause for internal stress, since in certain cases the stress often develops after plating has ceased. Bushrod and Hampson (141) in their studies on the internal stress of PbO_2, state that with PbO_2 electrodeposition onto nickel there is considerable lattice mismatch, but do not think this is the prime reason for the development of internal stress. They believe that one of the possible reasons for the development of internal stress is the codeposition of hydrogen or oxygen. This mechanism was first suggested by Shibaski (209) who thought that the codeposition of hydrogen could occur and be present either as interstitial hydrogen or as an unstable metal hydride. The mechanism for the inclusion of hydrogen proposed by Bushrod and Hampson was that it may arise from the discharge of H^+ from an intermediate complex in the production of PbO_2. The formation of which occurs via the following mechanism.

$$Pb^{2+} + 2OH^- \longrightarrow Pb(OH)_2 \qquad (a)$$

$$Pb(OH)_2 \longrightarrow Pb(OH_2)^{2+} + 2e \qquad (b)$$

$$Pb(OH_2)^{2+} \longrightarrow PbO_2 + 2H^+ \qquad (c)$$

Reaction (c) can be considered as the deposition of absorbed H^+, and it is possible that H^+ could enter the lattice via this mechanism. Evidence for the inclusion of hydrogen in the lattice was obtained by Bagshaw et al (144), who found analytical evidence for bound hydrogen in PbO_2 deposits.

The adsorption of certain organic acid ions e.g. citrates, tartrates at the electrode may well affect the H^+ desorption step and explain the unusual effects of these anions on the development of stress in electrodeposited PbO_2.

The codeposition of oxygen may also occur during the deposition of PbO_2, although the mechanism of this process is not understood.

They also noticed that there was no observable change in the α to β-PbO_2 ratio for the wide differences in deposit stress and that this is not an important factor in determining stress.

Gnanasekaran (145) states that the internal stress may arise as a result of chemical or structual changes or that the distortion may be due to the deposition of foreign ions or molecules.

A number of different methods have been developed to study the magnitude of the internal stress in electrodeposits, a review of which is given by Gabe and West (146).

Bushrod and Hampson (141) used a method first suggested by MacNaughton and Hothersall (147). They observed that an increase in the $Pb(NO_3)_2$ concentration from 0.3M to 1.2M resulted in a decrease in the compressive stress range of β-PbO_2 electrodeposited at 23°C, the magnitude of the decrease was from 9 to 6 $kgmm^{-2}$.

At c.d.s less than 7 Adm^{-2} no significant difference in stress level was observed, and although at higher values there were reductions in the compressive stress and the deposit was found to be non-adherent. Stirring appeared to give deposits that were stress-free or that contained only a slight tensile stress.

In contrast to Indian workers (145) and work performed in these laboratories (148 - 152) the level of stress was found to be independent of charge passed (deposit thickness) and was found

not to change after the deposition current was discontinued. Gnanasekaran (145) et al studied the effects of c.d., pH, temperature and addition agents on the internal stress of β-PbO_2 electrodeposited from a standard nitrate bath of composition 320-330 gl^{-1} $Pb(NO_3)_2$, and 20-22 gl^{-1} $Cu(NO_3)_2$ using a Hoar and Arrowsmith stress-meter. They found that at all c.ds studied the mean stress developed was always tensile during deposition and increased with c.d.; the value of the tensile stress tended to decrease with thickness. After the cessation of current, the mean stress changed quite quickly (i.e. approximately 120s) from tensile to compressive. Variations in pH over the range 1.2 to 4.2 had little effect on the internal stress, while the mean stress was lower for anodes deposited at 20^oC and 55^oC than for those deposited at 28^oC. This was shown by the fact that anodes deposited at room temperature were more likely to crack than those deposited at higher temperatures.

MacAllister and Shreir (149) studied the deposition of β-PbO_2 at 2 Adm^{-2} and 50^oC from a solution of 360 gl^{-1} $Pb(NO_3)_2$ at pH 4 using a Hoar and Arrowsmith stress-meter. They produced a deposit in a state of mean tensile stress up to a thickness of 6.5 μm with a peak stress of 6 $kgmm^{-2}$ at 1 μm. With increase in deposit thickness the stress fell very quickly passing through "zero" stress at 6.5 μm and then continued to fall rapidly to higher values of compressive stress, the mean stress at a thickness of 13 μm being -4 $kgmm^{-2}$. The value of the compressive stress increased still further after the current was switched off, though no quantitative figure for this was given. MacAllister also allowed samples of PbO_2 electrodeposited onto nickel under the same conditions to age for 7 days and measured the increase in stress using the Stoney technique (153), and found that the compressive stress level increased by some 15%. He also investigated the effect of c.d. on the internal stress of PbO_2 deposited from the same solution (150). He observed that an increase in the c.d. up to 5 Adm^{-2} resulted in an increase in the value of compressive stress. The mean compressive stress at 1 Adm^{-2} was -5 $kgmm^{-2}$ at 2 Adm^{-2}

it was -10 $kgmm^{-2}$, 4 Adm^{-2} it was -13.2 $kgmm^{-2}$ and at 5 Adm^{-2} it was -14.3 $kgmm^{-2}$. All these compressive stresses are values of the instantaneous stress at the same thickness i.e. 10 µm. The values quoted at 2 Adm^{-2} disagree with those quoted in a previous report (149) in that the latter gave higher values of compressive stress and lower thicknesses at which the changeover from mean tensile to compressive stress occurs. Nishihara et al (143) have also undertaken measurements of the internal stress of β-PbO_2 electrodeposited from $Pb(NO_3)_2$ solutions. Their results show that the internal stress is dependent on thickness, c.d. and temperature, but their results are neither quantitative nor very informative.

Studies on the internal stress of α-PbO_2 are not as numerous as those on β-PbO_2 yet some have been undertaken by the same researchers.

Gnanasekaran et al (145) studied α-PbO_2 deposited from an electrolyte consisting of 293 gl^{-1} $Pb(CH_3COO)_2$ and 17.7 gl^{-1} $Cu(CH_3COO)_2$ from which the stress was entirely compressive with the mean stress at 10 Adm^{-2} being lower than that at 5 Adm^{-2}. There was a tendency for the compressive stress to decrease once the current was turned "off" but it never became tensile; the instantaneous stress level at a thickness of 9µm was - 4.1 $kgmm^{-2}$ at 10 Adm^{-2} and - 3.3 $kgmm^{-2}$ at 5 Adm^{-2}. Gnanasekaran also investigated the internal stress of PbO_2 deposited from a sulphamate bath, but found these deposits to be poorly adherent.

Vasandra (154) et al have measured the internal stress of PbO_2 in conjunction with their studies of the effect of $Pb(CH_3COO)_2$ additions to $Pb(NO_3)_2$ solutions on the electrodeposition of PbO_2. They observed a compressive stress for the deposition of PbO_2 from $Pb(CH_3COO)_2$ solutions which was thickness dependent but remained compressive even after removal of current. The value for the instantaneous stress at 9 µm was quoted as -4 $kgmm^{-2}$.

However, results in these laboratories as yet unpublished (144) on the deposition of α-PbO_2 from a solution containing 409 gl^{-1} of $Pb(CH_3COO)_2$ show that α-PbO_2 is deposited in a state of mean tensile stress. The exact value of instantaneous stress is thickness dependent with a peak stress of 7 $kgmm^{-2}$ followed by a slow decline to + 2 $kgmm^{-2}$ at 15 μm; for comparison with Gnanasekaran (148) and Vasundra's (154) results the value at 9 μm is -3.3 $kgmm^{-2}$ and -4 $kgmm^{-2}$ respectively.

There appears to be conflicting reports in the literature especially with regard to the internal stress of α-PbO_2. Gnanasekaran and Vasundra's results are in close agreement with each other, yet MacAllister's are completely opposite to theirs in that he found the deposit to have a tensile not a compressive stress.

Apart from Bushrod and Hampson all the other workers have observed a variation in stress level with deposit thickness and c.d., and that the stress varies after the current is switched off, though there is agreement that in the case of β-PbO_2 the resultant stress is always compressive.

1.3.3.1 The effect of additives on the internal stress of PbO_2

The effect of the addition of monobasic acids such as acetic acid to $Pb(NO_3)_2$ solutions, that are used for the electrodeposition of PbO_2 has been studied by Bushrod and Hampson (141), and by Vasundra et al (154). Bushrod found that in the case of the addition of acetate to a 1.2M $Pb(NO_3)_2$ solution, an increase in the acetate concentration resulted in a decrease in compressive stress, which finally became tensile at 0.366M acetate. The addition of polybasic acids such as citrates and tartrates to 1.2 M $Pb(NO_3)_2$ solutions was more effective and only 0.03 M of the acid was necessary to cause a change from compressive to tensile stress. It was not possible, however, to increase the concentration of polybasic acids above this concentration (i.e. 0.03M) without severely affecting the adherence of the deposit.

Vasundra et al (154) made additions of $Pb(CH_3COO)_2$ to a standard bath of composition 300-350 gl^{-1} $Pb(NO_3)_2$ and 20-35 gl^{-1} $Cu(NO_3)_2$. The concentration range of the $Pb(CH_3COO)_2$ additions was 0 to 200 gl^{-1} and Vasundra not only observed the internal stress at each acetate concentration but also, the α to β-PbO_2 ratio, the throwing power, and the solution's polarisation characteristics. The mean values of stress were found to increase with $Pb(CH_3COO)_2$ concentration up to 50 gl^{-1} and then to decrease above that concentration. Only tensile stresses were observed during plating, though after removal of the current the stress became compressive in all cases.

Gnanasekaran et al (145) investigated the effect of some addition agents, i.e. saccharin, p-toluenesulphonamide and cetyl trimethylammonium bromide (CETB) on internal stress. They found that there was no difference in peak stress using either saccharin or p-toluenesulphonamide and although the tensile stress developed during deposition was considerably reduced, it still reverted to compressive even after removal of current. The addition of CETB however prevented the stress becoming compressive after deposition. Gnanasekaran et al (155) in a later paper concentrated their studies on the effect of various surfactants including CETB on the electrodeposition of β-PbO_2. They found that CETB not only lowered the mean stress but also facilitated the deposition of smooth pinhole-free PbO_2. At c.ds up to 1 Adm^{-2} the mean stress remained tensile until 18 μm of PbO_2 had been deposited, but at higher c.ds (2 and 3 Adm^{-2}) the mean stress rapidly became compressive at thicknesses of 6 to 7 μm, when deposited from a $Pb(NO_3)_2$ and $Cu(NO_3)_2$ solution containing 350 gl^{-1} and 25 gl^{-2} respectively plus 2 gl^{-1} CETB. The influence of various cationic, anionic and non-ionic surfactants on the

internal stress of PbO_2 has also been reported by Shibaski (142), and work has been carried out in these laboratories to investigate the effect of various anionic and non-ionic surfactants and also the complexant ethylenediaminetetraacetic acid (EDTA) on the internal stress of β-PbO_2 (150, 151, 152).

MacAllister and Shreir used a standard solution of 360 gl^{-1} $Pb(NO_3)_2$ at pH 4, which is the composition of the solution used to obtain coatings of β-PbO_2 on Ni, for use in the $Pb/HBF_4/PbO_2$ battery. They found that the addition of EDTA to the $Pb(NO_3)_2$ solution in the concentration range studied (0 to 1 gl^{-1}) had little effect in the tensile region, but it caused the changeover to a compressive stress to be delayed whilst the maximum value of the compressive stress is reduced with increasing concentration of EDTA. The instantaneous stress level at a deposit thickness of 10 μm from a solution containing 1 gl^{-1} EDTA was reported as -1.4 kg mm^{-2} whilst from a non-additive bath a deposit to the same thickness plated at 2 Adm^{-2} gave a mean stress of -11.4 kg mm^{-2}. The X-ray diffraction patterns of the deposit obtained from the $Pb(NO_3)_2$ solution containing $1gl^{-1}$ EDTA, showed the existence of α-PbO_2 in the deposit and a reduction in the grain size of the PbO_2.

In their studies on the effect of various anionic and non-ionic surfactants on the electrodeposition of β-PbO_2, MacAllister and Shreir selected a number of proprietary surfactants. In general, they found that the addition of non-ionic surfactants produces deposits with stress levels similar to those from the pure $Pb(NO_3)_2$ solution. On the other hand, additions of anionic surfactants caused a considerable reduction in the stress levels in both the tensile and compressive region. The stress level in some electrodeposits of β-PbO_2 obtained with certain of these addition agents was recorded and the voltage rise time of each electrode in 48% HBF_4 at -32°C measured. Tabulation of MacAllister's results enables a direct comparison of the relationship between the stress in certain β-PbO_2 electrodeposits and the voltage rise time (see Table 5):

TABLE 5

The relationship between internal stress of PbO_2 electrodeposited from a 360 gl^{-1} $Pb(NO_3)_2$ solution at 2 Adm^{-2} and 50°C and voltage rise time at -32°C for a $Pb/HBF_4/PbO_2$ battery

Addition Agent	Stress $kgmm^{-2}$	Cell Voltage (Volt) at a selected time after activation at -32°C	
		100ms	500ms
0.003% Triton	-6.0	1.232	1.262
0.003% Mannoxol 1B	-6.3	1.233	1.267
No addition agent added	-8.9	1.242	1.285
0.003% Tween 80	-9.85	1.315	1.324
0.003% BRIJ 35	-10.2	1.267	1.298
0.01% Tween 80	-11.15	-	-
Electrodeposited β-PbO_2 heat treated at 250°C for half an hour	-35.5	1.265	1.314

MacAllister's results show that in general the anionic surfactants appear to have a detrimental affect on electrode activation. In contrast to deposits prepared from baths containing the non-ionic surfactants, in particular Tween 80 which shows activation times lower than those prepared from the standard $Pb(NO_3)_2$ solution. The particular interest in the relationship between stress and voltage rise time arises as a direct result of Smith's (9) earlier work, where he noted the improved activation time of β-PbO_2 after it had been stressed by heat treatment.

MacAllister and Shreir have also investigated the development of stress in PbO_2 as a result of heat treatment of β-PbO_2 electrodeposited under standard conditions.

1.3.4 Other mechanical properties of PbO_2

The investigation of a number of mechanical properties such as brittleness, hardness and internal stress of PbO_2 electrodeposited onto a nickel electrode from an alkaline plumbite solution has been undertaken by Bakhchisaraitsyan et al (156) as a function of formation conditions and additions of ethylene glycol. High organic additive concentrations were found to lead to a reduction in microhardness, brittleness, brilliance and an increase in compressive stress. In an organic-free electrolyte the properties of the deposit apart from brilliance depended upon c.d. only to a limited extent, whilst for high additive concentrations an increase in c.d. lead to an increase in compressive stress. Bakhchisaraitsyan correlated these changes with changes in microstructure and deposit condition. The internal stress changes he linked with the changes in the volume of the deposit due to a variation in its PbO content, which increased with increasing ethylene glycol concentration.

The variation of PbO_2 hardness with potential in H_2SO_4 electrolytes was shown by Leikis and Venstrem (157) to exhibit a maximum at +1.78V vs (SHE) so confirming the potential of zero charge (E_{pzc}) determined by Kabanov et al (158). Volgina et al (159) studied the hardness and brittleness of PbO_2 electrodeposited from an EDTA containing solution, as a function of electrode potential, and found that hardness, brittleness, and internal stress were dependent on electrode potential.

1.3.5 Electrical properties of PbO_2

Lead dioxide is quite often referred to as a semi-conductor yet it has characteristics which more closely approach those of metals, since its resistivity, which is much lower than most semi-conductors, increases with temperature. In fact, it's resistivity approaches that of bismuth and mercury and is lower than that of carbon.

One of the first workers to investigate the electrical properties of β-PbO_2 was Thomas in 1948 (160). He obtained values for the resistivity of β-PbO_2 that were in the range 1×10^{-4} to 3×10^{-4} ohm cm, and values of the Hall Coefficent of -1.7×10^{-2} to -3.4×10^{-2} cm^3/C. From this Thomas concluded that conduction was via electrons, the carrier concentration of which was between 10^{20} and 10^{21} per cm^3.

Studies on the electrical properties of α-PbO_2 were carried out at a later date by White and Roy (186), yet the more authoritative study on the electrical properties of both α and β-PbO_2 was conducted by Mindt (161). In the case of electrodeposited β-PbO_2 he obtained a resistivity of 1×10^{-4} ohm cm, which was virtually independent of deposit thickness above 1 μm whilst for α-PbO_2 he found the resistivity to be 9×10^{-4} ohm cm, i.e. almost an order of magnitude higher. This is mainly as a result of the lower electron mobility in the α-phase i.e. 7 $cm^2\ V^{-1}sec^{-1}$ as compared with 100 $cm^2\ V^{-1}sec^{-1}$ in the β phase, which compensates for the higher electron concentration in the α phase of 1.4×10^{21} cm^{-3} in comparison to 5×10^{20} cm^{-3} for the β phase.

PAGINATION ERROR IN

ORIGINAL THESIS

The electron conduction mechanism is via free electrons that arise as a result of either deviations from stoichiometry or the incorporation of hydrogen and other impurities in the lattice. It is well known that PbO_2 exists in a wide range of non-stoichiometry which has been determined by Katz (162) as PbO_x, which ranges from 1.87 to 2.00. Each oxygen vacancy donates 2 free electrons into the PbO_2 conduction band.

Ruetschi and Cahan (163) have also suggested that the free electrons may in part be due to OH^- groups substituted for oxygen in the lattice, as an appreciable amount of bound hydrogen has been found in PbO_2 deposits by Bagshaw et al (144). However, it was not possible to decide whether non-stoichiometry or incorporated hydrogen gave rise to electronic conductivity as the chemical analysis was insufficently exact to distinguish between H in the lattice as part of OH^- groups and H^+ as part of absorbed water.

The different electron mobilities in α and β-PbO_2 are attributed to several factors by Mindt. Firstly the smaller grain size of α-PbO_2 i.e. 200μm, as compared to 500μm for β-PbO_2 giving a larger grain boundary area in the case of the latter, since this corresponds to a larger number of lattice defects at which electrons are scattered.

1.3.6 Electrochemistry of PbO_2

A review of the electrochemical properties of the PbO_2 electrode has been carried out by Carr and Hampson (164) and by Kelsall (165), whilst the thermodynamics of this system as a function of electrode potential is covered in some detail by Pourbaix (166).

In view of the commercial importance of the lead acid battery, most of the interest in the electrochemical properties of the PbO_2 electrode has concentrated on studies of PbO_2 in H_2SO_4. There exists in the literature a number of surveys on this subject, notably the ones by Carr and Hampson (164), Vinal (167), Burbank et al (168), Bode (132) and Kuhn (25) whilst the thermodynamics of the PbO_2/H_2SO_4 system is covered in some detail by Duisman and Giaque (169). As their studies bear no direct relationship to the present investigations they will not be reviewed here, since the present work is concerned primarily with the electrodeposition of PbO_2 from aqueous solutions of Pb^{2+} salts and in the reduction of PbO_2 to yield soluble reaction products. It is these aspects of the PbO_2 electrode that will now be considered in this review.

1.3.6.1 Nucleation of PbO_2

The process of nucleation of α-PbO_2 onto an inert electrode from a $Pb(CH_3COO)_2$ solution was first studied by Fleischmann et al (170) who also discussed the theoretical background to the nucleation process (171) and investigated the nucleation of PbO_2 from $PbSO_4$. They also investigated the potential and concentration dependence of the various nucleation rate constants. The rate of formation of nuclei is potential dependent, they therefore pre-formed a large number of nuclei at a high overpotential, and then studied their growth at low overpotential. Under these conditions the formation of new nuclei at low overpotentials may be neglected and the time dependence of the current, reflects the geometry of the growing crystal.

The current-time relationship they observed was found to be :

$i = BNt^2$ where i is the current density

B is the potential dependent nucleation constant

N is the number of nuclei formed at the higher overpotential

t is the time

This square relationship of time to current reflects a three dimensional growth of the nuclei.

Two nucleation laws have been observed. If virtually instantaneous nucleation of all the possible nuclei (N_o) at the preferential sites for nuclei formation occurs, the nucleation obeys a first-order law.

$$N = N_o (1 - \exp^{-At})$$

where A is a nucleation constant, and N is the number of nuclei at time t; for small times this approximates to a linear law

$$N = A N_o t$$

At potentials where the competing processes of nucleation and growth occur simultaneously, the current time relationship was calculated by Fleischman and Liler (172) who assumed a linear relationship between a current and time. Then for 3-dimensional nuclei formation:

$$OH^- - e \longrightarrow OH_{ads} \qquad (a)$$

$$Pb^{2+} + OH_{ads} + OH^- \longrightarrow Pb(OH)_2^{2+} + e \longrightarrow PbO_2 + 2H^+ \qquad (b)$$

in which the electron transfer stage was considered to be the rate determining step.

In a more recent paper Gilroy and Stevens (173) have investigated the potentiostatic deposition of β-PbO_2 from acidifed $Pb(NO_3)_2$ onto a Ti electrode and also the effect of F^- ions on the current transient and on the size distribution of the nuclei. They also found the growth step obeyed an i vs t^2 relationship and that in the initial stages of growth, the nuclei were spherical in shape.

The nucleation density was low 10^6 to 10^7 cm^{-2} compared to 10^9 cm^{-2} observed on Pt by Fleischman et al (174) and on SnO_2 by Laitinen and Watkins (175). In the absence of F^- it was found difficult to observe progressive nucleation as all the sites became rapidly saturated. The addition of F^- retarded the overall growth rate at a given potential, which they attributed to competitive absorption of the F^- ions on the growing lattice.

Beck (176) has carried out cyclic voltammetry studies on the deposition of PbO_2 from fluoroborate-containing solutions. From his results he postulated a reaction mechanism involving a sequence of both chemical and electrochemical steps:

$$Pb^{2+}(aq) \longrightarrow Pb(OH)^{+}(aq) + H^{+} \qquad (a)$$

$$Pb(OH)aq^{+} \xrightarrow{rds} Pb(OH)_2^{+} + H^{+} + e \qquad (b)$$

$$Pb(OH)_2^{+} \longrightarrow Pb(OOH)^{+} + H^{+} + e \qquad (c)$$

$$(PbOOH)^{+} \longrightarrow PbO_2 + H^{+} \qquad (d)$$

The slow step leads to the formation of a Pb (III) intermediate, $Pb(OH)_2^+$, and this is further verified by the fact that the solution soluble Pb (III) species was observed. Beck (176) also studied the effect of various anions on the anodic overvoltage (η_A) for PbO_2 formation, and found that they had a marked influence on (η_A) with NO_3^- ions lowering η_A to the greatest extent. The order of effectiveness of different anions was found to be:

$$NO_3^- > ClO_4^- > BF_4^- > SiF_6^{2-} > NH_2SO_3^- > CH_3COO^-$$

1.3.6.2 Cathodic dissolution of PbO_2

The reduction of α and β-PbO_2 in $HClO_4$ has been the subject of considerable research by Hampson, Jones and Phillips (177, 178). They consider that the time to passivation of PbO_2 in $HClO_4$ under galvanostatic polarisation, can be expressed in terms of a modified diffusion equation:

$$(i - i_L)t_p^{1/2} = K_p$$

where K_p = a constant characteristic of the system
i_L = limiting c.d. below which passivation does not occur
i = current density
t_p = time to passivation

Passivation is due to the formation of a film of $Pb(ClO_4)_2$ which causes a potential change as a result of the transition from reaction (a) to reaction (b) shown below:

$$PbO_2 + 4H^+ + 2e \longrightarrow Pb^{2+} + 2H_2O \qquad (a)$$

$$Pb^{2+} + 2e \longrightarrow Pb \qquad (b)$$

They showed that both i_L and K_p were dependent on $[H^+]$. The values for i_L obtained at higher acid concentrations (3M) were the same for both α and β-PbO_2 i.e. 0.05 Acm^{-2}; however, at low acid concentrations the values of i_L were higher for α than for β-PbO_2. Typical values were 0.007 Acm^{-2} for α-PbO_2 at 0.05M H^+ and 0.006 Acm^{-2} for β-PbO_2 at 0.24M H^+.

Hampson et al evaluated the mean values of capacitance of α-PbO_2 and β-PbO_2 in 3M $HClO_4$ as 138 $\mu F cm^{-2}$ and 79 $\mu F\ cm^{-2}$ respectively, and the difference was accounted for by the higher surface area of α-PbO_2; the values appeared to vary little with acid concentration.

Values for the exchange c.d. for α-PbO_2 were measured and found to be approximately twice those of β-PbO_2, and some of the values obtained are outlined in Table 6 below:

TABLE 6

Values of the exchange current density (i_o) for the reaction $PbO_2 \rightleftharpoons Pb^{2+}$ in $HClO_4$

Lead Concentration Moles l^{-1}	Acid Concentration Moles l^{-1}	Working Electrode	i_o Acm^{-2}
0.063	3	α-PbO_2	1.96×10^{-4}
0.5	3	α-PbO_2	2.71×10^{-4}
0.045	3	β-PbO_2	0.96×10^{-4}
0.47	3	β-PbO_2	1.53×10^{-4}

The temperature dependence of i_o obtained for β-PbO_2 indicated an activation enthalpy of 31 kJ $mole^{-1}$. In the case of α-PbO_2 the Arrhenius plot showed two distinct linear regions

for the exchange current density, with the break occurring at 40°C, and the values were 12.6 kJ mole^{-1} and 42 kJ mole^{-1} below and above 40°C, respectively.

From their investigation of the polarisation characteristics and measurements of the transfer coefficient, which remained constant only over a limited potential range, they concluded that in the low overpotential region, reduction occurs via a 2-electron transfer process whilst in the high overpotential region the reaction involves two consecutive single-electron transfers. The rate determining step (r.d.s.) was found to be the one that resulted in the formation of a Pb(111) intermediate and the reaction mechanism they proposed was as follows:

$$PbO_2 + 2H^+ \longrightarrow PbO_2\,(H^+)_2 \text{ ads}$$

$$PbO_2(H^+)_2 \text{ ads} + e \longrightarrow (Pb(OH)_2)^+$$

$$(OH\ PbOH)^+ + e \longrightarrow Pb(OH)_2 \quad \text{fast}$$

$$Pb(OH)_2 + 2H^+ \longrightarrow Pb^{2+} + 2H_2O$$

1.3.7 Electrodeposition of PbO_2 onto an inert substrate

The choice of a suitable substrate to act as a base for PbO_2 deposition is limited by the fact that it must be a good conductor, possess good mechanical properties, must not corrode in the event of a pinhole in the PbO_2 layer, and remain passive in the PbO_2 plating electrolyte. Graphite, Ti, Ni magnetite, and Ta are all possible substrate materials. Of these, Ti is the only one that satisfies all the above requirements; graphite and magnetite do not possess good mechanical properties, Ni will gradually dissolve when the PbO_2 is used in certain environments whilst Ta will anodise.

Ti is therefore the most commonly used substrate material, especially in applications where the PbO_2 is used in chemical synthesis. However, for positive electrodes in reserve batteries Ni is used as the electrode material because it is easily formed into thin sheets and remains passive in the PbO_2 plating electrolyte.

In view of the fact that modifications to the existing $Pb(NO_3)_2$ solution were necessary to obtain acceptable deposits of Pb it was important to review the work that had been conducted into improvements in the properties of PbO_2 by the addition of certain additives to the standard $Pb(NO_3)_2$ plating solution. In particular, it is important to consider additives that although improving the Pb deposit, would not have a deleterious effect on the properties of the PbO_2 deposit, particularly its adherence.

1.3.8 The PbO_2 electrodeposition process

In theory, PbO_2 may be electrodeposited from any soluble lead salt providing that the anion is relatively stable at the PbO_2 formation potential. There are, however, a limited number of readily available soluble lead salts for use in electrolytes for PbO_2 anode production, but successful deposits of PbO_2 under carefully controlled conditions are reported for Pb salts of the following anions: ClO_4^-, NO_3^-, BF_4^-, SiF_6^{2-}, $NH_2SO_3^-$ (179). However, Bushrod and Hampson (180) claim that at c.ds above 0.5 Adm^{-2}, BF_4^- and SiF_6^{2-} solutions produce unacceptable deposits of PbO_2 which are highly stressed, poorly adherent and flake off. Only NO_3^- and ClO_4^- salts were found to give acceptable PbO_2 deposits at a satisfactory rate.

The addition of certain anions such as CH_3COO^- and dibasic carboxylic acids to solutions of $Pb(NO_3)_2$ that are

used to produce electrodeposited PbO_2 has also been reported by Bushrod et al (141). The addition of polybasic acids to a $Pb(NO_3)_2$ solution at concentrations greater than 0.03M had a deleterious effect on the PbO_2 deposit adherence, though no such marked effect was observed when CH_3COO^- was added.

The use of $Pb(ClO_4)_2$ solutions for the preparation of PbO_2 deposits is precluded owing to the dangers caused by the high oxidising power of this solution, which may ignite organic materials and consequently requires considerable care in its use and handling. Indeed, it is only solutions based on $Pb(NO_3)_2$ that have any practical significance in the deposition and production of PbO_2 anodes. The only other soluble lead salt not discussed so far is $Pb(CH_3COO)_2$. However, deposits of α-PbO_2 are obtained from these solutions which are highly stressed, poorly adherent and therefore not suitable for use as battery material.

In the formation of PbO_2 there is a rapid decrease in solution pH, which is particularly important in the deposition of PbO_2 on nickel for reserve energisers. Smith (9) reports that a decrease in pH has a marked effect in increasing the voltage rise time. However, in addition, decrease in pH decreases the ability of Ni to passivate, and if it reaches too low a value, the nickel becomes active and corrodes. In practice, the acidity of the solution is maintained at pH 3.5 to 4 by circulating the electrolyte through a bed of PbO (lithage), which reduces the acidity, forming Pb^{2+} and H_2O.

This treatment also has the beneficial effect that the solution is replenished with Pb^{2+}. The increase in acidity may also be decreased by adding basic lead carbonate or copper carbonate.

During the operation of the bath NO_3^- is reduced to NO_2^- at the cathode or even to NH_4^+ in the presence of a Cu^{2+} catalyst, and oxidation of NO_2^- at the anode may lead

to a serious decrease in the current efficiency for PbO_2 formation (see Fig. 1) which was taken from the work of Bushrod and Hampson (180).

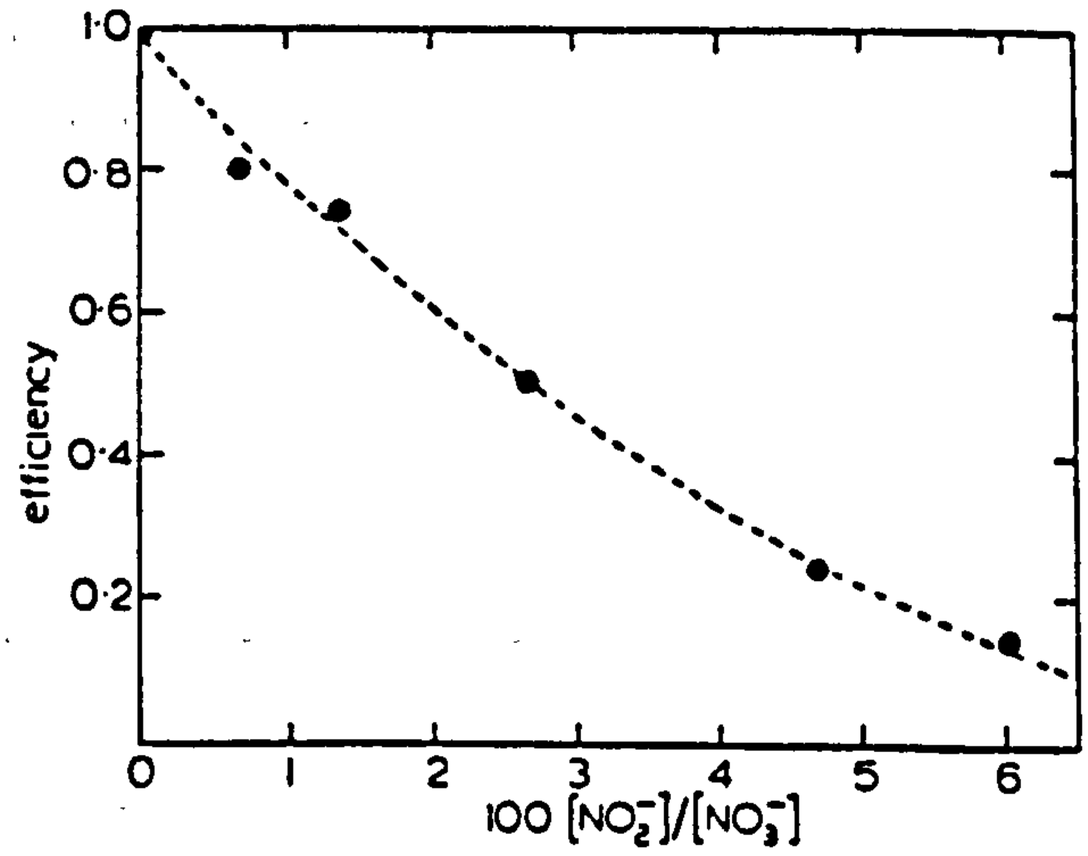

Fig 1. Effect of the nitrite ion on the faradaic efficiency for the anodic electrodeposition of PbO_2 from lead nitrate electrolyte.

Periodic additions of 35% H_2O_2 have been used to oxidise the NO_2^- and thus maintain the current efficiency at a high level. The circulation of the electrolyte over a bed of Pb_3O_4 has also been used as a method of chemically oxidising the NO_2^-. Other impurities that have a detrimental effect on current efficiency for PbO_2 deposition are Fe^{2+} and Co^{2+} since they may tend to be oxidised at the anode, and the presence of Co^{3+} is particularly undesirable since it may catalyse oxygen evolution on PbO_2.

1.3.9 The commercial electrodeposition of PbO_2 from $Pb(NO_3)_2$ solutions

A number of reviews exist in the literature on the production of PbO_2 electrodes on an inert base (25, 165), and details are provided of pre-treatments prior to deposition and of the deposition process. However, no account will be given here of the pre-treatment processes as these are mainly associated with Ti or graphite substrates, which are not of relevance to the present studies. An account of the pre-treatment process necessary for nickel prior to successful PbO_2 deposition is given by Smith (9).

The Pacific Engineering and Production Company of Nevada (PEPCON) have patented a number of modifications to the conventional $Pb(NO_3)_2$ electrolyte e.g. D.A.S 1,182,211; (1960) US patent 2,945,791 (1960) and D.A.S 1,496,962 (1966). Gibson describes in US Patent 2,945,791 and later in British Patent 1,159,241 a PbO_2 plating solution that operates in the temperature range 72 - 82°C and at c.ds up to 10 Adm^{-2}. The electrolyte consists of 200 gl^{-1} $Pb(NO_3)_2$, 10 gl^{-1} $Cu(NO_3)_2$, 10 gl^{-1} $Ni(NO_3)_2$ and 0.75 gl^{-1} of a surface active agent of the alkyl phenoxy polyethoxyethylene ethanol class and 0.5 gl^{-1} NaF with the pH adjusted to 4.

The $Ni(NO_3)_2$ addition is claimed to give a finer grain size (183), whilst additions of NaF inhibit the oxygen evolution reaction (184, 185). The surfactant was added to reduce gassing, improve throwing power and aid bubble release. Grigger reports the use of a surfactant of the above type (trade name Igepal (0-880) which is reported to break down in operation; the breakdown products are removed from solution by the addition of n-amyl alcohol which removes the residual surface active agents as a liquid layer that floats on the surface of the solution and can be decanted off. Regeneration of the plating bath is accomplished by the addition of the surface

active agent. The purpose of $Cu(NO_3)_2$ additions is to prevent the deposition of Pb dendrites at the cathode that could result in shorting out of the cell. This is achieved since Cu deposition occurs in preference to Pb deposition.

In a later patent Gibson (183) suggests a PbO_2 plating solution containing fewer additives, i.e. no $Ni(NO_3)_2$ and no surfactants that could have a detrimental effect on the PbO_2 deposit; this bath can operate at a low pH.

Narasimham and Udupa (187, 188) have added cetyltrimethyl ammonium bromide to $Pb(NO_3)_2$ solutions and claim this produced a stress-free smooth PbO_2 surface.

Shibaski (189) in his studies on the deposition of PbO_2 claimed that the most suitable conditions for strong, bright PbO_2 deposits were (a) a smooth substrate surface, (b) a high Pb^{2+} concentration (c) a pH in the range 1-4, a c.d. in the range 1 to 5.5 Adm^{-2} and an operating temperature of 0^oC to 20^oC and (d) the presence of Al^{3+}, Mn^{2+}, p-toluenesulphonamide or polyethoxyethylenealkyl ether.

Wabner (190) however states that deposition of PbO_2 onto Ti at low temperatures results in anodes that give higher overvoltages in subsequent use. The US Bureau of Mines (191) reports cracking of the deposit when deposition takes place above 70^oC, and in practical commercial baths the temperature is maintained in the range 50^oC to 60^oC.

UK patent 1,192,344 covers the use of a bath containing 300 gl^{-1} $Pb(NO_3)_2$, 3 gl^{-1} $Cu(NO_3)_2$ and 0.92 gl^{-1} Tergitol (a sodium alkyl sulphate). Another bath containing selected additives is described in UK patent 1,373,611 and contains $Pb(NO_3)_2$, Cu and Ni salts, free HNO_3, NaF and heptafluorobutanol. It is operated at 70^oC. using a two-stage deposition process.

1.4 Adhesion of electrodeposited β-PbO_2 onto a Ni foil substrate

The adhesion of -PbO_2 to Ni and its importance in relation to the lead acid primary battery has already been discussed (see Section 1.1), and interest in this subject arose from the fact that the adhesion of β-PbO_2 to certain batches of Ni was poor when compared to others having no significant differences in composition. Ramanathan and Shreir (192) have conducted a detailed study on the subject of the adhesion of β-PbO_2 to different batches of nickel foil and found that the adhesion to Ni270 foils was good, whereas that to Ni200 foil was poor. No clear reason for this phenomenum was found, but it was concluded that electrolytic etching of the nickel foil prior to electrodeposition of PbO_2 was an essential pre-requisite to obtain good adhesion and that certain differences in the etched surfaces of the two foils were evident. The samples of Ni270 etched in 4M H_2SO_4 at 50°C and a current density of 2.7A dm^{-2} were all faceted and etched in a random manner whereas the Ni200 samples all exhibited elongated pits and were covered by a thin brown film.

The thin brown film formed on the Ni200 samples was analysed and found to consist mainly of Cr_2O_3 and removal of this film subsequent to etching, actually increased the adhesion of β -PbO_2.

The electrochemical properties of various Ni samples in 4M H_2SO_4 at different temperatures were also investigated. The values of the rest potential were all essentially the same as were the values of i_{pp}. However, E_{pass} for Ni270 was found to be +0.55V vs SHE whilst for Ni200 a value of +0.62V vs (SHE) was recorded. The values of i_{pass} were recorded but no significant differences observed. The double layer capacitance for Ni270 at -0.16V was found to be 43μF cm^{-2} whilst that for Ni200 at the same potential was 37.7 μF cm^{-2} for samples etched at 2.5 Adm^{-2}, indicative of a higher etched surface area for Ni270.

However, the observation of Ramanatham and Shreir (192) that Ni270 foils exhibited "good" adhesion for electrodeposited PbO_2 whilst with Ni200 "bad" adhesion of PbO_2 was observed was not confirmed by more recent work (193,194) where the converse was observed. There is at present no apparent explanation for this variation in adhesion of PbO_2 to different samples of Ni foil.

1.4.1 The mechanism of adhesion

Adhesion can be defined as the summation of the intermolecular forces (ionic, covalent, polar or Van der Waals) between two different materials, the magnitude of which depends on the proximity of the materials and the nature of the interaction. In practice adhesion is measured in terms of force per unit area, i.e. the force required to separate or disrupt the interface between the two materials. The values obtained are often lower than the theoretical values, with failure occurring at flaws in the interface.

The maximum work (W) required to separate two surfaces is given by:

$$W = \gamma_1 + \gamma_2 - \gamma_1\gamma_2$$

where γ_1 is the surface energy of material 1

γ_2 is the surface energy of material 2

and $\gamma_1\gamma_2$ is the interfacial energy between the two materials.

In the case of two solid interfaces the forces of attraction between them will be atomic since the distance of separation is small and short range molecular forces may operate. Other theories have also been proposed to explain adhesion e.g. the diffusion theory of Voyutski (195) where mutual diffusion of the surface layers occurs which applies to polymeric systems or by electrostatic adhesion as suggested by Derjaguin (196).

The adhesion between two surfaces in contact is influenced by a number of factors.

1) The load at the interface which in the case of an electrodeposited film is simply the weight of the film.

2) An intrinsic compressive or tensile stress in the deposit.

3) The area of contact with a large area of intimate contact increasing the number of bonds and therefore the total force required to break them.

4) The presence of oxide films which may prevent intimate contact between two materials, has been shown to considerably reduce the level of adhesion (197).

1.4.2 Methods of adhesion measurement

A detailed account of the various methods used for adhesion testing on electrodeposited coatings has been given elsewhere and the interested reader is referred to these works (192, 198).

The measurement of the adhesion of electrodeposited β-PbO_2 to a nickel foil, is carried out by deforming both the subtrate and coating in a specially constructed jig, so that the tip of the deformed specimen can be examined visually to ensure the coating has not detached itself from the Ni substrate. This quantitative test is refered to as 'The Bending Adhesion Test' and the adhesion of the coating quantitatively assessed by the degree of detachment of the PbO_2 coating. The degree of adhesion of not only the PbO_2 but also the Pb coating is determined in the production of battery plate material.

Most of the tests used to assess adhesion are qualitative with any quantitative test used designed specifically for the particular system under investigation.

A detailed account of the experimental method to measure the adhesion of PbO_2 is given in Section (2.1.6).

1.5 Electrodeposition

Electrodeposition consists of two processes : (a) the path taken by an ion in solution to move up to and be incorporated in the lattices of the crystals constituting the electrode and (b) crystallisation, in which the individual atoms deposited link up to form crystals.

The whole process of electrocrystallisation is extremely complicated and only a brief outline of the fundamentals involved will be provided in this review.

1.5.1 Deposition

The process whereby a hydrated metal cation in the outer Helmholtz plane is reduced and becomes incorporated in the electrode lattice may be represented by the following equation :

$$M^{n+}_{(aq)} + ne \rightleftharpoons M$$

This is only a simplified picture, since deposition occurs via a number of different steps, one of which is slower than the others and thus determines the overall rate. This is referred to as the rate determining step (r.d.s.). First the hydrated metal ion has to receive one or more electrons to free itself from its hydration sheath before it can be incorporated into the metal lattice.

The level of free electron emmission from an electrode surface is very small, by virtue of the fact that this process has a high activation energy. The only possible explanation for the mechanism of charge transfer is by a process known as 'electron tunnelling'. If an electron in the metal has an energy equal to that of an empty level in the receptor ion, then quantum mechanics has shown that transfer of electrons can occur from the metal to receptor, to enable the release of the water molecules still co-ordinated (electron tunnelling). The driving force for this process is the increased stability offered by greater co-ordination with the metal atoms in the lattice. (199).

In cases such as nickel or copper deposition, where the overall reduction process involves a two-electron transfer, the two electrons are not transferred in a single step since calculations have shown (200) that the activation energy for this would be too high for the process to proceed at any reasonable rate. Therefore such metal deposition processes occur via two seperate steps. The electrodeposition of Pb^{2+} from a nitrate solution is also thought to occur via two one-electron steps (201).

$$Pb^{2+} + e \xrightarrow{r.d.s} Pb^{+}_{ads}$$

$$Pb^{+}_{sds} + e \longrightarrow Pb_{lattice}$$

Once an ion has transferred from the solution it may take up any position on the metal surface, the choice of position being determined by the energetics for the process, with some sites being more favourable than others.

The different types of sites available for deposition can be classified as (a) planar, (b) edge of a step, (c) kink site, (d) surface vacancy or (e) direct incorporation in a hole on the surface of the metal lattice.

The metal ion deposited onto the metal lattice does still retain some of its ionic character and is referred to as an adion, and these form surface dipoles with electrons in the conduction band of the metal and are stabilised by the residual hydration sheath. The number of water molecules in the hydration sheath is solely dependent upon the site occupied.

Bockris and Conway (200) have calculated the energy of activation for direct charge transfer to each site at the potential of zero charge for Ag^{+} and Cu^{2+} deposition, taking into account the distortion of the hydration sheath by certain sites and the gain in energy from increased co-ordination by the metal atoms in the substrate lattice. Their results clearly indicate that planar sites are the most energetically favourable for deposition. The energy difference is such that transfer to a planar site has a rate constant 10^{6} times greater than that at any other site and most deposition of 'adions' therefore occurs at these sites.

Before the adion can become incorporated it has to lose its hydration sheath. This is acheived by the diffusion of the adion along the surface from its planar site to a step site where it loses one water molecule, and increases its co-ordination number of metal atoms. The deposition process then continues by surface diffusion of the adion to a kink site where it loses yet another water molecule until after a series of these acts the adion has lost all its hydration sheath and has zero charge; it then becomes incorporated in the metal lattice.

The actual process of surface diffusion is not field-affected since the field at the interface is normal to the surface and the diffusion of adions occurs by a randon walk diffusion movement across the surface until collision with a step occurs.

The actual process of deposition therefore consists of a number of different stages: charge transfer, surface diffusion, tranfer from surface to edge of growth site, etc. Indeed at potentials near the reversible potential both surface diffusion or charge transfer may be the rate determining processes whilst at high cathodic overpotentials it is the charge transfer process which is rate-determining.

1.5.2 Electrocrystallisation

The process of charge transfer to form adions, subsequent surface diffusion to steps, diffusion along steps and then lattice incorporation is refered to as 'electrodeposition', which is sometimes abbreviated to 'deposition'. It is apparent that steps must occur at different sites before electrodeposition of the metal is observed visibly, and the cumulative effect of all these individual acts resulting in the growth of electrodeposits is termed "electrocrystallisation".

As a number of ions undergo the deposition process more and more adions join the step and the step begins to advance. The more adions incorporated in a step, the farther it advances until eventually a stage is reached where there is no step on the surface and the step disappears. However, steps are a necessary condition for deposition, since without steps the adion concentration on the plane builds up, the surface coverage of adions increases and the sites for deposition decrease until deposition should eventually stop. This, in fact, does not happen since the crystals are not perfect but contain dislocations i.e. regions of atom mismatch within the crystal. If a screw dislocation is present on the surface of a crystal, this acts as a self-perpetuating step, for as the adions add on to the edge, the step still remains but moves its position resulting in a spiral type growth.

The step described above is a microstep, since it is only atomic layers in height and cannot be seen by an optical microscope.

Apart from screw dislocations, two other sources of microsteps are possible, one resulting from two-dimensional nucleation and the other resulting from the misorientation in the cutting of the given crystal.

The microsteps discussed so far are of the order of one layer in height, and when they reach a size of several thousand A^{o} units they are then known as macrosteps.

The macrosteps themselves are formed by bunching of microsteps, for as the microsteps move across the surface they encounter imputity molecules and move at a slower rate, or even stop growth completely. On top of this first microstep, a second microstep moves as far as the first and is then blocked; this successive growth continues until 1,000 steps have formed on top of each other and a macrostep is formed.

The macrosteps may then grow upward or laterally, with the distance between the steps increasing as the deposit grows thicker. Correspondingly, the height of the steps increases with the total thickness of the deposit, i.e. when the whole deposit is increasing in thickness the height of one step over the one beneath it increases.

Each crystal may also contain only one screw dislocation which will act as a site from which a rotating microspiral can be produced. Since there are a large number of screw dislocations on a polycrystalline substrate, each step as it grows from a screw dislocation will eventually collide with another, providing the two screw dislocations are rotating in different directions. The merger of two screw dislocations results, not in their annihilation but in the production of a step running from the axis of one screw dislocation to the other from which further growth may then continue, with one half of the step spiralling left and the other right, forming a closed loop spiral. This results in the formation of a macrospiral.

Electrodeposits do not appear as smooth faced single crystals with the occasional macrospiral, and in practice display only certain crystallagraphic planes and exhibit examples of non-uniform growth such as dendrites.

Each growing crystal with a plane of exposed atoms is referred to as a facet. However, some facets grow faster than others, and the reason for this lies in the nature of the exposed facet. The number of underlying atoms in contact with the adion depends on the particular crystal plane, e.g. for an FCC crystal an adion sitting on the (111), (100) and (110) planes will have 3, 4 and 5 close atomic neighbours, and the strength of adion bond increases with the number of close neighbours, the stronger the bond the faster the charge transfer step.

The different deposition rates on different crystals means that the faster growing crystals tend to disappear whilst only the slower growing ones survive.

With a polycrystalline material, all the processes are the same as those described so far, for a single crystal; a polycrystalline material can be regarded as a number of single crystals with a small grain boundary area, and only at the grain boundary area will growth be different.

1.5.3 The nucleation and growth process in electrocrystallisation

The experimental investigation of the kinetics of metal electrocrystallisation has proved difficult, primarily because although the nature of a surface may be defined before measurement it will vary continuously once the current is applied. Transient techniques must be used, therefore, so that insufficient time is available for a significant change in the surface to occur. The surface itself should be free from dislocations to enable reproducible results to be obtained, and for this purpose mercury

is often used as the substrate on which to study the kinetics of the nucleation process, especially since the deposited metal is often completely soluble in the mercury so that no new phase is produced. The early theories on vapour deposition have been used as the basis for the explanation of electrochemical nucleation, since there are many similarities except that in the former the solvent is absent and the atoms are uncharged.

The mechanism of deposition where the lattice grows at step lines by adatoms diffusing along the surface has been outlined in the previous Section. The actual formation and growth of an electrodeposited phase is a complex process for which several models have been proposed. Indeed, Fleischman and Thirsk (210) have reviewed in some detail the different types of growth processes that are likely to occur when the depositing metal is the same as the substrate. However, in most plating operations the nucleation and growth processes occur initially on a foreign substrate.

Thirsk and Harrison (211) show that it is possible to describe the current time relationship at a given potential for the growth of discrete centres before the onset of overlap for different types of growth, whether it be one dimensional in the case of needles, two-dimensional as in the case of cylindrical forms or three-dimensional as in the case of hemi-spherical or spherical growth.

Palmisano (212) states that in the case of Pb deposition the r.d.s. in the growth process is Pb diffusion to the growth site and not the process of incorporating the Pb into the growth site.

Astley et al (214) have derived an expression for the diffusion controlled three-dimensional growth of a hemispherical nucleus, which is the growth process for Pb. In terms of linear diffusion, the current time relation for the growth of N_o nuclei formed instantaneously is given by:

$$I_{(t)} = \frac{8 N_o z F M c^3 D^{3/2} t^{1/2}}{\rho^2 \pi^{\frac{1}{2}}}$$

where $I_{(t)}$ = Current at time (t)

ρ = Density of deposit

D = Diffusion coefficient of electrodepositing species

M = Molecular weight

c = Concentration

and all other terms have their usual significance.

For progressive nucleation, i.e. nucleation occurring linearly with time, the corresponding expression is given as:

$$I_{(t)} = \frac{16 K_n N_o z F M^2 c^3 D^{3/2} t^{3/2}}{3\rho^2 \pi^{\frac{1}{2}}}$$

where K_n is the nucleation rate constant

Hills et al (215) consider it is more likely that diffusion will be hemispherical and that in this case the current for instantaneous nucleation is given as:

$$I_{(t)} = \frac{z F N_o (2Dc)^{3/2} M^{1/2} \pi t^{1/2}}{\rho^{\frac{1}{2}}}$$

and for progressive nucleation

$$I_{(t)} = \frac{4 \; F \; K_n \; N_o \; (Dc)^{3/2} \; M^{1/2} \; t^{3/2} \pi}{3\rho^{\frac{1}{2}}}$$

The difference between instantaneous and progressive nucleation is their time dependence, and this can be used to differentiate between the two processes.

1.5.4 Electrochemistry of Pb deposition

The kinetics of Pb deposition from $Pb(NO_3)_2$ solutions have been investigated in some detail by Chernenko (202). He used a coulostatic technique to measure i_o for Pb deposition at different Pb concentrations. This technique involves passing a current pulse and recording the resultant voltage versus time curve; the method of analysing these results has been outlined by Delahay (205), Reinmuth (206) and by Chernenko (207). Chernenko records a value of the exchange density of Pb deposition from a solution of 1 mole cm^{-3} $Pb(NO_3)_2$ as 1.12 Acm^{-2} at 25°C, and a value of β of 0.5, which was found to vary only slightly with temperature. Earlier determinations of i_o for Pb deposition from 0.05M $Pb(NO_3)_2$ + 1M KNO_3 report a value of 0.1 Acm^{-2} (204), but Strochkova (203) states that only the lower limit of i_o can be determined and for the above solution it exceeds 0.5 Acm^{-2}. The electrode capacitance (C) of Pb was also found to vary with Pb concentration, with a linear relationship existing between dlog C / dlog $[Pb^{2+}]$, the slope of which was 0.5. This phenomenom is attributed to an absorption capacitance and the increase with concentration is due to the increasing concentration of surface adions; a value of 4.17 $\mu F \; cm^{-2}$ at 1 mole cm^{-3} Pb^{2+} is quoted. Analysing the variation of C and i_o with temperature also allowed a determination of the energetic parameters for Pb deposition, and values of 7.4 kcal/g atom for adion formation and 3.6 kcal/g atom for the activation energy for surface diffusion are reported.

Other researchers have also studied the kinetics of Pb^{2+} deposition from NO_3^- solutions. Haruyama (216) obtained a value of 0.09 Acm^{-2} for i_o in 0.05M $Pb(NO_3)_2$ at room temperature, a value of β of 0.63 and a value for the enthalpy of charge transfer of 5 kJ $mole^{-1}$. Hampson and Larkin (217) used an impedance technique and a double potential pulse method for determining values of i_o and double layer capacitance at different Pb^{2+} concentrations and temperatures.

The value of i_o they determined varied depending on the technique used to obtain them; for example a value of i_o for 0.05M $Pb(NO_3)_2$ of 0.0468 Acm^{-2} was obtained from the measurement of the faradaic impedance, where as using the double-potential pulse technique the value was 0.064 Acm^{-2}. The value for the charge transfer coefficient β was found to be 0.8 and the enthalpy of charge transfer 12.6± 2 kJ $mole^{-1}$ which is considerably higher than the value of 5 kJ $mole^{-1}$ reported by Haruyama, a fact which is attributed to the higher reactivity of the Pb electrode used by Haruyama. The variation of electrode double layer capacitance, at the rest potential, with Pb^{+2} concentration was also reported and a value of 4.9 $\mu F\ cm^{-2}$ at 0.05 M $Pb(NO_3)_2$ is quoted. Hampson concluded from these results that the process of charge transfer is the r.d.s.

Similar studies for Pb deposition from $Pb(ClO_4)_2$ solutions have also been recorded. (215, 218) Miyashita (208) reports studies on Pb deposition from a $PbSiF_6$ solution containing 80 gl^{-1} free Pb and 80 gl^{-1} H_2SiF_6 in which the potential decay curve with time was analysed after application of a constant c.d to obtain i_o and the double layer capacitance. The effect of gelatin concentration on the double layer capacitance in this solution was investigated, with an increase in capacitance being observed with an increase in gelatin concentration, which reached a maximum at 2 Adm^{-2}. Typical values of capacitance at this c.d. were 250 $\mu F\ cm^{-2}$ at 0.5 gl^{-1} gelatin and 410 μFcm^{-2} at 1.5 gl^{-1}. The transfer coefficient was found to be 0.6 at 1 Adm^{-2} and it decreased with increasing c.d. with a value of i_o of 0.001 Acm^{-2} quoted.

Palmisano et al (212) have investigated the electrodeposition of Pb from $PbCl_2$ in 0.1M HCl on to a glassy carbon electrode by cyclic voltammetry and pulse potentiostatic techniques. The value of $Ep-Ep_{/2}$ was found to be dependent on sweep rate, but only linearly dependent on the logarithm of the sweep speed at low sweep rates and a linear relationship between peak potential and logarithm of Pb^{2+} concentration also observed. The slope of which is different to that predicted from theory for reversible metal deposition. They suggest therefore that the electrodeposition of Pb on vitreous carbon proceeds irreversibly. Values for the diffusion coefficient of Pb^{2+} at different concentrations were also obtained from plots of i_o versus $v^1/2$ (sweep rate) $^1/2$ and were found to decrease with increasing Pb^{2+} concentration. Typical values for D were 1.37 x 10^{-5} cm^2 sec^{-1} in 0.0005M Pb^{2+} and 6.1 x 10^{-6} cm^2 sec^{-1} in 0.00844M Pb^{2+}.

A linear relationship between i and $t^{1/2}$ at constant over potential was also found and values for the nucleation density of Pb quoted. The early stages of Pb deposition are reported to be due to instantaneous nucleation followed by hemispherical growth.

A critical review of Palmisano's work is however given by Hills et al (215). Hills states that the growth of small three-dimensional nuclei is best described in terms of hemi-spherical mass transfer rather than in terms of linear diffusion which Palmisano infers from a determination of the nucleation density. Hills supplements his criticisms still further by giving i vs t plots for Pb electrodeposited onto a Pt micro electrode from 0.008M $Pb(NO_3)_2$ and an explanation of Palmisano's work in relation to previous work (219, 220, 221).

The deposition of Pb onto Ag at a rotating disc electrode from 0.003M of $Pb(NO_3)_2$ in 1M KCl and from 0.05M $Pb(CH_3COO)_2$ in 1M $Na(CH_3COO)$ has been investigated by Harrison et al (222) using cyclic voltammetry.

A three dimensional nucleation and growth of Pb deposits under diffusion control was proposed and in addition, a relationship between potential and rotational speed on the number of growth sites was demonstrated.

The formation of an adsorbed mono layer of Pb on a foreign metal substrate prior to bulk deposition at potentials anodic to the reversible potential for electrodeposition has been reported for Pb on Au by Adzic (223) et al and on Ag by Schmidt and Wurtlich (224).

1.5.5 Morphology of Pb electrodeposits

Preliminary investigations into the growth of Pb deposits from 0.5M $Pb(ClO_4)_2$ in 0.5M $HClO_4$ have been carried out by Keen and Farr (225) in conjunction with their work on Cu electrodeposits,with Pb deposits showing ridge and platelet structures similar to those observed for copper electrodeposits.

A more detailed study on the deposition of Pb from $Pb(ClO_4)_2$ and $Pb(BF_4)_2$ solutions on Pb single crystals has been conducted by Bicelli (226), using the (100), (110) and (111) planes of single crystals and depositing at c.d.s between 0.5 and 5 A dm^{-2}. The Pb deposits on the (100) and (110) planes were all equiaxed and only on the (111) plane at a c.d.s. greater than 73 Adm^{-2} were deposits twinned with respect to the substrate observed. The deposits on this plane showing stepwise growth layers whose number increased with thickness, whilst on the (110) plane square base pyramidal deposits were noted.

Similar studies have been reported by Itoh (227) et al who deposited Pb onto single crystals from $Pb(CH_3COO)_2$ solutions. Deposition on the Cu(111) plane resulted in trigonal or hexagonal equiaxed deposits of Pb, but on the (001) plane two different types of deposit were observed with two types of paralell planes on the substrate surface Pb(001), Cu(001) and Pb(111) Cu(001).

The nucleation density increased with increasing overpotential, and nucleation was found to be easier on Cu (110) than on Cu(100) or Cu(111).

Wranglen (228) has investigated the production of Pb dendrites from various Pb plating solutions. He grew two main types of Pb dendrite, one flat and growing in a <110> direction and the other 3 dimensional and growing in a <100> direction, with the latter favoured by solution depletion.

Ogburn (229) later extended the work carried out by Wranglen by studying the production of Pb dendrites from 0.5M $Pb(CH_3COO)_2$ formed at rates varying from 0.001 to 1mm min^{-1}, corresponding to a c.d. at the tip of the dendrite of 1.8 to 1,800 Adm^{-2} respectively. The direction of dendritic growth was assumed to be parallel to the long axis of the dendrite. The structure of the dendrites was found to be essentially two crystals having a twist relationship about a common 111 pole which was normal to the flat surface. The direction of growth was either halfway between the <211> direction of one crystal and a neighbouring <211> direction of the second crystal or halfway between the <110> directions.

1.5.6 Effect of organic additives on the process of electrocrystallisation

It has been well known for some time that the addition of certain organic substances at very low concentrations to metal plating solutions may result in an improvement in the deposition characteristics of the solution or more important in the structure of the deposit (28).

Addition agents may reduce grain size, modify the deposits physical properties, suppress dendritic growth, reduce pitting, increase hardness and strength and give improved coverage, smoothness and brightness (230). Not all the effects of addition agents are beneficial, some may even be detrimental such as an increase in electrical resistivity and internal stress or a reduction in ductility.

The magnitude of the change brought about is dependent on the concentration and nature of the additive.

Addition agents may affect the morphology of deposits e.g. microscopic appearance of the surface, structural properties of deposits. These factors are all indicative of a modification in the steps of the electrocrystallisation process by addition agents.

The most likely explanation for the effectiveness of certain organic substances on this process, is adsorbtion on the electrode surface inhibiting the electrode process. A clear correlation has been established by Volk (231) between the adsorbtion of certain organic compounds, as measured by a decrease in the double layer capacitance and the modification of the electrode process. Most of the early work on the adsorption of organic substances was conducted on mercury electrodes which enabled both capacitance and surface tension measurements to be made simultaneously. However, measurements have also been conducted on solid electrode surfaces for which the surface coverage of certain organic substances with potential, has resulted in a parabolic relationship (232). The surface coverage of the organic compound reaches a maximum value at a certain potential and the parabolic shape of the curve results from competition between water and organic molecules for the surface sites. When the metal has a nett positive charge the water molecules have their oxygen atoms facing the electrode and when the electrode has a nett negative charge the orientation of the water molecules reverses. Therefore, maximum surface coverage of organic molecules will occur when the water molecules are least adsorbed, i.e. at the potential of zero charge. In practice however the adsorption maxima are shifted from the point of zero charge, because the strength of adsorption of each water molecule is not equal for both orientations of water. The extent to which any particular substance adsorbs is not only dependent on potential but also on the free energy of adsorption of the organic material on a water free surface.

The difference in adsorbance between different substances may vary by up to 10,000 times, so in theory it should be possible to select a compound that would adsorb at any potential (199).

A survey of the current theory relating to the effect of the adsorption of organic substances on electrochemical reaction kinetics is given by Damaskin (233). He discusses the blocking of surface sites by organic substances, their modification of the potential distribution in the double layer and the effect of this on the discharge process and also the mechanism of electrochemical reactions at surfaces where the surface coverage of adsorbate is high. Vijh and Randal (234) have also investigated electrochemical reduction processes at high surface coverage of the electrode and the influence of pH on the electrochemical reduction of Cd^{2+} in the presence of certain addition agents, showing that as the pH increases, the degree of inhibition also increases.

The adsorption of different organic substances from solution is found to be dependent on the surface charge on the electrode surface. The addition agent may even form a chemical bond to the metal surface by electron transfer, the strength of which will be dependent on the functional group of the additive. Electron transfer is particularly favoured in the presence of loosely bonded electrons, e.g. d electron systems or from atoms with lone pair electrons. The actual mechanism for addition agent action is therefore extremely complex and no simple mechanism can be proposed. One of the most detailed accounts of the possible mode of operation of addition agents is given by Bockris and Razumney (199). They show that addition agents modify the free energy for elementary charge transfer steps, and hence effect the rate constant i_o and reduce the area overwhich the charge transfer reaction can occur. The mean free path of lateral diffusion of adions will therefore be shortened, which would be equivalent to a decrease in the diffusion coefficient of adions.

This can result in (a) an increase in surface diffusion control and (b) an increase in adion concentration to such a point that the rate of two dimensional nucleation becomes appreciable.This results in a decrease in surface diffusion control due to a reduction in the distance between growth steps. This increased frequency of nucleation leads to a reduction in grain size.

Preferential adsorption of additives may also occur at certain growth steps, which would explain the dependence of growth form on the addition of even small amounts of impurities. Furthermore uneven surface coverage of the substrate by the adsorbtate may occur, and regions of high current density would exist were the additive concentration is low.

For the production of bright electrodeposits, by the use of selected additives in the plating solution, the surface produced must be smooth so that the magnitude of the irregularities is less than the wavelength of the reflected light being used. This is achieved because the more active facets constitute preferred sites for adsorbtion, and if the adsorbed substance inhibits deposition this would lead to an equalisation of the growth rates at different points on the surface, the absence of faceting and the elimination of microroughness, all of which result in bright deposits.

It is often practice to use combinations of additives to obtain the desired deposit properties, and the overall results cannot be predicted from the known effects of each additive individually. The coating of the cathode by the additives or their breakdown products depends on the deposition conditions, electrolyte composition and nature of the deposited metal and the optimisation of each system has to be carried out empirically.

In the presence of a depositing metal film the organic additive may be incorporated into the film. e.g. benzotriazole in Cu (235) or coumarin and thiourea in Ni deposits (236) under these conditions equilibrium coverage of the electrode by the organic additive can no longer be maintained. In these non equilibrium conditions the effectiveness of an addition agent will also be determined by the competition between its rate of incorporation into the metal film and the diffusion of the additive to the electrode surface, though this diffusion control is only apparent at very low additive concentrations.

1.6 Electrochemistry of nickel

Nickel dissolution has been studied by a number of workers in both acid and alkaline solutions using potentiostatic, potentiodynamic and galvanostatic techniques (237).

Indeed most studies have been concentrated in acid solutions, primarily dilute sulphuric acid because of the weak absorption tendency of the SO_4^{2-} ion, although other solutions have been investigated.

The most widely used technique to investigate Ni dissolution is anodic polarisation with a typical anodic polarisation curve resulting in three different regions (see Fig. 2).

1. An active region AB characterised by a steady state potential E, and a linear Tafel line AB.

2. An active / passive transition BC defined by the co-ordinates of the principle peak (E_{pp} or E_{crit} and i_{pp} or i_{crit})

3. A passive region starting at C and characterised by the passive potential E_{pass} and i_{pass} (the rate of dissolution of the passive metal).

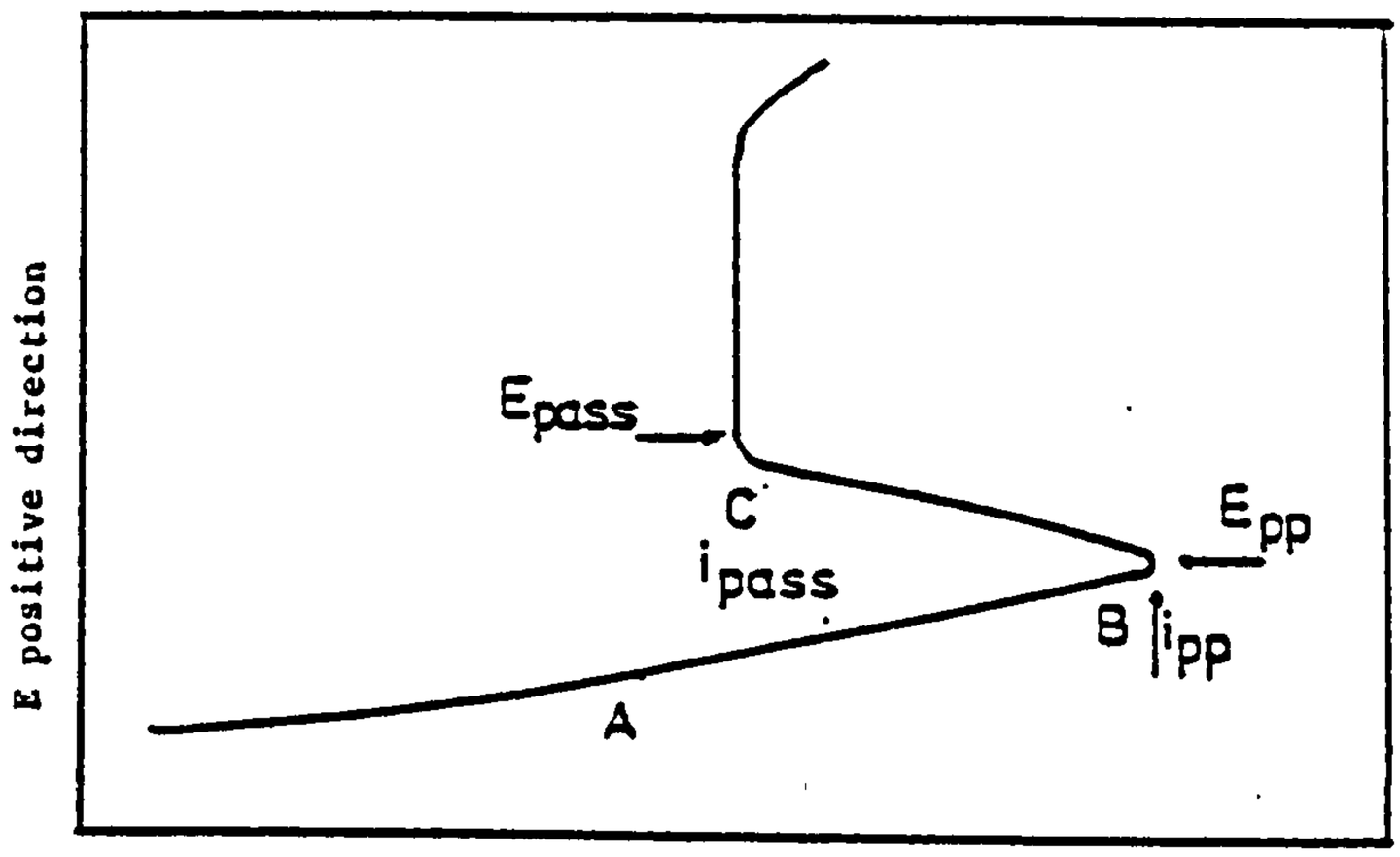

log i

Typical anodic potentiostatic curve for an active-passive metal.

FIGURE 2

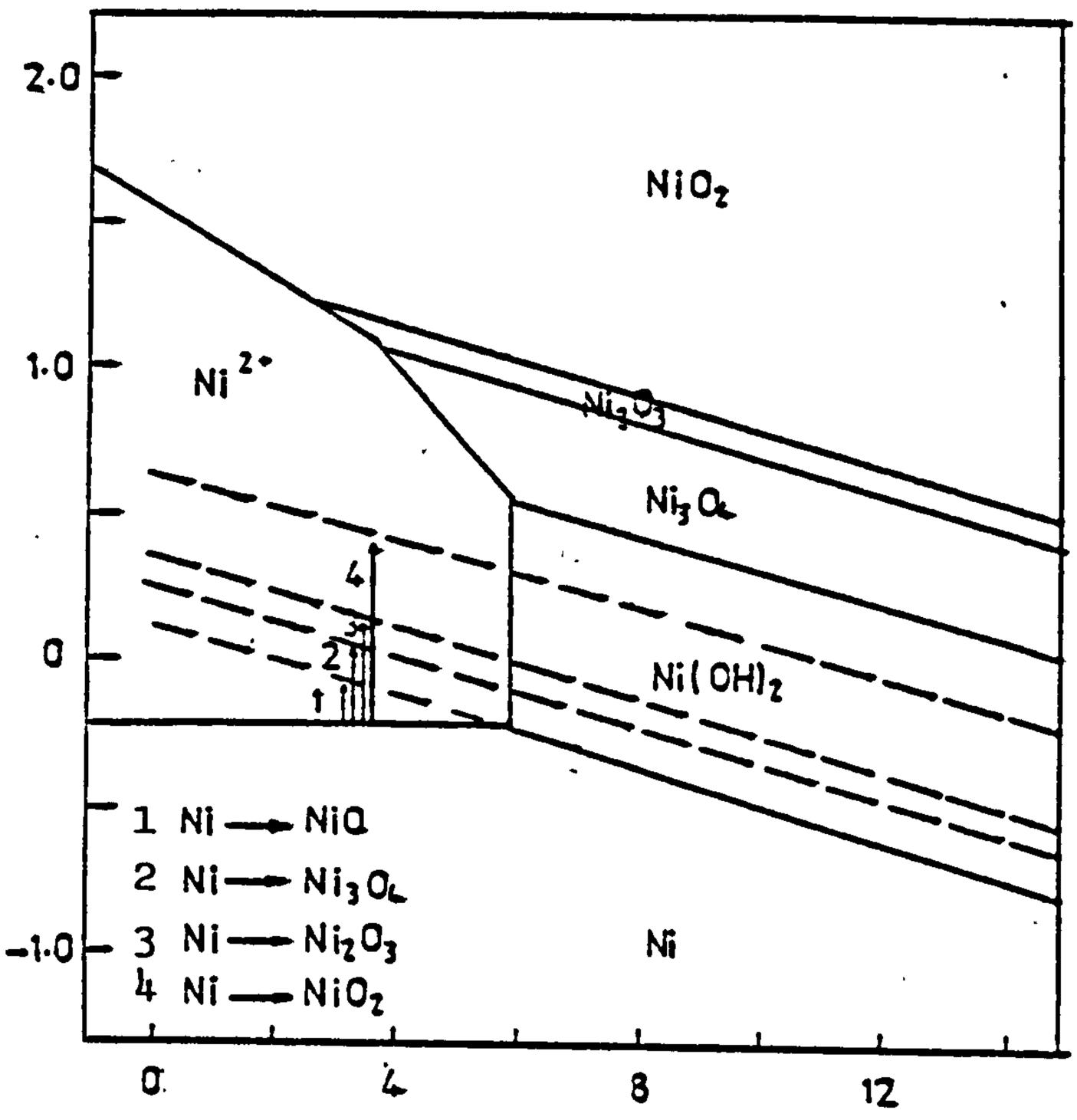

Modified potential versus pH diagram for the $Ni-H_2O$ system.

FIGURE 3

1.6.1 Active dissolution of Ni

The mechanism of nickel dissolution results in the entry of Ni^{2+} ions into an aqueous solution and is often represented by the equation.

$$Ni \rightleftharpoons Ni^{2+} + 2e$$

The reaction mechanism given above would indicate that nickel dissolution is independent of pH, however a number of workers have demonstrated that this is not the case.

Sato and Okamato (238) in their studies of nickel dissolution in 0.5M SO_4^{2-} solutions, of pH varying between 0 and 3 observed a Tafel slope of 0.030 volt per decade at 45°C and a variation of rest potential (E_r) with pH of (dE_r/dpH) = 0.105 volts. Increase in pH resulted in a shift of the anodic polarisation curve in a less noble direction and a decrease in the dissolution rate at a given potential, with a value of $(d\ln i/dpH)E = 1$, at a constant potential. From the results of their studies Sato and Okamato proposed the following mechanism for Ni dissolution.

$$NiOH^- \longrightarrow OH_{ad} + e \qquad (a)$$

$$NiOH_{ad} \longrightarrow NiOH^+ + e \qquad (b)$$

$$NiOH^+ \longrightarrow Ni^{2+} + OH^- \qquad (c)$$

With the rate determining step changing from a) to c) as the $NiOH^+$ concentration increases in the vicinity of the electrode surface.

Heusler and Gaisler (239) investigated the anodic dissolution of spectroscopically pure Ni in both 1M $NaClO_4$ and 1M $Ba(ClO_4)_2$ solutions and on the basis of their results also proposed a dissolution mechanism involving OH^-, as follows :

$$Ni\ [Ni(OH)_{ad},\ Ni(OHNi)_{ad}] + OH^- \longrightarrow NiOH^+ + \text{catalyst} + 2e \qquad a)$$

$$NiOH^+ + H^+ \longrightarrow Ni^{2+}_{aq} + H_2O \qquad b)$$

Reaction a) is split into the following steps:

$$Ni + H_2O \longrightarrow Ni(OH)_{ad} + H^+ + e \qquad 1)$$

$$Ni + Ni^{2+}_{aq} + e \longrightarrow Ni(OHNi)_{ad} + H^+ \qquad 2)$$

$$Ni\ (OH)_{ad} + Ni^{2+}_{aq} + 2e \longrightarrow Ni(OHNi)_{ad} \qquad 3)$$

The surface complexes formed are refered to as 'catalyst' and reaction 3) is assumed to be the rate determining step, with the overall rate of reaction given by :

$$i = 2Fk_3 a_{Ni(OHNi)ad}\ a^-_{OH}\ \exp - [z\alpha F_\eta /RT] \qquad a)$$

The observed Tafel slope obtained from the stationary E vs i curve was found to be 0.037 ± 0.004 volts per decade compared to the calculated value of 0.0276 volts and the reaction order with respect to OH^- determined as 1.75 ± 0.03.

Piatti, Arvia and Podesta (240, 241) investigated nickel dissolution in 2M NaCl and 2M $NaClO_4$ solutions at a variety of temperatures and Ni^{2+} activities. A Tafel slope of 0.060 volts per decade was obtained and values of i_o for Ni dissolution found to be between 10^{-8} and 10^{-10} A cm^{-2} and pH dependent. The value of H for nickel dissolution was found to be dependent on the solution, in Cl^- solutions a value of 13 ± 3 kcal $mole^{-1}$ was obtained, whilst for ClO^-_4 solutions the value was 18 ± 3 kcal $mole^{-1}$.

The values of E_{rest} were found to be dependent on pH and the nature of the anion but independent of Ni^{2+} concentration. A reaction mechanism for Ni dissolution similar to that of Sato and Okamato (238) was proposed involving both OH^- and an NiOH intermediate:

$$Ni + H_2O \longrightarrow NiOH_{ad} + H^+ + e \qquad a)$$

$$(NiOH)_{ad} \xrightarrow{rds} NiOH^+ + e \qquad b)$$

$$NiOH^+ \longrightarrow Ni^{2+} + OH^- \qquad c)$$

and

$$NI + OH^- \xrightarrow{rds} (NiOH)_{ads} + 2e \qquad d)$$

$$(NiOH)_{ads} \longrightarrow Ni^{2+} + OH^- \qquad e)$$

Reactions a) to c) explain most of the experimental results obtained particularly at low pH, however the anodic slope is lower than would be predicted for a simple electron transfer process and coincides with the one predicted by reactions d) and e).

However, if the reaction takes place on a surface covered by an oxide film a Tafel slope larger than 2 RT/3F may be recorded and reactions a) to c) are favoured over reactions d) and e).

Schwabe and Voigt (242) in their studies on Ni dissolution found no straight Tafel line but that the reaction rate was pH dependent, and a reaction order of 0.5 to 0.6 reported.

More recent work by Burstein and Wright (243) has been undertaken to study the dissolution of Ni in both CH_3COO^- and ClO_4^- electrolytes. A mechanism involving a NiOH intermediate was proposed and the reaction order with respect to OH^- found to be 0.2 ± 0.1.

$$Ni + H_2O \longrightarrow NiOH_{ads} + H^+ + e \qquad 1$$

$$NiOH_{ads} \longrightarrow NiOH^+ + e \qquad 2$$

$$NiOH^+ + H^+ \longrightarrow Ni^{2+} + H_2O \qquad 3$$

The reproducibility of results obtained was found to be better at high sweep rates, with no linear Tafel region observed at slow sweep rates, a phenomenom which Burstein and Wright attributed to the presence of a pre-passive film. The kinetics of dissolution were complicated by dissolution through this solid film intermediate.

Other workers have reported that the dissolution of Ni is pH independent, Kronberg et al (244) observed Tafel slopes of 0.110 to 0.120 volts per decade for Ni dissolution in ClO_4^- and SO_4^{2-} with the reaction rate independent of pH. Whilst Ovari and Rotingan (245) in their studies on the dissolution of electrodeposited Ni over the pH range 0.75 to 3.0 in $NiCl_2$ solutions also found the rate of dissolution independent of pH and proposed the following reaction mechanism.

$$Ni \longrightarrow Ni^+ + e$$

$$Ni^+ \xrightarrow{r.d.s.} Ni^{2+} + e$$

Nevertheless it is generally accepted that the anodic dissolution of Ni is pH dependent and does proceed via an NiOH intermediate.

The temperature dependence of Ni dissolution in $NiSO_4$ and $NiCl_2$ has been investigated by Vagramyan et al (260-264) over a range of temperatures from 25 to 75°C.

A Tafel slope of 0.095 volts per decade and value of i_o of 3.5 x 10^{-6}, A cm^{-2} were recorded.

1.6.1.2 The effect of different anions on Ni dissolution

The mechanism and rate of Ni dissolution is not only governed by pH and temperature but also the presence of other anions.

CH_3COO^- (246, 247) and other ions have been found to hinder Ni dissolution where as SO_4^{2-} and Cl^- accelerate it.

Kolotyrkin (248) in his studies on the anodic dissolution of Fe showed that it was not only pH dependent but also on the activity of SO_4^{2-} with OH^- ions being displaced by SO_4^{2-} and he proposed the following mechanism:

$$M + H_2O \longrightarrow M\,OH^-_{ads} + H^+ \qquad a)$$

$$MOH^-_{ads} \longrightarrow MOH_{ads} + e \qquad b)$$

$$MOH_{ads} + HSO_4^- \longrightarrow MSO_4 + H_2O + e \qquad c)$$

$$MOH_{ads} + SO_4^{2-} \longrightarrow MSO_4 + OH^- + e \qquad d)$$

$$MSO_4 \longrightarrow M^{2+} + SO_4^{2-} \qquad e)$$

Reactions d) and e) are the rate determining steps and Cl^- ions because of their ease of penetration are thought to act as follows:

$$M + Cl^-_{ads} + OH \longrightarrow MOH^+ + Cl^-_{aq} + 2e$$

Other ions notably S^{2-} effect Ni dissolution with various theories proposed to explain this observation. The most commonly accepted is that the S^{2-} ion strongly absorbs on the Ni surface and reduces the bond energy between Ni atoms and thus promotes dissolution or that a process involving HS^- adsorbtion leading to the formation of a MHS^+ intermediate which is then hydrolysed by water occurs.

Feller, Kesten and Ratzer-Scheibe (250) investigated the effect of the addition of halide ions to 0.5M H_2SO_4, with F^- having little effect on the E vs i characteristics, the effect increasing in the order $Cl^- > Br^- > I^-$, (the order of surface absorbtion) with I^- the most strongly absorbed.

F^- ions have little effect on the active dissolution region, but have an effect on i_{pass}. In contrast, the addition to a 0.5M H_2SO_4 solution of 0.0001M I^- was seen to shift the dissolution potential to +0.350V where as in pure H_2SO_4 the Ni electrode is already passive at this potential.

The halide ions absorbed on the metal surface inhibit the dissolution of Ni which is only overcome at more noble potentials. Kolotyikin (248) proposed that Ni dissolves into solution as a charged halide complex.

$$Ni + mX^- \longrightarrow NiXm^{+(m-n)} + ne$$

Whilst Feller, Kesten and Ratzer Scheibe (250) put forward the following mechanism for halide absorbtion at the Ni interface

$$\underset{a}{Ni + X^-_{ads}} \longrightarrow \underset{b}{Ni\ (-)\ X} \longrightarrow \underset{c}{Ni - X + e}$$

With only some areas of the nickel interface covered by the specifically absorbed intermediate Ni(-)X.

Feller, Kesten and Krupski (251) studied the influence of SO_4^{2-} ions on the dissolution of Ni. They observed two peaks in the dissolution of Ni one at +0.150V and the other at +0.300V with the absorbed sulphate ions participating in the metal dissolution process, in the course of which the SO_4^{2-} ions are reduced to HS^- ions. These latter ions remain on the surface and catalyse Ni dissolution by the reaction mechanism given below:

$$Ni + SH^- \longrightarrow NiSH_{ads} + e$$
$$NiSH_{ads} \longrightarrow NiSH^+ + e$$
$$NiSH^+ \longrightarrow Ni^{2+} + SH^-$$

Zamin and Ives (252) have studied the effect of an increase in Cl concentration on the anodic dissolution of Ni using both electrochemical and metallographic techniques. An increase in

Cl^- concentration was found to effect the active to passive transition. A high Cl^- concentration also resulted in a change over from pitting to general corrosion with attack in low concentration solutions, being concentrated at grain boundaries, then spreading to the grain interior in high Cl^- solutions.

Burstein and Wright (243) showed that the addition of F^- to CH_3COO^- solutions had no effect on the Tafel slope recorded and a plot of log i against log $[F^-]$ at constant potential yielded a slope of dlog i/ d log [F] of 0.1. The fact that linear Tafel slopes were observed at low sweep rates, Burstein and Wright attributed to the fact that F^- inhibits the growth of the pre-passive film whilst not participating directly in the dissolution reaction.

Sury (253) also found i_{pp} and i_{pass} increased with Cl^- concentration and that S^{2-} ions have a considerable influence on the kinetics for Ni dissolution.

1.6.1.3 Ni dissolution in nitric acid

Electrochemical studies on Ni dissolution in HNO_3 have been conducted by Touscek (254) who carried out similar work on Ni dissolution in H_2SO_4 and H_3PO_4.

More recent work by Lisac and Karsulin (249) has been carried out on nickel dissolution in high concentration HNO_3 solutions. The rest potential of nickel was determined at different HNO_3 concentrations over the range 1 to 14.6M. Nickel was found to remain active at concentrations below 10M and to passivate at concentrations in excess of this.

Saturation of an 8M HNO_3 solution with $Ni(NO_3)_2\ 6H_2O$ was found to decrease the corrosion rate of Ni when compared to the unsaturated solution and also affect the nature of the anodic polarisation curve obtained.

Tousek found both E_{pp} and i_{pp} increased with increase in HNO_3, concentration with values of 0.44V and 5 Adm^{-2} respectively for Ni in 1M HNO_3 at a sweep rate of 0.017 V sec^{-1}. The E vs log i curves for HNO_3 and H_3PO_4 where found to be similar, only one i_{pp} was observed the value of which decreased with repeated cycling. In H_2SO_4 Tousek observed two current maxima one at +0.200V and the other at +0.385V. These values he attributed to the formation of NiO and Ni_3O_4 respectively.

The addition of K_2SO_4 in small concentrations to HNO_3 on the dissolution of Ni was also studied with SO_4^{2-} moving the value of E_{pass} in a less positive direction, and decreasing the value of i_{pp}. However, Tousek's results on the effect of Cl^- ions on Ni dissolution in 1M HNO_3 are not clearly defined with the only observable difference on the addition of Cl^-, namely being the increase in the value of i_{pass} in the region of secondary passivity.

1.6.1.4 Effect of impurities and mechanical treatment on Ni dissolution

Hoar (255) in his early work on the dissolution of Ni in $NiSO_4$ solutions at various Ni^{2+} concentrations and temperatures, found the Tafel slope for Ni dissolution to be 0.059 volts per decade at 25°C and that the Ni^{2+} concentration had no effect on the rate of dissolution. The value of i_o density for Ni dissolution was also measured over a range of temperatures, which enabled a value of H for Ni dissolution of 10.6 kcal $mole^{-1}$ to be determined. Subjecting annealed Ni to 20% cold work, Hoar observed that the current density at any given potential increased by 10 times, yet the value of H remained the same.

Hoar deduced that 10^8 atoms cm^{-2} provide active sites for metal dissolution in cold worked material, compared to 10^7 atoms cm^{-2} for annealed material.

The effect of structure and heat treatment of Ni on its polarisation characteristics in H_2SO_4 were also investigated by Di Barr and Petrocelli (256) who concluded that additive content had a greater effect on reactivity than structure.

The principal effect of cold work was on the active to passive transition, although in the samples of Ni200 studied, extensive pitting was only observed in the cold rolled samples.

Minor changes in the degree of purity also affected the overall reactivity of Ni with small amounts giving an increased tendency for pit formation. The effect of additives on i_{pp} was used to study the order of reactiveness which was found to be S Se Te P C Si. The values of i_{pp} recorded for Ni dissolution in 1M $NiSO_4$, pH 2.0 for alloys containing the maximum impurity level of individual elements were given as:

P	increased i_{pass}	from 0.06 Adm^{-2}	to	0.05 Adm^{-2}
Se	increased i_{pass}	from 0.06 Adm^{-2}	to	0.5 Adm^{-2}
Te	increased i_{pass}	from 0.06 Adm^{-2}	to	1 Adm^{-2}
S	increased i_{pass}	from 0.06 Adm^{-2}	to	5 Adm^{-2}

Cathodic pre-treatment afforded to samples of Ni prior to polarisation studies has also been found to effect the E vs i curves obtained. MacDougall and Cohen (257) observed that the magnitude of i_{pp} was affected by cathodic pre-treatment i.e. making the specimen the cathode at a set potential/current prior to polarisation. The longer the cathodic pre-treatment, the greater the value of i_{pp} observed and the potential range over which dissolution occured. This they attributed to reduction of NiO at the electrode surface. Burstein and Wright (243) also reported a similar effect in their work on Ni dissolution in ClO_4^- solutions whilst Worch (259) also reported that pre-treatment of Ni affected the rate of dissolution of single crystals of Ni in $NiCl_2$

1.6.1.5 The effect of crystal structure on Ni dissolution

Saburo et al (258) observed that Ni with a (211) orientation is more reactive than the (110) or (210) planes with values of i_{pp} for Ni dissolution in 5% H_2SO_4 at a sweep rate of 0.125 V min^{-1} of 0.19, 0.14 and 0.12 Adm^{-2} respectively.

Worch (259) also noted that chemically polished single crystals dissolved at different rates, depending upon orientation with the plane with the greatest atomic density (111) found to dissolve at a faster rate than the (110) and (100) planes which dissolved at identical, yet slower rates.

Latanision and Staehle (265) have however shown that Ni polarisation in 0.5M H_2SO_4 was essentially insensitive to crystal orientation.

1.6.2 Nickel passivity

Passivity can be defined as the reduction in the reactivity of Ni by the formation of a protective film on the electrode surface and has been extensively and systematically studied in the past (237, 266).

The thermodynamics of Ni corrosion and passivity have been summarised by Pourbaix (166) in the form of a potential pH diagram for the Ni - H_2O system. However, studies have indicated that not only can the hydroxides and oxides exist in a stable state but also in a meta-stable state formed from the metal in acid solutions. The resulting modified potential vs pH diagram is shown in Fig.3 and shows the four oxides that may be formed either directly from the metal or indirectly from each other, depending upon pH and potential. The diagram only demonstrating the thermodynamically stable states but does not give the rate of reaction, or the effect of other anions on passivity.

Passivity is exhibited when the potential of the Ni is made more positive until a certain potential is reached at which point the process of active Ni dissolution is inhibited to such an extent that the current drops sharply, as exemplified by region BC of a typical E vs log i curve for Ni (see Fig.2). The potential at which the current falls sharply is refered to as E_{pp} (E primary passivation or E critical (E_{crit})) and the current at this potential i_{pp} or i_{crit} whilst the potential at which the passivation current ($i_{passive}$)is also a minimum is refered to as E passive (E_{pass}) or the Flade potential (E_f) which for Ni in the pH range 0 to 3 is given by :

$$E_f = E_f^o - 0.059pH \qquad \text{at } 25^oC$$

Where E_f^o - is the Flade potential at pH 0, (0.355V vs SHE).

The passive layer formed was attributed to the formation of NiO with film thickness of up to $40A^o$ measured, the film thickness increasing at more anodic potentials.

Raub and Disam (267) have obtained various values for E_f from studies of the anodic polarisation of Ni in 0.05M H_2SO_4, that fell into 3 distinct groups - 0.11V, 0.30 to 0.60V and 0.41 to 0.67V. These results were similar to the work of Greene (268) who also reported three different Flade potentials at 0.14V, 0.24V and 0.42V for Ni in 0.5M H_2SO_4.

Other workers have observed different Flade potentials, Sato and Okamato (269) reported two distinct potential arrests in the passivation of Ni in 0.5M H_2SO_4. The first at 0.15V and noted that some corrosion still occurs even at a high anodic potential of 1.35V.

DeGromoboy and Shreir (272) in their investigations on the behaviour of spectroscopically pure Ni in acetic acid and sulphate buffers at varous pHs observed four distinct Flade potentials which they attributed as corresponding to an

Ni_xO_y/N_1 reversible potential. The four different oxides not necessarily NiO or $Ni(OH)_2$ formed on the surface by direct metal oxidation and passivation. The most frequently observed value of E_f^o is +0.36V probably a Ni_3O_4/Ni system and is similar to the value of 0.30V recorded by Hug, Rosenberg and Markides (271) who also attributed passivation to the formation of a Ni_3O_4 and NiO oxide.

Osterwald and Uhlig (270) in their studies on the anodic polarisation of Ni and Ni-Cu alloys in 1M H_2SO_4 also observed a pH dependence of both E_{pp} and i_{pp}:

With an increase in the copper content, increasing the values of both i_{pp} and i_{pass}.

The value of E_{pp} of 0.12V was in close correlation with the thermodynamic formation potential calculated from values of G of +0.108V for the formation of NiO

$$Ni + H_2O \longrightarrow NiO + 2H^+ + 2e$$

Ratzer - Scheibe and Feller (273) in their investigations on Ni passivity observed a number of potential arrests in the E vs log i curve for Ni, some of which were pH dependent and attributed to the formation of different nickel oxides. The values of the potential arrests quoted were:

$$E_p = 0.120 - 0.057\ pH$$

For the reaction: $Ni + H_2O \longrightarrow NiO + 2H^+ + 2e$

$$E_p = 0.366 - 0.066\ pH$$

For the reaction: $3Ni + 4H_2O \longrightarrow Ni_3O_4 + 8H^+ + 8e$

$$E_p = 0.422 - 0.066\ pH$$

For the reaction: $2Ni + 3H_2O \longrightarrow Ni_2O_3 + 6H^+ + 6e$

Schwabe and Dietz (274) have studied the passivity of Ni in weak acid solutions and found that the passivation potential was independent of Ni^{2+} concentration but dependent on pH and that the potential pH diagram exhibited a slope that was dependent upon the nature of the anion.

The work on the determination of E_f is confusing, with a general agreement on the pH dependence of E_f but disagreement on the actual values and their significance.

The pH dependence of passive Ni corrosion has been studied by a number of workers (275, 276, 277, 278, 279).

Sato and Okamato (277) considered the passive film formation was due to the formation of Ni_3O_4 as represented by the following mechanism:

$$Ni + OH^- \longrightarrow NiOH^+ + e$$
$$3NiOH^+ + OH^- \longrightarrow Ni_3O_4 + 4H^+ + 2e$$

Although three distinct potential arrests were recorded, all were attributed to the formation of the different oxides NiO/Ni, Ni_3O_4/Ni and Ni_2O_3/Ni_3O_4.

The rate of Ni dissolution in the passive potential region was also quoted as being independent of potential but dependent on pH.

$$\log i = K - 0.46 \quad \text{where } K = 0.19 \text{ A dm}^{-2} \text{ at } 25^{\circ}C$$
$$K = 1.09 \text{ A dm}^{-2} \text{ at } 40^{\circ}C$$

The dissolution of the oxide film proceeding by the following mechanism:

$$Ni^{2+}_{(oxide)} + OH^{-} \longrightarrow NiOH^{+} \qquad (a)$$

$$NiOH^{+}_{(s)} \xrightarrow{r.d.s} NiOH^{+}_{(aq)} \qquad (b)$$

$$NiOH^{+}_{(aq)} \longrightarrow Ni^{2+}_{(aq)} + OH^{-} \qquad (c)$$

The rate of dissolution of the transpassive film Sato and Okamato regarded as the sum of the dissolution current of the passive film i and the dissolution current through active patches in the passive film i_B. The value of the Tafel slope for Ni dissolution in the passive region was found to be 0.120 volts per decade similar to the values of 0.140 volts per decade recorded by Vetter (276). The values of i_B observed at a critical potential (E_{cp}) reach a maximum value that increases with pH where as the value of E_{cp} decreased with pH, E_{cp} = 1.68 - 0.08pH.

Ammar and Darwish (278, 281, 282) in their studies on Ni passivity in 0.5M H_2SO_4 over the potential range of 0.76V to 2.0V observed a potential maxima at + 1.72V and suggested the formation of a pore free passivating oxide which undergoes oxidation from NiO to NiO_2 at high potentials, with no effect on the E vs i curve observed on addition of KNO_3.

The transpassive dissolution of nickel is characterised by a current maximum i_m followed by a current minimum indicating secondary passivity. Petit (283) studied the influence of temperature and pH on both i_m and E_m under potentiostatic control and like Okamato and Sato observed these to be dependent on pH and also the rate of polarisation.

The temperature effect on the dissolution of the passive film has been studied Ishikawa and Okamato (284) who measured an increase in current density with temperature at a fixed potential of +0.6V and recorded an activation energy of

21.2 kcal mole^{-1} for Ni dissolution at this potential. The temperature dependence of the active to passive transition on the kinetic behaviour of Ni in K_2SO_4 over a wide range of pHs has been investigated by Cowan and Stahle (285) who found the active to passive transition absent above 100°C.

Ebersbach, Schwabe and Koenig (287) in subsequent work studied the current time curves for a rotating Ni disk electrode in 0.5M H_2SO_4 and 1M $HClO_4$. They found no dependence of stirring on the rate of passivation and that at a constant potential the current fell exponentially with time in the passive region, with the slope of d log i/dt increasing exponentially with potential in the passive region.

Ebersbach, Schwabe and Ritter (288) have also investigated the kinetics of Ni passivation at various concentrations and temperature.

The kinetics of passivation they regarded as competition between anodic oxide formation with water and reactions that remove the oxide, with the following reaction scheme for passivation suggested :

$$Ni + H_2O \longrightarrow NiOH + H^+ + e \qquad (a)$$

$$NiOH + H_2O \longrightarrow Ni(OH)_2 + H^+ + e \qquad (b)$$

$$Ni(OH)_2 \longrightarrow NiO + H_2O \qquad (c)$$

and for breakdown of the passive film

$$NiO + 2H^+ \longrightarrow Ni^{2+} + H_2O \qquad (d)$$

$$NiO + H_2O + 2A^- \longrightarrow NiA_2 + 2OH^- \qquad (e)$$

where A^- is a solution anion.

Bockris, Reddy and Rao (289) have conducted elipsometric investigation on Ni passivity at 20°C in 0.01M H_2SO_4.

They reported that Ni is film free in the potential range -0.250 to -0.025V and that anodic metal dissolution without film formation occurs whilst between -0.025 to 0.00V elipsometric evidence of film formation was obtained, although the onset of film formation was not accompanied by any decrease in the dissolution current. The Ni dissolves as a soluble intermediate $NiOH^+$ which accumulates near the electrode surface until a $Ni(OH)_2$ precipate forms. The potential at which this forms is +0.048V. The passivity process associated with the formation of a semi-conducting passive film from the oxidation of $Ni(OH)_2$ to an oxide of composition $NiO_{1.5-1.7}$, the final thickness determined elipsometrically as 45A°. The conversion of $Ni(OH)_2$ to non stoichiometric oxides has been studied earlier by Wynne Jones and Briggs (290) using X-ray diffraction techniques. They also concluded that the composition of the final product was $NiO_{1.7}$.

The nature of the oxide film formed on Ni by polarisation in near neutral pH solutions has been studied by Okuyama and Haruyama (295), who concluded that dissolution of Ni stopped when a continuous film of NiO_2 was formed at high anodic potentials but that at intermediate potentials a mixed oxide of NiO and Ni_3O_4 is formed, the steady state film thickness of which is 12A°. Similar galvonostatic work but in Na_2SO_4 solutions over the pH ranges 2 to 8 have also been carried out by MacDougall (297) who concentrated his work on the growth of the anodic NiO film, whilst more recent work on Ni passivation in near neutral borate solutions has been conducted by Gassa et al (300).

The breakdown of the passive film on Ni by F^- has also been studied by Lochel et al (299) in 1M $HClO_4$ and weak alkaline buffers. They concluded that the passive film is thinned by the action of F^-. This results in a higher electrical field strength across the oxide film and hence an increased corrosion current density.

With the transfer of nickel ions to the electrolyte catalysed by the formation of a fluoride complex.

Lochel et al (299) have also conducted work to identify the nature of the passive film formed in F^- containing solutions.

In F^- free solutions an inner oxide and an outer hydroxide of thickness $8A^o$ were detected. The oxide thickness is potential dependent but independent of pH.

In F^- containing solutions yet at low potentials the oxide is thinned but absorbed F^- could be detected. At relatively high anodic potentials however the metal surface was seen to be covered with a fluoride layer of 20-70 A^o with the oxide thinned to $4A^o$. The fluoride corresponds to NiF_2 and has passivating properties which compensate for the reduction in oxide thickness. The thickness of the flouride film was found to be pH dependent.

1.6.2.1 The effect of Ni composition and foreign anions on Ni passivity

Desterat (294) observed that the secondary passivity of Ni is greatly affected by its carbon content, whilst more detailed work on the effect of impurities on the passive and active dissolution of Ni has been undertaken by Di Bari and Petrocelli and has already been discussed in Section (1.6.1.2).

The effect of anions on the active dissolution and to some extent the passivity of Ni has also been discussed earlier. However work has also been conducted by other workers on the effect various anions on Ni passivity.

Postlethwaite and Freese (291) have investigated both the active and passive dissolution of Ni in 0.05M H_2SO_4 containing small quantities of NaCl, NaBr, and NaI in the range of 0.0001M to 0.1M with all the additives lowering E_{corr} but raising E_{pp} and i_{pp}.

The effect of KBr on Ni passivity has also been investigated by Ammar (296), in 0.5M H_2SO_4 on a rotating Ni electrode who detected the appearance of a second maximum in the E vs log i curve.

The effect of Cl^- ions on the passive dissolution of Ni has been studied by Truempler and Keller (294) who showed that increase in Cl^- concentration displaced E_{pp} in a more noble direction increased i_{pass} and i_{pp}. Whilst Piron and Noble (293) found that at a NaCl concentration greater than 0.5% NaCl no active to passive transition could be observed.

Chatfield and Shreir (301) have studied the effect of the addition of H_2S to Ni in chloride solutions and concluded that passivation is due to the formation of an NiS film in these solutions with increase in H_2S concentration affecting both the active and passive dissolution.

2 EXPERIMENTAL

2.1 Specimen preparation of Ni foil prior to Pb and PbO_2 electrodeposition

Samples of Ni foil 4 x 3.5 cm were cut from N1200 sheet, 125 μm thick, which had already been shown to give acceptable levels of adhesion to electrodeposited PbO_2. A 5 cm length of Ni wire 0.5mm in diameter was then spot welded onto the Ni foil, so that electrical contact could be obtained for the subsequent etching and plating operations. The samples were then pre-treated prior to electrodeposition by the following method :

a) Vapour degrease in trichloroethylene for 10 minutes.

b) Cathodically degrease in a solution of 50 gl^{-1} NaOH, 50 gl^{-1} Na_2CO_3 and 10 gl^{-1} Na_2SO_4 at 5 Adm^{-2} and at room temperature, for 10 minutes.

The specimen to be degreased was made the cathode in the degreasing solution and placed between two stainless steel anodes. A Farnell 30 Volt, 5 amp constant current power source was used to provide current for the cathodic degreasing.

The specimens were removed from the bath, washed with de-ionised water and dried with iso-propanol.

c) The Ni foil specimens were then placed in a 30% by weight solution of H_2SO_4 at 50°C ± 2°C and anodically etched for 10 minutes at 2.7 Adm^{-2}.

The cathodes were sheet Pb and the Ni specimens were inserted between two Pb cathodes. A Farnell 5 amp constant current unit was used as the power source and the etch solution temperature maintained at the required value, using a stirrer hot plate.

Ni samples were removed from the solution after etching, washed thoroughly with de-ionised water and dried using iso-propanol.

d) The side of the Ni foil with the spot welded connection was then coated with 'Lacomit' (a proprietary lacquer) using a camel hair brush and allowed to dry, which enabled a known area of specimen to be defined.

The Ni foil electrodes prepared in the above manner were then used as the substrates for Pb and PbO_2 deposition from both conventional and simultaneous plating solutions.

2.1.1 Electrodeposition of Pb and PbO_2

For the simultaneous electrodeposition of both Pb and PbO_2 a cell was specially constructed so that the solution pH could be maintained within acceptable limits during the plating operation. Details of this cell are shown in Fig. 4.

In practice it was found difficult to maintain the pH of the solution between 3.5 and 4 using this design of cell. This was due to the relatively small volume of the plating solution and the anodically produced H^+ ions, which lowered the pH during the initial stages of PbO_2 deposition. Therefore, whilst neutralisation and replenishment of the $Pb(NO_3)_2$ solution with Pb^{2+} ions by addition of PbO was possible, it could not compete with the rate of the anodic formation of H^+. The solution pH in this event could only be maintained within the pH range 2.6 to 3.5 during the course of the experiment. The design of the cell meant that the solution could be regenerated after use, since direct addition of PbO to the plating solution often resulted in incorporation of fine PbO powder in the PbO_2 deposit. Increase in the solution pH was sometimes achieved by the addition of small quantities of KOH.

The power source used for all plating experiments was a Farnell 30 volt, 1 amp constant-current unit; details of the electrical schematic for the plating circuit are given in Fig. 5.

For all current efficiency determinations a copper coulometer was placed in series with the plating cell. The Ni substrates were weighed before and after deposition of Pb and PbO_2, as was the weight of the copper cathode in the coulometer.

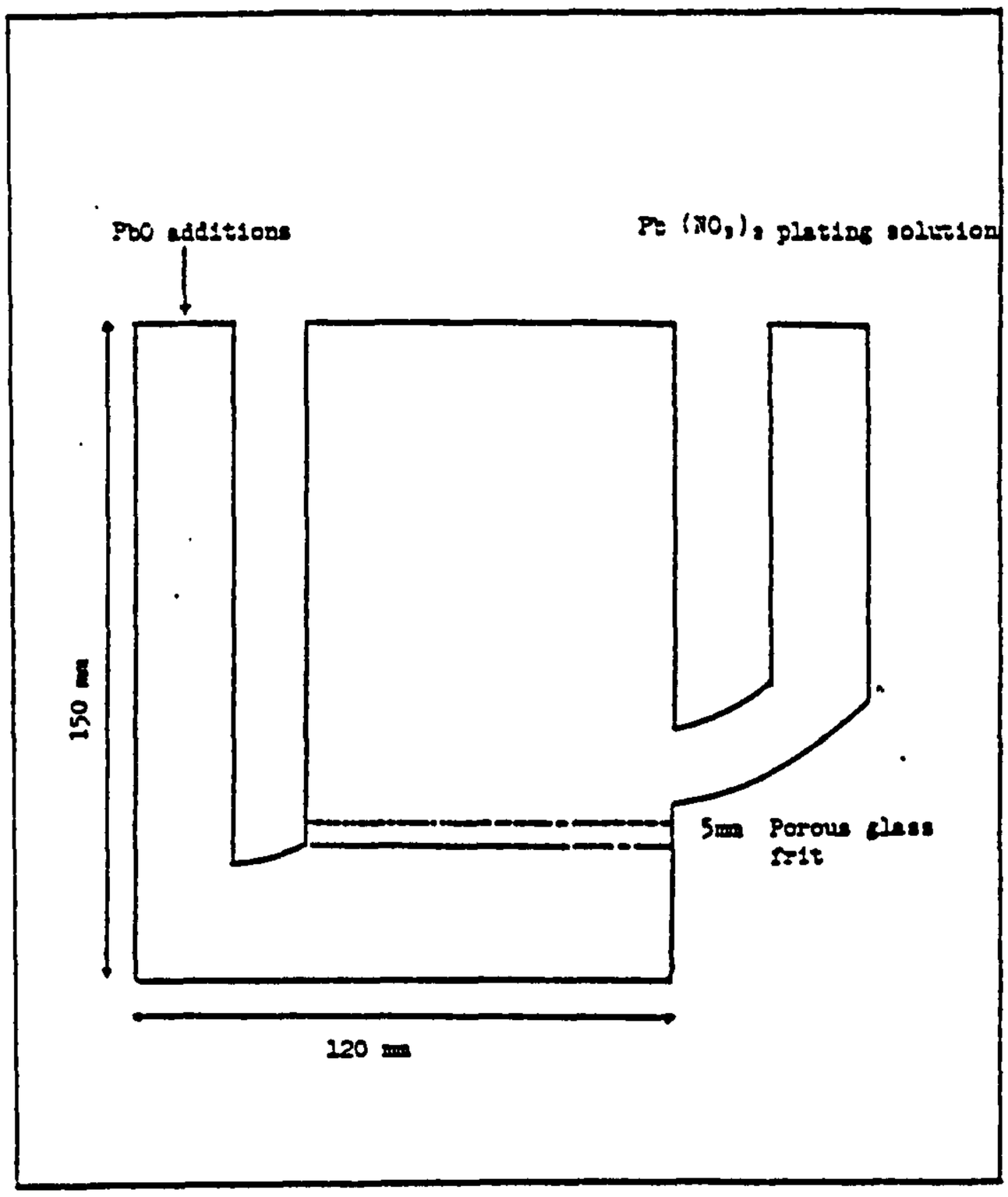

Schematic of the glass cell used for the simultaneous electrode position of Pb and PbO_2, with the facilities for addition of PbO for acid neutralisation.

FIGURE 4

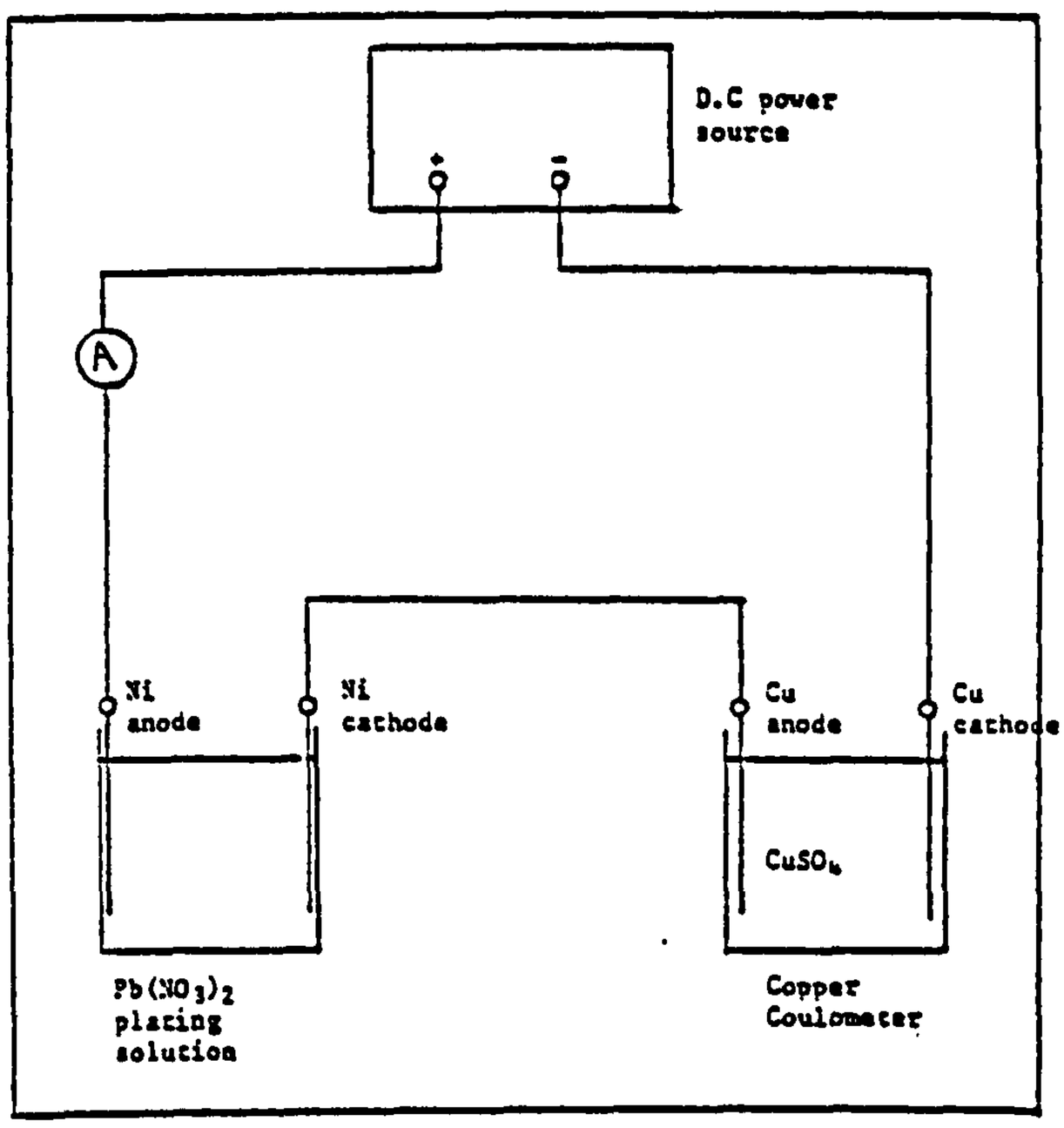

Schematic of the plating circuit used for the simultaneous electro- deposition of Pb and PbO_2 in laboratory studies.

FIGURE 5

In the case of the deposition of Pb from a $Pb(BF_4)_2$ solution polyethylene beakers were used and the anode was sheet Pb.

Temperature control of the plating solutions was via a hot plate, with the temperatures maintained to within ± 2°C of a pre-selected value.

2.1.2 Porosity determinations for Pb electrodeposited onto Ni

Samples of Pb electrodeposited onto Ni from a variety of different plating solutions were prepared in the same way as those for current efficiency determinations and S.E.M examination (see Section 2.1.1).

The 'Lacomit' coating on the back of each Pb-plated Ni sheet was removed with acetone, to enable electrical contact to be made to each specimen when placed in the specimen holder. Four circular sections, each of area 0.63 cm^2 were punched out using a specially constructed punch and die, from each sheet of Pb coated Ni. Each test piece was then inserted into the Teflon specimen holder (see Fig. 6), which allowed a specimen area of 0.238 cm^2 to be exposed to the solution. Electrical contact was made by tightening the brass locating screw onto the base of the test specimen. This also ensured a tight seal around the test piece and prevented any ingress of electrolyte.

The electrodeposited coating was then made the working electrode of a cell, details of which are shown in Fig. 7. The electrical circuitry and current monitoring equipment are shown in Fig. 8.

The method chosen to assess the level of porosity was measurement of the current obtained when Pb deposits on Ni sheets were anodically polarised in a 1.5M H_2SO_4 solution. This method relies on the fact that in this solution Ni is active, whilst the Pb becomes passive. Thus any current obtained is due to nickel dissolution, although a small amount is also due to $PbSO_4$ formation. It therefore follows that the greater the porosity of the coating the higher the current obtained. The ratio of i_{pp} for the electrodeposited Pb on Ni

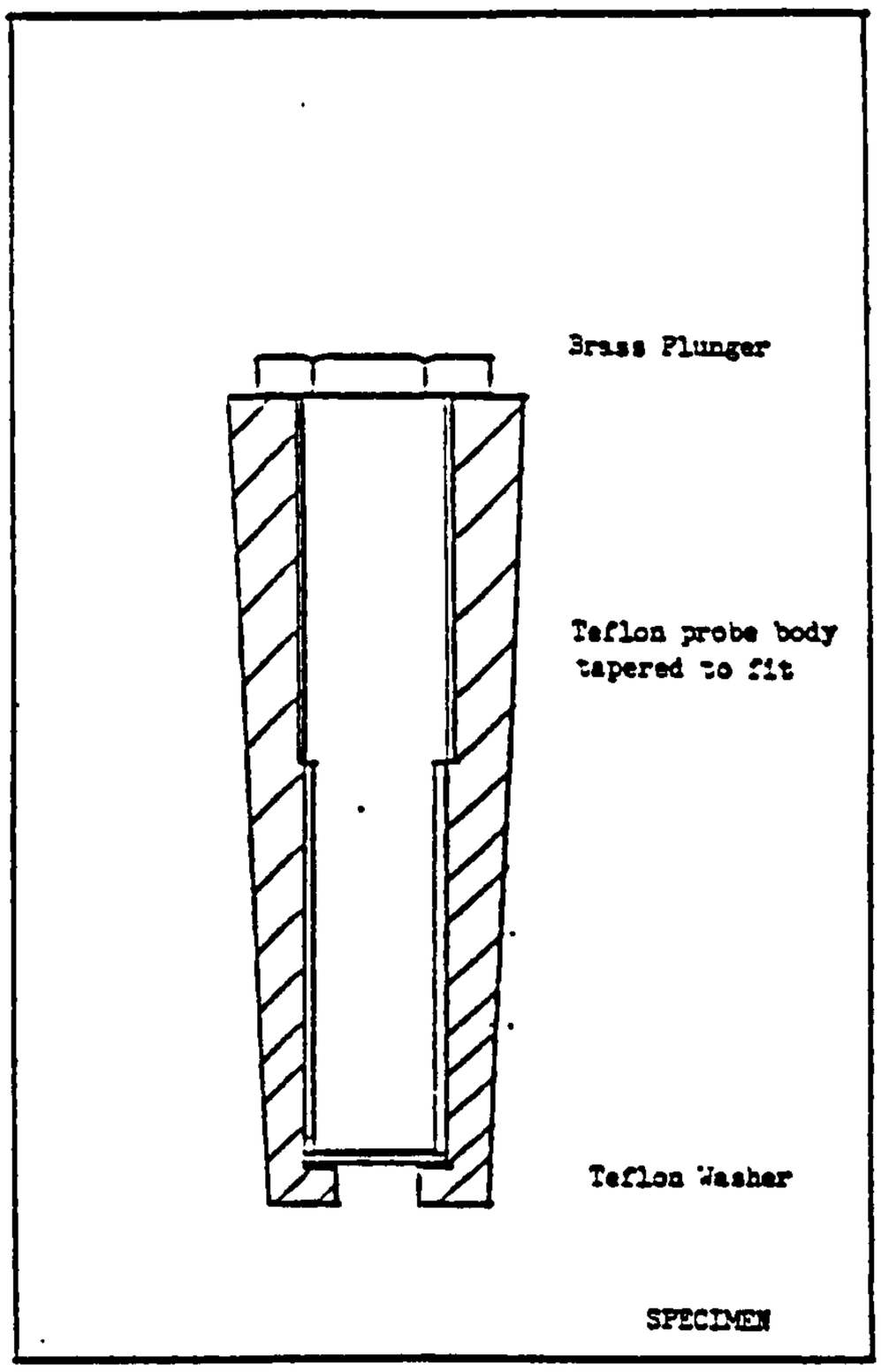

Teflon specimen holder used for porosity measurements on Pb electrodeposited onto Ni

FIGURE 6

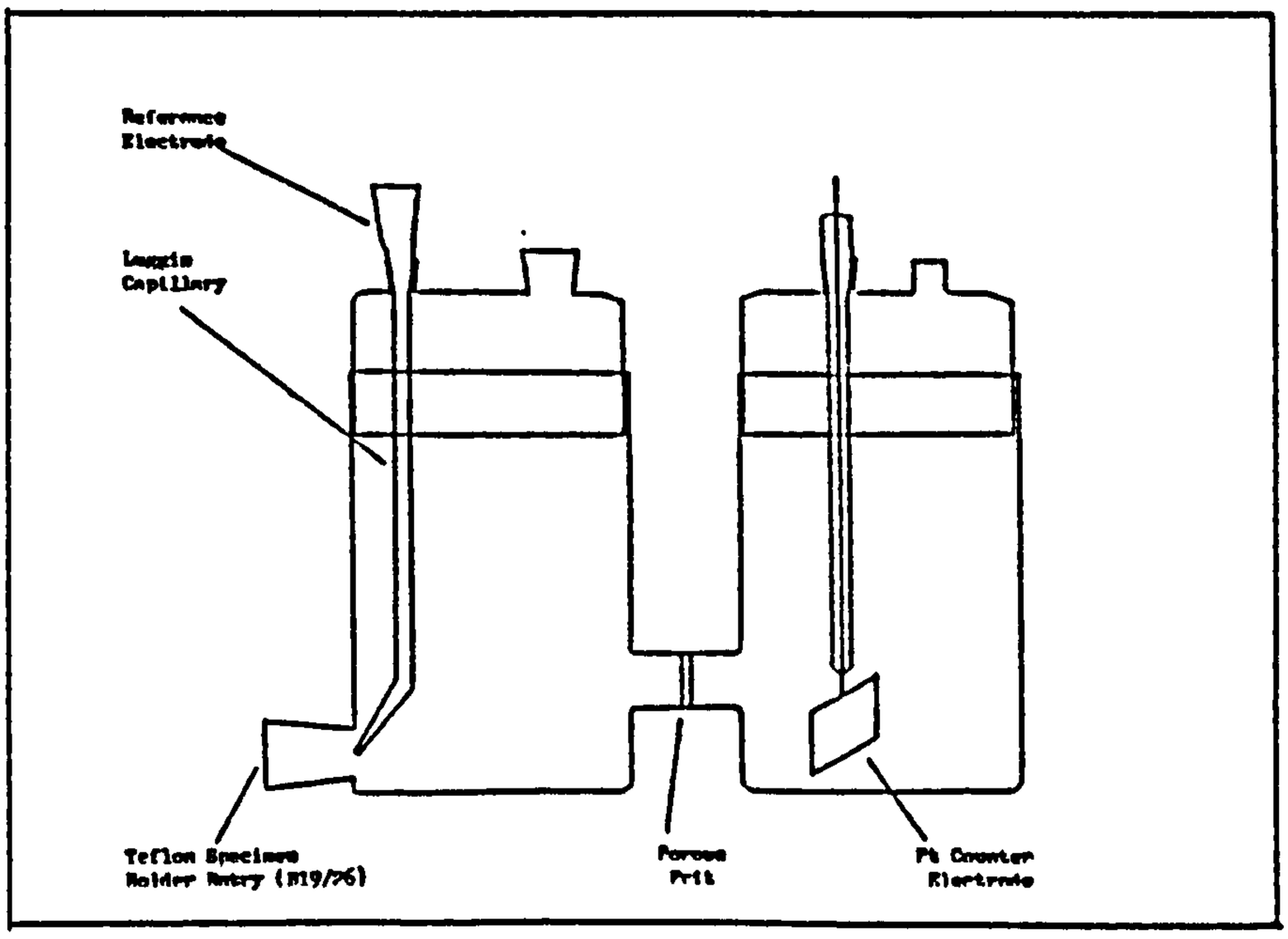

Porosity Determination Glass Cell

FIGURE 7

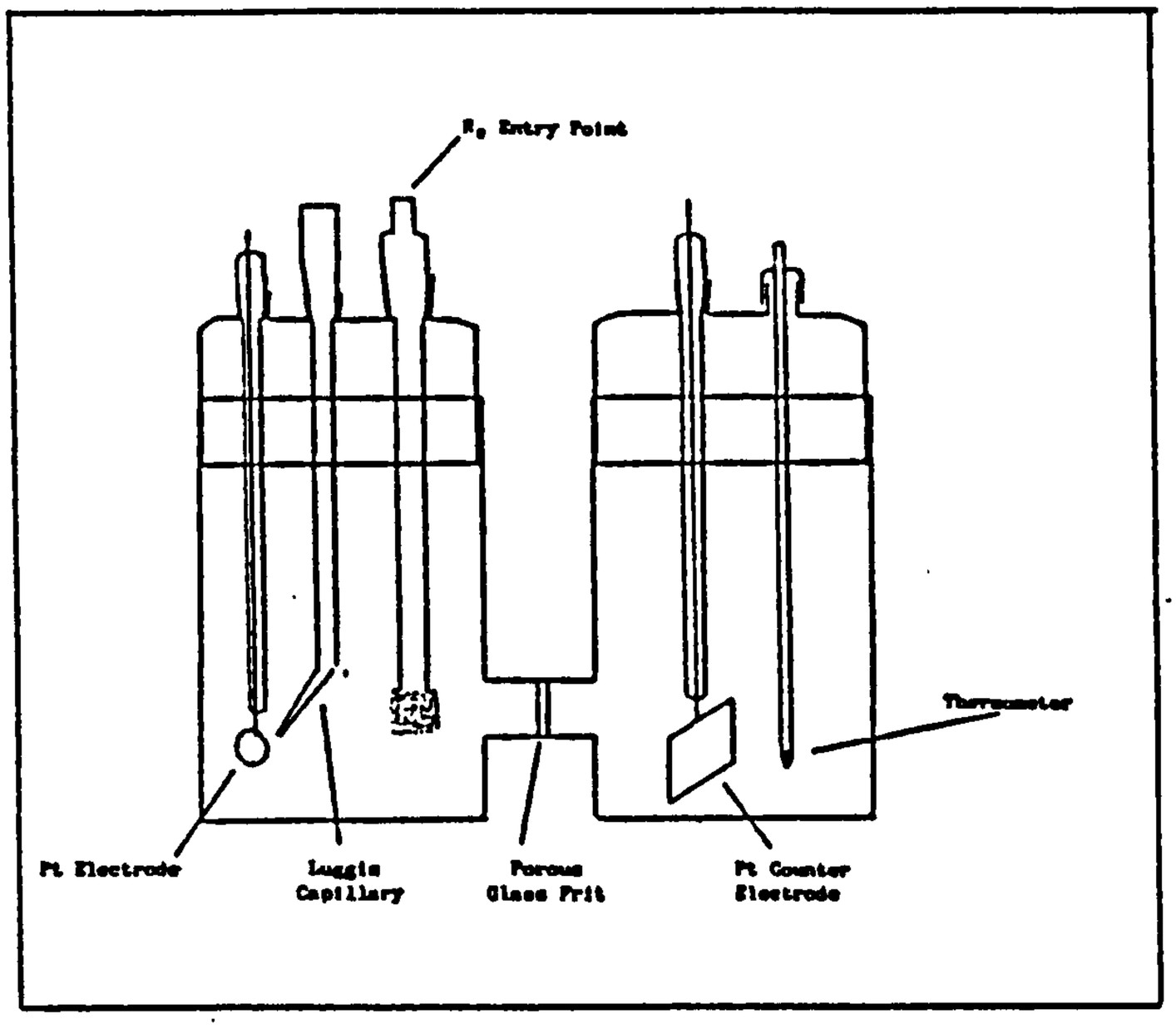

Cell for the anodic oxidation of addition agents

FIGURE 7A

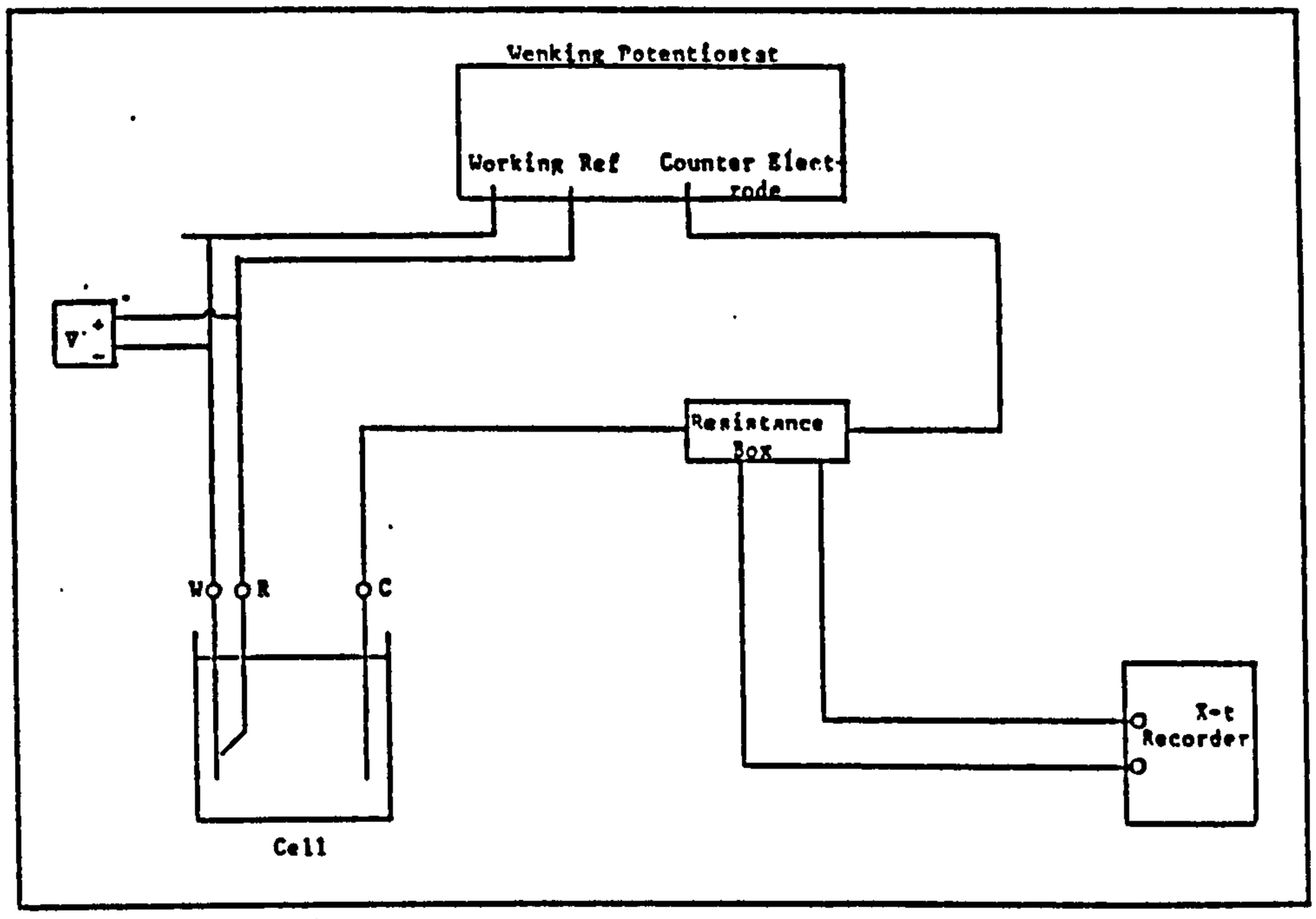

Circuit schematic for electrochemical studies on Pb electrodeposition and Ni passivation in various solutions.

FIGURE 8

to i_{pp} for pure nickel in this solution, at the same sweep rate, was selected as an index of the relative porosity of the deposit.

The Pb-plated nickel sheets were maintained at a potential of -0.160 V for 5 min, and then polarised at 3 mV sec^{-1} from this potential, (all potentials are quoted versus a Standard Hydrogen Electrode (SHE) unless otherwise stated). The current was continuously recorded on a Bryans 28000 chart recorder. The same procedure was adopted to obtain i_{pp} for pure nickel in this solution.

A total of 4 separate porosity determinations were made on each sheet of electrodeposited Pb and the mean value of the four readings was taken as the relative porosity.

2.1.3 Cell discharge experiments

Samples of electrodeposited β-PbO_2 on Ni were prepared for cell discharge experiments using the same deposition conditions as in the commercial production of battery plate, i.e from a solution of 360 gl^{-1} $Pb(NO_3)_2$, pH 3.5 - 4.0 and depositing at a c.d. of 2 Adm^{-2} with the temperature maintained at 50°C.

The samples of Pb electrodeposited onto a Ni substrate for use in cell discharge experiments, were produced from a solution containing 230 gl^{-1} $Pb(BF_4)_2$ + 22 gl^{-1} HBF_4 + 12 gl^{-1} H_3BO_3 + 0.1 gl^{-1} gelatin, at a c.d of 2.7 Adm^{-2} and at room temperature. The exposed area of the Ni foil substrate used for the deposition of Pb and PbO_2 was 14 cm^2 (4 x 3.5 cm), the reverse side being masked off with 'Lacomit'. Electrical connection to each foil was via a Ni wire spot welded onto the reverse face of the Ni foil. The Ni was pre-treated prior to plating, as outlined in Section 2.1 and each specimen was weighed before and after plating. These specimens were used in the determination of the discharge properties of cells constructed from conventional battery plate material and material prepared from simultaneous plating solutions.

The PbO_2 and Pb deposits on Ni obtained from "simultaneous baths" (i.e. $Pb(NO_3)_2$ plus additives) were also prepared under laboratory conditions, by plating for 15 minutes at 2 Adm^{-2} and 50°C. The same specimen preparation and geometry as that described earlier was used. The discharge cell for these experiments was that used for the determination of activation times and is described elsewhere (see Section 2.1.8). The specimens for the discharge experiments were each 3 x 1.7cm, although an area of only 0.63 cm^2 of substrate was exposed to the solution. Continuous determination of current and cell voltage was made possible by measuring the potential drop across the resistive load connecting the PbO_2 and Pb electrodes, using a Bryans 28000 series X-t chart recorder.

The test electrolyte for all experiments was 48% HBF_4. The electrolyte used in experiments carried out at 60°C was heated slightly above this temperature, and then immediately placed in the discharge cell. The temperature was measured soon after discharge and found to have fallen to only 57°C. Thus although no accurate control of temperature was made during each test, at elevated temperature, the temperature of the HBF_4 was found to remain reasonably constant.

2.1.4 Scanning Electron Microscope (SEM) examination of Pb and PbO_2 electrodeposits

Samples of Pb and PbO_2 electrodeposited onto Ni from different plating solutions were examined with the aid of an SEM. The bulk samples were cut to the required size and then mounted on an aluminium stud, electrical contact to which was made using a conductive silver paint. The samples were sputter coated with gold prior to examination to prevent surface charging.

An Hitachi and a Cambridge Scientific Microscope were used. An EDAX (Energy dispersive analysis of X-rays) was attached to the side of the microscope to enable a qualitative chemical analysis of the surface under examination to be carried out, if required.

Photographs of the surface were taken using a camera facility incorporated in the microscope.

2.1.5 X-ray diffraction studies

X-ray diffraction patterns were obtained for Pb and PbO_2 electrodeposits on the Ni substrate and on bulk samples of PbO_2; a Phillips 4211 diffractometer was used to obtain the diffraction patterns. The intensity of the diffracted X-rays was measured by a ion scintillation counter and the results continuously recorded on a chart recorder. Copper Kα radiation was used for all experiments and the diffractometer set at 40 kV and 20 mA. The specimens were rotated at 2 degrees $minute^{-1}$ to obtain the bulk diffraction patterns and 0.5 degrees $minute^{-1}$ when grain size determinations were conducted.

2.1.6 The determination of the adhesion of β-PbO_2 onto Ni foil substrates

Samples of β-PbO_2 electrodeposited onto etched Ni foil from conventional and simultaneous plating solutions were tested to see if the organic addition agents affected the levels of adhesion of PbO_2.

The method of adhesion testing has been described elsewhere (see Section 2.3.9).

2.1.7 Plant trials

Plant trials were undertaken by the Ionic Plating Co Ltd to evaluate the nature and properties of the Pb and PbO_2 deposits obtained from a large scale commercial plating solution based on $Pb(NO_3)_2$ plus selected addition agents. The initial work was conducted to determine the long term performance of a simultaneous plating solution consisting of 360 gl^{-1} $Pb(NO_3)_2$ 1.5 gl^{-1} 2 butyne 1,4 diol and 3 ml l^{-1} Triton X100. The total solution volume was 450 litres with the pH maintained within the range 1.5 to 3 by the addition of PbO.

The tank was fitted with a Pb anode and a carbon cathode, between which was inserted an unconnected Ni foil electrode in a bipolar system. The Ni foil electrode was held in position by a specially constructed jig that allowed only a very limited electrolyte leakage between the two compartments, and was not electrically connected to the terminals of any power source, a schematic of the cell construction is shown in Fig. 9.

Electrodeposition was carried out at 2.4 Adm^{-2} on Ni foils of size 610 x 190 mm. The solution was operated for a total of 1900 amp-hours and samples taken at selected intervals, to determine the concentration of organic addition agents. The thickness of the Pb and PbO_2 deposits obtained was measured using a Betascope.

Simultaneous plating solutions of similar $Pb(NO_3)_2$ concentration but containing different addition agents were also evaluated in this way.

2.1.8 Activation time determination

The time taken for Pb and PbO_2 battery plate material to reach a given voltage, after immersion in 48% HBF_4 at low temperatures, is an important parameter in determining the performance of battery plate material. Details of the method used to carry out these determinations have been described by Smith (9).

Pb and PbO_2 battery plate material obtained from conventional and simultaneous plating solutions were tested. Samples of Pb and PbO_2 on Ni were cut from bulk samples. A 0.5 mm diameter Ni wire was spot welded onto the uncoated side of the Ni foil and then the Pb and PbO_2 electrodes were masked off with insulating tape, so that only an area of 1 cm^2 was exposed. The Pb and PbO_2 electrodes were then fixed into a specially constructed, spring loaded jig, and a 56 ohm precision resistor connected between the electrodes. They were then placed into a refrigerator with the temperature maintained at $-32^{o}C$. The specimens were kept in the refrigerator for 4 hours, to allow a stable temperature to be reached.

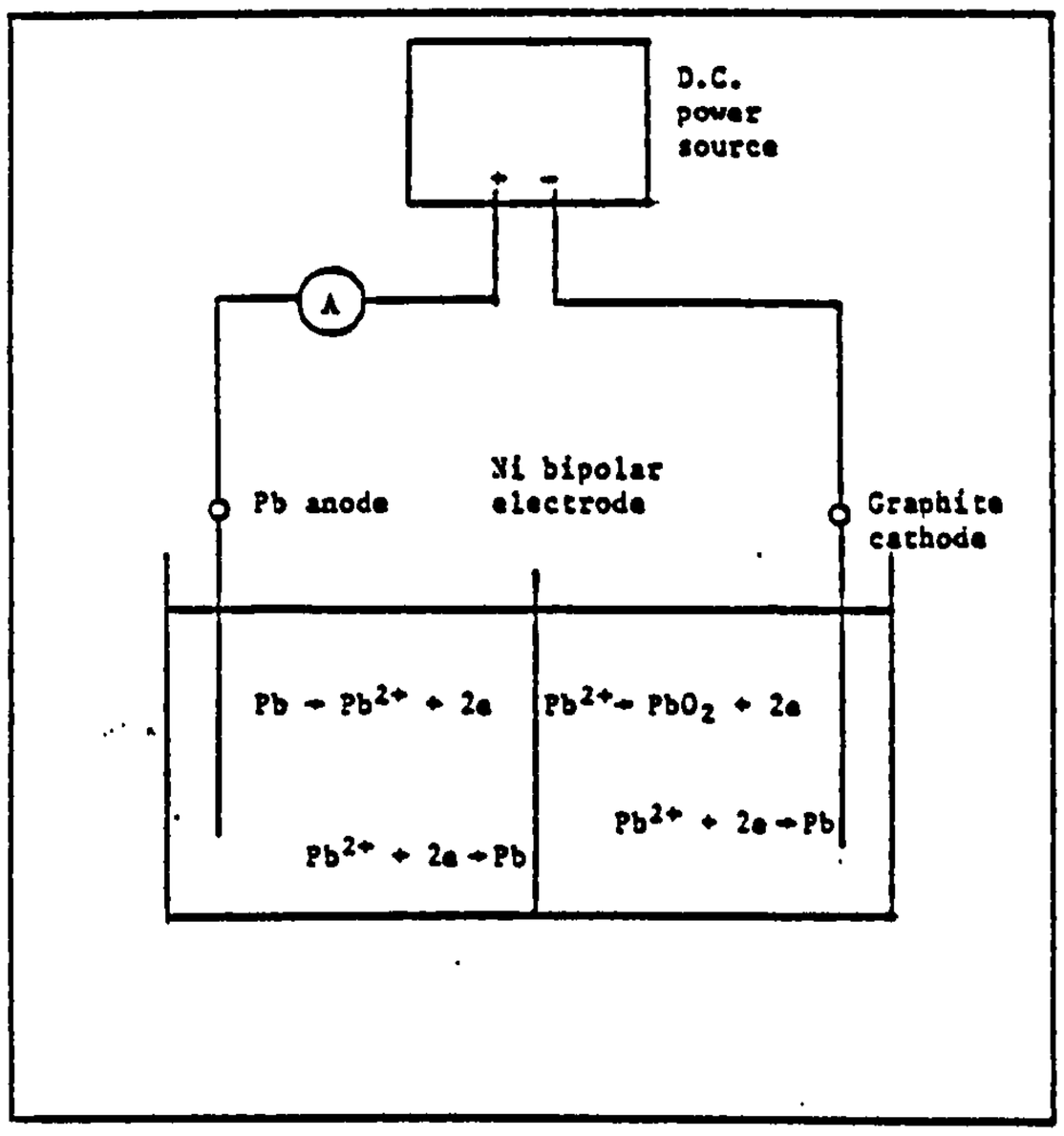

Schematic showing the simultaneous electro-deposition of Pb and PbO_2 onto a bipolar Ni foil electrode.

FIGURE 9

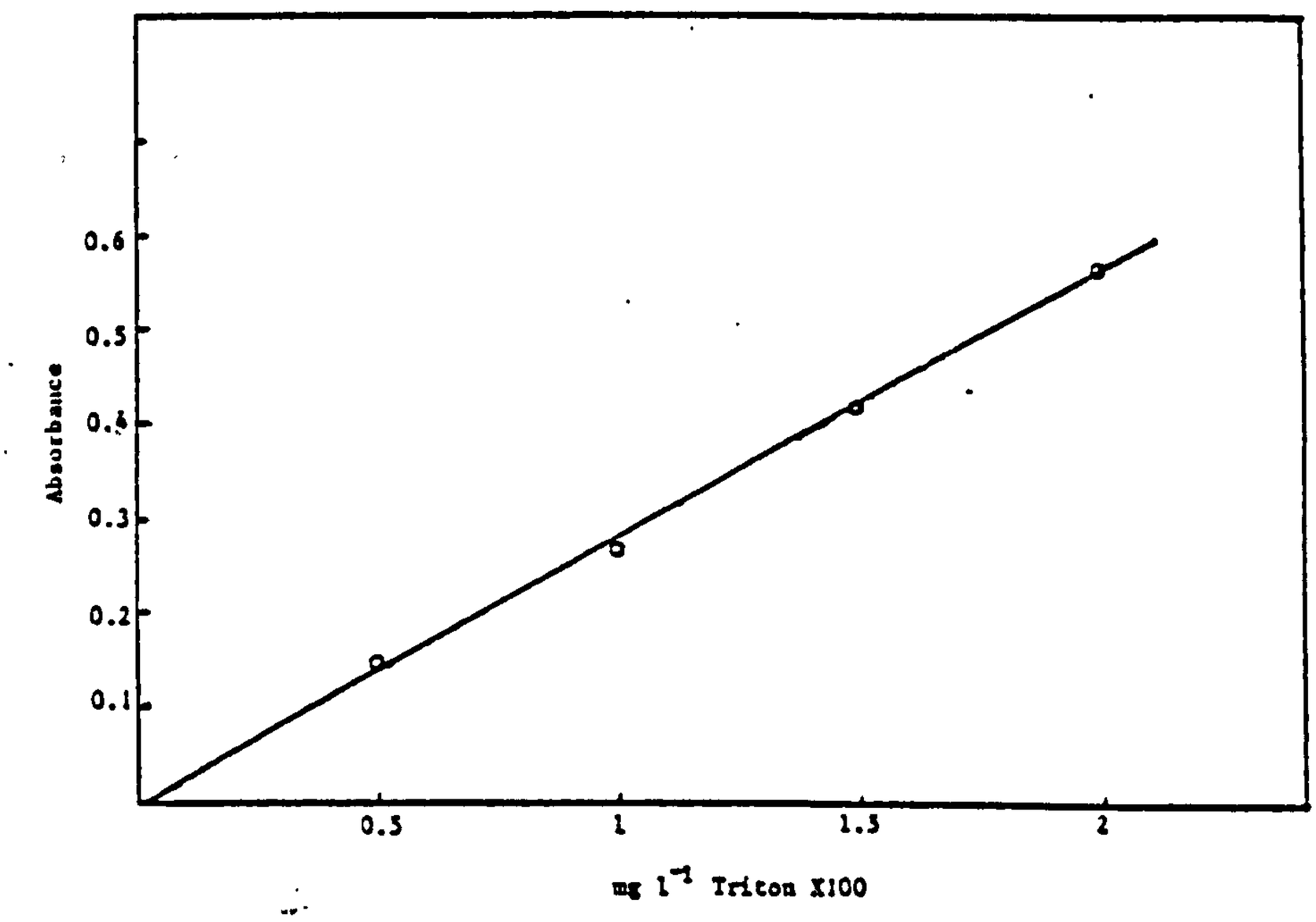

A graph of Triton X100 concentration versus absorbtion intensity for the colorimetric determination of Triton X100

FIGURE 10

The spring holding the electrodes in position was released by pressing an external switch which operated a relay fixed to the jig. The electrodes were immediately inserted in the electrolyte using this technique and the cell voltage continuously monitored using a Bryans Series 40,000 Ultra Violet chart recorder.

2.1.9 Analysis of Triton X100 and 2 butyne-1,4-diol in $Pb(NO_3)_2$ solutions

A solution of 360 gl^{-1} $Pb(NO_3)_2$, 3 ml l^{-1} Triton X100 and 1.5 gl^{-1} butyne 1,4 diol was used in the pilot plant at Ionic Plating Limited as the working electrolyte for the production of samples of $Pb/HBF_4/PbO_2$ battery plate material. Samples of this solution were taken before use and at different intervals during the plating operation, to determine the concentration of addition agents. Methods of analysis for each addition agent were sought to obtain a quantitative value for each addition agent concentration.

2.1.9.1 Triton X100 determination using a gravimetric method

The gravimetric method to determine Triton X100 concentration was first developed by Barber (301) and was carried out as follows :

20 ml of the $Pb(NO_3)_2$ solution plus addition agents was pipetted into 150 ml of 30 wt% HCl, then 20 ml of 10% $BaCl_2$ solution was added. The $PbCl_2$ precipitate obtained was filtered off and the filtrate brought to boil on a hot plate. 10 ml of a 20% dodecaphosphotungstic acid solution was then added and boiling continued for 1 to 2 mins to allow the precipitate to coagulate. The white precipitate formed was then filtered off and weighed. The amount of Triton X100 in the unknown sample was determined by a comparison of the weight of precipitate obtained, with the weight from a solution of known Triton X100 content.

2.1.9.2 Triton X100 determination using a colorimetric method

The method used for this determination was that outlined by Weber et al (302), however a few modifications to this method were found necessary. 1.5 ml of the unknown solution containing Triton X100 was made up to the total volume by the addition of 1.5 ml of 50% v/v absolute alcohol. 5 ml of a cobalt thiocyanate solution containing 178g ammonium thiocyanate and 28 ml of cobalt nitrate hexahydrate dissolved in 1000 ml of water was then mixed with the Triton X100 absolute alcohol mixture in a plastic beaker. The mixture was shaken with 10 ml of ethylene dichloride for 10 min to extract the complex formed, centrifuged, then the ethylene chloride removed and the absorbance measured at 620 μm against a blank sample. The same method was adopted to obtain a calibration curve of absorbance versus Triton X100 diluted with 50% absolute alcohol at various Triton X100 concentrations; the calibration curve is shown in Fig. 10.

2.1.9.3 2-butyne-1,4-diol determination by back titration

A 10 ml sample of the $Pb(NO_3)_2$ solution containing the addition agents 2-butyne-1,4-diol and Triton X100 was pipetted into a 200 ml solution of 2M H_2SO_4 and the resultant $PbSO_4$ precipitate filtered off. To this clear solution 50ml of 0.037M $KMnO_4$ solution was added. The solution was allowed to stand overnight, then 50ml samples were withdrawn from the solution and titrated against a stock solution of 0.15M $K_4Fe(CN)_6$ (potassium ferrocyanide) with ferroin as the indicator. The quantity of $K_4Fe(CN)_6$ required to reach an end point and the total volume of the solution were recorded.

A similar procedure was adopted to determine the quantity of $KMnO_4$ necessary to oxidise a known weight of Triton X100 and butyne 1,4 diol separately, for which stock solutions of known concentrations were used.

Once the concentration of Triton X100 had been determined by a separate analysis, it was then possible to calculate the quantity of $KMnO_4$ necessary to oxidise the Triton X100 in the sample solution. From a knowledge of the total concentration of $KMnO_4$ necessary to oxidise both the Triton X100 and butyne 1,4 diol and the actual concentration of Triton X100. It was possible to calculate the concentration of butyne 1,4 diol in the solution.

2.1.10 Electrochemical studies on the anodic oxidation of selected organic addition agents in aqueous solution

A stock solution of 0.2M Na_2SO_4 was made up with distilled water, with the pH adjusted to 2.0 using dilute H_2SO_4. To this stock solution known quantities of selected organic compounds that had found use as addition agents in the electrodeposition of Pb and PbO_2 were added.

A Pt electrode was used as the inert electrode and maintained at +0.60 V for 5 mins before polarisation so that the current due to $Pt(OH)_2$ formation reached a minimum level.

The electrochemical cell used for all experiments is that shown in Fig. 7A and the method for obtaining the cyclic voltammograms was similar to that described in Section 2.2.3.

2.2 Electrochemical studies on Pb deposition

2.2.1 Linear polarisation studies on a Pb electrode in $Pb(NO_3)_2$ solutions

A stock solution of 0.1M $Pb(NO_3)_2$ containing a supporting electrolyte of 0.1M HNO_3 was used as the electrolyte in which to study the effect of certain organic additives on the E vs i curve for Pb deposition.

The electrochemical cell used for these experiments is shown in Fig. 11. The Pb working electrode, cross sectional area 0.1 cm^2, was obtained by cold extruding lead rod. The Pb wire was then mounted in cold setting epoxy resin, and located on the end of a glass syringe. This design of working electrode enabled easy mechanical polishing of the electrode surface down to 800 grade emery paper and the production of a renewable Pb electrode of constant surface area. The counter electrode for all experi ments was Pb foil, located in a second compartment of the electrochemical cell, both compartments were separated by a No 2 porosity glass frit. A saturated calomel electrode (SCE) attached to a Luggin capillary was used as the reference electrode.

The Pb working electrode was connected up to the working electrode terminal of a Wenking PPT-70 potentiostat, which was connected to a PCA 72 M potential control amplifier and a fixed resistance box, was connected between the counter electrode terminal on the potentiostat and the Pb counter electrode. The potential across a selected precision resistor was recorded on a Bryans 28000 X-t chart recorder to enable continuous monitoring of the cell current. A linearly varying voltage was applied from a Wenking waveform generator type VSG 72 and all potentials were monitored with a high impedance Solartron 7045 digital voltmeter.

2.2.2 Rotating disc studies

The working electrode used for all rotating disc studies was AnalaR grade lead rod extruded to produce lead wire of the required thickness. A piece of lead wire was then inserted into the Teflon specimen holder and held in position using cold setting epoxy resin. Prior to each experiment the electrode surface was mechanially polished down to 800 grade emery paper. After polishing, the electrode and holder were then fixed to the drive shaft of a Chemical Electronics RDI rotating disc unit. Electrical contact to the working electrode was via an insulated wire, attached to the unexposed end of the working electrode and

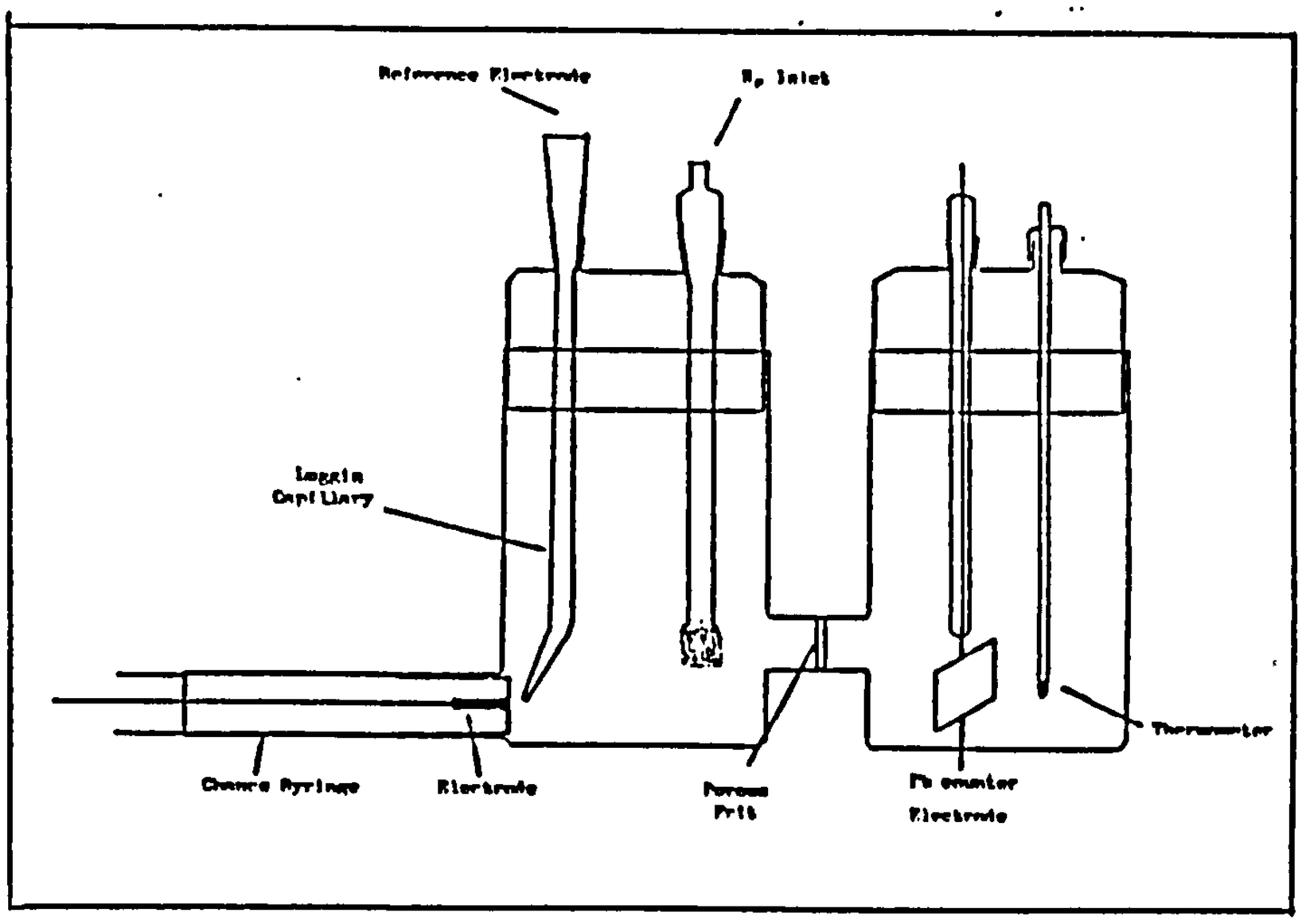

Cell for studies on the anodic dissolution of Ni and linear polarisation of Pb electrode in $Pb(NO_3)_2$

FIGURE 11

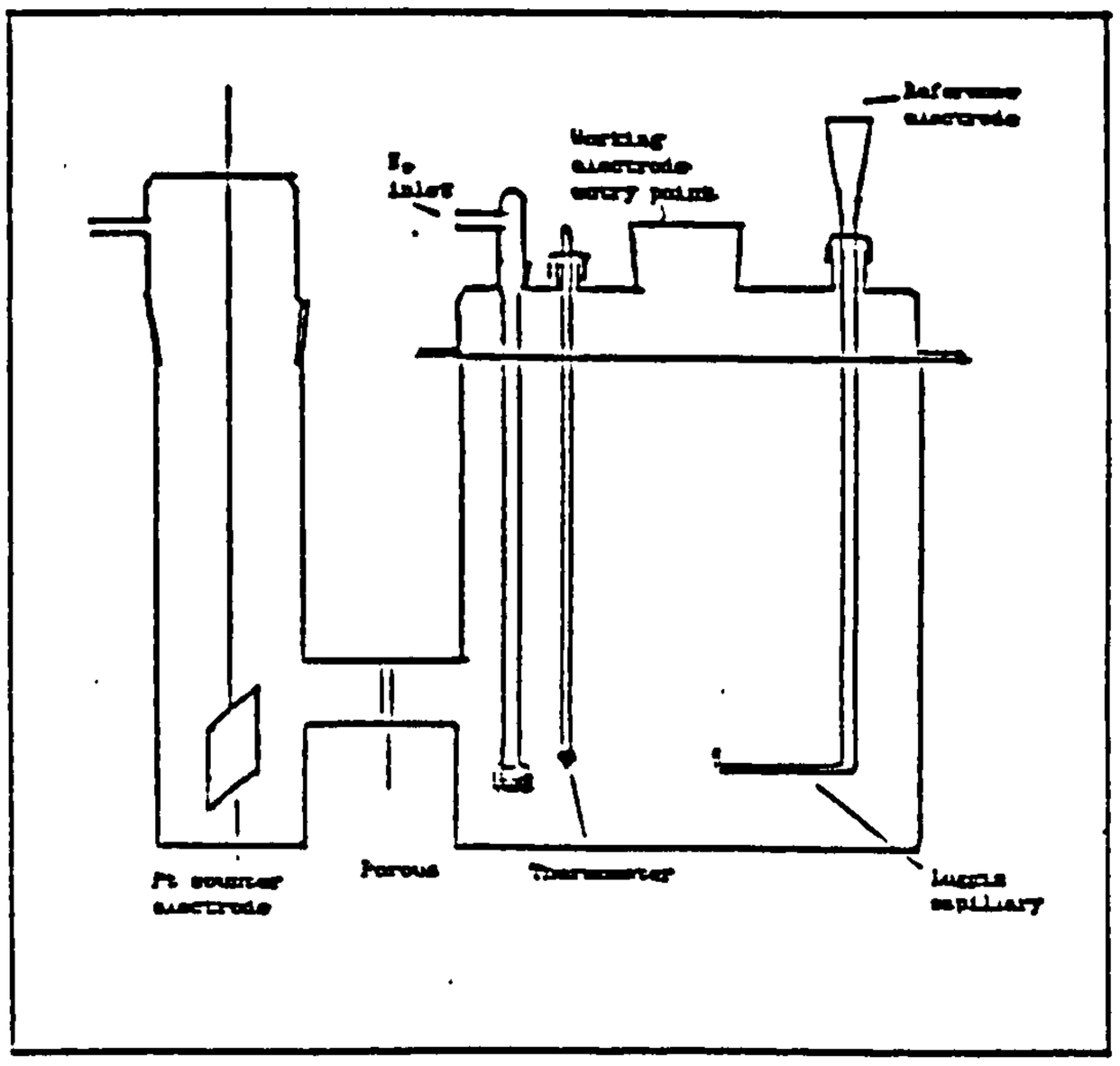

Rotating disc studies

FIGURE 12

fed up the hollow central axis of the drive shaft, to a bush connection on top of the drive shaft. This allowed the electrode to be freely rotated and provided continuous electrical contact between the working electrode and potentiostat.

The details of the chemical cell are given in Fig. 12, whilst the electronic circuitry is similar to that shown in Fig. 8.

The whole experimental cell, once in position, was immersed in a thermostatically controlled water bath, maintained at $25^{o}C \pm 0.2^{o}C$ unless otherwise stated. The test solutions, were made from AnalaR grade chemicals and a supporting electrolyte of 1M KNO_3 plus 0.1M HNO_3 was used to make up all solutions.

The specimen was allowed to reach its' rest potential for 10 mins, then polarised from this potential at a sweep rate of 0.5 mV sec^{-1}. The rotational speed was measured from a specially constructed "photo multiplier" that produced a digital readout of the rotational speed in revolutions per minute (RPM). This device was calibrated with the aid of a stroboscope.

A fixed value precision resistor was inserted between the counter electrode and potentiostat and the voltage drop across this resistor was used to measure the cell current.

The kinematic viscosity of all solutions was measured using an Ostwald Viscometer, the details of which are given in the literature (304).

2.2.2.1 Determination of i_o exchange current density

The exchange current density (i_o) for Pb deposition from 0.1M Pb $(NO_3)_2$ solutions with and without addition agents at certain temperatures was determined by extrapolation of the linear portion of the E vs log i graph, to zero overpotential. The working electrode was rotated at 3000 rpm in the solution under investigation, polarised to a fixed anodic potential, then cathodically polarised at a sweep rate of 0.5 mV sec^{-1}. Both

the anodic and cathodic currents were continuously recorded on the chart recorder. To enable both anodic and cathodic currents to be recorded a double pole switch was incorporated in the resistance box connected between the counter electrode and potentiostat and used in conjunction with a Bryans (28000 Series) X-t recorder.

A sweep rate of 0.5 mV sec^{-1} was selected since this was considered to be sufficiently slow to maintain near equilibrium conditions yet fast enough to help minimise effects due to the changing electrode area.

One other method of determining i_o, i.e. measurement of the linear portion of the E vs i curve at low overpotentials was also used as a confirmatory test for i_o determinations.

2.2.2.2 Studies on NO_3^- reduction at a Pb cathode

Experiments using the Pb rotating disc electrode were also carried out to study the nitrate reduction reaction on a Pb electrode at fixed rotational speeds. The nitrate concentration was held constant at 1M KNO_3 for all these experiments.

The parameters investigated were pH, oxygen concentration and the effect of plating additives.

De-oxygenation was effected by purging the solution with oxygen-free nitrogen, and all experiments were carried out at 25°C. The electrode was allowed to reach an equilibrium potential for 10 minutes prior to measurement, then cathodically polarised at a sweep rate of 1 mV sec^{-1} from this value.

2.2.3 Cyclic Voltammetry

The reduction of Pb^{2+} in NO_3^- solutions and the effect of certain addition agents on this process was investigated using cyclic voltammetry. The experimental cell consisted of a two compartment cell separated by a glass frit, one compartment housing the counter electrode assembly and the other the working electrode and reference electrode (see Fig.7A).

The SCE reference electrode used was located remote from the working electrode via a Luggin capillary tube. The working electrode was a circular Pt disc of area 0.34 cm^2 and a Pt gauze electrode was used as the counter electrode. The solution of 0.1M $Pb(NO_3)_2$, 1M KNO_3 and 0.1M HNO_3 was made from AnalaR reagents using distilled water. A Wenking PPT-70 potentiostat was used in conjunction with a Wenking PCA 72M potential control amplifier to maintain a fixed potential between the reference and working electrode and a Wenking VSG 72 scan generator was used to apply a linearly varying voltage to the working electrode. A Bryans X-Y chart recorder was used to record the potential versus current voltammograms, with the potential output obtained directly from the scan generator and the current output by measurement of the potential across a resistor connected between the counter electrode and the potentiostat.

The Pt working electrode was allowed 10 mins prior to each potential scan to reach equilibrium. After each potential scan the Pb deposited was removed by anodic polarisation of the working electrode to leave a fresh Pt electrode. The electrode was cleaned in aqua regia prior to immersion in any fresh additive containing solution so as to remove any adsorbed organic addition agents from the electrode surface.

2.2.4 Pulse potentiostatic studies

The current vs time transients at a fixed potential for Pb deposition onto a Ni electrode, in a 0.1M $Pb(NO_3)_2$, 0.5M KNO_3 solution with and without selected addition agents was investigated. This work was instigated to study the effect of certain addition agents on the nucleation and growth processes of Pb electrodeposited from practical plating solutions.

All the solutions were made from AnalaR grade reagents and Ni270 wire 0.6mm in diameter was used as the working electrode. To reduce the grain boundary and defect concentration the nickel

wire was annealed for 6 hr at 1400°C to produce a recrystalised nickel structure. The Ni wire was then placed in 5mm diameter glass tubing filled with cold setting epoxy resin to hold it in position, then polished down to 1 micron alumina powder to obtain a smooth surface.

The Ni electrode was placed in the electrochemical cell (see Fig. 7A), with a SCE reference electrode and a Pt counter electrode. These electrodes were then connected up to the respective terminals of a Ministat potentiostat. A Hi-Tek Waveform Generator was used to supply the pulse potential and the current was continuously recorded on a Nicolet Explorer 1 oscilloscope.

2.2.5 Impedance studies on a Pb electrode in $Pb(NO_3)_2$

The Pb electrode used for this work has been described elsewhere as has the electrochemical cell A (see Fig. 11). All the potential readings were taken with reference to a saturated calomel electrode; a Pt gauze located in a separate compartment of the cell was used as the counter electrode. The potential of the electrode was held constant with a Ministat potentiostat and the Faradaic impedance measurements were performed using a "Solartron Schlumberger" (type 1172) automatic frequency response analyser. The frequency response analyser consists of a digital programmable generator that provides the alternating signal, a correlater to analyse the systems response and printer output to present the results. The output frequency was selected between the desired limits and an a.c signal of 10mV amplitude used as the measuring voltage.

2.2.6 PbO_2 deposition onto a Pt disc electrode from $Pb(NO_3)_2$ solutions

The electrodeposition of PbO_2 onto a Pt disc electrode (0.34 cm^2) from a solution of 0.1 M $Pb(NO_3)_2$, 1M KNO_3 plus 0.1M HNO_3 with and without selected addition agents was investigated.

The cell used for these experiments is shown in Fig. 7A. whilst the electrical circuit was similar to that shown in Fig. 8. The potential of the Pt working electrode was maintained at a fixed value using a Wenking PPT-70 potentiostat, and the cell current and electrode potential were continuously recorded on a Bryans X-Y chart recorder.

The Pt electrode was cleaned by immersion in an aqua regia solution to remove any adsorbed chemicals prior to each experiment and washed thoroughly before being replaced in the test solution.

2.3 Investigation of factors that affect the adhesion of PbO_2 onto Ni substrates

2.3.1 Selection of material

In the present work, studies were undertaken to examine the varying degrees of adhesion of PbO_2 to different types of sheet Ni foil. The Ni foil used for these investigations was that found by the manufacturers of Pb and PbO_2 battery plate material to exhibit either 'good' or 'bad' adhesion of electrodeposited PbO_2 (see Section 1.4).

The foils found by the manufacturers to exhibit 'good' adhesion were invariably Ni200, whilst those found to exhibit 'bad' adhesion were invariably Ni270. This is in contrast to previous laboratory studies where Ni270 foils produced 'good' adhesion of PbO_2 and Ni200 foils resulted in 'bad' adhesion of the PbO_2 deposit. (192)

Part of the objective of the present studies was to identify the factors responsible for the bad adhesion of PbO_2 onto the nickel substrate and to see what effect, if any, the addition of additives to the PbO_2 plating solution had on the adhesion of PbO_2.

Since the development of a simultaneous plating solution for Pb and PbO_2 would not be of any commercial significance unless the problem of the varying adhesion of PbO_2 to Ni substrates could be eliminated, work was therefore undertaken to re-examine the problem of PbO_2 adhesion onto Ni. The foils used for these studies, their suppliers and appearance are listed in Table 7.

TABLE 7

Ni foils used to study the factors that affect the adhesion of PbO_2 onto a Ni foil substrate

Type of foil	Thickness (μm)	Adhesion	Source	Surface Appearance
Ni200	125	'good'	R.A.R.D.E	clean/glossy finish
Ni270	200	'bad'	R.A.R.D.E	dull
Ni270	125	'bad'	Ionic Plating Co	dull, with oil interference film
Ni270	200	'bad'	Ionic Plating Co	dull

2.3.2 Pre-treatment of Ni foil prior to electrodeposition of PbO_2

The pre-treatment afforded to the Ni foil specimens prior to investigations into the etching properties of Ni foil was that used for the commercial production of battery plate material, (see Section 2.1.1.)

2.3.3 Electrochemical studies on Ni foils

The anodic behaviour of Ni foils that exhibited both good and bad adhesion of β-PbO_2 was investigated in both H_2SO_4 and $Pb(NO_3)_2$ electrolytes.

The cell used for these experiments was that shown in Fig. 7 and consists of two compartments separated by a No. 2 porosity glass frit. In one compartment was placed the Pt gauze counter electrode and a thermometer, whilst the second compartment housed the Teflon working electrode holder and a Luggin capillary attached to an S.C.E. reference electrode. The Teflon holder (see Fig. 6) was inserted through the opening near the base of the cell and was tapered to fit. The working electrodes were circular discs of Ni which were inserted into the holder and secured in position by tightening the brass locating screw. This prevented electrolyte leakage into the holder and provided a means of obtaining electrical contact; the holder also ensured that the same surface area was exposed to the solution. The potentiostatic experiments were carrried out using a Wenking PPT-70 potentiostat in conjunction with a Wenking PCA-72M potential control amplifier, with the potential continuously varied at selected sweep rates using a Wenking VSG-72 sweep generator. The E vs i curves were recorded on a Bryans X-t 28000 series chart recorder and all potentials measured using a Solartron 7045 digital voltmeter. The details of the circuitry are similar to those shown in Fig. 8.

The potentiostat was also used as an galvanostat by connecting a precision resistor between the counter electrode terminal and the reference electrode terminals. The current was varied by adjusting the 10 turn potentiometer on the front of the potentiostat.

To obtain reproducible results in the galvanostatic experiments it was found necessary to automatically vary the current output. This was achieved by connecting the sweep generator to the potentiostat then selecting the sweep speed necessary to give the desired rate of change of output current. In the present studies a value of 156 $\mu A\ cm^{-2}\ sec^{-1}$ was used.

2.3.4 Chemical analysis of Ni foil by atomic absorbtion and XRFS

The quantitative determination of the impurity content of different samples of Ni foil was carried out using a Pye atomic absorption spectrophotometer.

Standard solutions of each element to be analysed were made up and a calibration plot of absorbtion intensity versus concentration obtained over the linear absorbtion range of each element to be studied, which for Cu was 0 to 1ppm, Fe 1 to 5ppm, Mn 1 to 5ppm, Si 5 to 25ppm, Cr 0 to 1ppm and Mo 1 to 5ppm.

The unknown samples prepared by dissolving Ni in 20% HCl were then diluted by a known amount until the absorption intensity recorded on the atomic absorbtion spectrophotometer was within the linear absorbtion range of the element. The impurity level of each element in the unknown sample was then obtained from the respective calibration curve.

A semi-quantitative X-ray fluorescent (XRFS) analysis of all the samples of 'good' and 'bad' adhesion Ni foils was also carried out using a Phillips P.W 1400 spectrophotometer which enabled analysis on selected areas of Ni foil to be carried out.

2.3.5 Hardness determinations

The hardness values of Ni foils that exhibited both 'good' and 'bad' adhesion of electrodeposited PbO_2 were measured on a Vickers macrohardness machine and also with a Vickers microhardness tester attached to a microscope. In the case of the macrohardness tests a 1 kg load was used, whilst the load for the microhardness determinations was 200 g.

2.3.6 The tensile properties of Ni foils

Standard test specimens of Ni foil that exhibited 'good' and 'bad' adhesion were prepared. Sections of foil were cut to the approximate final dimensions of the test piece, and these were

then clamped firmly between two brass templates and milled until they had assumed the same dimensions as the template. The gauge length of each specimen was 68 mm and width 12.54 mm. All the specimens were cut parallel to the direction of rolling and six samples of Ni200 (125 μm thick) 'good' adhesion foil and Ni270 (200 μm) 'bad' adhesion foil were prepared for testing.

The tensile properties of each foil were determined on an Instron tensile test apparatus and the stress continuously recorded on a chart recorder connected up to a 500 kg load cell. The strain rate for the tests was 6.35 mm min^{-1}.

2.3.7 Double layer capacitance determination on nickel foils in NaOH solutions

The double layer capacitance at a fixed potential is dependent upon surface area, and experiments were carried out to determine this area for the particular Ni foils under investigation. These results were then compared with those obtained in previous work (192). The method used for the determination of double layer capacitance was that described by Gagnon (305) and used by Ramanathan (192) in his investigations on the adhesion of electrodeposited PbO_2 on Ni.

A $30cm^2$ specimen of the etched Ni foil under investigation was immersed in a solution of 8M KOH. This was made the working electrode in the electrochemical cell shown in Fig. 11, by connecting up to a Wenking PPT-70 potentiostat. The Ni foil was held at a constant potential and an alternating triangular voltage of amplitude 60mV at a scan speed of 500 mV sec^{-1} applied. The current change that occurred during the fast forward and reverse sweep was measured. The current at the change overpoint is a result of double layer charging and is related to the double layer capacitance, (assuming no Faradaic current flow at the change over potential) in the following way.

$C = \frac{Q}{V}$ by definition, where C = capacitance (Farads)

Q = charge (Coulombs)

V = potential (Volts)

also $C = \frac{It}{V}$ I = current (Amps)

t = time (seconds)

dV/dt = sweep rate V sec^{-1}

and $C = I/\frac{dV}{dt}$

2.3.8 Auger and XPS analysis of nickel foils

To explain the uneven anodic etching of Ni270 foil samples when compared to Ni200 samples, a limited investigation of the surface of each foil prior to and after anodic etching was conducted using Auger spectroscopy (AES) and X-ray photoelectron spectroscopy XPS.

Four samples of Ni sheet were studied in this way and were identified as follows :

a) Ni200, 'Good' adhesion, as received sample.

b) Ni200, 'Good' adhesion, etched in 30% H_2SO_4 at 2.7 Adm^{-2}, 50°C for 10 min.

c) Ni270, 'Bad' adhesion, as received sample.

d) Ni270, 'Bad' adhesion, etched in 30% H_2SO_4 at 2.7 Adm^{-2} 50°C for 10 min.

Sections of approximately 1 cm^2 were cut from each sample and mounted in a V.G 'Escalab' instrument.

Widescan and high resolution electron binding energy spectra were recorded (using XPS) in conjunction with argon ion beam etching on all the samples. In addition AES was used to examine the areas of different surface appearance i.e the unetched and etched areas found on different samples of Ni foil.

2.3.8.1 A.E.S analysis of nickel foils

The Auger effect is observed when excited atoms emit electrons with specific energies, which are related to the binding energies of electrons in the atomic core. The energy of the emitted electron can therefore be used to identify the individual atom. Since each atom has its own characteristic set of Auger energies and those electrons with an energy of less than 1000 eV have an escape depth of less than 2nm. Only those electrons that are emitted from the outermost surface escape and this allows analysis of only the surface atoms to be undertaken. The source of excitation for the atoms is an electron beam with an energy of 2-3 keV.

2.3.8.2 XPS analysis of nickel foils

X-ray photoelectron spectroscopy is used for chemical analysis of surfaces. Photons from 'soft' or low energy X-ray sources bombard the surface causing it to emit electrons. The number and energy of these electrons determines the composition of the surface. Indeed like Auger spectroscopy the kinetic energy of the emitted electrons is less than 150 eV and therefore only the surface atoms are analysed since these have escaped depths of only 2-3nm.

The spartial resolution of this technique is low however and a beam size of 0.4 cm^2 is used whilst with AES the beam size is only 5-10 μm enabling higher resolution on individual regions.

2.3.9 The bend test for the determination of the level of adhesion of PbO_2 onto Ni foil

Samples of Ni foil were etched as described in Section 2.1 then coated with electrodeposited PbO_2 from a solution containing 360 gl^{-1} $Pb(NO_3)_2$. The degree of adhesion of the PbO_2 coating was then tested using the bend adhesion test, i.e physically bending the plated specimen and examining the specimen for any coating detachment. The greater the extent of coating attachment the better the adhesion.

The equipment used for this test consists of a hand press and 3 press dies one of which is in position in the press. The specimen of battery plate material is cut to sufficient size to fit into the press, by a specially constructed punch and placed in the test rig.

Then the test procedure consisting of 4 separate operations is commenced (see Fig. 13).

(1) Die 1 is positioned in the hand press and the specimen placed in die 1 as shown in Fig. 13. The press was then closed so as to bend the specimen.

(2) Die 1 is replaced by die 2 and the specimen straightened out.

(3) Die 3 is positioned in the hand press instead of die 2 and the specimen bent as shown.

(4) Die 3 is used again but the specimen is reversed and bent again.

After removal from the press the bent region of the specimen was dusted and subjected to visual examination to assess the level of adhesion.

Samples of battery plate material from production runs and samples of PbO_2 electrodeposited on Ni from certain additive containing solutions were tested in this way.

An attempt was also made to quantify values for the adhesion of PbO_2 onto nickel using a tensile test method, similar to the one described by Ramanathan (192). In this instance the apparatus consisted of a plated specimen, either side of which a known area was covered with an epoxy resin into which a brass bolt was embedded. The bolts with the specimen sandwiched between them were placed in an Instron tensometer and the force required to pull the PbO_2 from the Ni surface measured.

2.3.10 Scanning Electron Microscopy (SEM) on nickel foils

Samples of etched and unetched Ni200 and Ni270 foils and failed adhesion test specimens were examined on a Hitachi SEM. Certain specimens were sputter coated with a thin layer of gold prior to investigation and photographs of the surface taken at different magnifications.

2.3.11 Back reflection X-ray examination of nickel foil

Samples of Ni200 and Ni270 both etched and unetched were examined using a Laue back scatter diffractometer to see if any evidence of preferred orientation could be detected.

Samples of Ni foil, approximate dimensions 1 x 2 cm were placed inside the diffractometer. The specimen was subjected to copper K α radiation for 10 mins at 20 kV and the back scatter diffraction pattern recorded on a photographic plate.

2.4.1 Anodic and cathodic polarisation of Pb and PbO_2 electrodes in 48% HBF_4

The Pb electrode described in Section 2.2.1 was used as the working electrode for this work whilst the electrochemical cell used and details of the electrical schematic have also been described (see Section 2.2.3).

Temperature control was achieved using a thermostatically controlled water bath.

Because of the reactivity of HBF_4, this electrolyte was removed from the glass cell immediately after each experiment.

The PbO_2 electrodes were obtained by electrodeposition from a 360 gl^{-1} $Pb(NO_3)_2$ solution at 2 Adm^{-2} and 50°C onto a Ni foil substrate. A known surface area of PbO_2 was used for each experiment.

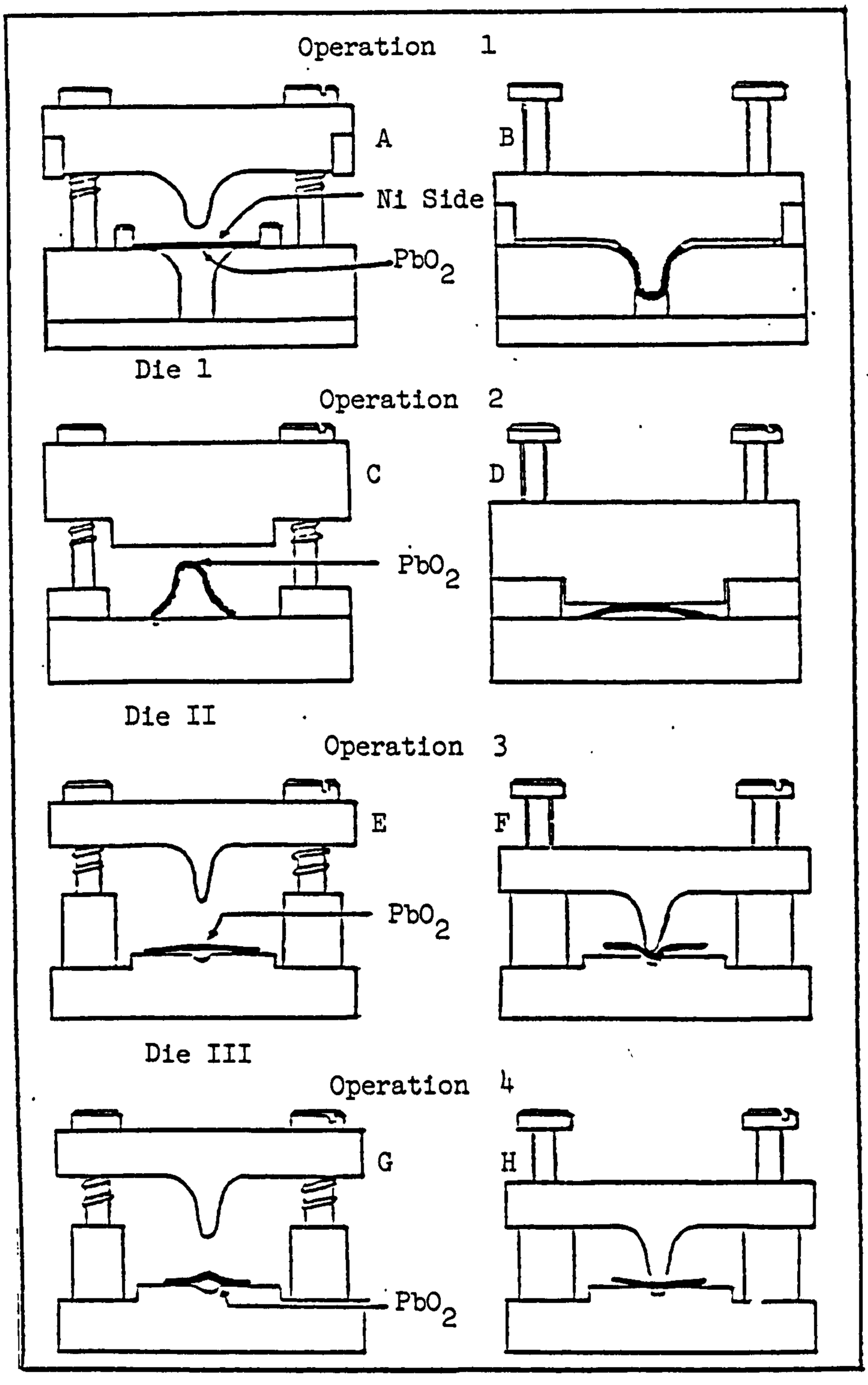

Schematic Illustration of the different Operations in the Bending Adhesion Test (reference RARDE Specification 91/71)

FIGURE 13

2.4.2 Electrochemical impedance meausrements on a Pb and PbO_2 electrode in 48% HBF_4

The Pb and PbO_2 electrodes were as described in Section 2.4.1 whilst the method of conducting the impedance measurements is that described in Section 2.2.5.

2.4.3 Thermal decomposition of PbO_2

A sample of PbO_2 was obtained by electrodeposition at 1 Adm^{-2} onto two sides of a Ni foil substrate, (4 x 3.5 cm) from a 360 gl^{-1} $Pb(NO_3)_2$ solution at 50°C, with the pH adjusted to 3.5. After 2 hr the Ni foil specimen was removed and the PbO_2 deposit detached from the Ni surface by bending the Ni foil. To aid easy removal of the PbO_2, unetched Ni foils were used.

A bulk sample of 50 g of PbO_2 obtained in this way, was then ground to a fine particle size using a pestle and mortar. The PbO_2 was then sieved through a 36 mesh to control the particle size.

The PbO_2 was dried in an oven at 110°C for 4 hr then removed and placed in a dessicator. Samples of PbO_2 approximately 1g in weight were then weighed and placed in a Stanton Thermal Balance, which had a sensitivity of 0.1 mg. The temperature was measured using a Pt/Ir thermocouple. The weight loss with time for samples of PbO_2 at selected temperatures was then recorded.

2.5 The electrochemical properties of Ni in NO_3^- solutions

High purity 99.999% cold drawn Ni rod, 5 mm in diameter and supplied by Koch Light Ltd was used as the working electrode for all experiments. Electrical connection to the Ni rod was achieved by soldering a wire to one end of the rod, and then encapsulating the Ni rod and wire connection point in epoxy resin. The Ni rod was mounted on the end of a Chance glass

syringe. This design of working electrode enabled easy mechanical polishing of the electrode surface down to 800 grade emery paper and the production of a renewable Ni surface.

The electrochemical cell shown in Fig. 11 was used for all experiments, since this allowed the position of the Ni working electrode to be adjusted as required. A Pt gauze electrode was used as the counter electrode and an S.C.E as the reference electrode.

All solutions were made up with AnalaR grade chemicals and the pH adjusted with HNO_3 or KOH to the required value. Accurate measurement of the solution pH was required and this was achieved using a Pye Unicam pH meter, calibrated with buffer solutions before each measurement.

Details of the electrical schematic and equipment used to conduct the linear polarisation and cyclic voltammetry studies have already been described (in Sections 2.2.1 and 2.2.3).

The Ni electrode was allowed to adopt a stable potential for 5 minutes in the test solution before polarisation. This standardisation of the immersion time was found necessary to achieve reproducible results.

Small quantities of selected inorganic anions and organic complexing agents were added to a 1M KNO_3 solution and the effect of these anions on the anodic polarisation characteristics of the Ni working electrode at a sweep rate of 10 mV sec^{-1} recorded.

3 RESULTS

3.1 Preliminary studies on the selection of addition agents for Pb deposition from $Pb(NO_3)_2$ solutions

The work on the selection of addition agents was concentrated on finding those additives that produced acceptable deposits of both Pb and PbO_2 from the same $Pb(NO_3)_2$ plating solution.

Previous work in these laboratories (306) had shown that the additives Triton X100 and 2-butyne-1,4-diol when added together to a $Pb(NO_3)_2$ solution, produced deposits of Pb and PbO_2 that were acceptable for use as the active material in the production of primary Pb acid batteries . However, only a few of the many possible additives for use in Pb and PbO_2 plating solutions were studied in this preliminary work, and for the present studies a more detailed search for suitable addition agents was instigated. A list of those investigated is given in Appendix 1.

Preliminary studies simply involved the addition of selected additives to a 360 gl^{-1} $Pb(NO_3)_2$ solution, electrodepositing Pb at 2 Adm^{-2} for 15 mins and then making a visual assessment of each deposit.

All the Pb deposits obtained by this method at room temperature exhibited an improved surface coverage of the nickel substrate when compared to the Pb deposited from an additive-free solution. The extent of surface coverage was dependent upon the addition agent used with the order of effectiveness for each of the few initial addition agents studied, based on visual examination found to be "Wafex" or "Wannin" (lignosulphonates) > Eugenol > hydroquinone > 2-butyne 1,4 diol > gelatin > peptone resorcinol > 2-amino-1,5-naphthol sulphonic acid.

In all these cases a nodular Pb deposit was observed with the extent of lateral growth insufficent to completely cover the substrate. An increase in the plating solution temperature to 50°C produced deposits that were non adherent and dendritic, irrespective of the additive used.

The current efficiency for Pb deposition was in most cases 90 to 95% although accurate values were difficult to obtain, since all the deposits exhibited dendrites on the edges of the nickel substrate. These often detached themselves from the Ni substrate thus giving apparently low values for the current efficiency for Pb deposition.

The effect of certain additives on the nature of the PbO_2 deposit and current efficiency for PbO_2 deposition was also investigated.

The addition of 1 gl^{-1} resorcinol to a 360 gl^{-1} $Pb(NO_3)_2$ solution from which PbO_2 was deposited at a current density of 2 Adm^{-2}, resulted in a decrease in the current efficiency for PbO_2 formation to 40%. The PbO_2 deposit itself was of poor quality and some areas of the nickel substrate remained uncovered. Hydroquinone also exhibited a similar effect to resorcinol in that this additive reduced the current efficiency for PbO_2 deposition (see Table 8).

As a result of the marked decrease in current efficiency for PbO_2 electrodeposition on the addition of the latter two additives, these were not thought worthy of further study.

The addition of eugenol (4-allyl-2-methoxyphenol) had little effect on the current efficiency for PbO_2 formation which was measured as 99%, although a yellow colouration was observed around the anode indicating some degradation of this addition agent. This additive was not completely soluble at a concentration of 1 gl^{-1} and exuded a pungent odour.

TABLE 8

The variation in the current efficiency for PbO_2 depositon at a c.d of 1 Adm^{-2} vs hydroquinone concentration in a 360 gl^{-1} $Pb(NO_3)_2$ solution at room temperature.

Hydroquinone concentration gl^{-1}	Current efficiency for PbO_2 formation at 1 Adm^{-2} %
0	98
1	88
5	54
10	21

The addition of peptone and gelatin at a concentration of 1 gl^{-1} resulted in the formation of highly stressed PbO_2 coatings, especially in the case of gelatin where the coating readily flaked off.

Wafex whilst not having such a pronounced effect on the appearance of the PbO_2 deposit at a concentration level of 1 gl^{-1} caused striatification of the PbO_2 deposit and a reduction in the current efficiency for deposition at higher concentrations. An increase in the concentration of Wafex to 5 gl^{-1} and deposition at 1 Adm^{-2}, produced a shiny PbO_2 deposit at a current efficiency of 85%.

The addition of 1 gl^{-1} butyne 1,4 diol to a 360 gl^{-1} $Pb(NO_3)_2$ solution produced PbO_2 deposits at a current efficiency of 99%,at 2 Adm^{-2} with black shiny striations in the PbO_2 deposit, which were visible on deposits obtained at room temperature, but disappeared on those produced at 50°C. Raising the additive concentration to 3 gl^{-1} did not effect the current efficiency, yet it did result in the formation of blisters in the PbO_2 deposit; this effect was only noticable at room temperature and was absent at 50°C.

The investigation of each addition agent individually was not shown to be fruitful and therefore this line of approach was discontinued. In favour of combinations of additives, which appeared to produce improved deposits of both Pb and PbO_2. Since Triton X100 was seen to be the most effective addition agent system further efforts were directed towards finding an additive that worked in conjunction with this chemical.

A stock solution of 100 gl^{-1} $Pb(NO_3)_2$ plus 2 gl^{-1} Triton X100 was made up and a second addition agent added at a concentration level of 0.5 gl^{-1}, which in some cases exceeded the saturated solubility for the additive in the stock solution. The method of assessment of the Pb coating was visual comparision of Hull Cell test panels obtained after plating at 1 A for 5 mins. The additives were then classified by their ability to produce either 'good', 'average' or 'poor' coverage of the test panel by the Pb deposit, and these results are presented in Table 9.

Some of the additives were only sparingly soluble, namely benzoin isobutyl ether; 4,4 methylene cyclohexamine; 1,4 naphthoquinone (produced a brown cloudy solution) and 2-naphthoxy acetic acid, others such as the anthraquinone disulphonic acids and mono-sulphonic acids were soluble only to a concentration level of 0.2 - 0.3 gl^{-1} whilst all the others were soluble to a concentration level of 0.5 gl^{-1}.

The additives that produced a poor surface coverage of the Pb deposit on the test panel were not used for further investigation, whilst all the other additives were investigated further by plating samples of Pb and PbO_2 at 2 Adm^{-2} from these solutions at 50°C and room temperature. The current efficiency for deposition was then determined and the surface appearance was examined visually and by SEM. These results are given in Table 10.

TABLE 9

The extent of coverage of a Pb deposit from a stock solution of 100 gl^{-1} $Pb(NO_3)_2$ + 2 gl^{-1} Triton X100 containing selected addition agents on a brass Hull Cell test panel, after a current of 1A was passed for 5 min at room temperature.

Good Coverage	Average Coverage	Poor Coverage
anthraquinone-1,5 disulphonic acid	1,5 naphthalene	eugenol
anthraquinone-2,6 disulphonic acid	1,5 aminonaphthalene	benzoin isobutyl ether
1-naphthol-4-sulphonic acid	naphtalene-1,3,6-trisulphonic acid	itaconic acid
2-naphthoylamine	gelatin	2-methoxy acetic acid
1-nitroso naphthalene disulphonic acid	2-butyne 1,4 diol	sacharin
1,4 naphthoquinone		4,4 methylene cyclohexamine
anthraquinone-2-sulphonic acid		10-camphor sulphonic acid
		glycine
		antipyrine
		2-napthoxy acetic acid

The work on linear polarisation of Pb in $Pb(NO_3)_2$ solutions (see Section 3.2.1) had shown that BRIJ 35 and Pluronic L64 (see Section 4.1.1) had a similar effect to Triton X100 on the polarisation characteristics for Pb deposition from a 0.1M $Pb(NO_3)_2$ solution. Indeed subsequent experiments showed these additives to be equally as effective as Triton X100 for Pb deposition when used in combination with another addition agent.

The low values of the efficiency for Pb deposition given on Table 10 are not attributed to the electrochemical reduction of additives or an alternative cathodic process, but to the poorly adherent nature of the Pb deposits from nitrate baths, which

TABLE 10

The variation of current efficiency and deposit appearance for Pb and PbO_2 deposited at a current density of 2 Adm^{-2} at 50°C from a solution of 100 gl^{-1} $Pb(NO_3)_2$ plus 2 gl^{-1} Triton X100 and a second addition agent.

Second addition agent	Pb efficiency %	PbO_2 efficiency %	Remarks on Pb deposit apperance	Remarks on PbO_2 deposit appearance
gelatin 0.3g/l	34.2	101	Poor coverage of substrate with Pb, some dendrites.	Smooth PbO_2 deposit, some evidence of pitting.
butyne 1,4, diol 1,5g/l	90.3	100	Poor coverage of substrate with Pb.	PbO_2 same as for a non additive solution.
anthraquinone 1,5 disulphonic acid 0.3g/l	105	98.2	Pb deposit coverage good, though some dendrites on edge of Pb specimen solution appeared.	Additive not completeley soluble at this concentration and some particlues trapped in PbO_2 deposit.
anthraquinon 2,6 disulphonic and 0.3g/l	100	99.0	Good coverage of substrate by Pb.	PbO_2 same as for non additive bath.
anthraquinone 2 sulphonic acid	97	99.0	Excellent coverage of substrate with no evidence of dendrites.	Slight staining of PbO_2 on edges, i.e. bright areas.
0.5g/l 1, naphthol 4 sulphonic acid	103	75.2	Good Pb coverage, dendrites formed on edge.	Dull smooth PbO_2 deposit.
0.5g/l 1,5 naphthylamine disulphonic acid.	91.2	96.1	Fairly good Pb coverage, evidence of dendrites on edge.	Shiny appearance highly stressed especially on edges.
0.5g/l 1,5 naphthalene disulphonic acid.	83	98.8	Fairly good Pb coverage, dendrites on edges.	Dull deposit not visibly affected by additives.
0.5g/l 1,4 naphthoquinone	101	101	Good coverage no dendrites on edges.	PbO_2 deposit the same as for the non additive solution.
0.5g/l 1,3,6 naphthalene trisulphonic acid.	80.9	99.3	Fairly good coverage on edge.	Smooth relatively uneffected.

readily detach themselves from the substrate surface during the plating or drying operations. The high values for PbO_2 current efficiencies are possibly due to incorporation of the additive in the deposit or the formation of an insoluble Pb compound on the deposit surface.

In the case of the use of the additive anthraquinone-1,5-disulphonic acid it was observed that a reddish deposit was formed at the Pb anode.

Plating at 2 Adm^{-2} from a solution of 0.5 gl^{-1} anthraquinone -1,5-disulphonic acid, 2 gl^{-1} Triton X100 and 100 gl^{-1} $Pb(NO_3)_2$ at room temperature produced an abhoreal red coloured deposit of Pb on the Hull Cell test panel at room temperature. At a lower current density of 1 Adm^{-2} the extent of dendritic growth was not as pronounced.

The use of the additives Pluronic L64 or BRIJ35 instead of Triton X100 also produced acceptable Pb deposits. However a combination of 1 gl^{-1} cetyltrimethylammonium bromide (CETB) plus 0.1 gl^{-1} anthraquinone-2-sulphonic acid when used for the electrodeposition of Pb at 2 Adm^{-2} and 50°C from a solution of 100 gl^{-1} $Pb(NO_3)_2$ resulted in only average coverage of the Ni foil substrate; Pb dendrites were produced on the edges of the Ni substrate, and the cathode efficiency was only 75%. The resultant PbO_2 deposit was smooth, fine grained and deposited at a current efficiency of 98.1%.

The work carried out by visual examination indicates that the most successful additive in terms of improving surface coverage was anthraquinone-2-monosulphonic acid when used in conjunction with Triton X100, BRIJ35 or Pluronic L64. This was indeed confirmed by more detailed SEM studies (see Section 3.1.4).

3.1.1 Studies on plating solutions found suitable for the simultaneous electrodeposition of Pb and PbO_2

The effect of $Pb(NO_3)_2$ concentration on the current efficiency for Pb and PbO_2 formation when deposited at 2 Adm^{-2} from a solution containing 360 gl^{-1} $Pb(NO_3)_2$ +0.1 gl^{-1} anthraquinone-2-sulphonic acid and 3 gl^{-1} of either Triton X100, BRIJ35 or Pluronic L64 is shown in Table 11. No marked variation in current efficiency was detected, although there was a tendency for the current efficiency for PbO_2 formation to be greater than 100%, whilst in the case of Pb deposition, the value was nominally 99%.

TABLE 11

The effect of $Pb(NO_3)_2$ concentration on the current efficiency for Pb and PbO_2 deposition from $Pb(NO_3)_2$ solutions containing 3 gl^{-1} surfactant plus 0.1 gl^{-1} anthraquinone-2-sulphonic acid, at 50°C

Concentration $Pb(NO_3)_2$	Current efficiency at at 2 Adm^{-2}		Surfactant
gl^{-1}	Pb%	PbO_2%	
360	99	101	Triton X100
	99	102	BRIJ35
	99	102	Pluronic L64
270	99	101	Triton X100
	99	102	BRIJ35
	99	100	Pluronic L64
180	99	99	Triton X100
	99	101	BRIJ35
	99	99	Pluronic L64
45	98	96	Triton X100
	98	98	BRIJ35
	98	90	Pluronic L64

The lower current efficiency for PbO_2 formation at low $Pb(NO_3)_2$ concentrations, is thought to be due to the accompanying process of oxygen evolution (see Table 12). However, the low PbO_2 formation efficiency for low concentration $Pb(NO_3)_2$ solutions containing Pluronic L64 is thought to be due to oxidation of this additive as well as oxygen evolution.

TABLE 12

The variation in current efficiency for PbO_2 deposition with $Pb(NO_3)_2$ concentration in a non additive solution at 50°C and at a c.d of 2 Adm^{-2}

Mean current efficiency %	Concentration of $Pb(NO_3)_2$ solution pH 3.6 gl^{-1}
100.6	360
98.4	180
97.4	90
95.1	45

In the case of Pb deposition from a 360 gl^{-1} $Pb(NO_3)_2$ solution containing 3 gl^{-1} Triton X100 and 0.1 gl^{-1} anthraquinone-2-monosulphonic acid, at a low c.d (1 Adm^{-2}) the deposit was of dull appearance with poor surface coverage; at higher c.d.s e.g 3 Adm^{-2} there was an increase in the extent of dendritic growth on the edges of the specimen with no apparent change in the surface coverage (see Table 13).

TABLE 13

The effect of the concentration of different surfactants in a solution of 0.1 gl^{-1} anthraquinone-2-sulphonic acid + 360 gl^{-1} $Pb(NO_3)_2$ on the current efficiency for Pb and PbO_2 deposition

Additive concentration gl^{-1}	Additive	Current efficiency for deposition at 2 Adm^{-2} Pb%	PbO_2%	Remarks
0	Triton X100	99	102	Increase in additive concentration decreases the amount of dendritic growth in the high c.d regions
0.5		82	100	
1		97	100	
1.5		97	99	
2		97	102	
3		99	102	
0	Pluronic L64	99	102	Solution goes cloudy on heating; increase in additive concentration decreases extent of dendritic growth on edges of specimen
0.5		86	102	
1		90	101	
1.5		97	100	
2		97	99	
3		101	102	
0	BRIJ35	99	101	Dull deposits of Pb in centre of specimen no dendrites on edges of specimen
0.5		97	100	
1		100	101	
1.5		100	102	
2		101	100	
3		101	103	

N.B. The results above are quoted to one significant place since they were the result of only one separate determination

3.1.1.1 The effect of $NaCH_3COO$ and other additives on Pb and PbO_2 deposits obtained from $Pb(NO_3)_2$ solutions

The addition of sodium acetate to a 180 gl^{-1} $Pb(NO_3)_2$ solution on the current efficiency for Pb and PbO_2 deposition from a solution containing the optimum additive concentration of 3 gl^{-1} Triton X100 and 0.1 gl^{-1} anthraquinone-2-mono sulphonic acid was also investigated, up to a concentration of 40 gl^{-1} $NaCH_3COO$. No apparent change in current efficiency with current density was observed. The nature of the Pb deposits obtained by plating at 2 Adm^{-2} and at 50°C was not visibly different to that obtained from the non-acetate solutions. However, at 40 gl^{-1} $NaCH_3COO$ a shiny PbO_2 deposit was produced whilst at 10 gl^{-1} $NaCH_3COO$ a dull-black smooth deposit was obtained. In the case of Pb deposits obtained from these solutions at room temperature under the same conditions the extent of dendritic growth increased with increase in the acetate concentration. At a current density of 0.5 Adm^{-2} no dendritic growth on the edges of samples was recorded until the acetate concentration reached 40 gl^{-1}.

The effect of certain additives on the efficiency for PbO_2 formation at selected current densities from a 360 gl^{-1} $Pb(NO_3)_2$ solution is given in Table 14.

A colour change was observed in the Wafex-containing solutions used for PbO_2 deposition, whilst with peptone as an additive a striated PbO_2 deposit was obtained at 2 Adm^{-2} and at a lower current density 0.5 Adm^{-2} a very smooth highly reflective PbO_2 surface was produced. Solutions containing CETB also produced a smooth PbO_2 deposit but did not improve the nature of the Pb deposit obtained.

TABLE 14

The variation of the current efficiency for PbO_2 deposition with current density and addition agent

Additive	Current efficiency for PbO_2 formation at selected current densities from a 360 gl^{-1} $Pb(NO_3)_2$ solution at 50°C		
	1 Adm^{-2}	2 Adm^{-2}	4 Adm^{-2}
No additive	98	100	101
Peptone 0.5 gl^{-1}	95	98	99
CETB 1 gl^{-1}	99	96	83
Wafex 1 gl^{-1}	94	95	67

3.1.1.2 Room temperature electrodeposition of Pb from $Pb(NO_3)_2$ solutions

The addition agents discussed so far were not particularly suited to room temperature deposition, primarily because of the ease with which dendrites where formed on the specimen edges even at low c.d.s. The nature of the Pb deposit obtained with certain additive combinations at room temperature was filamentary, and consequently very fragile. During the course of the present studies it was discovered that deposits of Pb obtained in the presence of the additive tannic acid at room temperature were non-filamentary, and showed no evidence of dendritic growth until relatively high c.d.s. The major drawback in the use of this additive for the simultaneous electro-

deposition of Pb and PbO_2 was that HNO_3 must be added to ensure complete solubility of the tannic acid. At the resulting low pH obtained using HNO_3, the nickel anode was found not to remain passive.

The optimum deposit properties in terms of surface coverage were achieved when tannic acid was used in combination with another addition agent. Aloin was used for the initial experiments but later work showed a combination of tannic acid and Wafex (a sodium lignosulphonate) to be the most effective.

Hull Cell tests on solutions of $Pb(NO_3)_2$ (of varying concentration) plus 20 gl^{-1} HNO_3, 2 gl^{-1} tannic acid and 2 gl^{-1} Wafex at room temperature were used to determine the optimum plating ranges over which deposition may occur.

For a $Pb(NO_3)_2$ solution concentration 45 gl^{-1}, the plating range was 3.5 to 0.1 Adm^{-2}, at 90 gl^{-1}, 7 to 0.7 Adm^{-2} and at 135 gl^{-1} between 15 to 0.8 Adm^{-2} all at room temperature. At elevated temperatures the Pb deposit was of noticeably inferior porosity and a wide plating range obtained at a given $Pb(NO_3)_2$ concentration.

3.1.2 Porosity determinations on Pb electrodeposited onto Ni

The technique of porosity determination has been described in Section 2.1.2 and involves measurement of the anodic polarisation properties of both Ni and Pb.

The values of i_{pp} for Ni in 1.5M H_2SO_4 were found to be dependent upon the pre-treatment afforded to the nickel foil prior to testing. Samples of Ni200 supplied by RARDE, cathodically cleaned but not subjected to an anodic etch in 30% H_2SO_4, were found to give lower values of i_{pp} than samples of the same foil subjected to cathodic cleaning and anodic etching in 30% H_2SO_4 at 50°C at a c.d of 2.7 Adm^{-2} for 10 min.

However, this effect is what would be expected, since the anodically etched specimens have a higher surface area. Indeed it is usual practice for all nickel specimens to be subjected to an anodic etch prior to Pb deposition, as this improves the adhesion of the Pb. The value of i_{pp} chosen as the standard for porosity determinations was therefore obtained on etched Ni200 foils. The substrate used for Pb deposition from simultaneous plating solutions.

An E vs log i curve for unetched Ni200 foil is shown in Fig 14. The value of i_{pp} of 11.5 Adm^{-2} for this foil is in good agreement with previously reported values, although the values of i_{pp} for different unetched Ni200 samples were not reproducable and were subject to some degree of scatter. The value of E_{pp} of + 0.3V is lower by 0.14V than previously reported values (192). However, this low value of E_{pp} appeared to be a valid result for this particular sample of foil.

In the case of etched nickel foil, the mean value of i_{pp} for a number of Ni200 foil samples was 35 Adm^{-2} and it was this value that was used as the constant in the porosity determinations.

A plot of E vs i for a specimen of pure Pb in 1.5M H_2SO_4 is shown in Fig 15. This specimen was held at -0.250V for 5 min and then anodically polarised at 3 mV sec^{-1} from this potential. The initially high current is due to the formation of $PbSO_4$ and decreases as the Pb potential is made more positive. At the value of E_{pp} for Ni in H_2SO_4 (+0.30V) i_{pass} for Pb is 0.0022 Adm^{-2} which is considerably lower than the value of i_{pp} obtained on unetched Ni of 11.5 Adm^{-2} at this potential. These figures indicate that the passivity of Pb and the activity of Ni in H_2SO_4 may well be a suitable method of measuring the porosity of the Pb plate, even at low values of porosity.

To test the suitability of the proposed method for assessing porosity, Pb was deposited from a standard $Pb(BF_4)_2$ bath (230 gl^{-1} $Pb(BF_4)_2$) at 2 Adm^{-2} for 15 min. The E vs i curve obtained when a section of this Pb plate was polarised at 3 mV sec^{-1} in 1.5M H_2SO_4 is shown in Fig. 16. The current (a) at E = 0.212V is the value of i_{pp} for Ni in this environment, less a value of i_{pass} for Pb at this potential. The value of i_{pass} was obtained by drawing a straight line between points (1) and (2) and noting the value of current on the line that is obtained when peak (a) is reached. The value of the exposed Ni area was then expressed as a percentage as follows :-

$$\text{Porosity value \%} = \frac{i_{pp} \text{ (electrodeposited Pb)} - i_{pass} \text{ Pb}}{i_{pp} \text{ etched Ni}} \times 100\%$$

In the case of Fig 16, the porosity value obtained is 0.015%. The value of E_{pp} for the electrodeposited coating is 0.1V lower than that for uncoated nickel, which may be attributed to concentration polarisation in the deposit pores i.e rapid build up of corrosion products, causing premature passivation of the exposed nickel surface. Indeed at this potential i_{pp} for Ni would not have been reached and the Ni dissolution current at this potential is lower than the value of i_{pp} used as the constant in the above equation. Therefore, using i_{pp} etched Ni in this case would in fact give an incorrect indication as to the exposed surface area of the Ni.

Fig. 17 shows the E vs i curve for Pb electrodeposited onto Ni from the same $Pb(BF_4)_2$ bath yet for 30 min at 2 Adm^{-2}, which corresponds to a coating thickness of 34 µm. A similar curve to Fig 16 is recorded except that E_{pass} for is lowered to + 0.190V and the value of i_{pp} (electrodeposited coating) - i_{pass} Pb, of 19 μAcm^{-2} is lower than the value of 54 μAcm^{-2} for a 17 µm coating.

The primary objective of this work was to assess the effect of different addition agents and deposition parameters on the porosity of Pb deposits, the method used does appear to provide

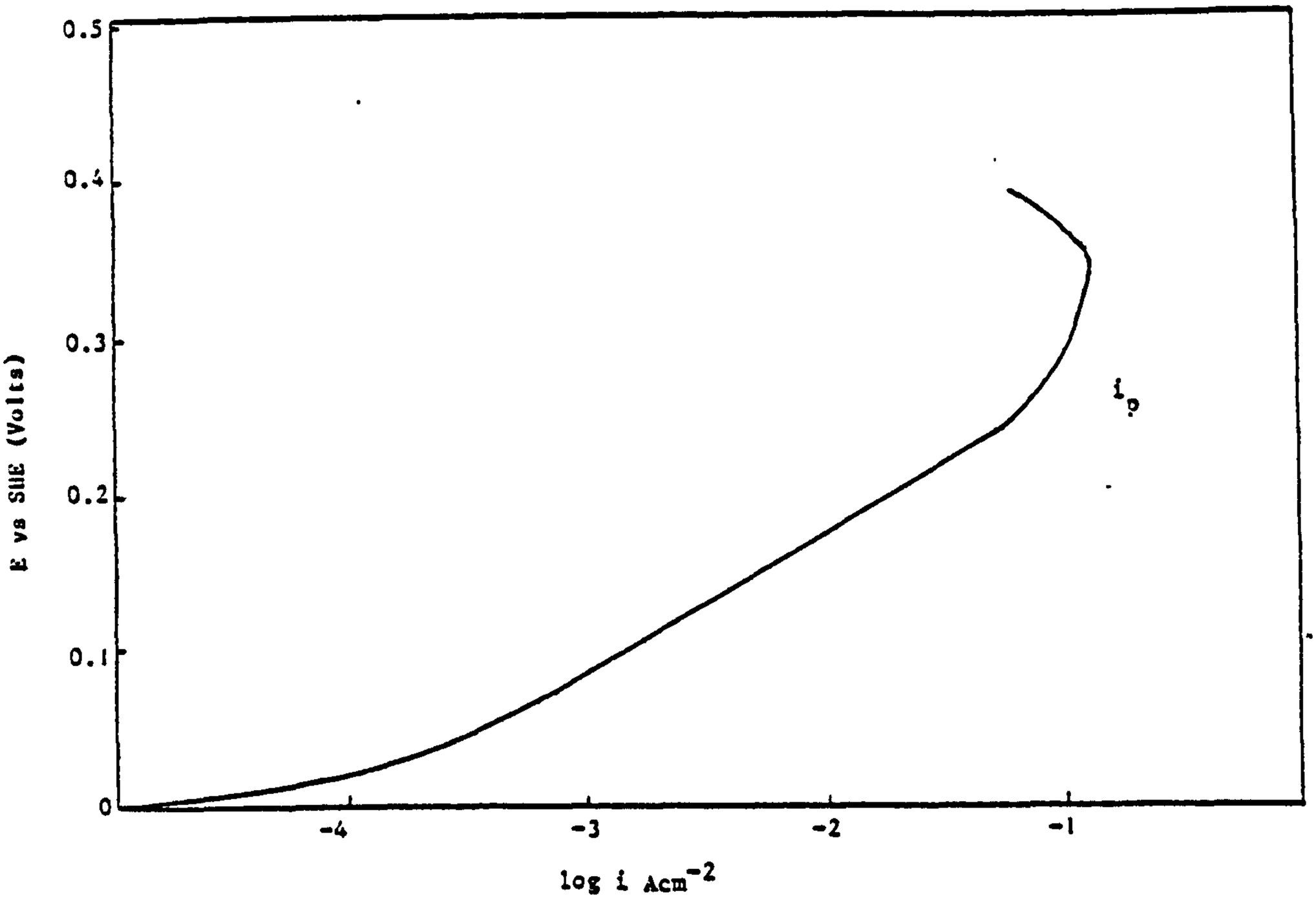

E vs log i curve for Ni200 anodically polarised at a sweep rate of 3mV sec^{-1} in a 1.5M H_2SO_4 solution at 25°C.

FIGURE 14

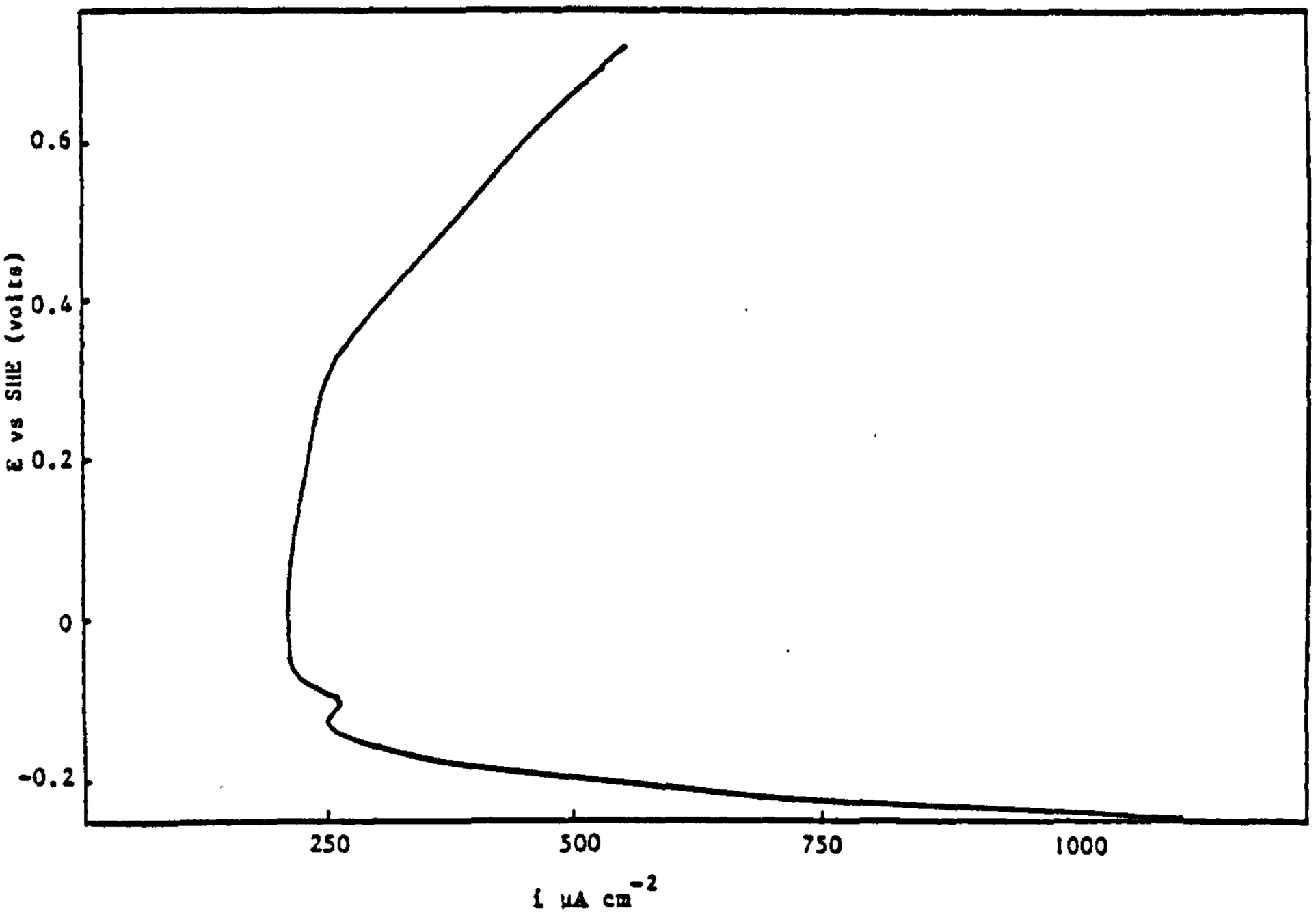

A graph of E vs i for a Pb electrode anodically polarised at a sweep rate of 3mV sec^{-1} in a 1.5 M H_2SO_4 solution. The specimen held at a potential of -0.250 Volts for 5 minutes before polarisation.

FIGURE 15

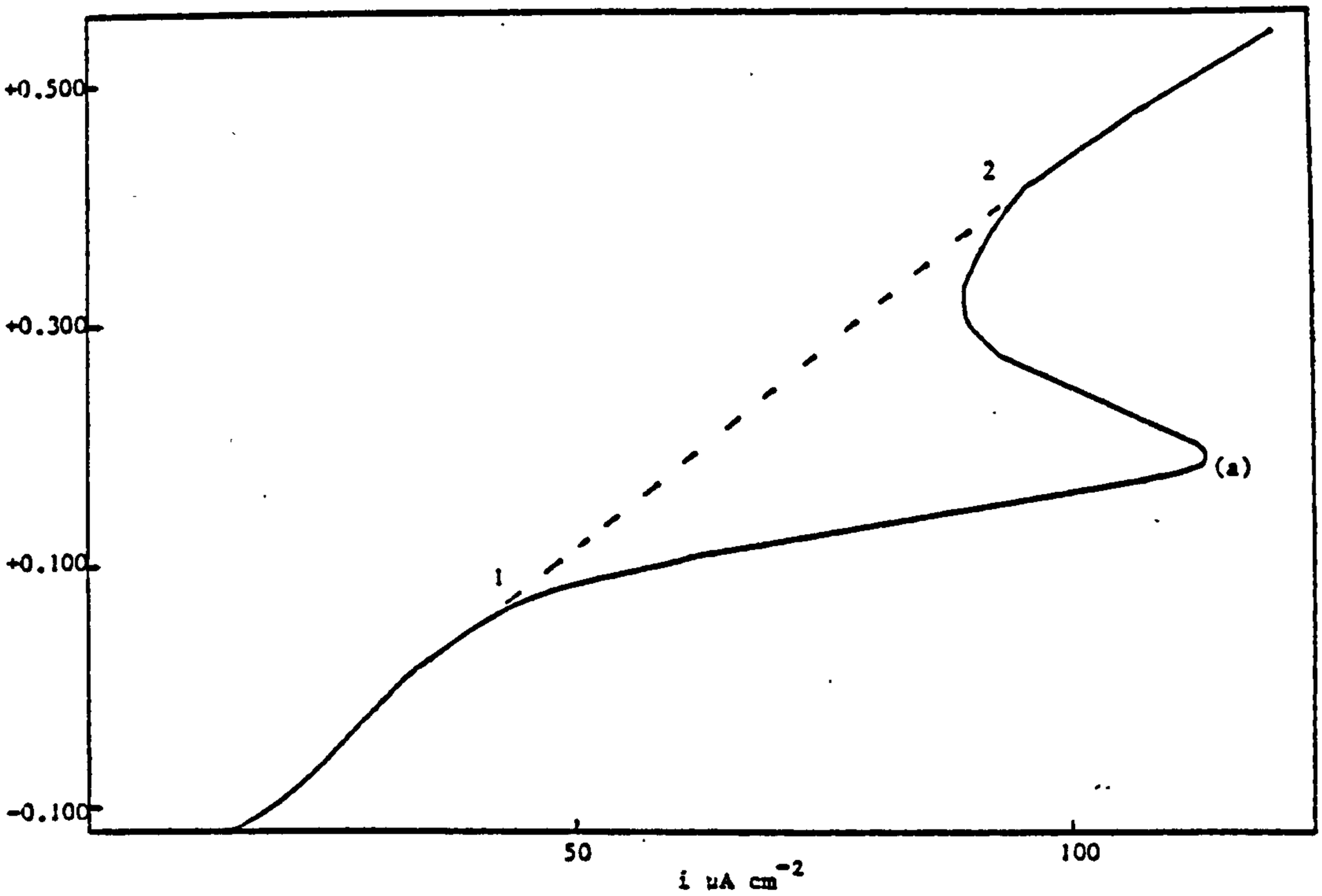

A graph of E vs i for a sample of Pb electrodeposited onto Ni at 2 Adm^{-2} for 15 minutes from a solution of 230 gl^{-1} $Pb(BF_4)_2$. The Pb electrodeposit anodically polarised at 3mV sec^{-1} in a solution of 1.5 M H_2SO_4 and held at a potential of -0.110 Volts vs SHE for 5 minutes before polarisation.

FIGURE 16

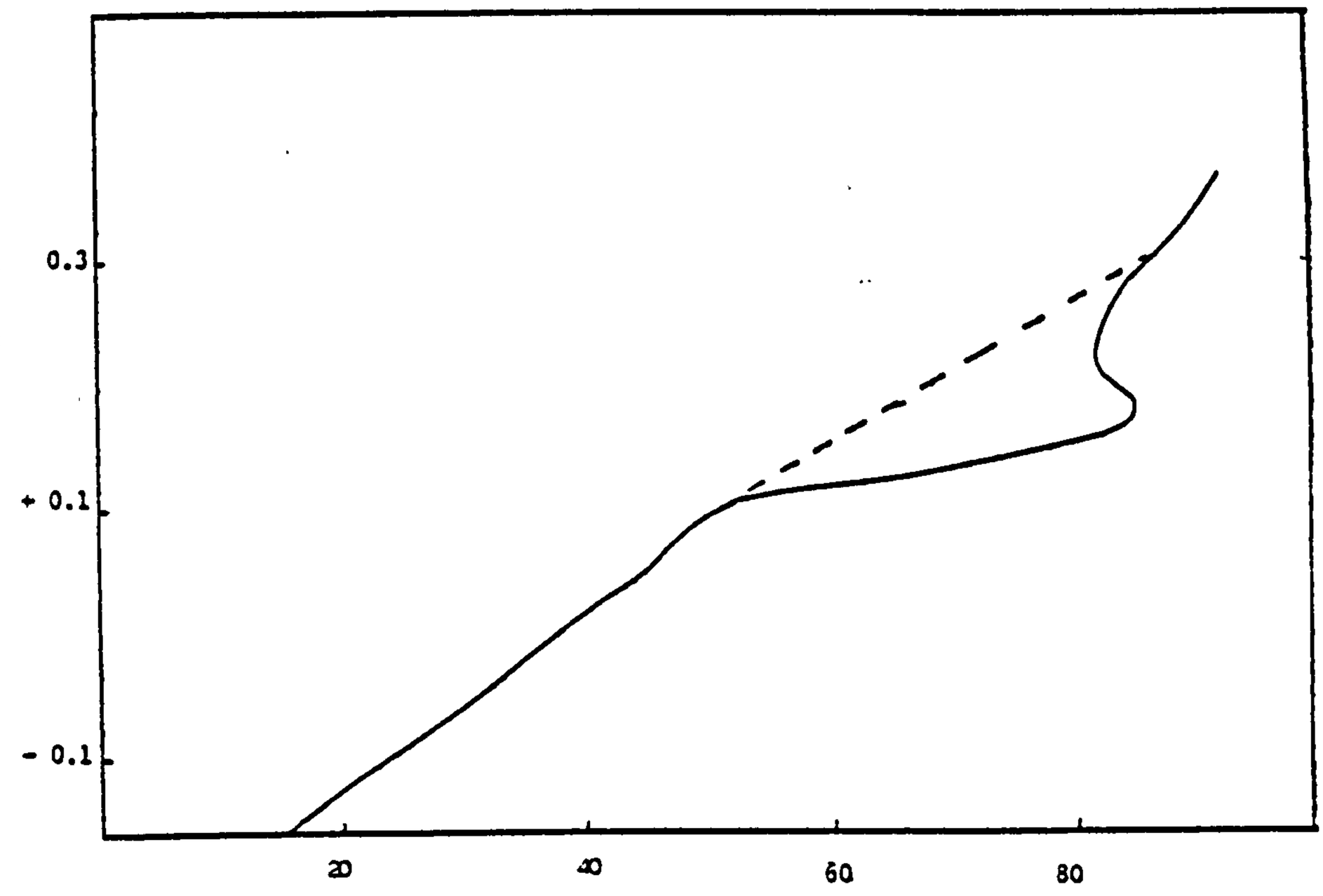

A graph of E vs i for a sample of Pb electrodeposited onto Ni at 2 Adm^{-2} 30 minutes from a solution of 230 gl^{-1} $Pb(BF_4)_2$. The Pb electrodeposit anodically polarised at 3mV sec^{-1} in a solution of 1.5M H_2SO_4 and held at a potential of -0.110 Volts vs SHE for 5 minutes before polarisation.

FIGURE 17

a reasonably satisfactory indication of porosity and surface coverage. There was some degree of scatter in the results obtained, which is as would be expected since the porosity was not considered to be uniform over the specimen surface. For example, the values of i_{pp} (coating) minus the value for the background current for Pb dissolution for 4 samples of Pb electrodeposited onto Ni from a $Pb(BF_4)_2$ plating solution for 15 minutes at 2 Adm^{-2} varied as follows :

54 μAcm^{-2}, 130 μAcm^{-2}, 140 μAcm^{-2} and 118 μAcm^{-2}.

Porosity determinations on Pb electrodeposited from $Pb(NO_3)_2$ solutions were used to assess the effectiveness of different addition agents, and the effect of addition agent concentration and c.d on the surface coverage of the Pb deposit.

The results on Pb coatings obtained from conventional plating solutions show that this technique is suitable for detecting small levels of porosity and is useful in comparing the porosity of these coatings with those obtained from $Pb(NO_3)_2$ plating solutions.

3.1.2.1 The effect of different addition agents on the porosity of Pb electrodeposited from $Pb(NO_3)_2$ solutions

Work on the selection of addition agents has shown that the additive Triton X100 in conjunction with another organic addition agent, produces acceptable deposits of Pb from $Pb(NO_3)_2$ solutions. To select a suitable second addition agent a stock solution of 100 gl^{-1} $Pb(NO_3)_2$ plus 2 gl^{-1} Triton X100 was made up and small quantities of addition agent were added. The deposits of Pb obtained from the stock solution plus the second addition agent were then examined visually and their porosity measured. The results of the porosity determinations for selected addition agents are given in Table 15. All the samples for porosity determination were of the same nominal Pb thickness (17 µm) and were obtained by plating at 2 Adm^{-2} for 15 min at 50°C. The temperature of the plating

solution was maintained at 50°C since this is the temperature at which PbO_2 is deposited from commercial $Pb(NO_3)_2$ solutions, and any bath used for the simultaneous deposition of both Pb and PbO_2 would have to be capable of operation at this temperature.

From Table 15 it can be seen that the best additive in terms of producing low porosity Pb deposits was anthraquinone-2-mono sulphonic acid, though at 0.3 gl^{-1} this additive is not completely soluble in the solution, since it forms insoluble lead salts. The additive 1,4 napthoquinone also showed promise, although the solubility of this additive is again limited. The additive anthraquinone-2-monosulphonic acid was selected for further studies in conjunction with Triton X100.

A decrease in c.d. from 2 Adm^{-2} to 1 Adm^{-2} was found to have no significant effect on the porosity value, and if anything slightly lower values where recorded at higher c.d.s, e.g for a solution of 100 gl^{-1} $Pb(NO_3)_2$ plus 2 gl^{-1} Triton X100 and 1.5 gl^{-1} butyne 1,4 diol, the mean porosity value was 19.3% at 2 Adm^{-2} and 23% at 1 Adm^{-2}.

A typical E vs i curve for Pb electrodeposited onto Ni from this solution at 2 Adm^{-2} for 15 min and subjected to the porosity test is shown in Fig. 18. Owing to the poor surface coverage of the nickel substrate by the Pb a high polarisation current is recorded, and E_{pass} for the coating is the same as for the pure Ni foil.

Using anthraquinone-2-monosulphonic acid as the selected addition agent for Pb deposition from $Pb(NO_3)_2$ solutions, experiments were conducted to determine the effectiveness of Triton X100 and other surface active agents, notably Pluronic L64 and BRIJ35 in improving the properties of the Pb deposit.

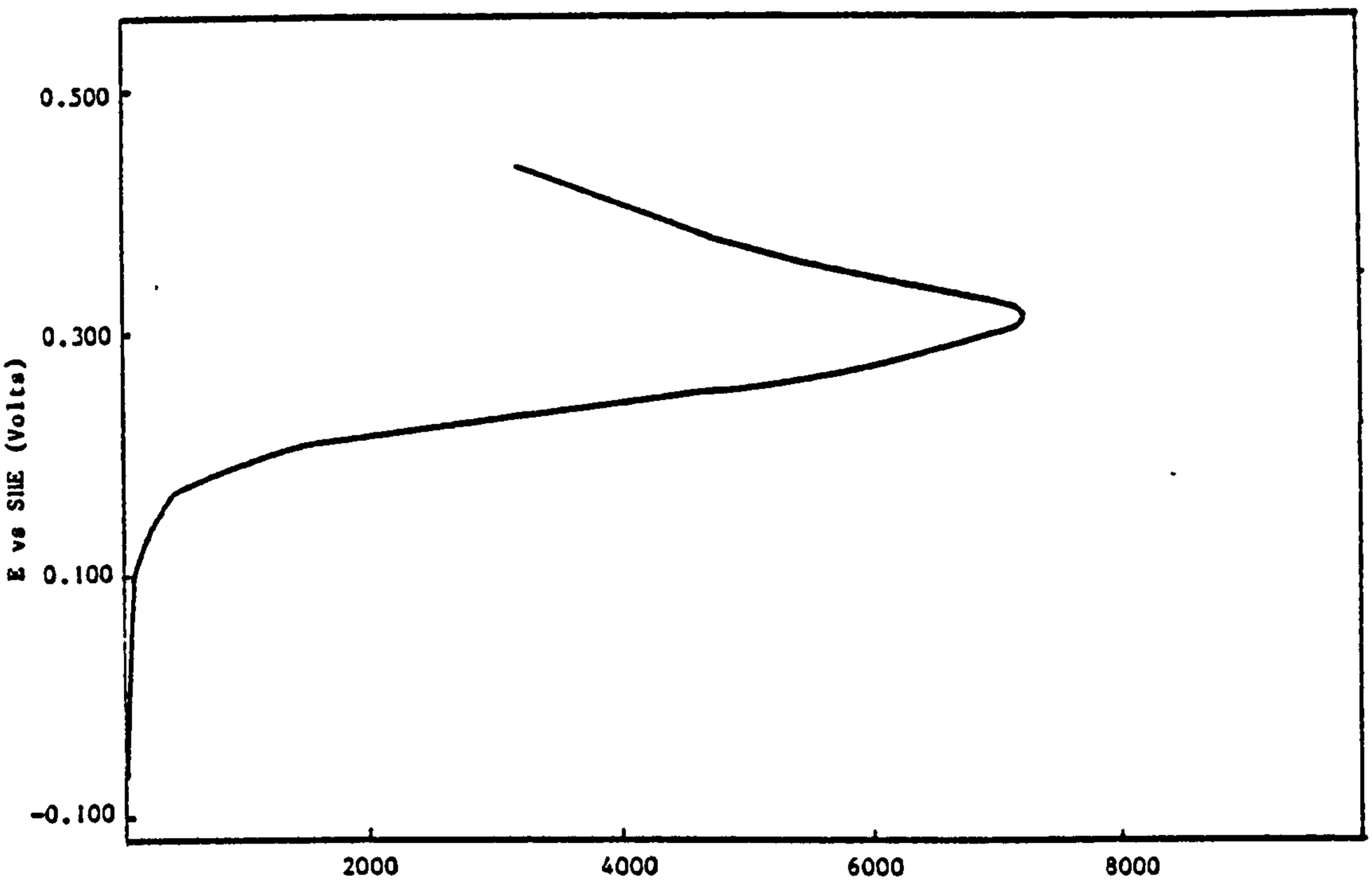

A graph of E vs i for a sample of Pb electrodeposited onto Ni at 2 Adm^{-2} for 15 minutes at 50°C from a solution of 100 gl^{-1} $Pb(NO_3)_2$ plus 2 gl^{-1} Triton X100, 1.5 gl^{-1} butyne 1,4 diol. The Pb electrodeposit anodically polarised at 3mV sec^{-1} in a solution of 1.5M H_2SO_4 and held at a potential of -0.11 Volts vs SHE for 5 minutes before polarisation.

FIGURE 18

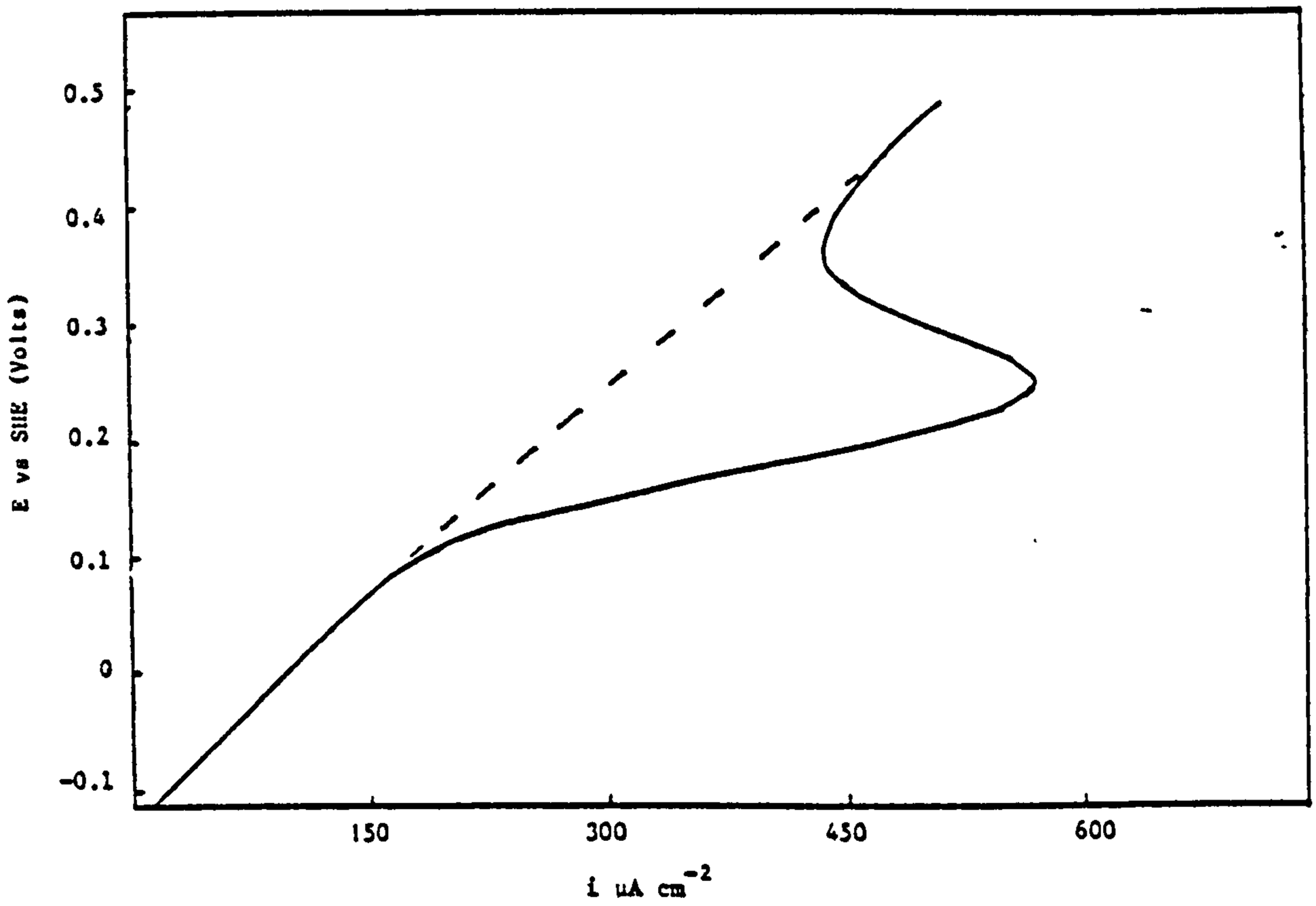

A graph of E vs i for a sample of Pb electrodeposited onto Ni at 2 Adm^{-2} for 15 minutes at a temperature of 50°C from a solution of 100 $gl^{-1}Pb(NO_3)_2$ plus 3 gl^{-1} Triton X100, 0.1 gl^{-1} anthraquinone-2-monosulphonic acid. The Pb electrodeposit anodically polarised a 3mV sec^{-1} in a solution of 1.5M H_2SO_4 and held at a potential of -0.110 Volts vs SHE for 5 minutes before polarisation.

FIGURE 19

TABLE 15

The effect of a second addition agent on the porosity of Pb electrodeposits. (Samples plated at 2 Adm^{-2} for 15 min at 50°C from a stock solution of 100 gl^{-1} $Pb(NO_3)_2$ plus 2 gl^{-1} Triton X100).

Concentration	Second Addition Agent	Mean Porosity %
0.5 gl^{-1}	naphthalene-1,3,6-trisulphonic acid	33.7
0.3 gl^{-1}	gelatin	25.6
0.3 gl^{-1}	naphthalene-1,5 disulphonic acid	24.8
0.3 gl^{-1}	naphthol	24.3
0.3 gl^{-1}	1 nitroso-3,6 naphthol disulphonic acid	21.0
1.5 gl^{-1}	butyne 1,4 diol	19.3
0.3 gl^{-1}	1-naphthylamine-6,8-disulphonic acid	15.0
0.5 gl^{-1}	1 naphthol 4 sulphonic acid	6.8
0.3 gl^{-1}	1,5 anthraquinone	5.9
0.3 gl^{-1}	anthraquinone-1,5-disulphonic acid	1.54
0.3 gl^{-1}	anthraquinone-2,6-disulphonic acid	1.15
0.5 gl^{-1}	1,4 naphthoquinone	0.4
0.3 gl^{-1}	anthraquinone-2-monosulphonic acid	0.21

Cetyltrimethylammonium bromide (CETB) was also used as an addition agent, but was found to be unsuitable for use in $Pb(NO_3)_2$ solutions e.g a value of Pb porosity of 52.5% was recorded for deposits obtained by electrodeposition at 1 Adm^{-2} from a 100 gl^{-1} $Pb(NO_3)_2$ solution containing 1 gl^{-1} CETB + 0.1 gl^{-1} anthraquinone-2-mono sulphonic acid. The results show that porosity is dependent upon Pb concentration and at very low concentrations approaches that of Pb electrodeposited from a $Pb(BF_4)_2$ bath (see Table 16).

TABLE 16

Variation of mean deposit porosity with $Pb(NO_3)_2$ concentration for Pb plated onto nickel at 2 Adm^{-2} for 15 min at 50°C from a $Pb(NO_3)_2$ solution containing 0.1 gl^{-1} anthraquinone-2-monosulphonic acid plus selected addition agents

$Pb(NO_3)_2$ concentration gl^{-1}	Porosity %		
	Triton X100 $3gl^{-1}$	Pluronic L64 $3gl^{-1}$	BRIJ35 $3gl^{-1}$
360	3.4	3.6	10.2
270	0.10	4.9	3.0
180	0.17	2.2	1.0
100	0.21	0.48	0.8
45	0.011	0.047	0.054

The highest values for porosity were recorded from a 360 gl^{-1} $Pb(NO_3)_2$ solution, with the porosity decreasing with decrease in $Pb(NO_3)_2$ concentration. It was found difficult to obtain reproducible results for porosity at high Pb^{2+} concentrations because of the difficulty in dissolving the additive anthraquinone-2-monosulphonic acid in these solutions. This problem was solved by dissolving this additive in water first before adding it to the plating solution, so as to achieve the optimum results.

An E vs i curve for Pb electrodeposited onto Ni from a solution of 100 gl^{-1} $Pb(NO_3)_2$ + 2 gl^{-1} Triton X100 + 0.1 gl^{-1} anthraquinone-2-monosulphonic acid, and polarised at 3 mV sec^{-1} in a solution of 1.5M H_2SO_4 is shown in Fig. 19. The porosity value of 0.08% for this particular sample is lower than the mean value of 0.21% obtained from other porosity determinations.

Table 17 shows the effect of Triton X100 concentration on the porosity of Pb electrodeposited from a solution of 0.1 gl^{-1} anthraquinone-2-monosulphonic acid and 100 gl^{-1} $Pb(NO_3)_2$. The results show that the porosity decreases with increase in concentration of Triton X100 and that the concentration of Triton X100 should be maintained above 2 gl^{-1} to obtain a low porosity and hence a high surface coverage of the substrate by the Pb deposit.

TABLE 17

The effect of Triton X100 concentration on the porosity of Pb deposited from a solution of 100 gl^{-1} $Pb(NO_3)_2$ plus 0.1 gl^{-1} anthraquinone-2-monosulphonic acid

Triton X100 concentration gl^{-1}	Mean porosity of Pb deposit after 15 min plating at 2 Adm^{-2} and a temperature of 50°C %
0	13.3
0.5	1.99
1.0	1.29
1.5	0.76
2	0.35
3	0.09

From the porosity values measured it was observed that samples of Pb electrodeposited from additive containing $Pb(NO_3)_2$ solutions exhibited lower porosities when deposited at 50°C than when deposited at room temperature.

3.1.2.2 Effect of current density on Pb porosity

The effect of c.d. at selected addition agent concentrations was also investigated. The addition agent combinations studied were BRIJ35, Pluronic L64 and Triton X100 each used in conjunction with 0.1 gl^{-1} anthraquinone-2-monosulphonic acid. The $Pb(NO_3)_2$ concentration was kept constant at 100 gl^{-1} and all samples were deposited at 50°C. The results of porosity at different current densities are shown in Tables 18, 19, and 20.

TABLE 18

The variation in the porosity of Pb electrodeposited from a solution of 100 gl^{-1} $Pb(NO_3)_2$ plus 0.1 gl^{-1} anthraquinone-2-monosulphonic acid at 50°C with c.d. and BRIJ35 concentration

Current Density Adm^{-2}	Porosity % at a given BRIJ 35 concentration				
	0.5 gl^{-1}	1 gl^{-1}	1.5 gl^{-1}	2 gl^{-1}	3 gl^{-1}
1				1.10	0.14
2	2.10	1.2	0.86	0.23	0.14
3				1.15	0.13
4				2.24	0.17
5				0.7	0.19

TABLE 19

The variation in the porosity of Pb electrodeposited from a solution of 100 gl^{-1} $Pb(NO_3)_2$ plus 0.1 gl^{-1} anthraquinone-2-monosulphonic acid at 50°C with c.d. and Pluronic L64 concentration

Current Density Adm^{-2}	Porosity % at a given Pluronic L64 concentration				
	0.5 gl^{-1}	1 gl^{-1}	1.5 gl^{-1}	2 gl^{-1}	3 gl^{-1}
1				0.25	0.66
2	2.9	1.18	1.05	0.17	0.25
3				1.17	0.39
4				2.0	0.10
5				5.0	0.14

TABLE 20

The variation in the porosity of Pb electrodeposited from a solution of 100 $gl^{-1}Pb(NO_3)_2$ plus 0.1 gl^{-1} anthraquinone-2-monosulphonic acid at 50°C with c.d. and Triton X100 concentration

Current Density Adm^{-2}	Porosity % at a given Triton X100 concentration				
	0.5 gl^{-1}	1 gl^{-1}	1.5 gl^{-1}	2 gl^{-1}	3 gl^{-1}
1				1.1	0.12
2	1.9	1.29	0.76	0.29	0.09
3				1.1	0.02
4				2.2	0.2
5				3.5	0.1

These results are difficult to interpret and all those quoted are the mean of at least 3 separate determinations. Further investigations would be required to determine the validity of these results.

TABLE 21

The variation of Pb porosity with thickness for Pb deposits from different plating solutions

Plating time (minutes)	Mean % porosity values for different plating solutions					
	230 gl^{-1} $Pb(BF_4)_2$ + 0.1 gl^{-1} Gelatin	360 gl^{-1} $Pb(NO_3)_2$ 2 gl^{-1} Triton X100 0.1 gl^{-1} An2S	180 gl^{-1} $Pb(NO_3)_2$ 2 gl^{-1} Triton X100 + 0.1 gl^{-1} An2S	180 gl^{-1} $Pb(NO_3)_2$ 2 gl^{-1} Pluronic L64 + 0.1 gl^{-1} An2S	180 gl^{-1} $Pb(NO_3)_2$ + 2 gl^{-1} Triton X100 + 1.5 gl^{-1} butyne diol	180 gl^{-1} $Pb(NO_3)_2$ 40 gl^{-1} $NaCH_3COO$ 2 gl^{-1} Triton 0.1 gl^{-1} An2s
3	0.97	8.8	7.4	9.9	12.3	7.0
9	0.20	6.6	9.5	8.1	13.4	7.7
12	0.35	4.0	4.4	1.2	10.3	2.9
15	0.025	3.4	0.18	2.2	10.2	0.78
30	0.005	1.03	0.54	0.52	(not measured)	0.27

N.B. An2S = anthraquinone-2-monosulphonic acid

TABLE 22

Thickness of the Pb deposit obtained from different plating solutions after different plating times at 2 Adm^{-2} and 50°C. The thickness measured on a betascope

Plating time at 2 Adm^{-2} time (minutes)	Theoretical deposit thickness at 2 Adm^{-2} at different plating times /µm	Plating Solutions						
		230 gl^{-1} $Pb(BF_4)_2$	360 gl^{-1} $Pb(NO_3)_2$ 3gl^{-1} Triton X100 + 0.1 gl^{-1} An2S	180 gl^{-1} $Pb(NO_3)_2$+ 3 gl^{-1} Triton X100 0.1 gl^{-1} An2S	360 gl^{-1} $Pb(NO_3)_2$ Triton X100 + 1.5 gl^{-1} butyne diol	180 gl^{-1} $Pb(NO_3)_2$ + 3 gl^{-1} Pluronic An2S 0.1 gl^{-1}	180 gl^{-1} $Pb(NO_3)_2$ + 10 gl^{-1} $NaCH_3COO$ + 3gl^{-1} Triton X100 + 0.1 gl^{-1} An2S	180gl^{-1} $Pb(NO_3)_2$ 40 gl^{-1} $NaCH_3COO$ + 3gl^{-1} Triton X100 + 0.1 gl^{-1} An2S
4	4.5	2.5	0	0	0	0	-	-
6	6.8	3.3	1.6	2.1	0	0.8	0.3	0
9	10.2	3.4	1.4	1.5	0	1.1	1.1	0.7
12	13.6	4.2	1.9	3.3	1.7	2.0	3.3	2.6
15	17.0	5.9	4.0	3.8	1.5	2.1	2.4	4.1
20	34.0	13.1	6.0	7.4	4.9	6.3	7.1	6.3

N.B. An2S = anthraquinone-2-monosulphonic acid

Triton X100 appears to be the most effective additive at a concentration of 3 gl^{-1}. At a concentration of 2 gl^{-1} a rapid increase in porosity is observed if the c.d is increased above 3 Adm^{-2}. This was also the case with Pluronic L64 at this concentration. In general, at surfactant levels of 3 gl^{-1} an increase in c.d up to 5 Adm^{-2} did not have any significant effect on porosity, but at 2 gl^{-1} an increase in c.d above 3 Adm^{-2} had a detrimental effect.

3.1.2.3 Effect of deposit thickness on Pb porosity

Pb was electrodeposited from the various solutions described in Table 21, for different plating times at a c.d of 2 Adm^{-2}. The concentrations of both $Pb(NO_3)_2$ and the addition agent used were varied.

$NaCH_3COO$ at a concentration of 40 gl^{-1} was also added to a solution of 180 gl^{-1} $Pb(NO_3)_2$ plus 0.1 gl^{-1} anthraquinone-2-monosulphonic acid and 2 gl^{-1} Triton X100 to see if it improved the deposit appearance and porosity.

Despite the fact that each of the porosity values quoted was the mean of 3 separate determinations, the porosity values obtained at varying thicknesses were not totally consistent. Therefore, these values were only used to compare individual plating solutions and show apparent trends rather than be taken as absolute values.

The thicknesses of Pb deposits obtained from each of the plating solutions was also measured on a Betascope (see Table 22) and the values in μm compared with the theoretical thicknesses that should be obtained at a deposition c.d of 2 Adm^{-2} (assuming a cathode efficiency of 100%).

The values of the deposit thickness were considerably lower than the theoretical deposit thickness, which may be attributable to

current density variations on the deposit surface due to the poor throwing power in $Pb(NO_3)_2$ solutions. Although it should be noted that the thickness of the deposit from the $Pb(BF_4)_2$ solution is lower than the theoretical Pb thickness at a given current density. This work needs further verification.

The weight per unit area for Pb deposit simultaneously deposited from a 360 gl^{-1} solution of $Pb(NO_3)_2$ + 2 gl^{-1} Triton X100 + 0.1 gl^{-1} anthraquinone-2-monosulphonic acid at 2 Adm^{-2} for 15 min was 0.0126g cm^{-2}. This equates to a deposit thickness of 11.1 μm.

3.1.2.4 Porosity determinations on Pb deposits obtained using tannic acid as an addition agent

Good lead deposits from $Pb(NO_3)_2$ at room temperature with no dendritic growth on the edges of the substrate were obtained using tannic acid + Wafex. Since tannic acid is insoluble in $Pb(NO_3)_2$ unless HNO_3 is added, a supporting electrolyte of 20 gl^{-1} HNO_3 was added to all the solutions.

The optimum additive concentration was found to be 1 gl^{-1} Wafex + 1 gl^{-1} tannic acid with tannic acid being the most effective additive in reducing porosity. This is exemplified by values for the porosity of 13.5% for Pb obtained from a solution of 45 gl^{-1} $Pb(NO_3)_2$, 20 gl^{-1} HNO_3 + 0.5 gl^{-1} Wafex, plated at 2 Adm^{-2} for 15 min. In the case of the same solution containing 0.5 gl^{-1} tannic acid and no Wafex, the porosity value was as low as 0.53%. The variation of porosity with $Pb(NO_3)_2$ concentration for Pb plated at 2 Adm^{-2} for 15 min from a solution containing 1 gl^{-1} tannic acid and 1 gl^{-1} Wafex is given in Table 23.

TABLE 23

The effect of $Pb(NO_3)_2$ concentration on the porosity of Pb electrodeposited at 2 Adm^{-2} for 15 min from a $Pb(NO_3)_2$ solution plus 1 gl^{-1} tannic acid + 1 gl^{-1} Wafex

$Pb(NO_3)_2$ Concentration gl^{-1}	Porosity % %
45	0.24
90	0.40
135	0.54

3.1.2.5 The effect of CH_3COO^- on the porosity of Pb deposits

The porosity of Pb deposits obtained from a solution of 180 gl^{-1} $Pb(NO_3)_2$ + 2 gl^{-1} Triton X100 and 0.1 gl^{-1} anthraquinone-2-monosulphonic acid containing 0, 10, 20 and 40 gl^{-1} $NaCH_3COO$ at room temperature and 50°C was measured. No marked improvement in porosity was recorded when this additive was used, although a decrease in porosity with increase in c.d. from 0.5 Adm^{-2} to 2 Adm^{-2} was recorded.

The values of porosity for Pb deposited from the stock solution of 180 gl^{-1} $Pb(NO_3)_2$ with different $NaCH_3COO$ concentrations at 2 Adm^{-2} for 15 min are given in Table 21.

The value for the porosity of Pb electrodeposited from the stock solution plus 40 gl^{-1} $NaCH_3COO$ at 0.5 Adm^{-2} for 1 hour was 2.0%, whilst that from the same solution plated at 2 Adm^{-2} for 15 min (i.e to the same thickness) was 1.3%. The Pb deposit obtained from the stock solution without any acetate and deposited at 0.5 Adm^{-2} for 1 hour was 2.5%.

3.1.2.6 The porosity of Pb battery material produced on the pilot plant

A sample of battery plate material produced on the pilot plant from a solution of 360 gl^{-1} $Pb(NO_3)_2$, 1.5 gl^{-1} butyne 1,4 diol and 3 ml^{-1} Triton X100 and supplied by Ionic Plating was tested for Pb porosity. A total of 5 separate determinations were made and the mean value of porosity was found to be 20.8%.

The other values obtained were 15.1%, 18.0%, 25.2%, 23.7% and 22.0% and thought to indicate the variation in porosity over the specimen surface.

3.1.3 The discharge properties of the $Pb/HBF_4/PbO_2$ primary battery

Typical discharge curves for β-PbO_2 in 48% HBF_4 at various discharge c.ds are shown in Fig. 20.

The PbO_2 was obtained by electrodeposition from a conventional $Pb(NO_3)_2$ bath, the composition of which and conditions of deposition, have been outlined in Section 2.1. The electrodeposited Pb anode used in the discharge experiments was prepared by electrodepositing Pb from a $Pb(BF_4)_2$ plating solution, onto a Ni substrate for 30 min at 2 Adm^{-2}, to ensure that the amount of Pb obtained was at least double that of the PbO_2 deposited. This was done so that in the calculation for the coulombic efficiency of PbO_2 the decrease in cell voltage, was due solely to the reduction of all the active PbO_2.

At high discharge c.ds (36 Adm^{-2}) a rapid decrease in cell voltage was observed (see Fig. 21) as the active material is quickly consumed and passivation of the cathode with $Pb(BF_4)_2$ occurs. At 22 Adm^{-2} the cell voltage remains constant for most of the discharge period.

The coulombic efficiency for a PbO_2 electrode at each c.d was calculated by determining the mean cell voltage and the time taken for the cell voltage to fall below 1V. This permitted a

determination of the number of coulombs that could be obtained from this cell in practice. The theoretical number of coulombs available for discharge was calculated from the total weight of active material available for discharge, and the coulombic efficiency simply taken as a ratio of the experimentally determined number of coloumbs over the theoretical number.

The results of the coulombic efficiency determinations at different discharge c.ds are given in Table 24.

The values of coulombic efficiency were different for each electrode studied and those quoted above were the mean of 5 separate determinations. An example of the degree of variation is shown by the values obtained at a discharge c.d of 5.5 Adm^{-2}, which were 71, 68, 64, 61 and 56%. The values for coulombic efficiency were generally more reproducible at the higher c.ds than at the lower. On removal of the discharged electrodes from the test electrolyte flakes of PbO_2 were clearly visible on the bottom of the cell. This unused active material helps explain why values for coulombic efficiency do not approach the theoretical limit. This is attributed to the brittle nature of the PbO_2 deposit and its poor adherence to the electrode surface. The lower efficiency at low c.ds may also be associated with self corrosion of the PbO_2 deposit, during the duration of the test, which at 0.6 Adm^{-2} may last for 15 min.

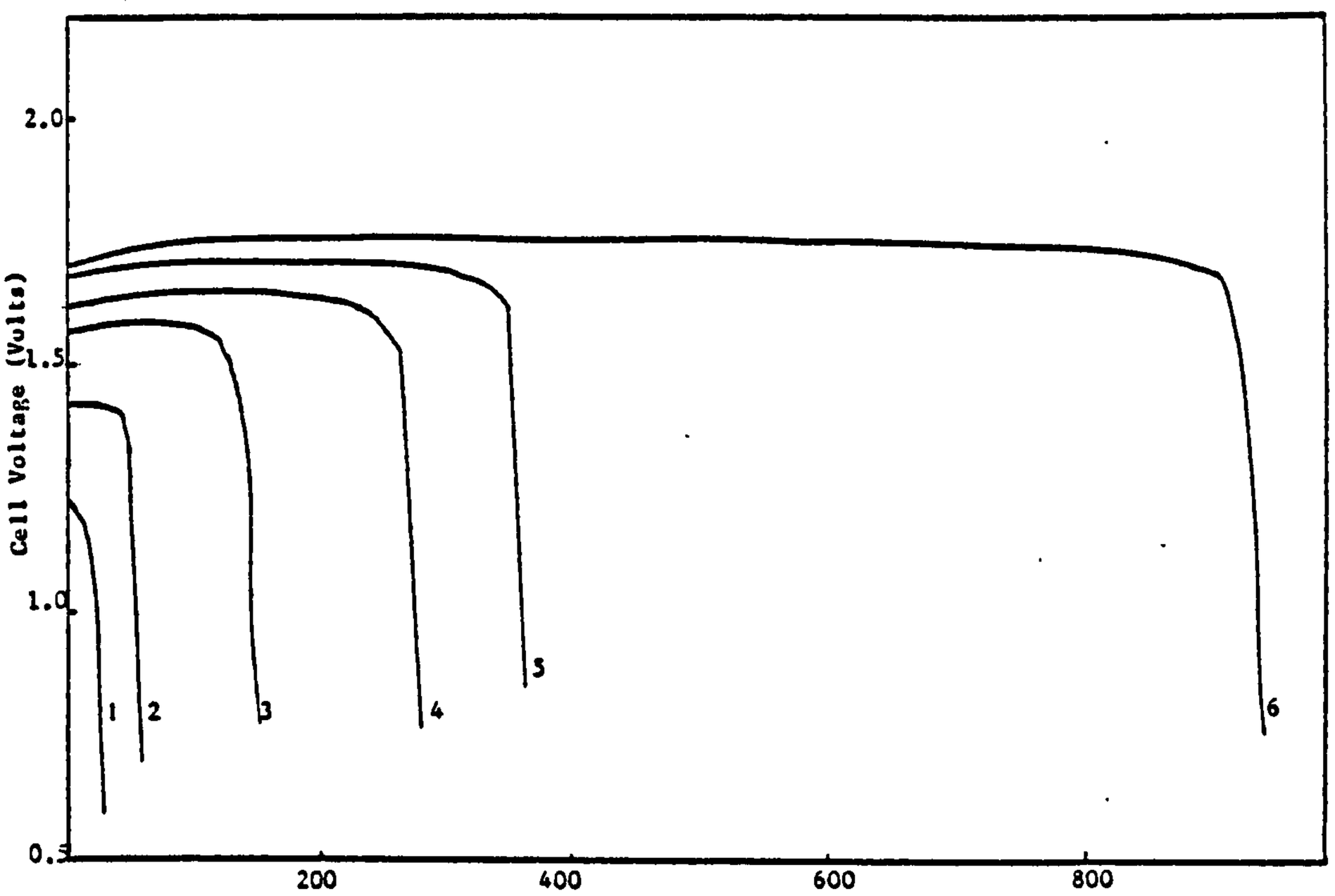

Room temperature discharge curves for a $Pb/HBF_4/PbO_2$ cell at different initial discharge current densities, containing Pb foil and 0.0223 gcm^{-2} of PbO_2.

1 = 36 Adm^{-2} 2 = 22 Adm^{-2} 3 = 11 Adm^{-2} 4 = 5.5 Adm^{-2}
5 = 2.7 Adm^{-2} 6 = 0.63 Adm^{-2}

FIGURE 20

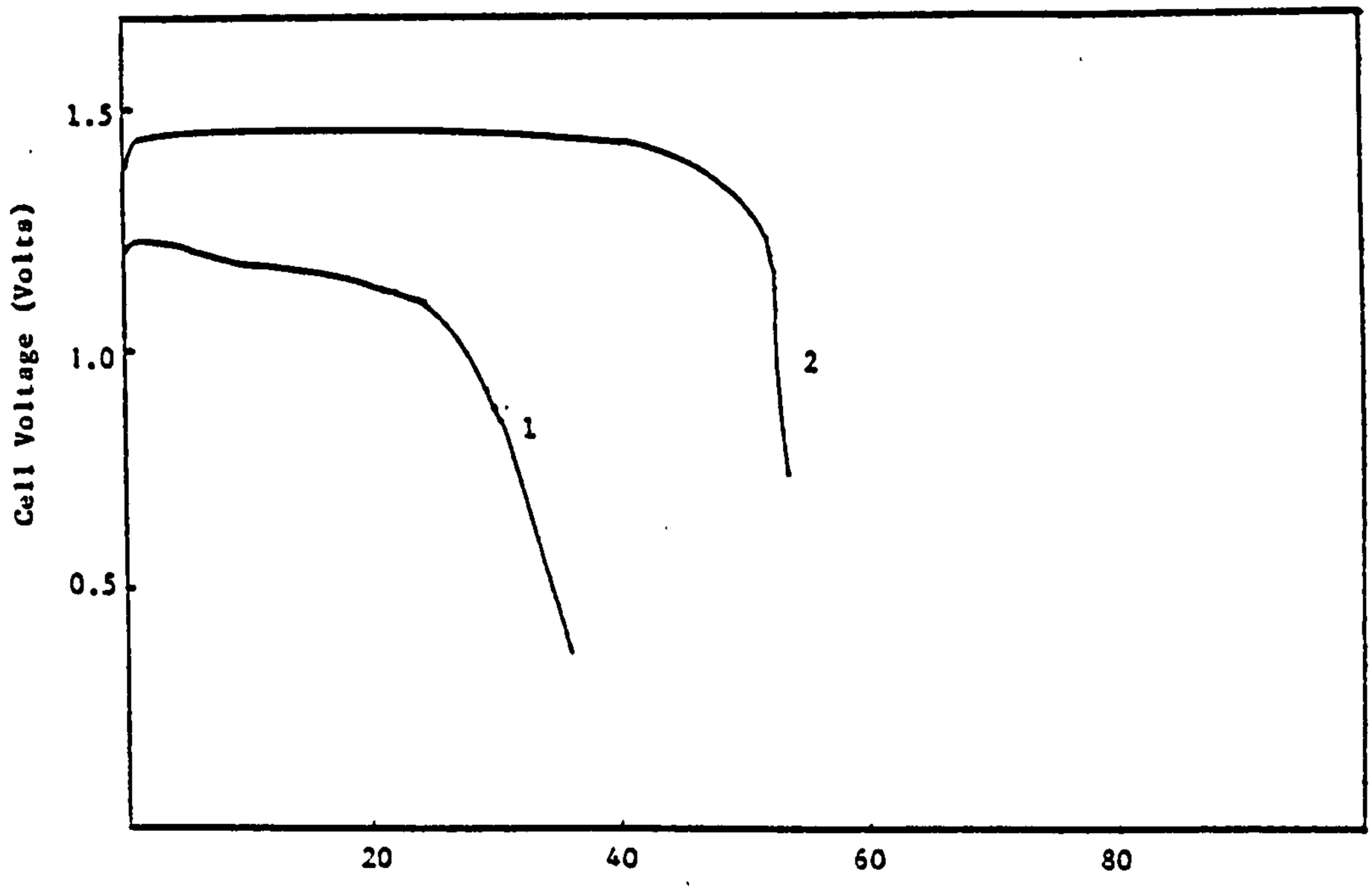

Room temperature discharge curves for a $Pb/HBF_4/PbO_2$ cell in 48% HBF_4 at 25°C with different initial discharge current densities.

1 = 36 Adm^{-2}

2 = 22 Adm^{-2}

FIGURE 21

TABLE 24

The variation of coulombic efficiency for PbO_2 reduction with discharge c.d. for a $Pb/HBF_4/PbO_2$ primary battery at room temperature

Discharge c.d. Adm^{-2}	Mean coulombic efficiency %
36	50
22	67
11	69
5.5	64
2.7	59
0.6	40

3.1.3.1 The room temperature discharge properties, for $Pb/HBF_4/PbO_2$ primary batteries constructed from material produced by the simultaneous electrodeposition of Pb and PbO_2 from $Pb(NO_3)_2$ solutions

In order to test the suitability of battery plate material obtained from "simultaneous baths" the discharge curves for these cells were compared with those for conventional battery plate material, discharged through a 47 ohm resistor; in both cases the electrode area was 0.64 cm^2. Simultaneous baths found to give acceptable deposits were used to produce the battery plate material. The simultaneous baths studied were :

1) 360 gl^{-1} $Pb(NO_3)_2$ + 3 gl^{-1} Triton X100 and 1.5 gl^{-1} butyne 1,4 diol.

2) 360 gl^{-1} $Pb(NO_3)_2$ + 3 gl^{-1} Triton X100 and 0.1 gl^{-1} anthraquinone-2-monosulphonic acid.

3) 360 gl^{-1} $Pb(NO_3)_2$ + 3 gl^{-1} Pluronic L64 and 0.1 gl^{-1} anthraquinone-2-monosulphonic acid.

These solutions will be referred to simply by the additives they contain. In all cases the Pb and PbO_2 deposits were produced under the same conditions i.e by plating at 2 Adm^{-2} for 15 min.

Fig. 22 shows the typical discharge curves for Pb and PbO_2 electrodes both of area 0.64 cm^2 produced from various baths and discharged through a 47 ohm resistor. Curve 1 is for the conventional battery plate material, curve 2 for Pb and PbO_2 electrodeposited from the Triton X100, anthraquinone-2-monosulphonic acid bath and curve 3 is for the deposits from the Triton X100, butyne 1,4 diol bath.

The weight of the PbO_2 available for discharge was essentially the same at 0.014 g in all cases although the Pb weight varied as follows : 0.0125g, 0.0126g and 0.0083g for curves 1,2 and 3 respectively. The weight per unit area of Pb electrodeposited from the Triton X100, butyne 1,4 diol bath was lower than that in the other two cases, although the same deposition time and current density were used. This is due to the fact that the deposits from the latter bath were visibly of lower surface coverage of the nickel when compared to those from the anthraquinone-2-monosulphonic acid baths. The Pb dendrites produced on the edges of the plated specimens were fragile and were removed before weighing. The production of dendrites on the Ni substates resulted in a lower c.d on the remainder of the electrode surface and consequently a lower Pb coverage.

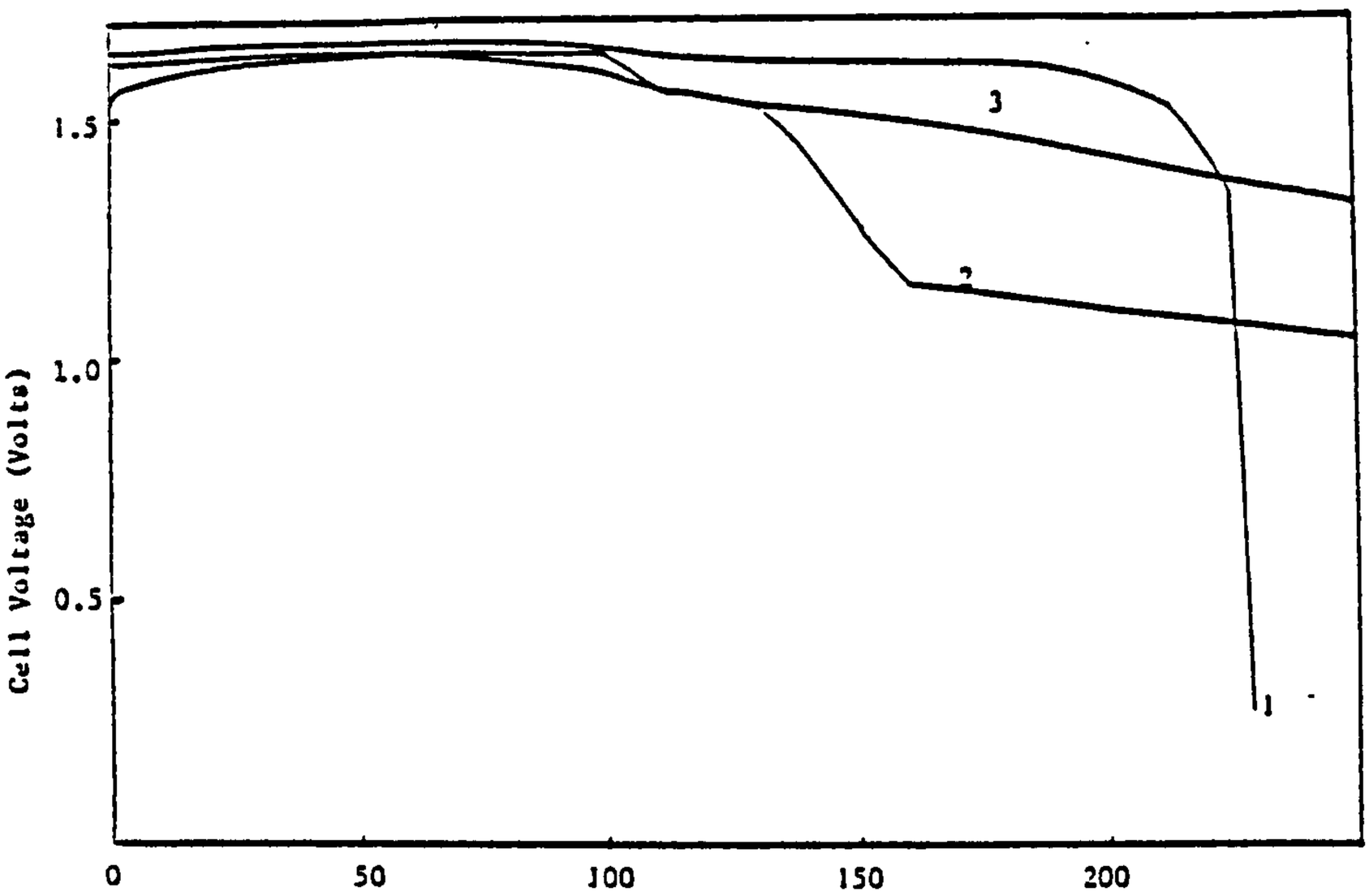

Discharge curves for Pb and PbO_2 electrodeposits in 48% HBF at 25°C. The Pb and PbO_2 material produced from different plating solutions and discharged through a 47 ohm resistor with 0.638 cm^2 of material exposed.

1 = Conventional Pb and PbO_2 battery plate material
PbO_2 weight = 0.0143g

2 = Pb and PbO_2 electrodeposits obtained from a solution of 360 gl^{-1} $Pb(NO_3)_2$ plus 2 gl^{-1} Triton X100, 0.1 gl^{-1} anthraquinone-2-monosulphonic acid of
PbO_2 weight = 0.0141g

3 = Pb and PbO_2 electrodeposits obtained from a solution of 360 gl^{-1} $Pb(NO_3)_2$ plus 2 gl^{-1} Triton 100, 1.5 gl^{-1} butyne 1,4 diol
PbO_2 weight = 0.0139g

FIGURE 22

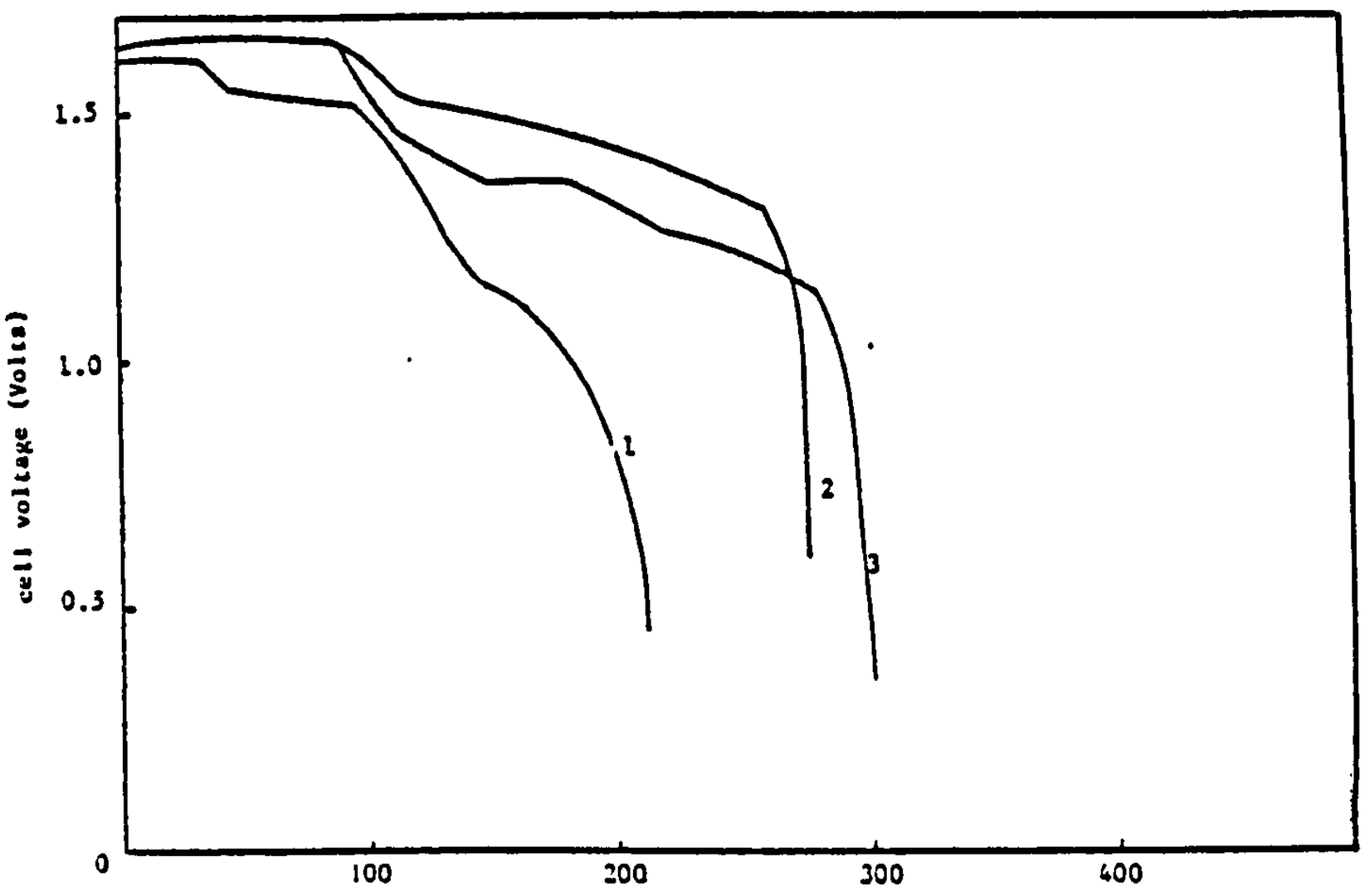

Discharge curves for different Pb and PbO electrodeposits in 48% HBF. The deposits obtained by electrodeposition from a solution of 360 gl^{-1} $Pb(NO_3)_2$ plus 3 ml l^{-1} Triton x100, 1.5 gl^{-1} butyne 1,4 diol at 2 Adm^{-2} for 15 minutes at 30°C. The electrodes of surface area 0.638 cm^2 and discharged through a 47 ohm resistor.

1 = weight of Pb = 0.0085g, weight of PbO_2 = 0.0139g

2 = weight of Pb = 0.0085g, weight of PbO_2 = 0.0139g

3 = weight of Pb = 0.0085g, weight of PbO_2 = 0.0139g

FIGURE 23

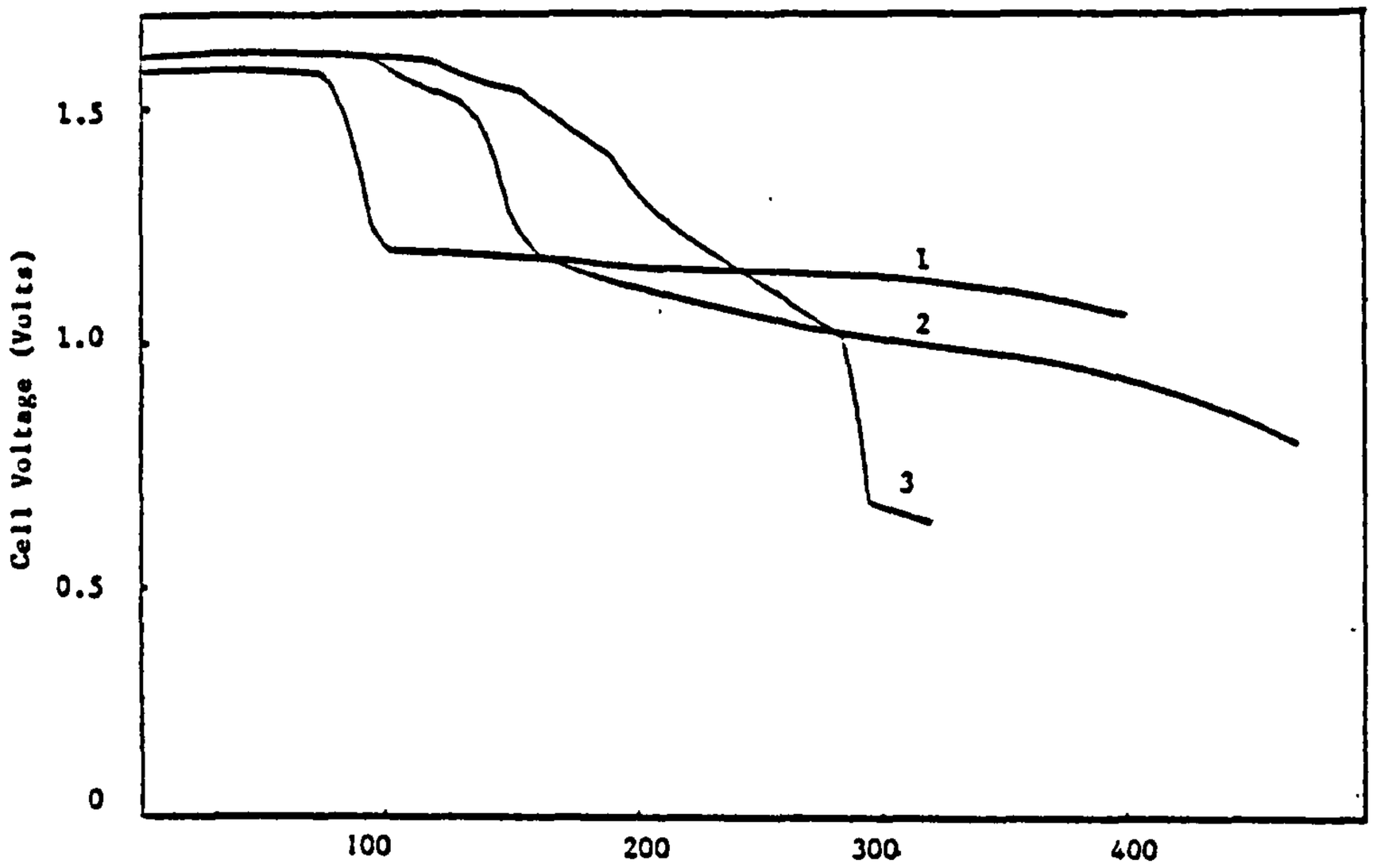

Discharge curves for different Pb and PbO_2 electrodeposits in 48% HBF_4. The deposits obtained by electrodeposition from a solution of 360 gl^{-1} $Pb(NO_3)_2$ plus 2 gl^{-1} Triton X100, 0.1 gl^{-1} anthraquinone-2-monosulphonic acid at 2 Adm^{-2} for 15 minutes at 50°C. The electrodes of surface area 0.638 cm^2 and discharged through a 47 ohm resistor.

1 = weight of Pb = 0.0113g, weight of PbO_2 = 0.0140g

2 = " " = 0.0126g, " " = 0.0141g

3 = " " = 0.0126g, " " = 0.0141g

FIGURE 24

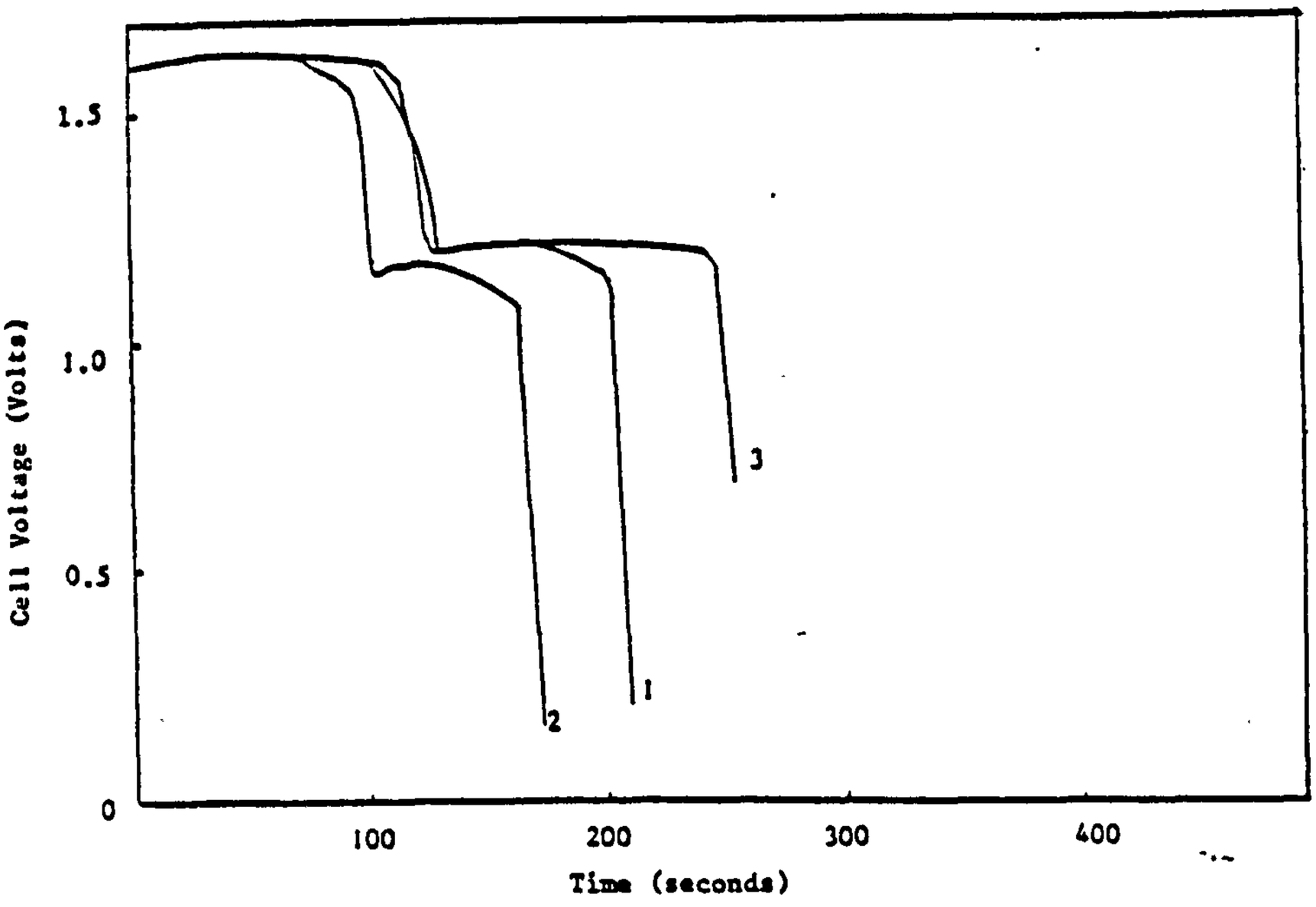

Discharge curves for different Pb and PbO_2 electrodeposits in 48% HBF_4. The deposits electrodeposited from a solution of 360 gl^{-1} $Pb(NO_3)_2$ plus 2 gl^{-1} Pluronic L64, 0.1 gl^{-1} anthraquinone-2-monosulphonic acid at 2 Adm^{-2} for 15 minutes at 50°C. The electrodes were of surface area 0.638 cm^2 and discharged through a 47 ohm resistor.

1 = weight of Pb = 0.0085g , weight of PbO_2 = 0.0138g

2 = " " = 0.0085g , " " = 0.0138g

3 = " " = 0.0085g , " " = 0.0138g

FIGURE 25

From Fig. 22 it can be seen that with conventional plate materials a constant cell voltage is maintained until all the active material is consumed, after which point the cell voltage falls off rapidly. In the case of the Pb and PbO_2 deposits produced from the simultaneous baths a constant cell voltage was only maintained for the first 100s of discharge and after this period a gradual fall in cell voltage was recorded.

The reproducibility of the voltage output from cells constructed from Pb and PbO_2 electrodeposits obtained from the simultaneous baths is poor as can be seen from Fig. 23 for the Triton X100, butyne 1,4 diol bath and from Fig 24 for the Triton X100, anthraquinone-2-monosulphonic acid bath. No apparent differences are noticable between the voltage-time curves for the deposits from a Triton X100, butyne 1,4 diol bath and the Triton X100, anthraquinone-2-monosulphonic acid solution, except that the time taken for the voltage to drop below 1 Volt is invariably longer for the latter, presumably because of the thicker Pb deposits obtained from these solutions at the same c.d and deposition time.

The voltage vs time curves for deposits of Pb and PbO_2 obtained from a Pluronic L64, anthraquinone-2-monosulphonic acid bath were essentially the same as for the other "simultaneous baths" as can be seen from Fig. 25. Some dendritic growth of Pb was visible on the nickel electrode when plated from this solution, which explains the low weight per unit area of Pb measured on these specimens.

The reason for the fall in cell voltage with time after the first 100s of discharge, for the deposits obtained from the "simultaneous baths" is not clearly understood. It may be due to a decrease in the coulombic efficiency of the PbO_2 electrode as a result of internal stresses created in the PbO_2 when deposited from an additive bath and or a reduction in the deposit adherence. This could result in some of the active material detaching itself from the substrate during the discharge process. Another reason may be poor adhesion of the electrodeposited Pb on the nickel substrate, when deposited from a simultaneous plating solution.

A graph of voltage versus time for the discharge of Pb electrodeposited onto nickel from two different simultaneous plating baths with a PbO_2 electrode obtained from the standard $Pb(NO_3)_2$ solution is shown in Fig. 26. These are typical discharge curves and help to show the general trend. The results clearly indicate that it is the nature of the Pb electrode rather than the PbO_2 electrode that is responsible for the inferior discharge characteristics of cells constructed using material deposited from a simultaneous plating solution.

In fact, a regular a.c voltage superimposed on the d.c cell voltage was observed during the discharge of certain of the Pb deposits obtained from a 360 gl^{-1} $Pb(NO_3)_2$ + 3 gl^{-1} Triton X100 + 1.5 gl^{-1} butyne 1,4 diol solution, as can be seen from Fig. 26.

Visual examination of the Pb deposit from the simultaneous baths after discharge showed that most of the Pb still remained although areas of exposed nickel were clearly visible.

The typical discharge curve for a PbO_2 deposit obtained from the same simultaneous baths against a standard Pb deposit is shown in Fig. 27. The coulombic efficiency for this deposit was found to be approximately 65%.

The effect of the addition of 1 gl^{-1} cetyl trimethyl ammonium bromide to a 360 gl^{-1} $Pb(NO_3)_2$ solution on the discharge properties of the PbO_2 electrodeposited from this solution is shown in Fig. 28.

The use of this additive appears to have a detrimental effect on the discharge curve as can be seen from Fig. 28, when it is compared to the discharge curves shown in Figs. 20, 22 for a PbO_2 electrode produced from a $Pb(NO_3)_2$ solution without any additive. The voltage output initially remained steady, but then decreased. The mean coulombic efficiency for this electrode was found to be low, 53% compared to 64% for a conventional PbO_2 deposit.

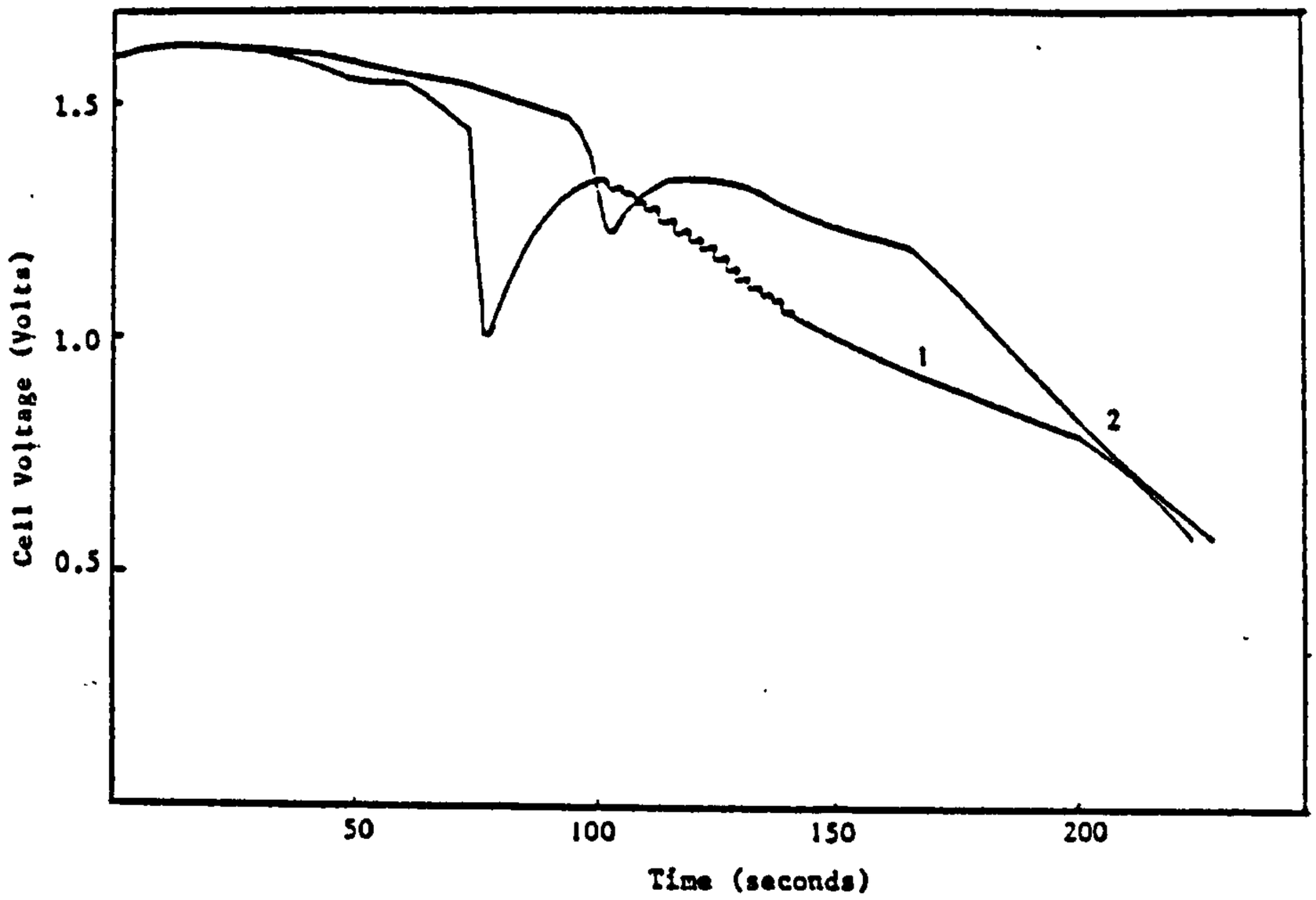

Discharge curves for a PbO_2 deposit obtained by electrodeposition from a 360 gl^{-1} $Pb(NO_3)_2$ solution without additives at 50°C and discharged against a Pb denosit obtained from a different plating solution. The electrodes of surface area 0.638 cm^2,,discharged through a 47 ohm resistor.

1 = Typical Pb deposit obtained from a solution of 360 l^{-1} $Pb(NO_3)_2$ plus 3 gl^{-1} Triton X100, 1.5g l^{-1} butyne 1,4 diol for15 minutes at 2 Adm^{-2} and 50°C. Pb weight = 0.009g

2 = Typical Pb deposit obtained from a solution of 360g l^{-1} $Pb(NO_3)_2$ plus 2 gl^{-1} Triton X100, 0.1 gl^{-1} anthraquinone-2-monosulphonic acid for 15 minutes at 2 Adm^{-2} and 50°C. Pb weight = 0.0125g

FIGURE 26

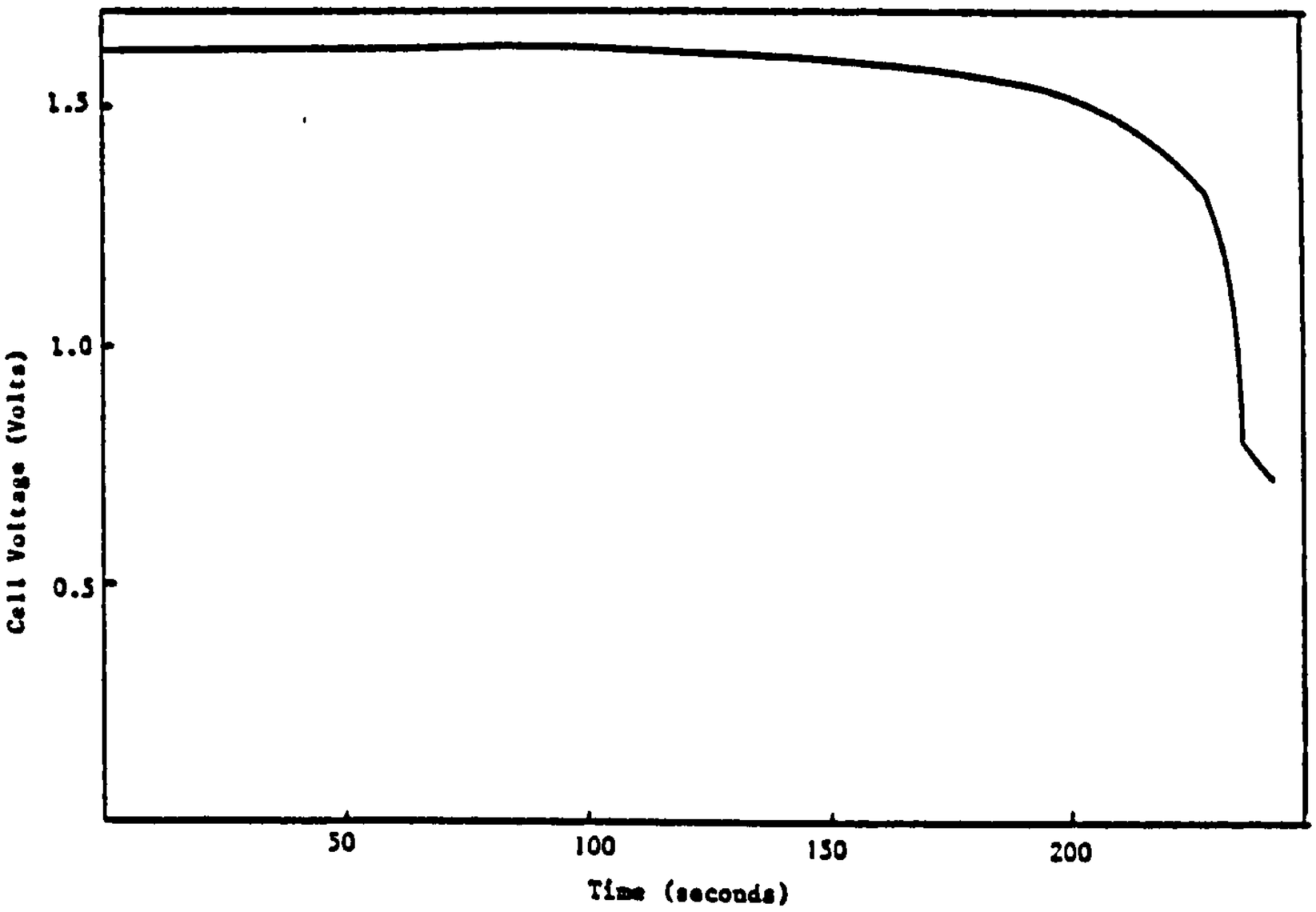

Typical discharge curve for PbO_2 electrodeposited from a solution of 360 gl^{-1} $Pb(NO_3)_2$, plus 2 gl^{-1} Triton X100, 0.1 gl^{-1} of anthrquinone mono sulphonic acid and discharged against Pb foil in 48% HBF_4. The electrode of an exposed surface area of 0.638 cm^2 and discharged through a 47 ohm resistor.

FIGURE 27

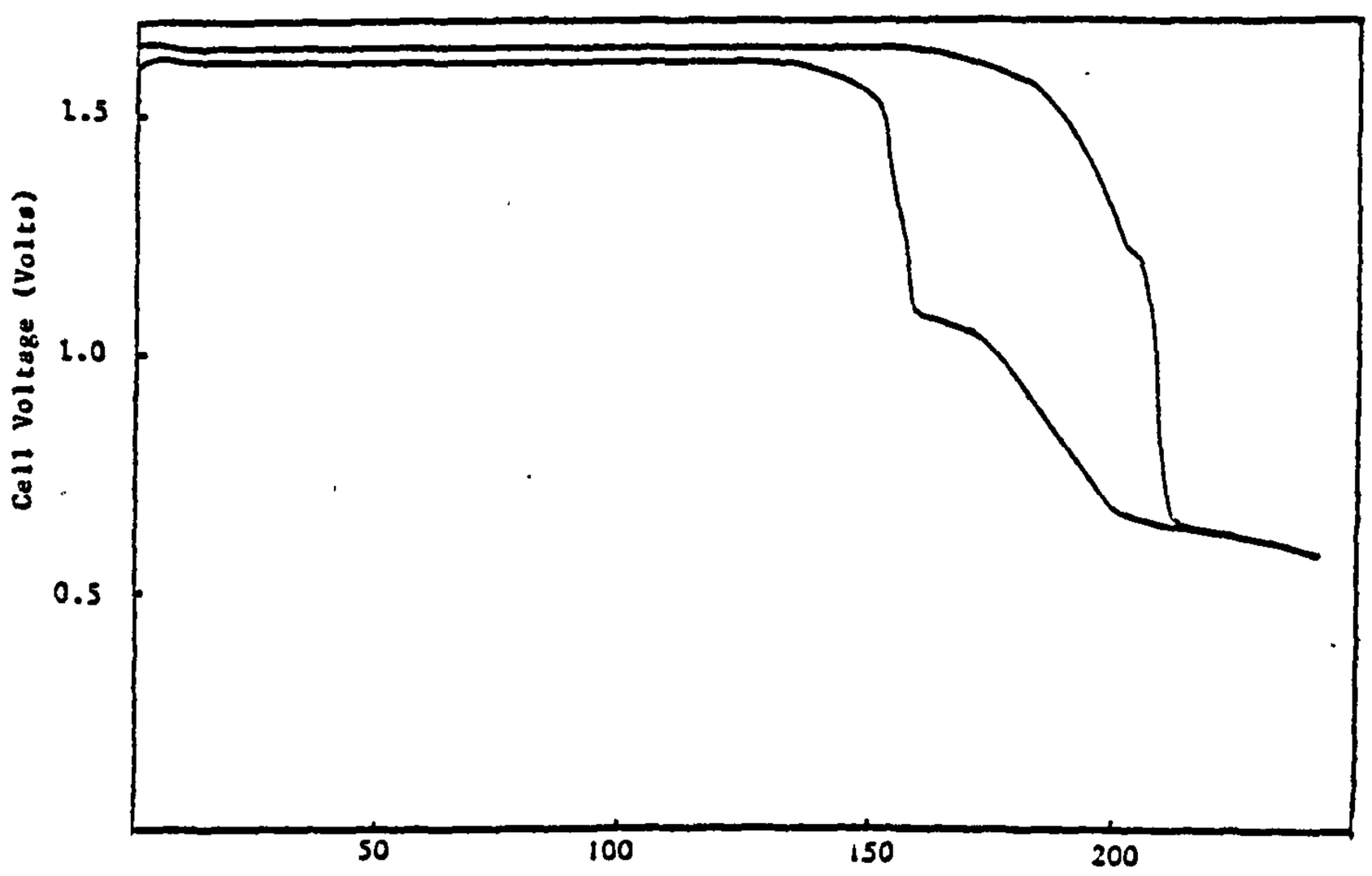

Discharge curves for PbO_2 electrodeposited from a solution of 360 gl^{-1} $Pb(NO_3)_2$, plus 1 gl^{-1} CETB for 15 minutes at 2 Adm^{-2} and 50°C, then discharge against a Pb foil electrode in 48% HBF_4. The electrodes of exposed surface area 0.638 cm^2 and discharged through a 47 ohm resistor.

FIGURE 28

Typical discharge curves for PbO_2 and Pb electrodes in 40% HBF_4, at 60°C, the electrodes were produced from different plating solutions each of surface area 0.64 cm_2 and discharged through a 47 ohm resistor.

1 = Pb and PbO_2 electrodeposits obtained from a solution of 360 gl^{-1} $Pb(NO_3)_2$ plus 3 gl^{-1} Triton X100, 1.5 gl^{-1} butyne 1,4 diol at 2 Adm^{-2} and 50°C.

2 = Pb and PbO_2 electrodeposits obtained from a solution of 360 gl^{-1} $Pb(NO_3)_2$ plus 2 gl^{-1} Triton X100, 0.1 gl^{-1} 2 anthraquinone mono sulphonic at 2 Adm^{-2} and 50°C.

3 = Pb and PbO_2 conventional battery plate material.

FIGURE 29

3.3.3 The discharge properties of the $Pb/HBF_4/PbO_2$ primary battery at $60^{o}C$

Fig. 29 shows typical voltage vs time curves for conventional battery plates of Pb and PbO_2 of area 0.64 cm^2 immersed in 48% HBF_4 and discharged through a 47 ohm resistor together with those of battery plate material obtained from baths containing Triton X100 plus butyne 1,4 diol, and Triton X100 plus anthraquinone-2-monosulphonic acid. The voltage vs time curves from these materials were similar to those obtained at room temperature except that a higher cell voltage was recorded. The Pb and PbO_2 deposits produced from simultaneous baths all exhibited a contant voltage for the first 80 to 100s of discharge, which was followed by a gradual decrease in cell voltage. The deposits obtained from the Triton X100 plus anthraquinone-2-monosulphonic acid baths were slightly superior to those from the Triton X100 plus butyne diol baths at elevated temperatures, in as much as the voltage was maintained constant for slightly longer periods.

The mean value for the coulombic efficiency for discharge of the conventional battery plate material in 48% HBF_4 at $60^{o}C$ was found to be about 60%. The mean cell e.m.f at this temperature at a discharge c.d of 5.9 Adm^{-2} was 1.72 V.

3.1.4 Scanning Electron Microscopy

3.1.4.1 Pb deposit morphology

Deposits of Pb from a solution of $Pb(NO_3)_2$ with no additives are non-adherent, filamentary and unsuitable for use in commercial plating solutions.

Fig. 1P shows the nature of the Pb deposit on a nickel foil substrate obtained from a solution of 360 gl^{-1} $Pb(NO_3)_2$. Large single crystals of Pb are visible, as is the presence of a small number of Pb crystals. The deposit is by no means

continuous with large areas of the Ni foil substrate still bare even after 15 min plating at 2 Adm^{-2}. At higher magnifications (Fig. 2P), different facets on the Pb crystals can also be seen.

Lead deposits obtained from a $Pb(BF_4)_2$ plating solution (see Fig. 3P) are continuous and of a much smaller grain size when compared to those from a $Pb(NO_3)_2$ solution. Macro steps in the Pb deposit are also visible see Figs. 3P and 4P.

When selected organic addition agents are added to the $Pb(NO_3)_2$ plating solutions, the nature of the Pb deposit obtained alters. In the case of the use of the additive combination 3 gl^{-1} Triton X100 plus 1.5 gl^{-1} butyne 1,4 diol to a solution of 360 gl^{-1} $Pb(NO_3)_2$, the nature of the Pb deposit obtained at room temperature is shown in Figs. 5P and 6P. The coverage of the Ni substrate by the Pb deposit is considerably better than in the case of the non additive $Pb(NO_3)_2$ solution but pores in the deposit are still visible. At room temperature the Pb deposit is porous and filamentary with small dendrites radiating out from the central Pb crystals, the structure of which cannot be easily identified (see Fig. 6P).

Deposition of Pb from a solution of 360 gl^{-1} $Pb(NO_3)_2$ plus 3 gl^{-1} Triton X100 and 1.5 gl^{-1} butyne 1,4 diol at an elevated temperature (35°C), increased the extent of surface coverage of the nickel substrate by the Pb deposit (see Fig. 7P) and prevented the formation of a filamentary Pb deposit, (see Fig.8P). Deposition from the same solution yet at a slightly higher temperature still failed to improve the degree of surface coverage of the Ni substrate; if anything it decreased it from that obtained at 35°C. (see Fig. 9P). The Pb crystals formed where rounded and the different crystal facets could not be identified at a low magnification (see Fig. 10P).

The use of 2 gl^{-1} Triton X100 in conjunction with 0.1 gl^{-1} anthraquinone-2-monosulphonic acid as addition agents for Pb deposition from $Pb(NO_3)_2$ solutions was found to be a more effective additive combination. The extent of surface coverage of the Ni substrate can be seen in Figs. 11P and 13P for two different samples of Ni plated from the same $Pb(NO_3)_2$ solution.

At high magnification the Pb crystals can be identified (Fig 14P) as can micro pores in the Pb deposit (see Fig. 12P). The Pb crystals are visibly larger than those obtained from a $Pb(BF_4)_2$ solution; they are faceted and macro steps in the Pb deposit can be seen. At lower magnifications macro pores in the deposit were visible but in some areas no pores could be detected (Fig. 16P).

A decrease in the $Pb(NO_3)_2$ concentration does have an effect on the deposit morphology. At very low $Pb(NO_3)_2$ concentrations (45 gl^{-1}) pyramidal crystals of Pb were seen (Figs. 17P and 18P). Indeed at high magnification macro steps in the Pb pyramids were visible (see Fig. 18P).

The effect of other additive combinations on the morphology of Pb deposits from $Pb(NO_3)_2$ solutions was also studied using S.E.M; this applied particularly to those thought suitable for use in simultaneous Pb and PbO_2 plating. However, none of those investigated produced pore-free deposits and surface coverage of the Ni substrate by the deposit was incomplete. Fig. 19P shows the nature of the deposit, obtained from a solution of 360 gl^{-1} $Pb(NO_3)_2$ containing 3 gl^{-1} BRIJ 35 plus 0.1 gl^{-1} anthraquinone-2-monosulphonic acid. Pores in the deposit can be seen with the larger ones appearing to be concentrated around an etch pit on the Ni200 substrate. Fig. 20P shows the extent of surface coverage obtained when anthraquinone-2,6-disulphonic acid is used as the addition agent in preference to anthraquinone-2-monosulphonic acid.

An interesting phenomenon was observed when anthraquinone-1,5-disulphonic acid was used in conjunction with Triton X100 as a plating additive, since filamentary deposits of Pb were obtained at room temperature. No pores in the Pb deposit appeared visible yet these were presumably masked by Pb filaments radiating out over the substrate surface (see Figs. 21P and 22P).

The effectiveness of other addition agents namely gelatin and naphthalene-1,5-disulphonic acid when used in conjunction with Triton X100 to deposit Pb from a 100 gl^{-1} $Pb(NO_3)_2$ solution can be seen in Figs. 23P-24P; cetyltrimethylammonium bromide (CETB) also produced inferior surface coverage of the Ni substrate (see Fig. 25P).

Tannic acid was also found to be a suitable addition agent for Pb deposition from $Pb(NO_3)_2$ solutions. Unfortunately this addition agent would only dissolve in acidified $Pb(NO_3)_2$ solutions, which cannot be used for the simultaneous deposition of Pb and PbO_2, since the nickel foil does not remain passive when anodically polarised in acid solutions.

Tannic acid in conjunction with Wafex (a sodium lignosulphonate) was found to be more effective in improving the properties of the Pb deposit produced from $Pb(NO_3)_2$ solutions than the individual additives. Fig. 26P shows the extent of surface coverage of a Pb deposit obtained at 2 Adm^{-2} for 15 min at room temperature from a solution of 360 gl^{-1} $Pb(NO_3)_2$, 2 gl^{-1} Wafex, 2 gl^{-1} tannic acid and 20 gl^{-1} HNO_3. A higher magnification view of the Pb deposit is shown in Fig. 27P which shows pores or discontinuities in the deposit. Increase in the deposition temperature resulted in an increase in the number of pores in the Pb coating and hence a decrease in the extent of coverage of the Ni substrate (see Fig. 27P). A reduction in the $Pb(NO_3)_2$ concentration results in an improved surface coverage of the Ni substrate by the Pb deposit (see Fig. 28P).

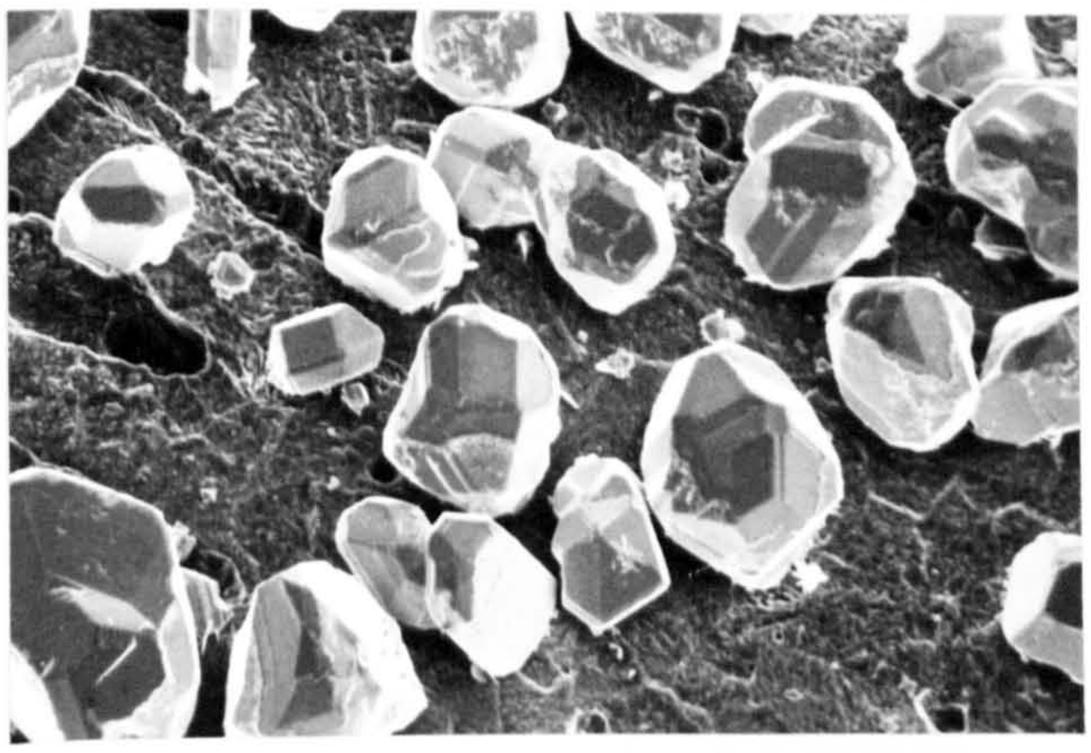

FIGURE 1P

Pb electrodeposited at 2 Adm^{-2} for 15 minutes at 50°C onto a Ni substrate, from a solution of 360 gl^{-1} Pb $(NO_3)_2$ pH 3.5, without addition agents.

(Magnification 700X)

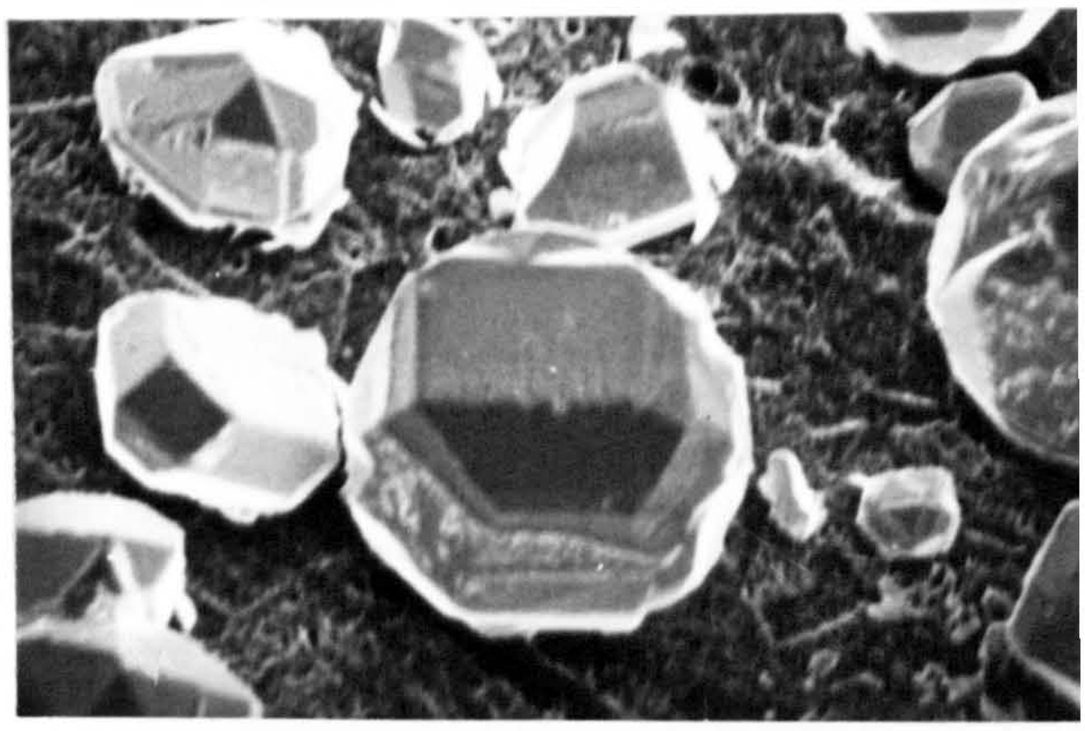

FIGURE 2P

Higher magnification view of Pb deposit shown in Figure 1P.

(Magnification 1000X)

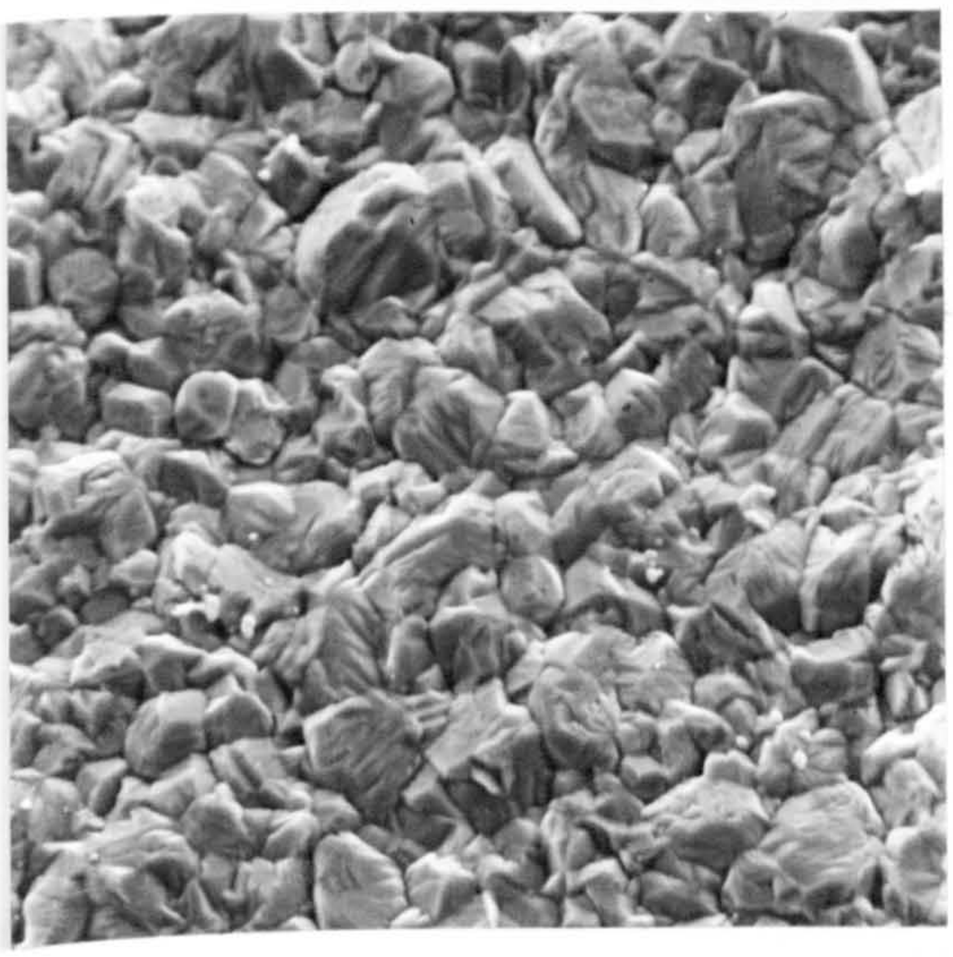

FIGURE 3P

Pb electrodeposited at 2.7 Adm^{-2} from a 230 gl^{-1} Pb $(BF_4)_2$ solution at room temperature.

(Magnification 1000X)

FIGURE 4P

Higher magnification view of the Pb deposit shown in Figure 3P.

(Magnification 5000X)

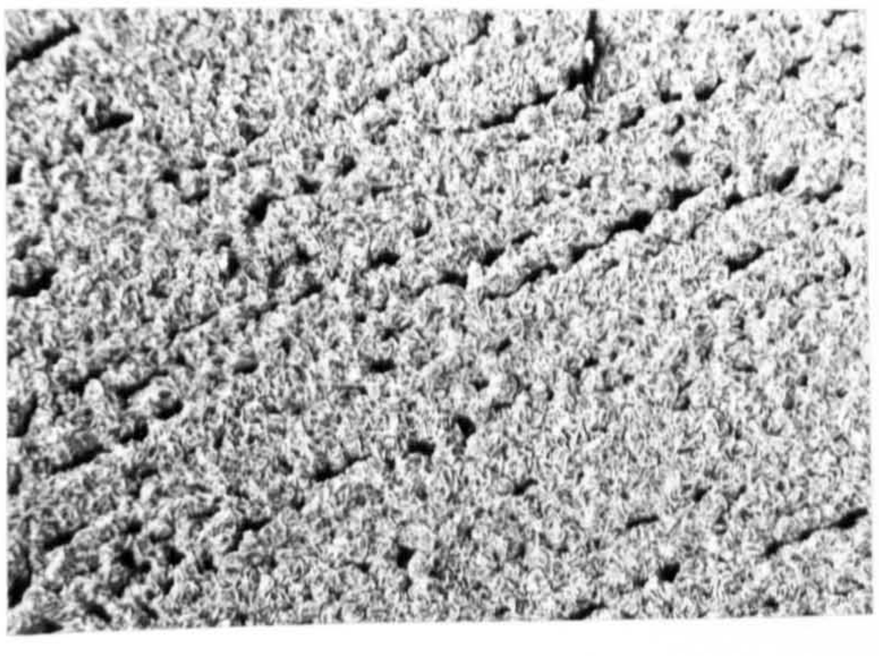

FIGURE 5P

Pb electrodeposited from a 360 gl^{-1} $Pb(NO_3)_2$ solution + 3 gl^{-1} Triton X100 + 1.5 gl^{-1} butyne 1,4 diol deposited at 2.4 Adm^{-2} at 20°C.

(Magnification 100X)

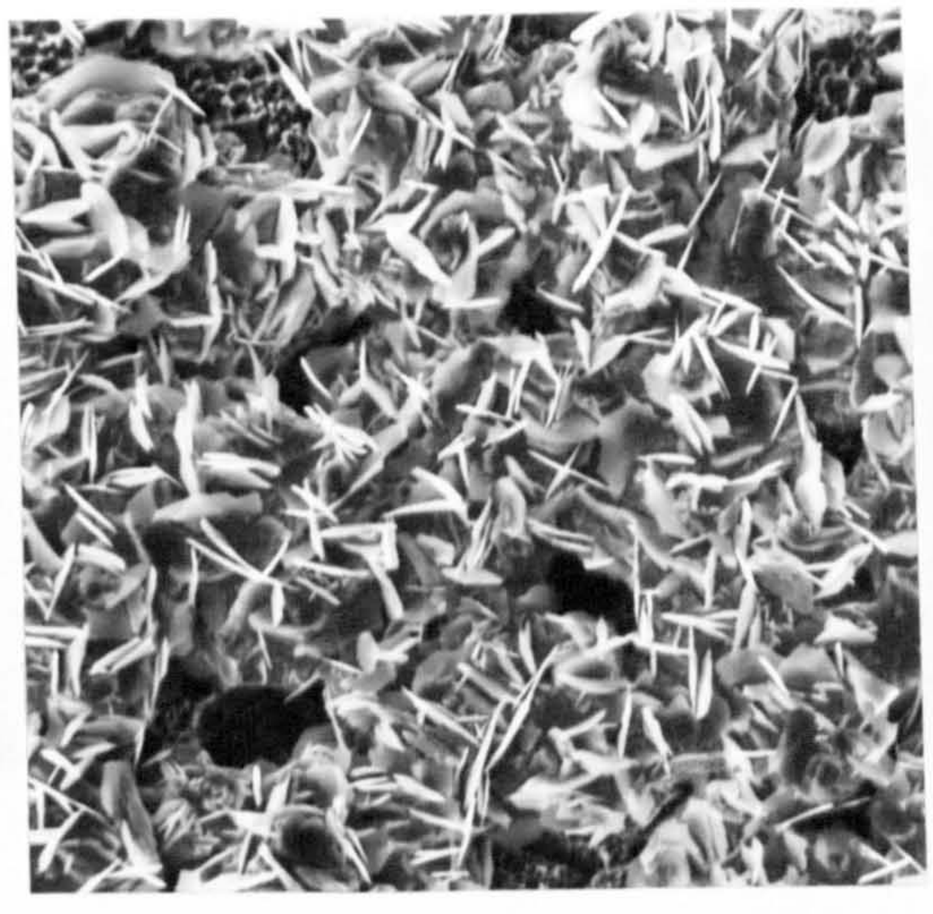

FIGURE 6P

Higher magnification view of the Pb deposit shown in Figure 5P.

(Magnification 1000X)

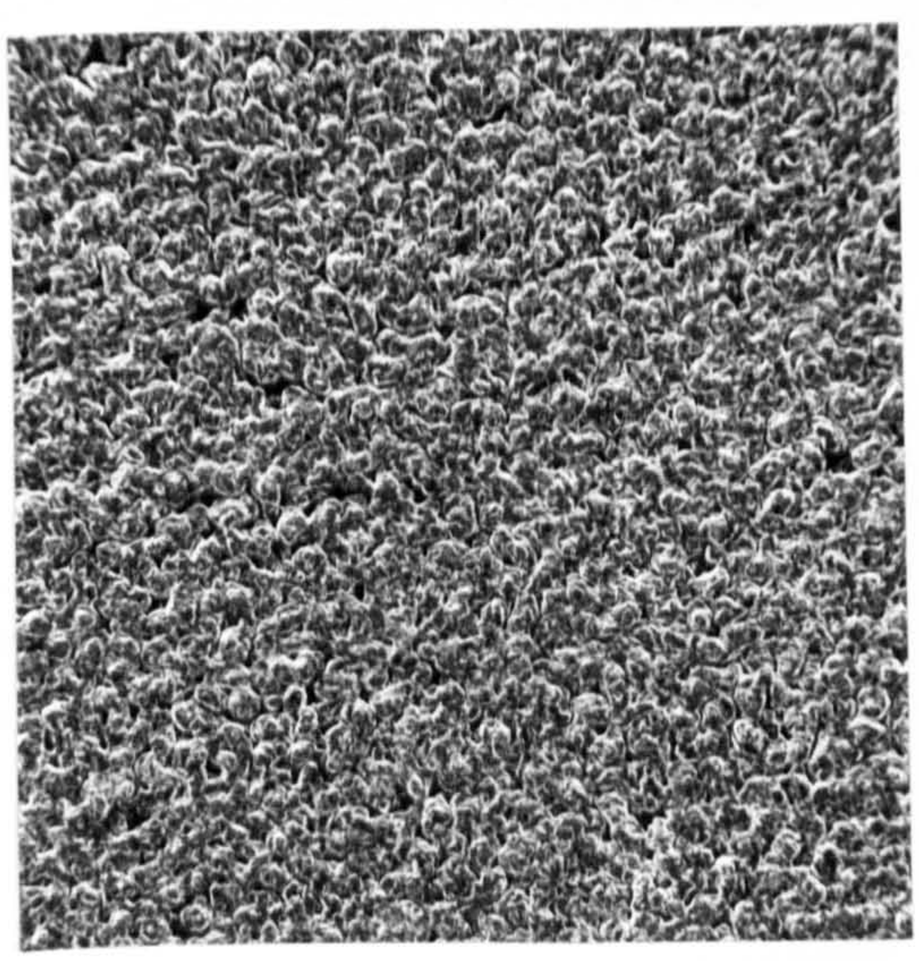

FIGURE 7P

Pb electrodeposited from a 360 gl^{-1} $Pb(NO_3)_2$ + 3 gl^{-1} Triton X100 + 1.5 gl^{-1} butyne 1,4 diol, at 2.4 Adm^{-2} and at 35°C.

(Magnification 100X)

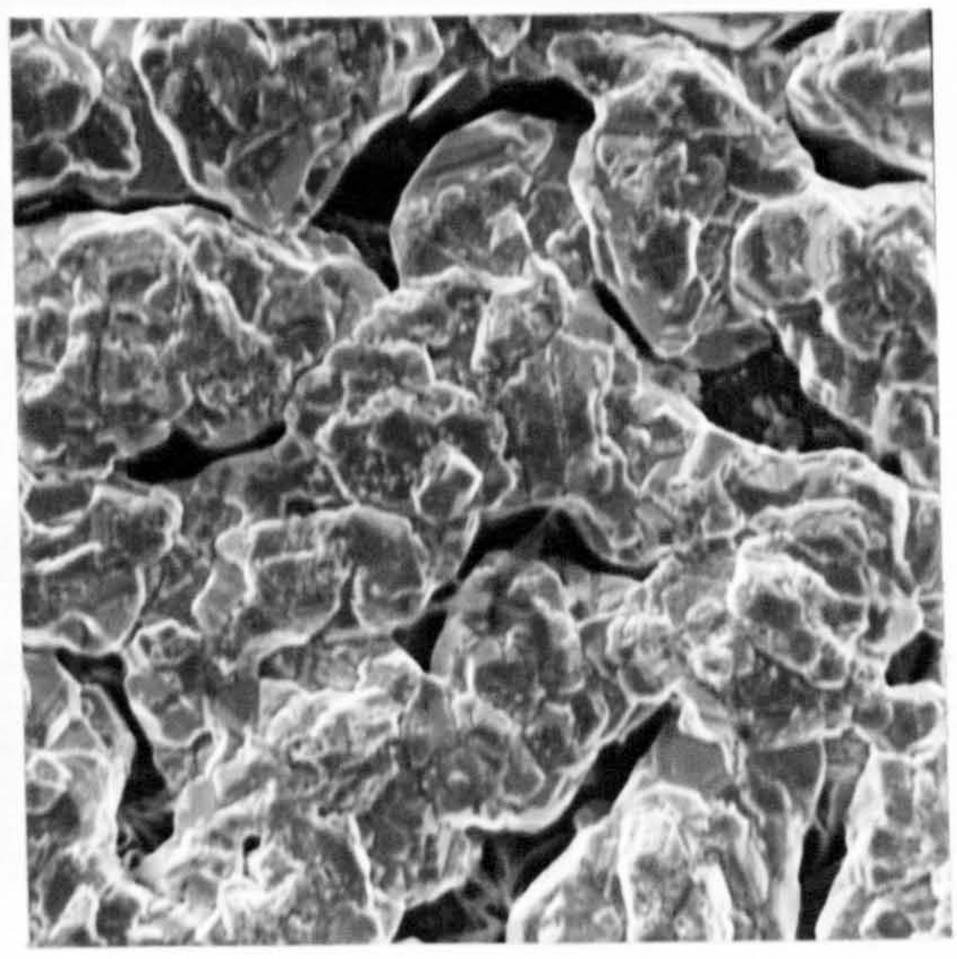

FIGURE 8P

Higher magnification view of the Pb deposit shown in Figure 7P.

(Magnification 1000X)

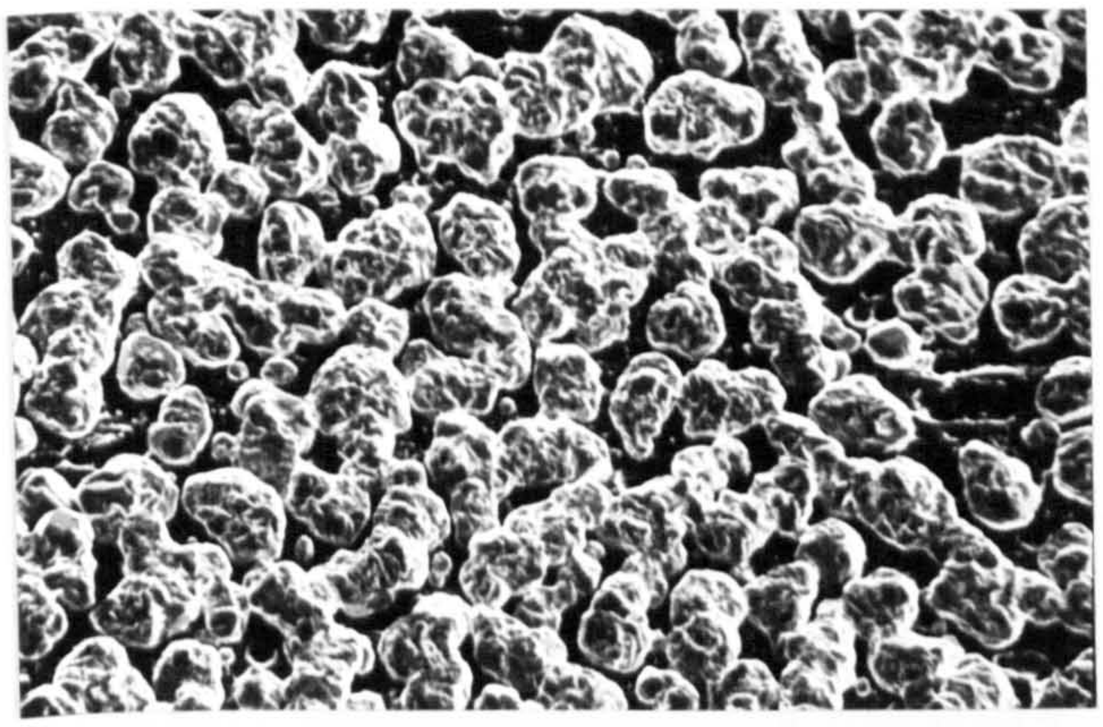

FIGURE 9P

Pb electrodeposited from a 360 gl^{-1} $Pb(NO_3)_2$ solution + 3gl^{-1} Triton X100 + 1.5 gl^{-1} butyne 1,4 diol at 2 Adm^{-2} and at 50°C.

(Magnification 200X)

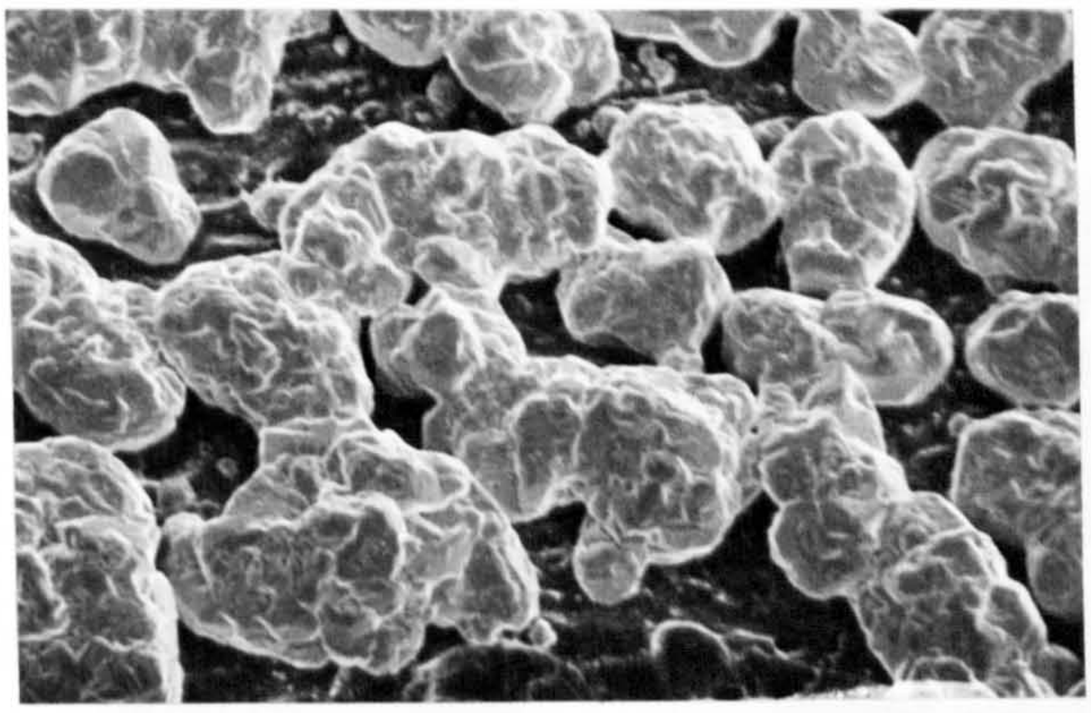

FIGURE 10P

Higher magnification view of the deposit shown in Figure 9P.

(Magnification 1000X)

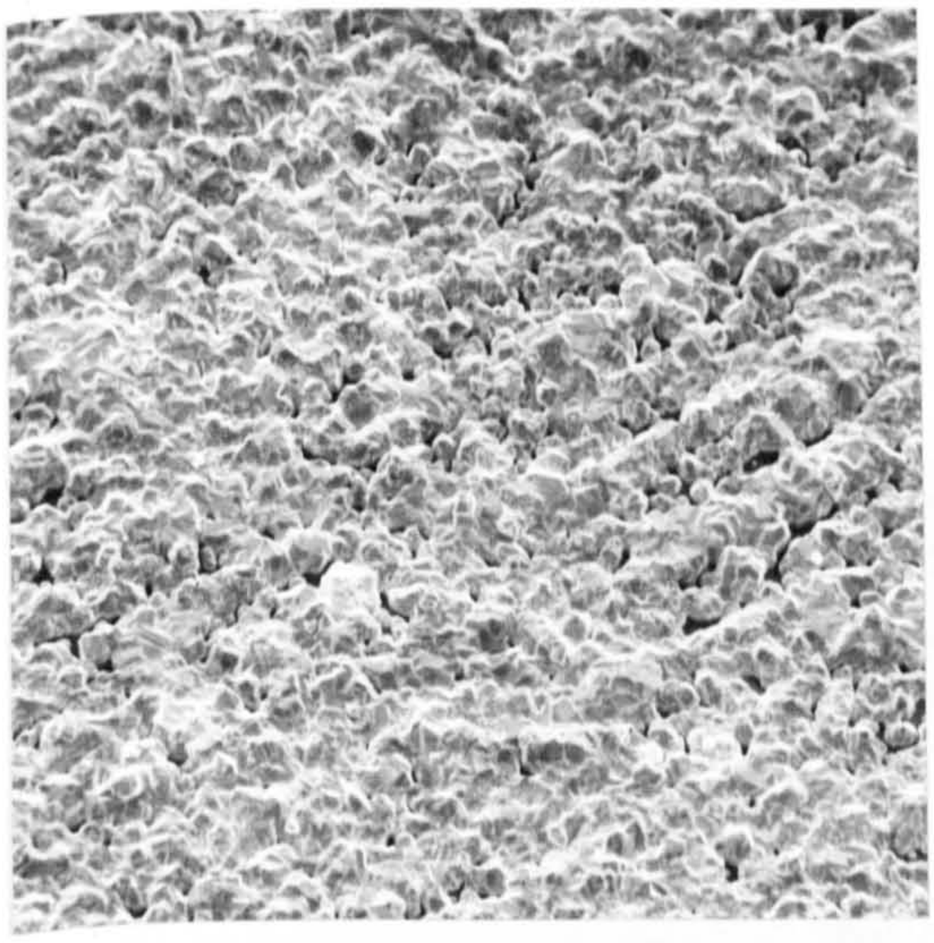

FIGURE 11P

Pb electrodeposited from a 360 gl^{-1} $Pb(NO_3)_2$ solution plus 2 gl^{-1} Triton X100 + 0.1 gl^{-1} anthraquinone-2-monosulphonic acid, at 2 Adm^{-2} and at 50°C.

(Magnfication 200X)

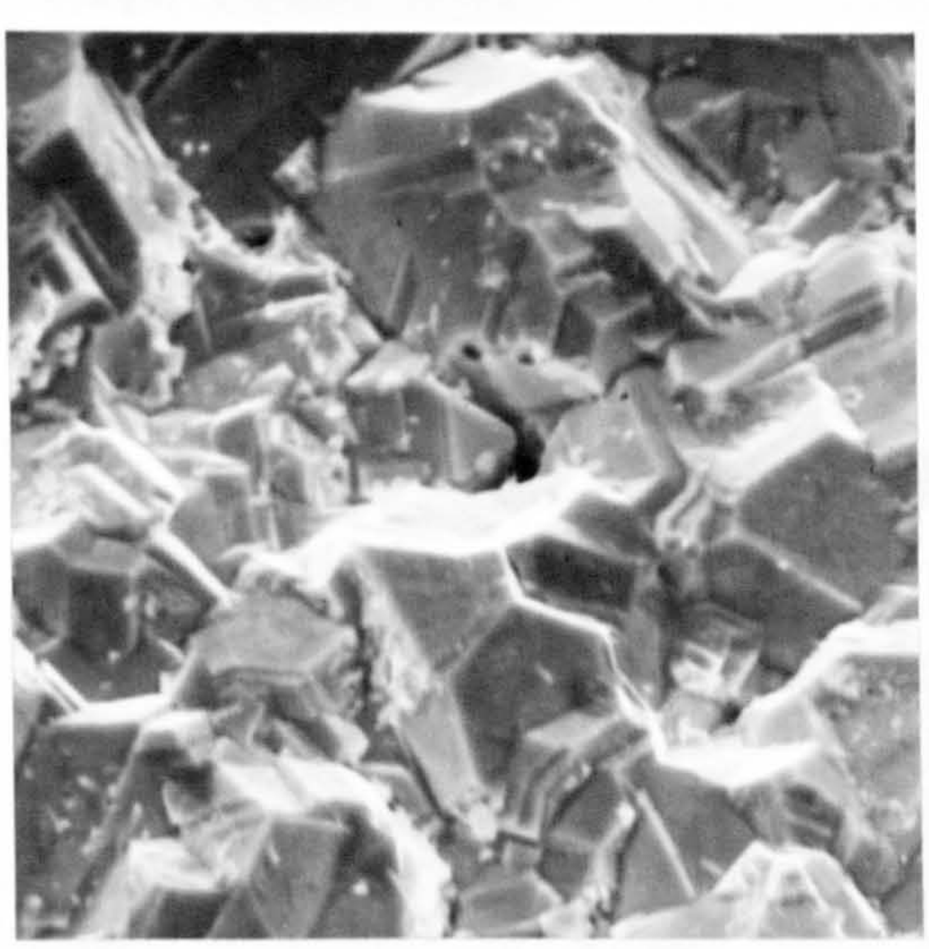

FIGURE 12P

Higher magnification view of the Pb deposit shown in Figure 11P.

(Magnification 5000X)

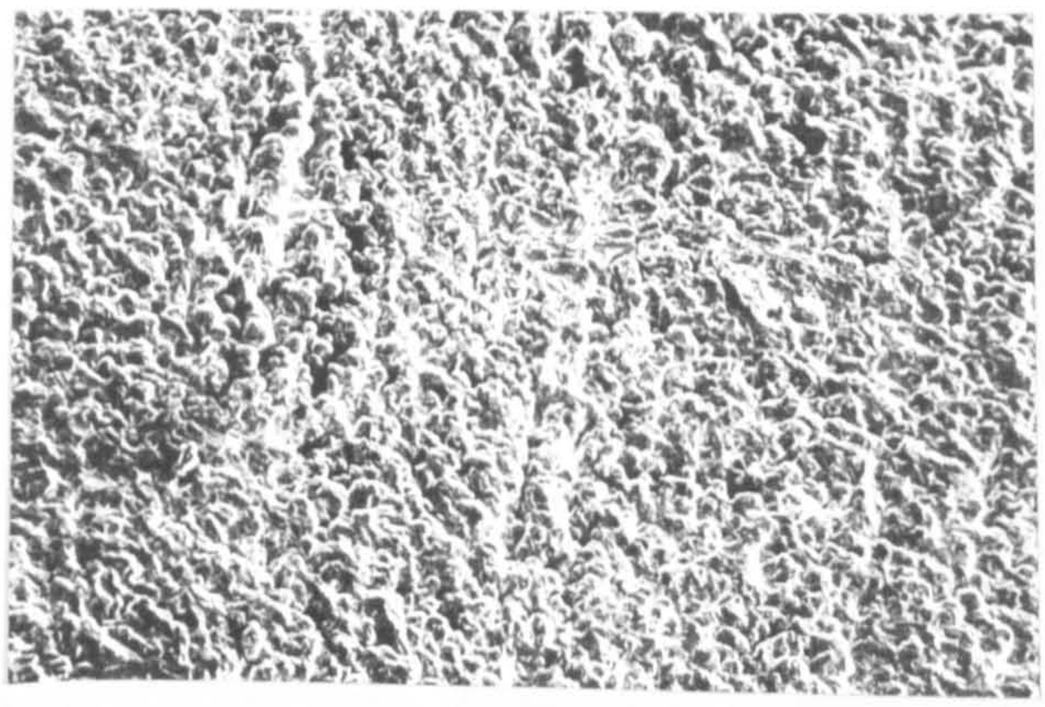

FIGURE 13P

Pb electrodeposited from a 360 gl^{-1} $Pb(NO_3)_2$ solution plus 2 gl^{-1} Triton X100 + 0.1 g^{-1} a anthraquinone -2- monosulphonic acid, at 2 Adm^{-2} and at 50°C.

(Magnification 200X)

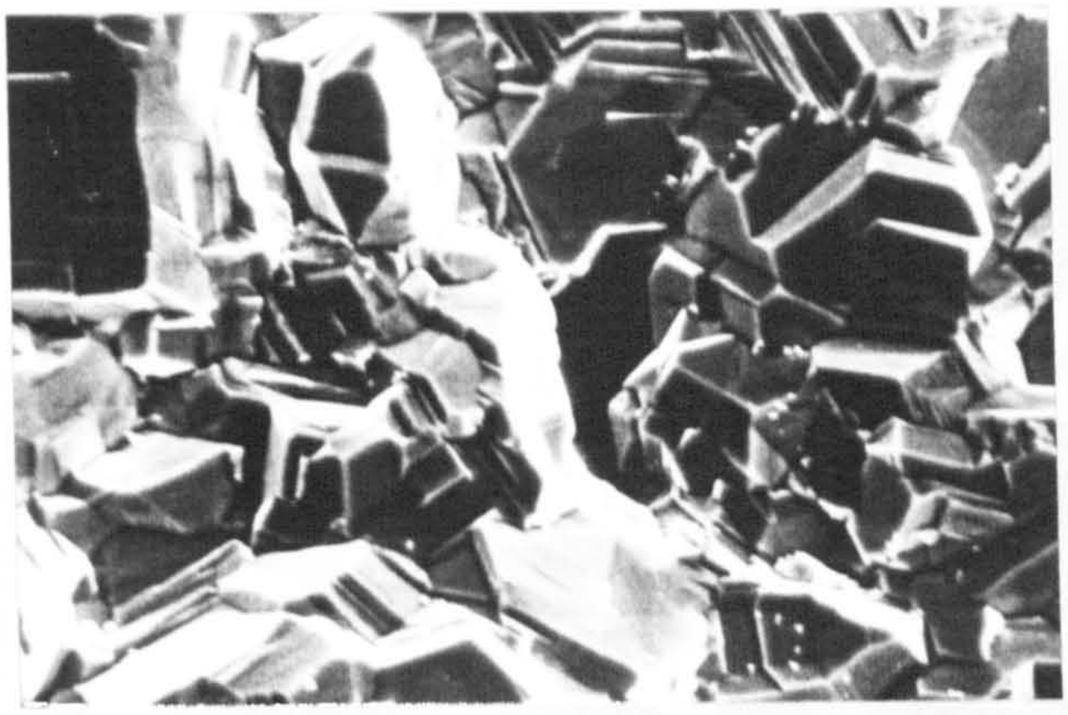

FIGURE 14P

Higher magnification view of the Pb deposit shown in Figure 13P.

(Magnification 3000X)

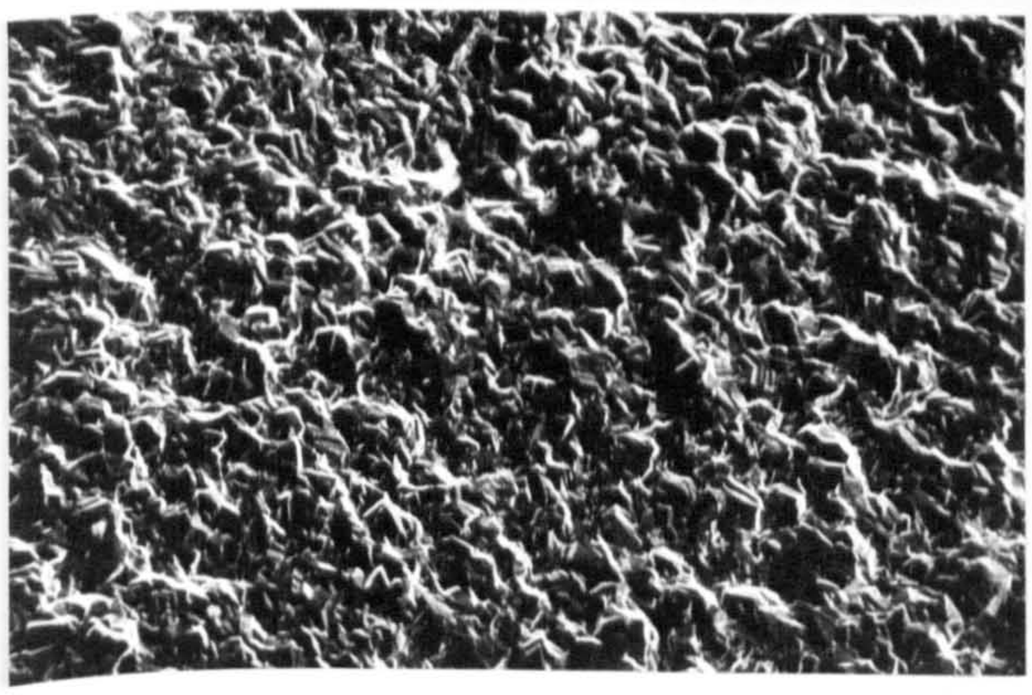

FIGURE 15P

View of the Pb deposit shown in Figure 13P.

(Magnification 400X)

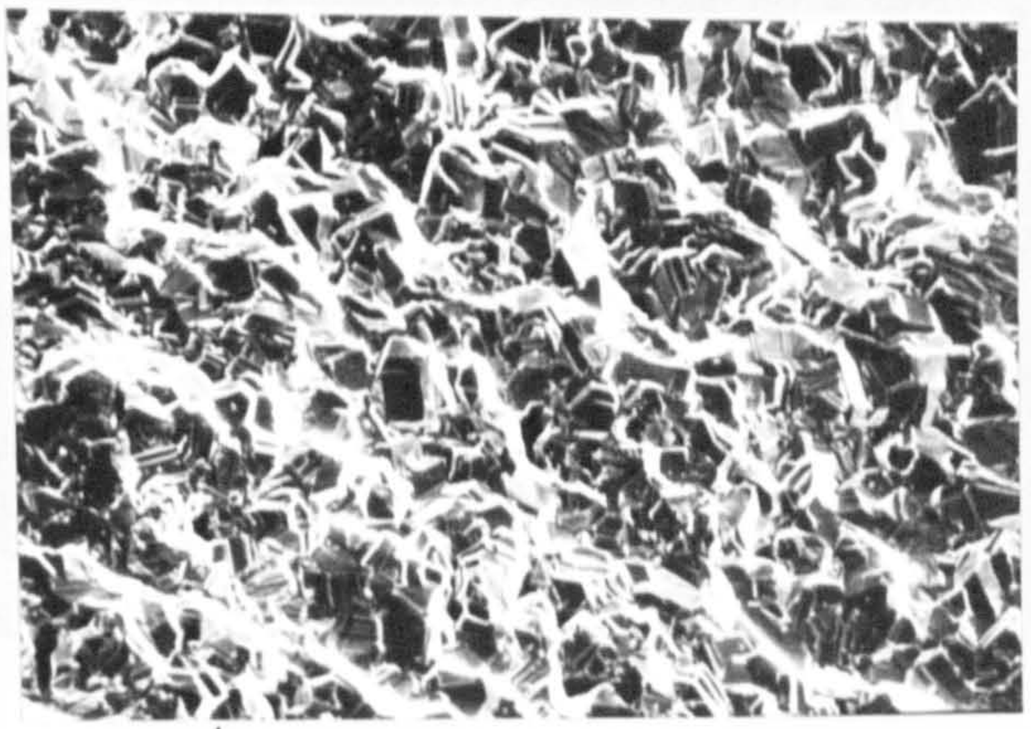

FIGURE 16P

A view of the Pb deposit shown in Figure 13P, without surface pores.

(Magnification 700X)

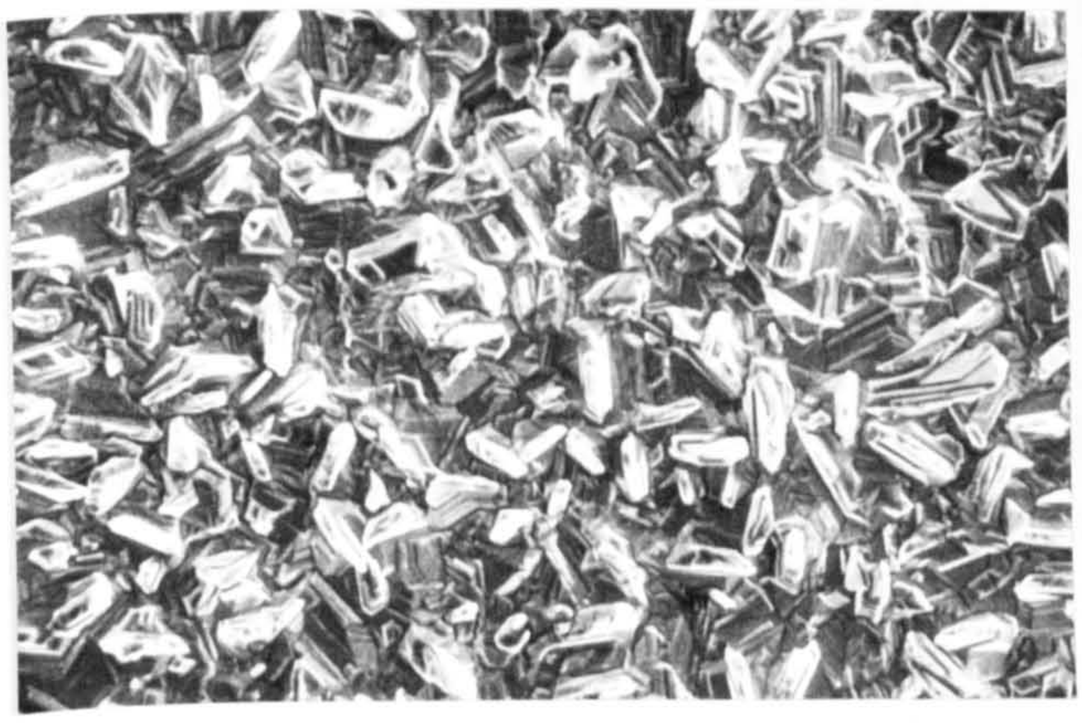

FIGURE 17P

A view of the Pb deposit obtained from a solution of of $45gl^{-1}$ Pb $(NO_3)_2$ + 3 gl^{-1} Triton X100 + 0.1 gl^{-1} anthraquinone -2- monosulphonic acid by electrodeposition at 2 Adm^{-2} at 50°C.

(Magnification 1000X)

FIGURE 18P

A view of the pyramidal Pb deposit shown in Figure 17P.

(Magnification 3000X)

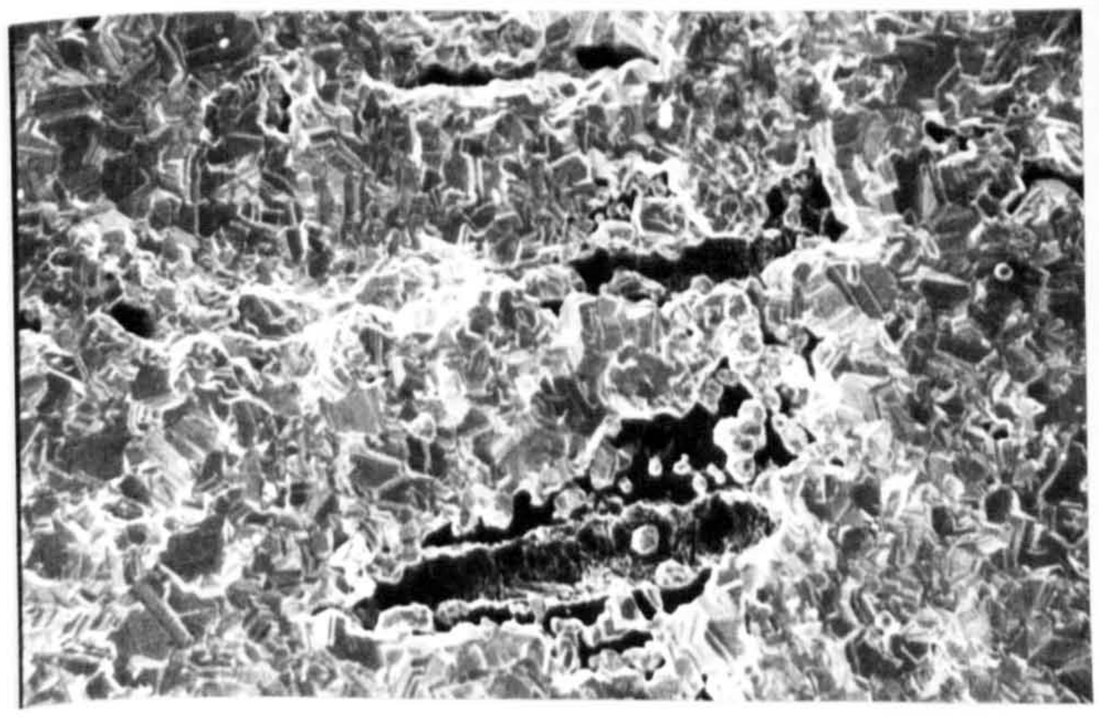

FIGURE 19P

Pb electrodeposited from 360 gl^{-1} solution of Pb Pb $(NO_3)_2$ + 3 gl^{-1} BRIJ 35 + 0.1 gl^{-1} anthraquinone 2-monosulphonic acid at 2 Adm^{-2} and 50°C.

(Magnification 700X)

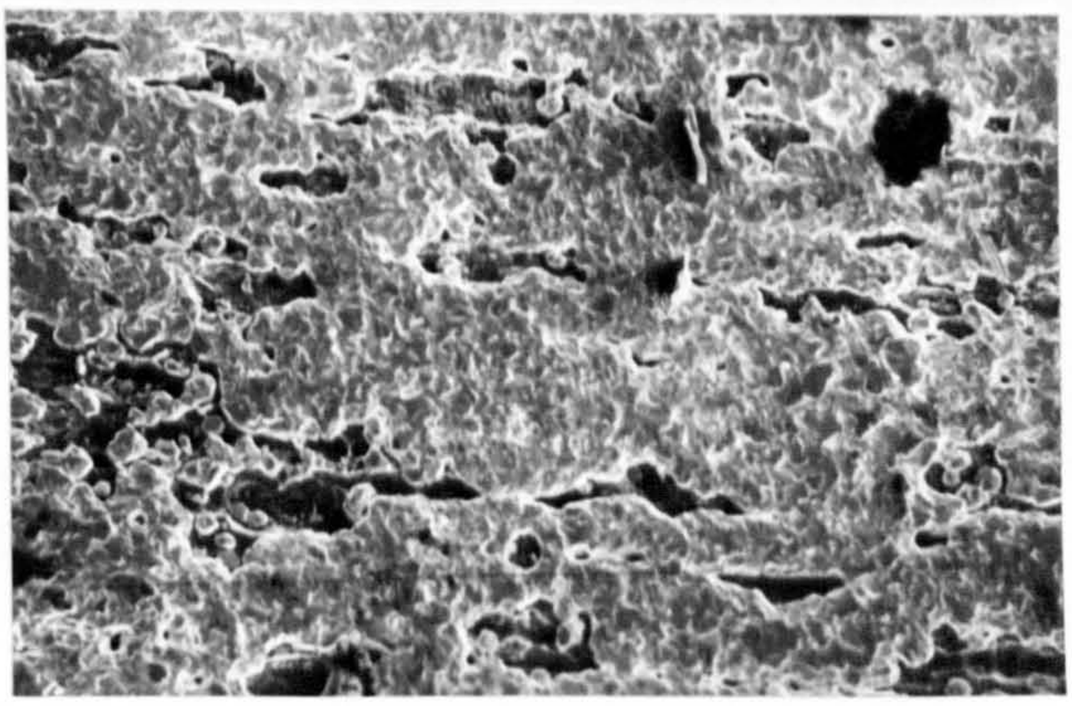

FIGURE 20P

Pb deposit obtained from a solution of 100 gl^{-1} Pb $(NO_3)_2$ + 2 gl^{-1} Triton X100 anthraquinone -2,6- disulphonic acid at 2 Adm^{-2} and 50°C.

(Magnification 400X)

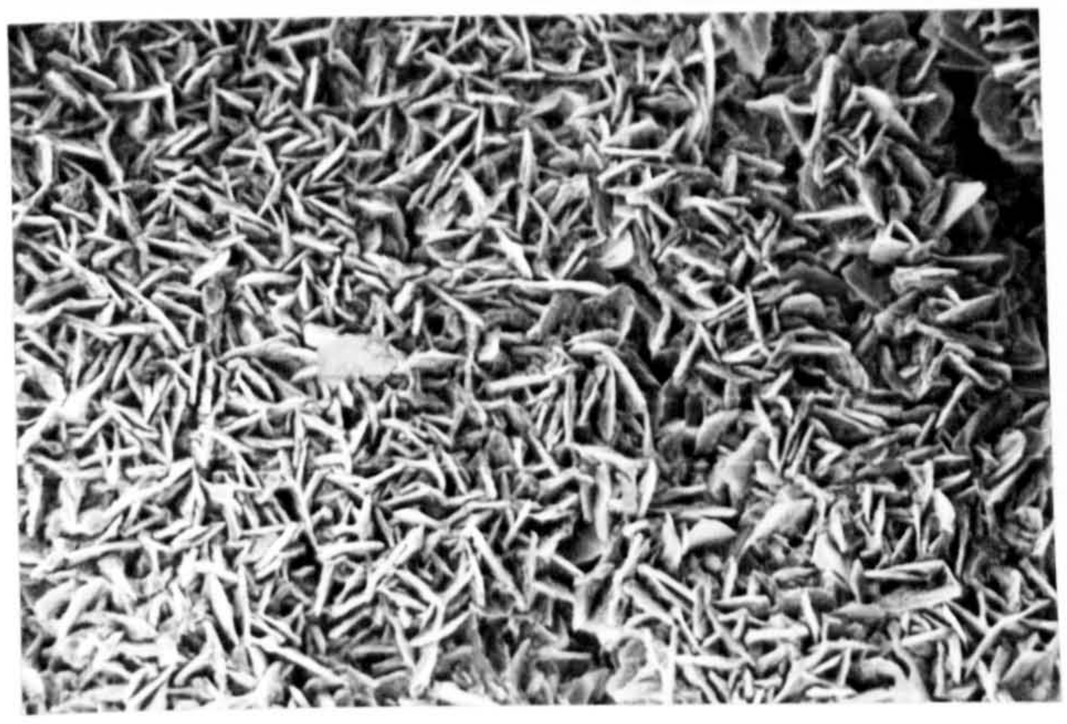

FIGURE 21P

Pb electrodeposited from a solution of 100 gl^{-1} disulphonic acid $Pb(NO_3)_2$ plus 0.1 gl^{-1} anthraquinone -1,5- + disulphonic acid + 2 gl^{-1} Triton X100 at 1 Adm^{-2} and at room temperture.

(Magnification 200X)

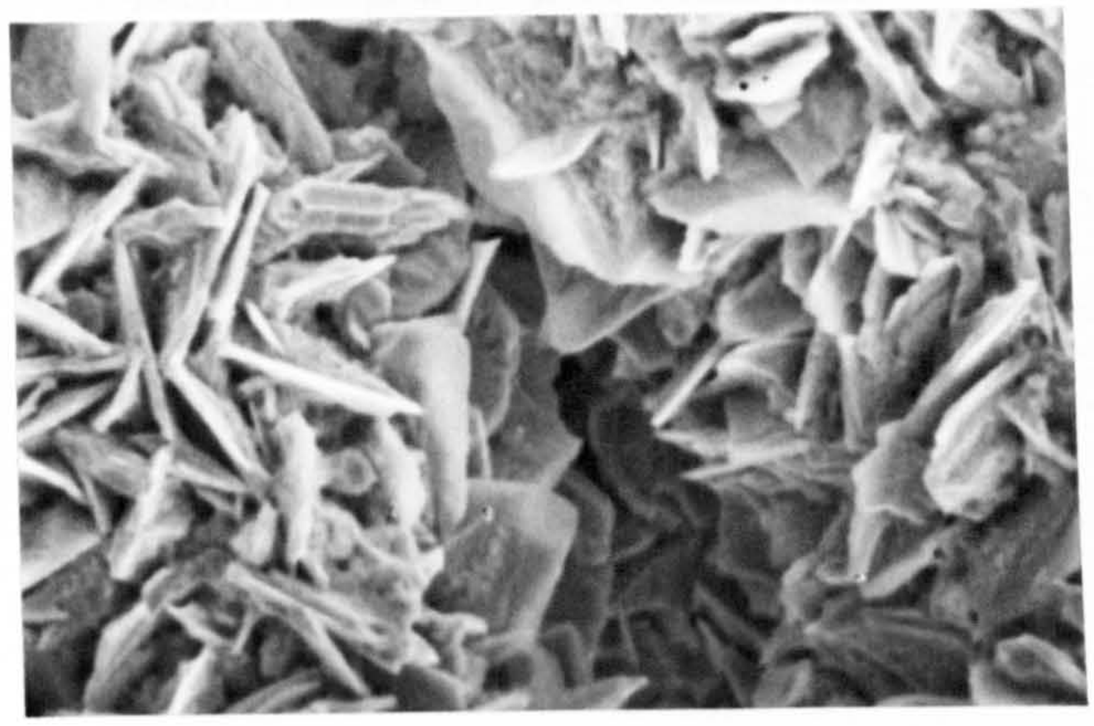

FIGURE 22P

High magnification view of the Pb deposit shown in Figure 21P.

(Magnification 1000X)

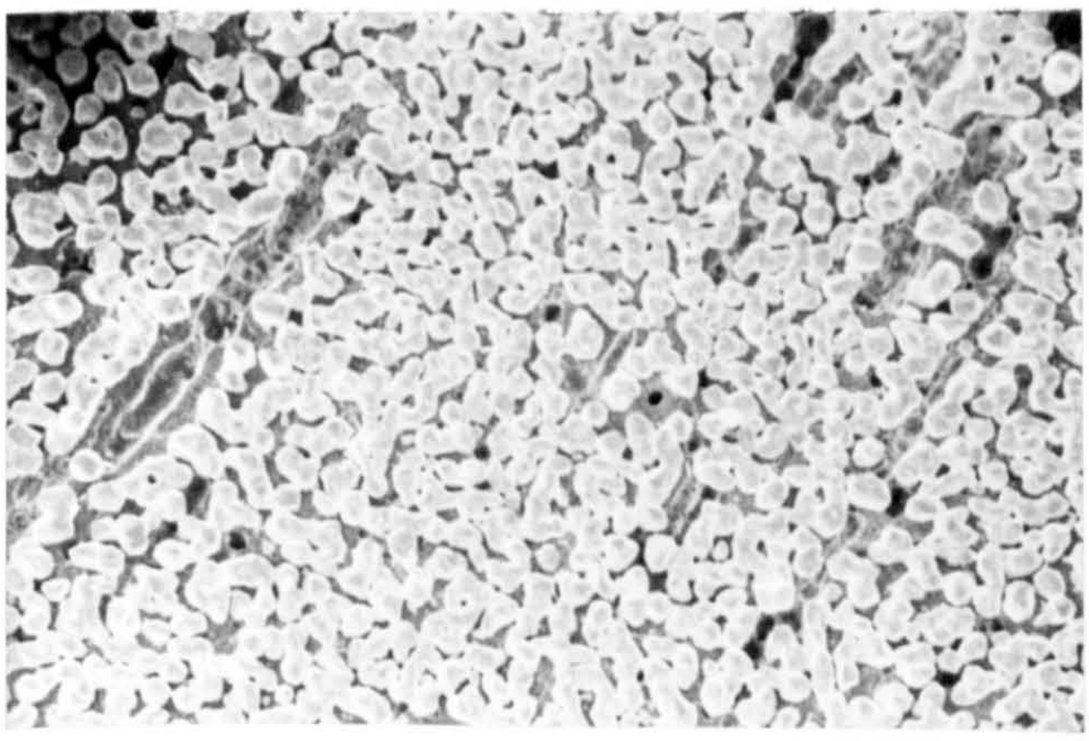

FIGURE 23P

Pb electrodeposited from a solution of 100 gl^{-1} $Pb(NO_3)_2$ plus 2 gl^{-1} Triton + 0.5 gl^{-1} gelatin at 2 Adm^{-2} and at 50°C.

(Magnification 200X)

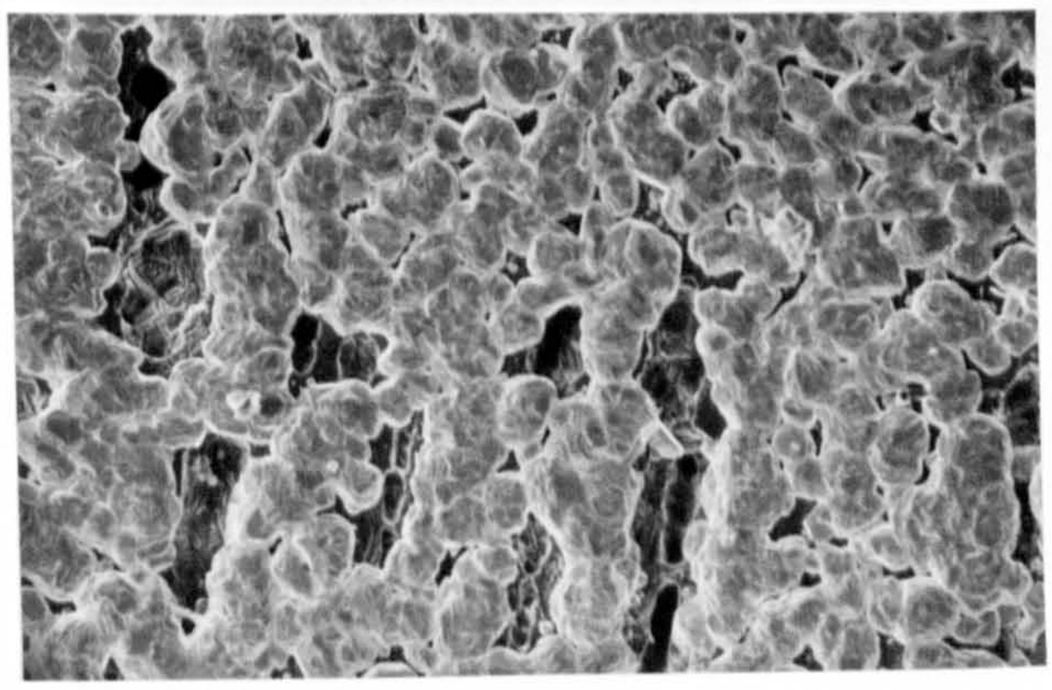

FIGURE 24P

Pb electrodeposited from a solution of 100 gl^{-1} $Pb(NO_3)_2$ + 2 gl^{-1} Triton X100 + 0.3 gl^{-1} napthalene -1,5- disulphonic acid at 2 Adm^{-2} and at 50°C

(Magnification 400X)

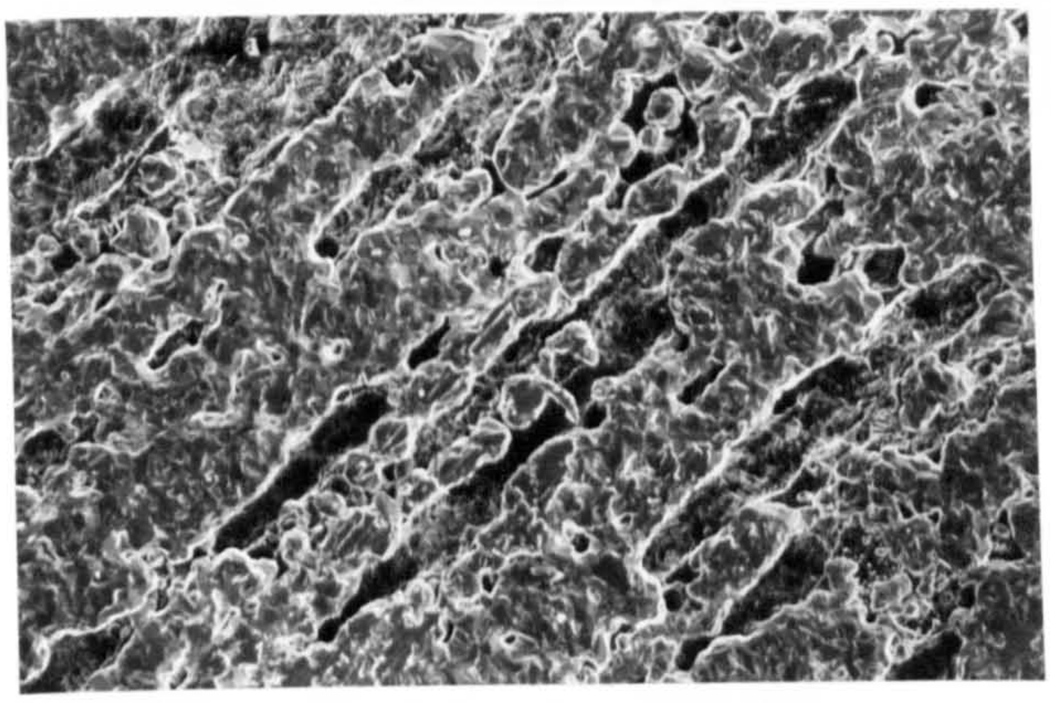

FIGURE 25P

Pb electrodeposited from a solution of 100 gl^{-1} $Pb(NO_3)_2$ + 2 gl^{-1} cetyltrimethylammonium bromide at 2 Adm^{-2} and at 50°C.

(Magnification 200X)

FIGURE 26P

Pb electrodeposited at 2 Adm^{-2} from a 15 minutes from a solution of 360 gl^{-1} $Pb(NO_3)_2$, 2 gl^{-1} Wafex, 2 gl^{-1} tannic acid at room temperature

(Magnification 100X)

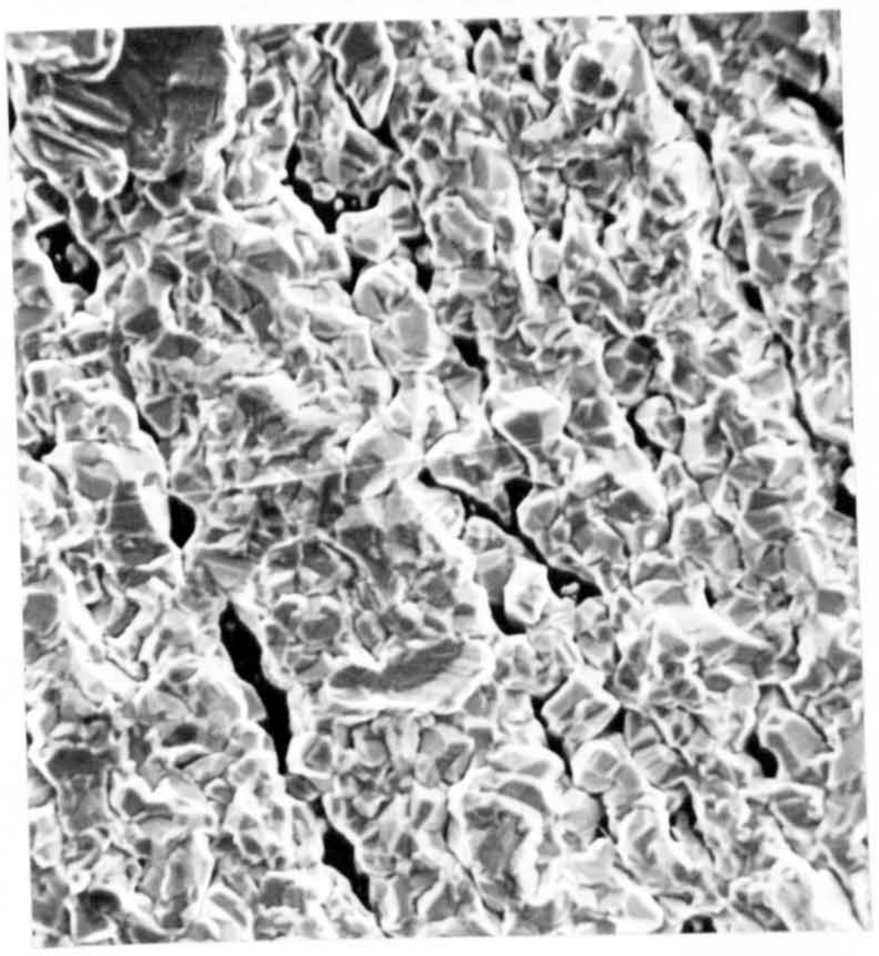

FIGURE 27P

Pb electrodeposited from a solution of 45 gl^{-1} $Pb(NO_3)_2$ + 2 gl^{-1} Wafex + 2 gl^{-1} tannic acid at 4 Adm^{-2} and room temperature

(Magnification 1000X)

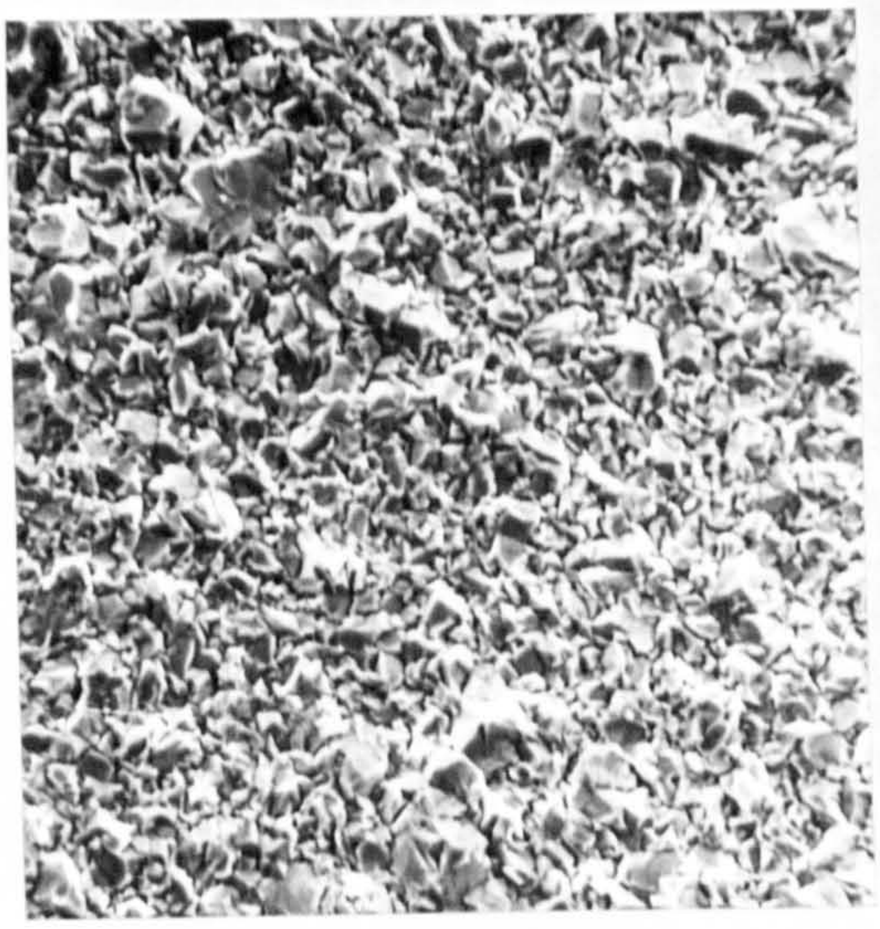

FIGURE 28P

Pb electrodeposited from a solution of 45 gl^{-1} $Pb(NO_3)_2$ + 2 gl^{-1} tannic acid at 1 Adm^{-2} and room temperature

(Magnification 1000X)

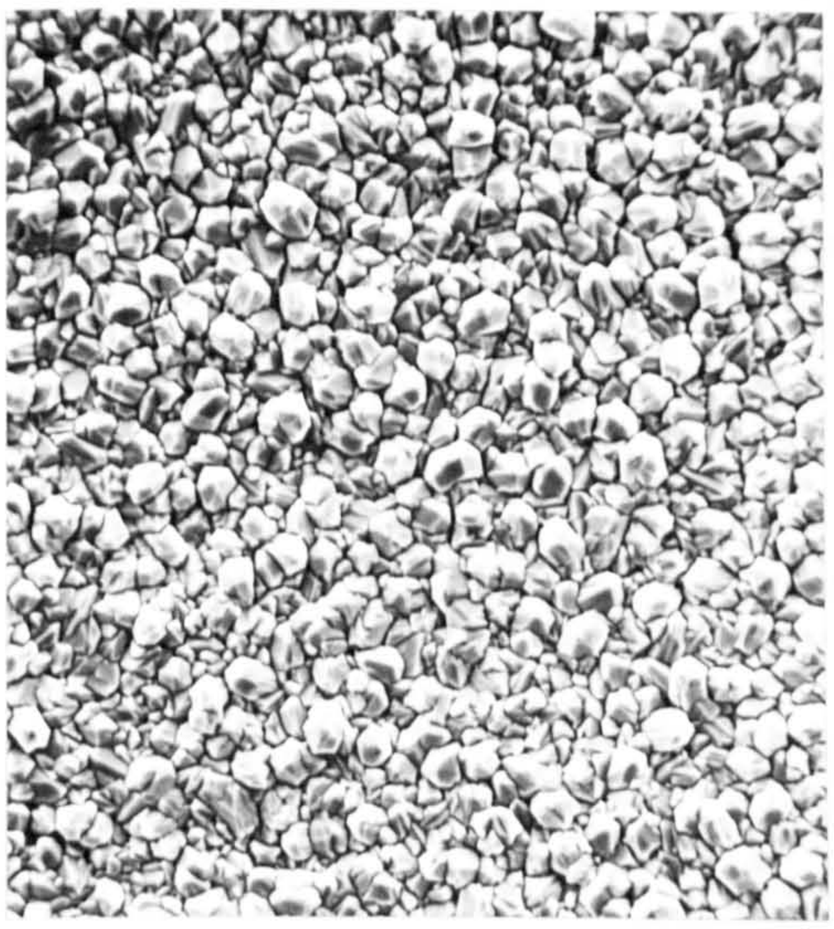

FIGURE 29P

Pb electrodeposited at 4 Adm^{-2} from a solution of 45 gl^{-1} $Pb(NO_3)_2$ + 2 gl^{-1} tannic acid + 2 gl^{-1} Wafex + 20 gl^{-1} HNO_3

(Magnification 1000X)

FIGURE 30P

Higher magnification view of the Pb deposit shown in Figure 29P

(Magnification 2500X)

FIGURE 31P

Pb electrodeposited from a solution of 22 gl^{-1} $Pb(NO_3)_2$ + 2 gl^{-1} Wafex + 2 gl^{-1} tannic acid + 20 gl^{-1} HNO_3 at 1 Adm^{-2} and room temperature

(Magnification 2500X)

FIGURE 32P

Pb electrodeposited from a solution of 45 gl^{-1} $Pb(NO_3)_2$ + 2 gl^{-1} Wafex + 2gl^{-1} tannic acid + 20 gl^{-1} HNO_3 at 2 Adm^{-2} and 50 ^{o}C

(Magnification 1000X)

The effect of increase in the deposition c.d. from 2 Adm^{-2} to 4 Adm^{-2} on the deposit obtained from a 45 gl^{-1} $Pb(NO_3)_2$ solution can be seen in Fig. 29P; no pores in the Pb deposit could be seen (Fig. 30P). A further decrease in the Pb $(NO_3)_2$ concentration to 22 gl^{-1} $Pb(NO_3)_2$ did not result in a change in the deposit morphology (see Fig. 31P). Although a reduction in c.d. did produce a deposit of smaller grain size (compare Fig. 30P with Fig. 31P). Deposition of Pb at elevated temperatures results in a deposit that does not have such a clearly defined structure when compared to the room temperature deposit (see Fig. 32P).

The use of Wafex alone resulted in the formation of inferior Pb deposits whilst Wafex in combination with aloin did not produce any noticeably improvement in surface coverage.

3.1.4.2 S.E.M. examination of PbO_2 deposits when electrodeposited onto a Ni substrate from $Pb(NO_3)_2$ solutions containing different addition agents.

A view of the PbO_2 deposit obtained by electrodeposition from a non-additive containing solution of 360 gl^{-1} $Pb(NO_3)_2$ at 50°C is shown in Fig. 33P. The pore seen in this micrograph is thought to be due to PbO_2 deposition occuring inside an etch pit on the Ni substrate, rather than a crack in the PbO_2 coating. A higher magnification view of the PbO_2 deposit is seen in Fig. 34P. The deposit appears to consist of a number of irregularly shaped crystals.

The nature of the PbO_2 deposit obtained from low $Pb(NO_3)_2$ concentration solutions namely 180 gl^{-1} $Pb(NO_3)_2$ and 100 gl^{-1} $Pb(NO_3)_2$ using the same deposition parameters can be seen in Figs. 35P to 38P. No readily apparent change in the deposit morphology with decrease in $Pb(NO_3)_2$ concentration could be observed.

The morphology of the PbO_2 deposit obtained when Triton X100 was added to a $Pb(NO_3)_2$ plating solution in conjunction with anthraquinone-2-monosulphonic acid (Fig. 39P) and butyne 1,4 diol (Fig. 40P) was not noticeably different from that obtained from a non additive bath, except that a possible reduction in grain size with the latter additives was observed.

However, the use of other organic additives for the simultaneous electrodeposition of both Pb and PbO_2 from a $Pb(NO_3)_2$ solution did have a significant effect on the resultant PbO_2 deposit. The addition of 0.5 gl^{-1} peptone to a 180 gl^{-1} $Pb(NO_3)_2$ solution maintained at a 50°C followed by deposition at a c.d. of 0.5 Adm^{-2} onto a Ni substrate, produced a smooth, bright, highly reflective PbO_2 deposit (see Fig. 41P). This deposit was highly stressed as is evident by the cracks seen in the deposit and showed no definable crystal structure for PbO_2 even at relatively high magnification (see Fig. 42P). PbO_2 deposits obtained from the same solution yet at a higher c.d. (4 Adm^{-2}) are of a different appereance. Rounded craters can be seen in the PbO_2 deposit, presumably due to oxygen evolution occuring at this c.d. with the gas bubbles so formed adhering to the deposit surface reducing the rate of PbO_2 formation and thus producing craters (see Figs. 43P and 44P). No evidence of cracks in the deposit could be detected and small crystals of PbO_2 could be seen, even at relatively low magnification. At higher magnification (Fig. 45P) the PbO_2 crystals can be seen to be of small grain size when compared to the deposit obtained from a non-additive solution under the same conditions (Fig. 36P). The PbO_2 crystals are all of similar appearance i.e elongated pyramids rather than the hexagonalshaped crystals formed from the non-additive solution.

The use of Wafex as an addition agent also resulted in the formation of craters in the PbO_2 deposit (see Fig. 46P). Cracks in the deposit were visible and appeared to originate at the centre of the craters, the edges of which were smooth with no definable crystal structure (see Fig. 47P). The PbO_2 deposit obtained from a Wafex containing solution of $Pb(NO_3)_2$ was of a regular appearance and consisted of small

elongated pyramids of PbO_2. Deposition of PbO_2 from the same solution but at a slightly decreased c.d. also produced a deposit in which the individual grains in the PbO_2 deposit could be identified (see Fig. 48P). The grain size of the deposit from this solution can be seen to be considerably smaller than that from a non-additive solution by comparing Fig. 48P with Fig. 35P. Cracks in this deposit were visible presumably due to its' high internal stress.

Other organic addition agents when added to $Pb(NO_3)_2$ plating solutions also resulted the production of fine grained PbO_2 deposits. In the case of addition of 1,5 napthylamine to a 100 gl^{-1} $Pb(NO_3)_2$ solution no crystal structure could be identified (see Fig. 49P) except under high magnification and then only at the edges of cracks in the PbO_2 deposit (see Figure 50P). The PbO_2 deposit obtained using this additive was dull, with the micrographs showing an undulating highly stressed PbO_2 deposit. The use of 0.5 gl^{-1} 6,8 napthylamine instead of 1,5 napthylamine did not have such a marked effect on the nature of the PbO_2 deposit obtained (see Figs. 53P and 54P).

The use of 1 nitroso-2-napthol-3,6-disulphonic acid also resulted in a reduction in the PbO_2 deposit grain size and the formation of regular pyramidal crystals of PbO_2 (see Figs. 51P and 52P). Similar effects were also obtained using 1-napthol-4-sulphonic acid and napthalene-1,3,6-trisulphonic acid (see Figs. 55P to 57P).

Gelatin when added to a $Pb(NO_3)_2$ plating solution produced some decrease in PbO_2 grain size but resulted in the formation of a highly stressed deposit (see Fig. 58P) with cracks in the coating visible.

The additive CETB has been used by other workers to produce smooth pinhole-free deposits of PbO_2. Yet this additive was found to be unsuccessful when used in the simultaneous deposit of Pb and PbO_2, since it failed to improve the extent of Pb surface coverage on the Ni substrate. Micrographs of the PbO_2

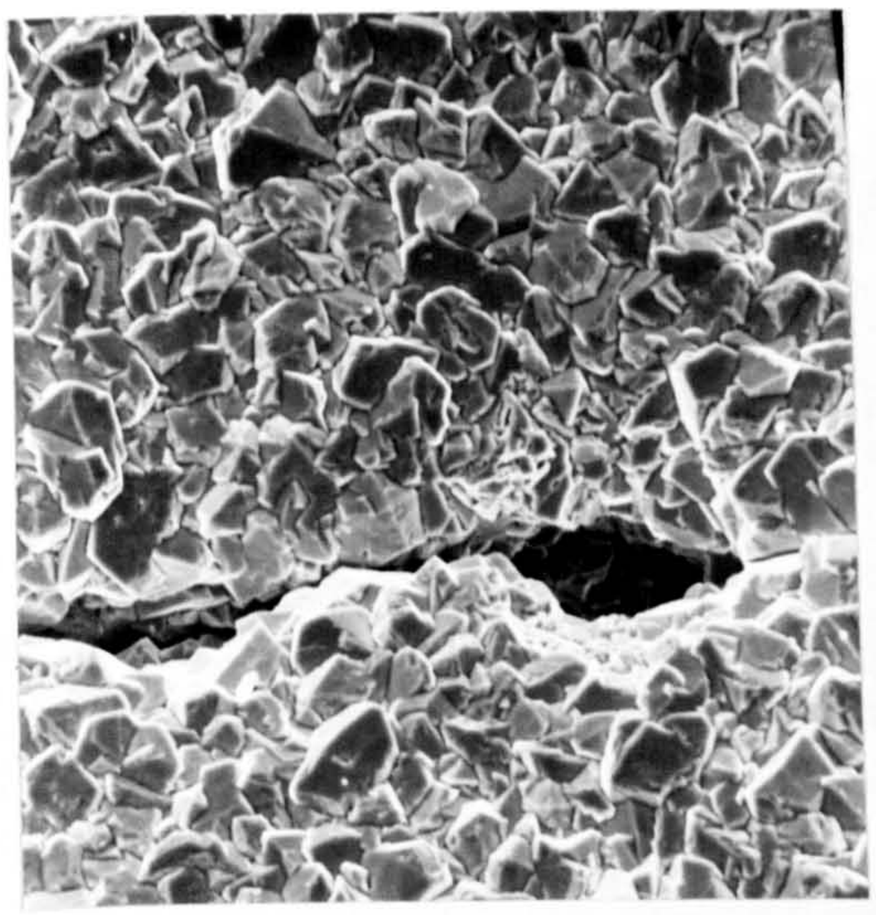

FIGURE 33P

PbO_2 electrodeposited from a solution of 360 gl^{-1} $Pb(NO_3)_2$ at 2 Adm^{-2} and 50 ^{o}C

(Magnification 1000X)

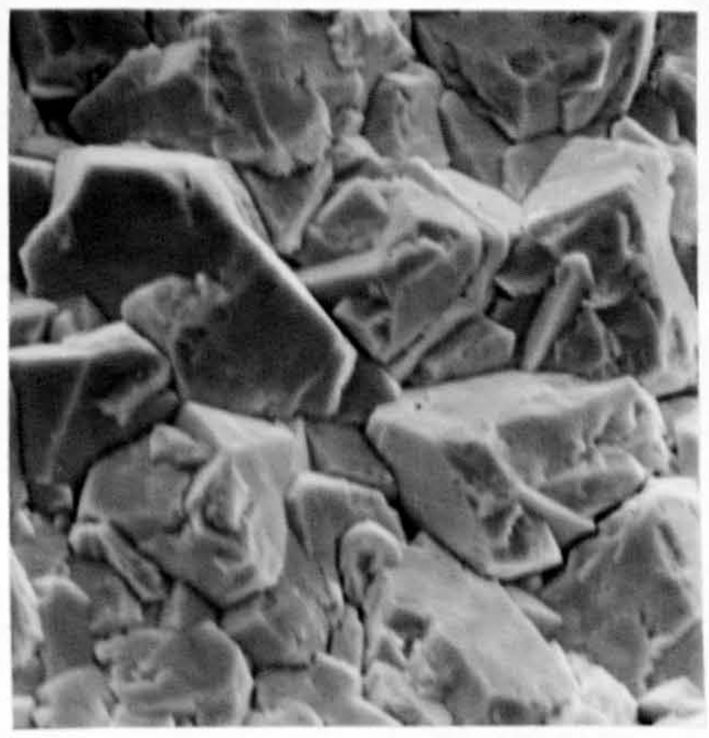

FIGURE 34P

Higher magnification view of the PbO_2 deposit shown in Figure 33P

(Magnification 2500X)

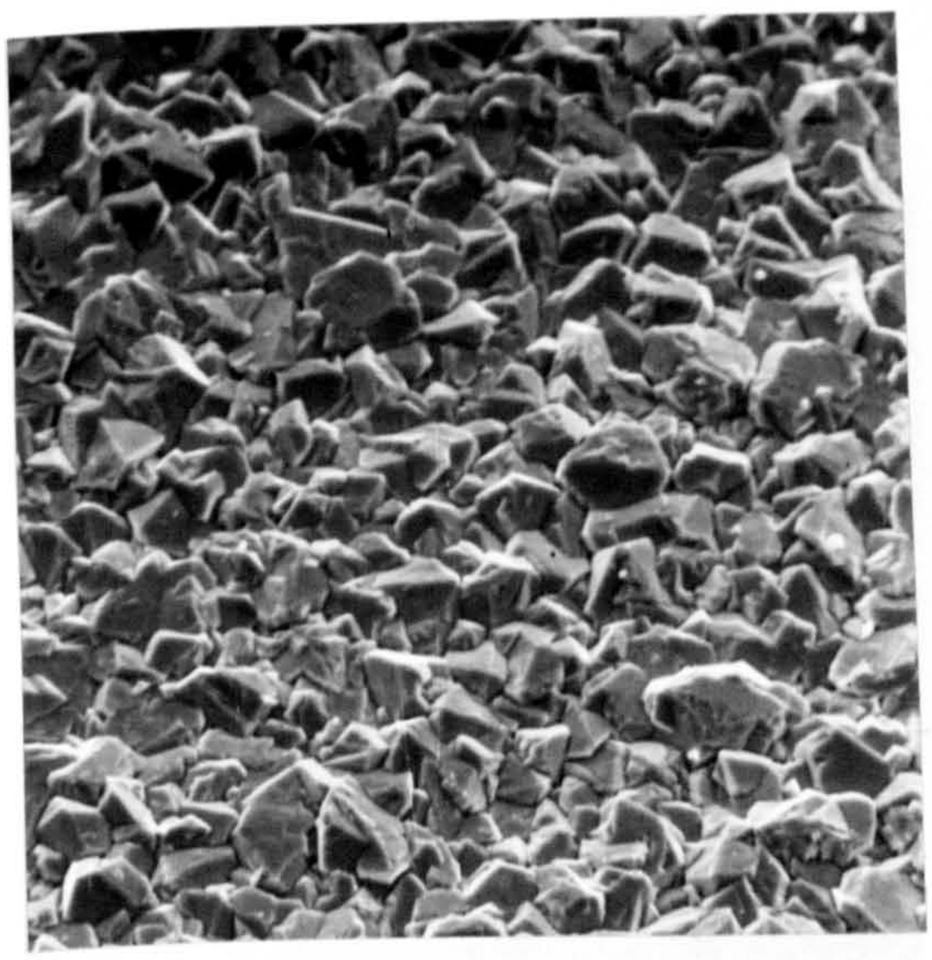

FIGURE 35P

PbO_2 electrodeposited from a 180 gl^{-1} $Pb(NO_3)_2$ solution at 1 Adm^{-2} and 50 ^{o}C

(Magnification 1000X)

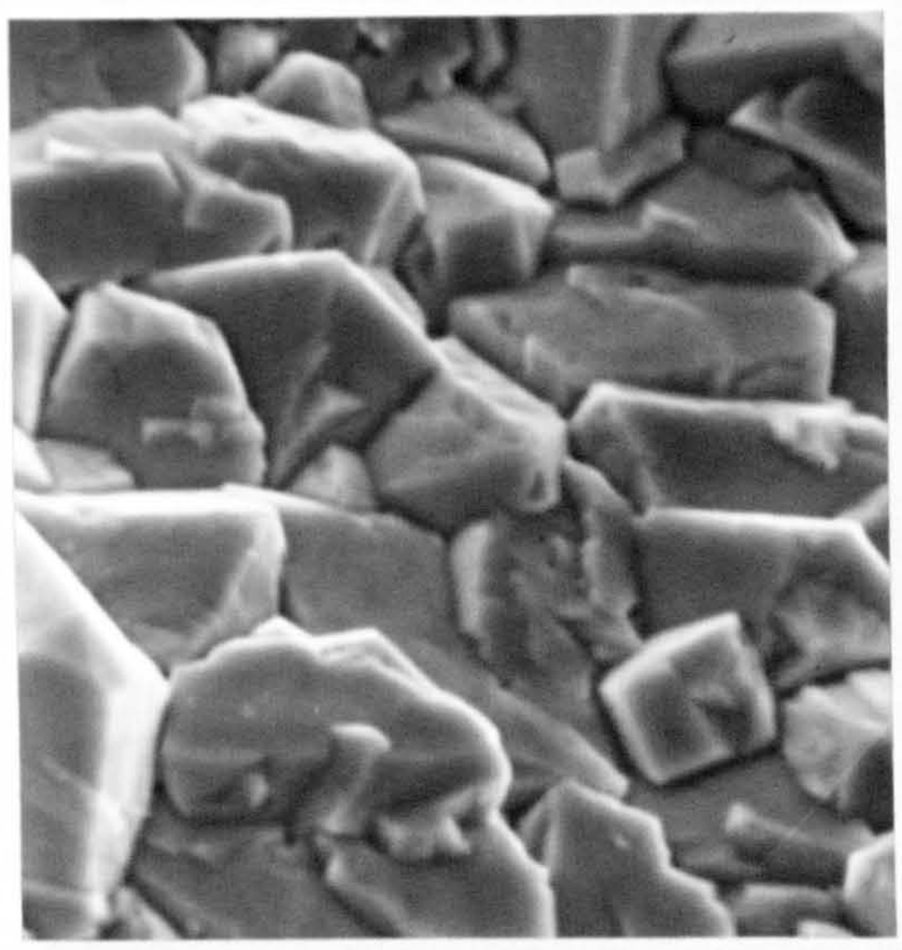

FIGURE 36P

Higher magnification view of the PbO_2 deposit shown in Figure 35P

(Magnification 5000X)

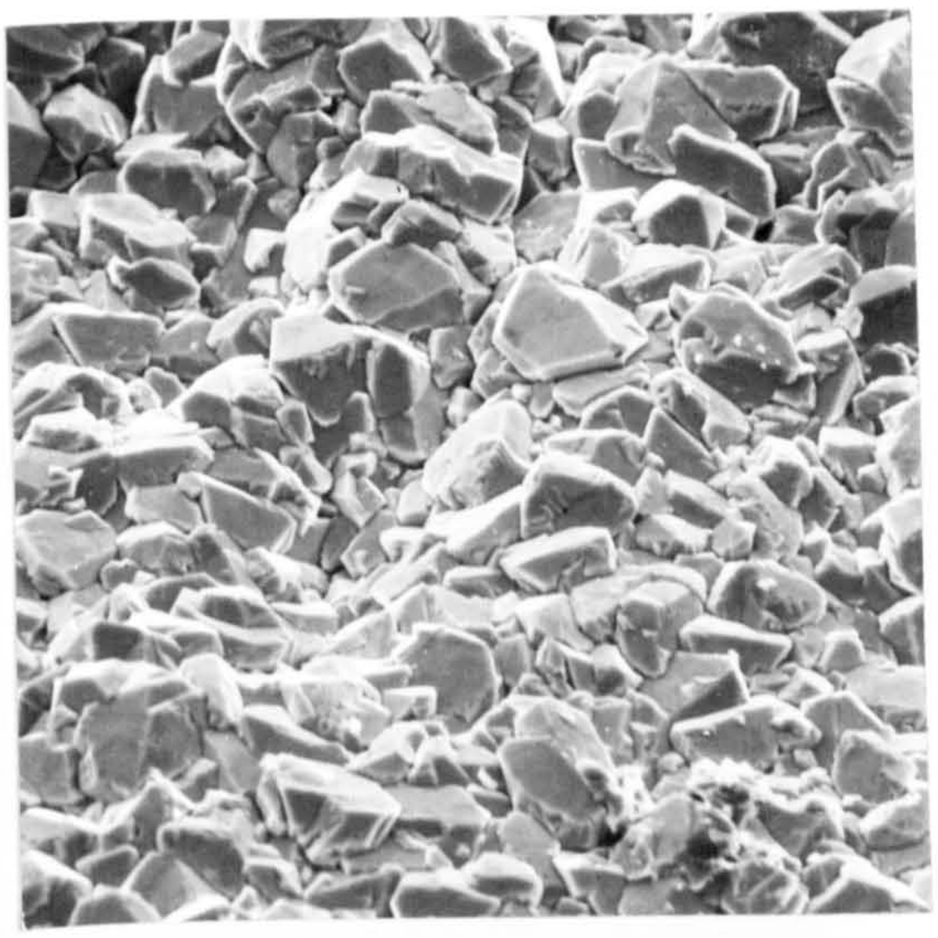

FIGURE 37P

PbO_2 electrodeposited from a solution of 100 gl^{-1} $Pb(NO_3)_2$ at 2 Adm^{-2} and 50 ^{o}C

(Magnification 1000X)

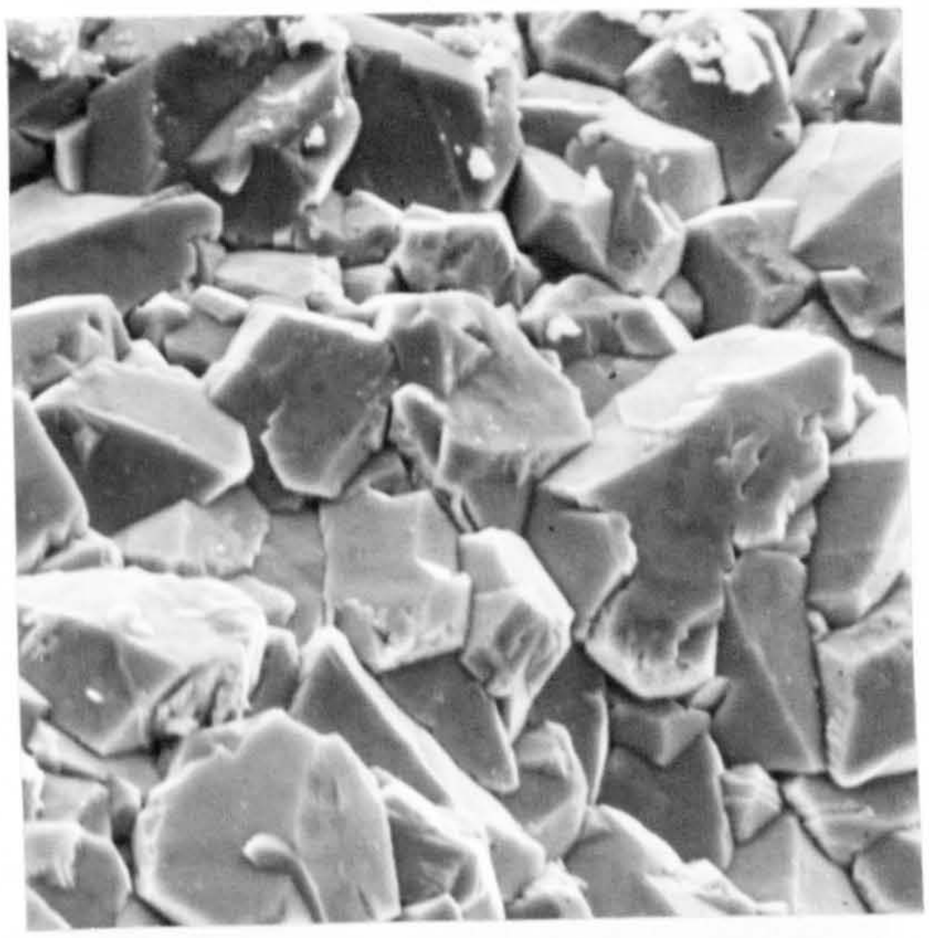

FIGURE 38P

Higher magnification view of PbO_2 deposit shown in Figure 37P

(Magnification 2500X)

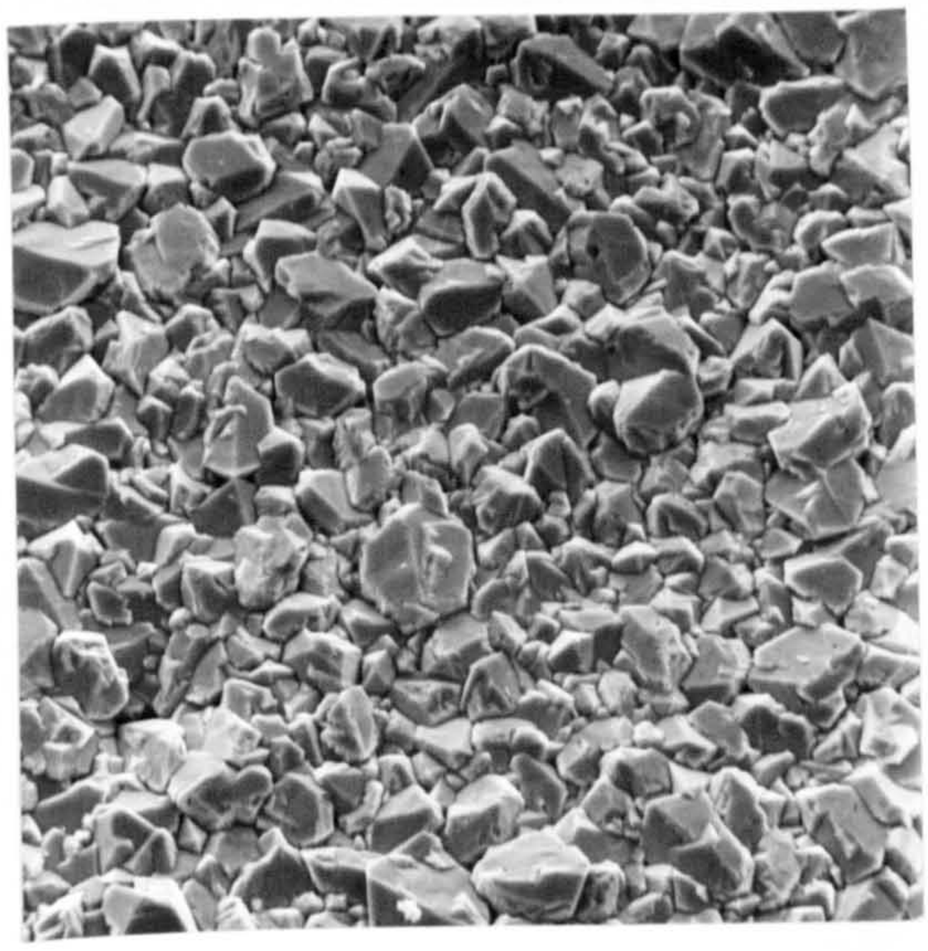

FIGURE 39P

PbO_2 electrodeposited from a solution of 360 gl^{-1} $Pb(NO_3)_2$ 2 gl^{-1} Triton X100 + 0.1 gl^{-1} anthraquinone -2-monosulphonic acid at 2 Adm^{-2} and 50 ^{o}C

(Magnification 100X)

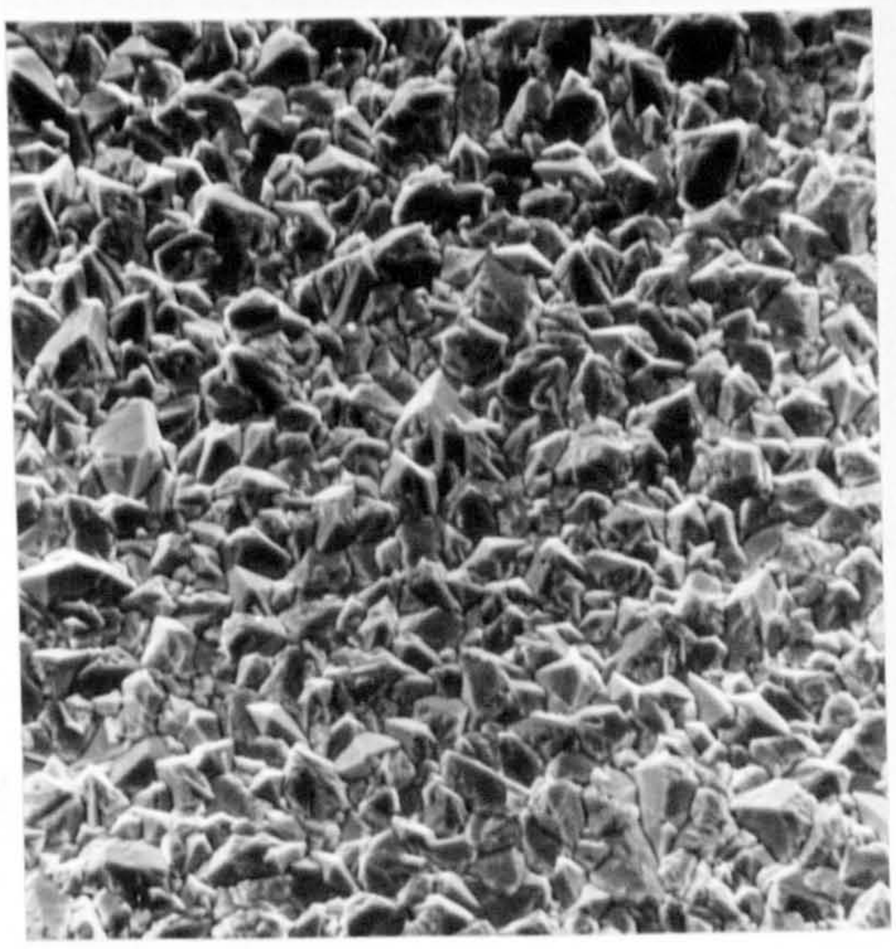

FIGURE 40P

PbO_2 electrodeposited from a solution of 360 gl^{-1} $Pb(NO_3)_2$, 3 gl^{-1} Triton X100 + 1.5 gl^{-1} butyne 1,4 diol at 2 Adm^{-2} and 50 ^{o}C

(Magnification 1000X)

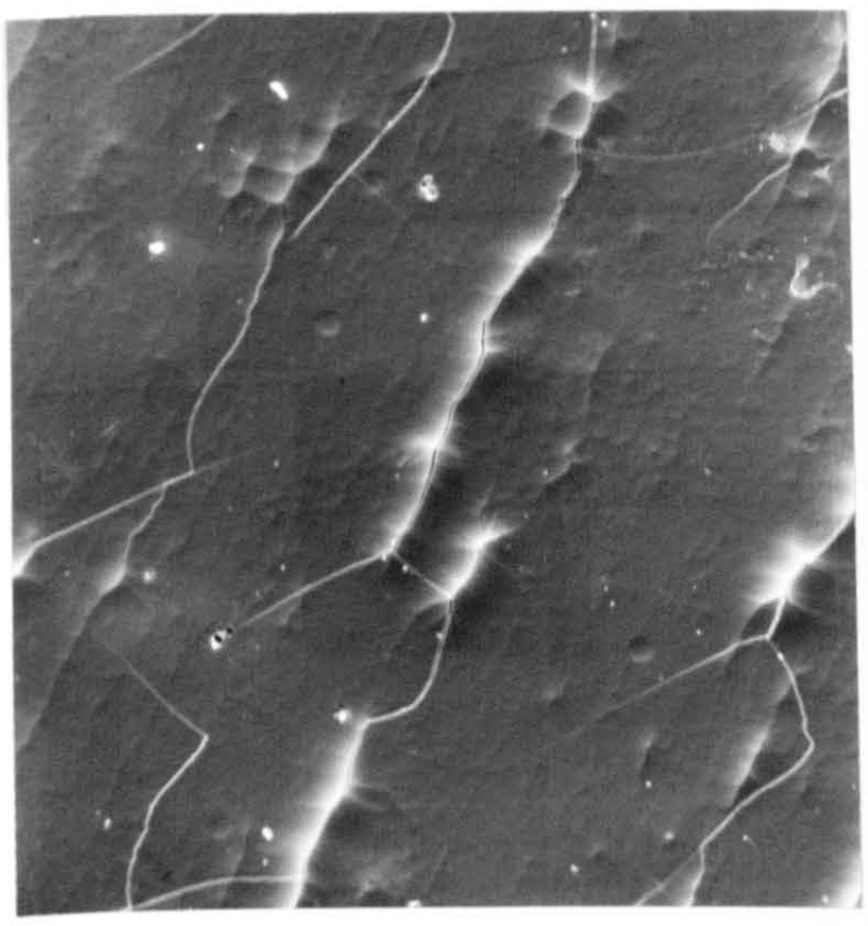

FIGURE 41P

PbO_2 electrodeposited at 0.5 Adm^{-2} from a solution of 180 gl^{-1} $Pb(NO_3)_2$ + 0.5 gl^{-1} peptone at 50 °C

(Magnification 250X)

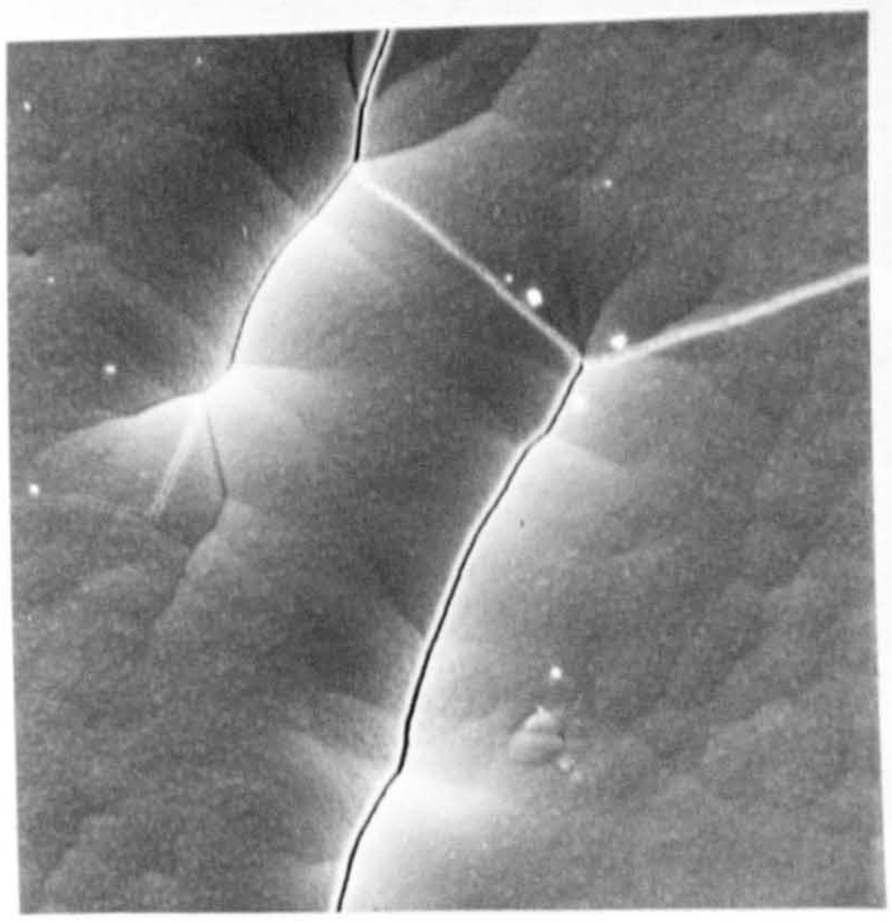

FIGURE 42P

Higher magnification view of the PbO_2 deposit shown in Figure 41P

(Magnification 1000X)

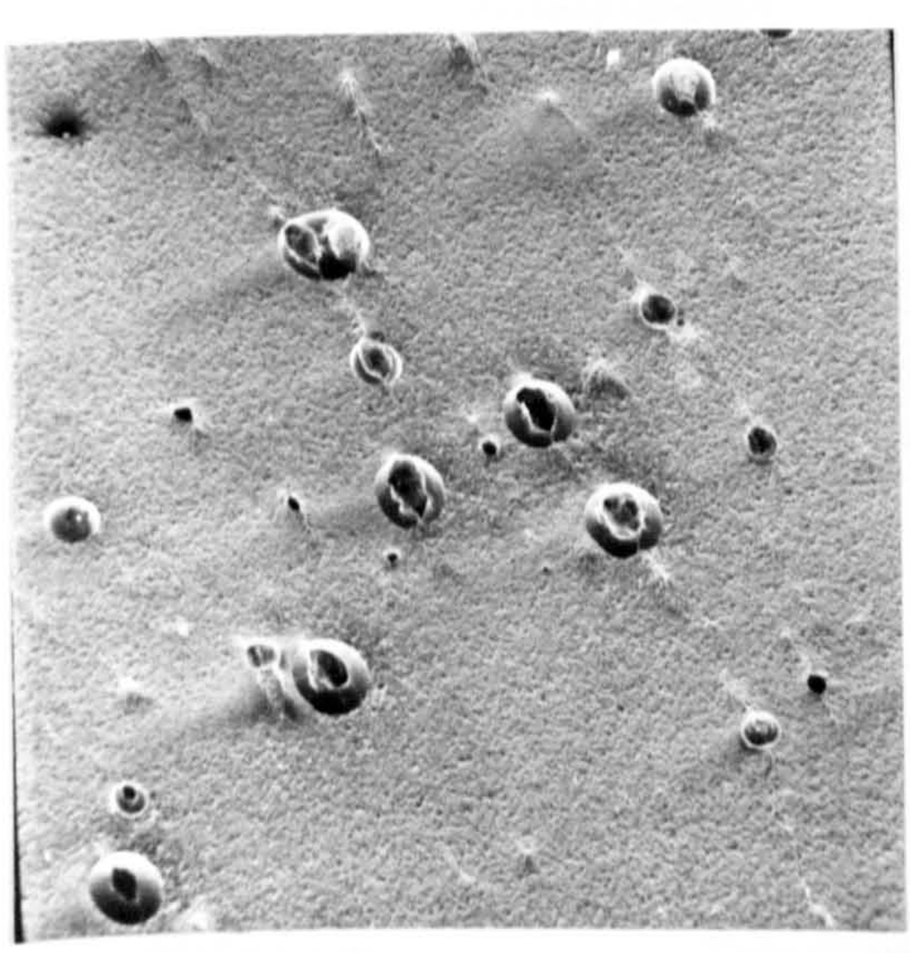

FIGURE 43P

PbO_2 electrodeposited from a solution of 180 gl^{-1} $Pb(NO_3)_2$ + 0.5 gl^{-1} peptone at 4 Adm^{-2} and 50°C

(Magnification 100X)

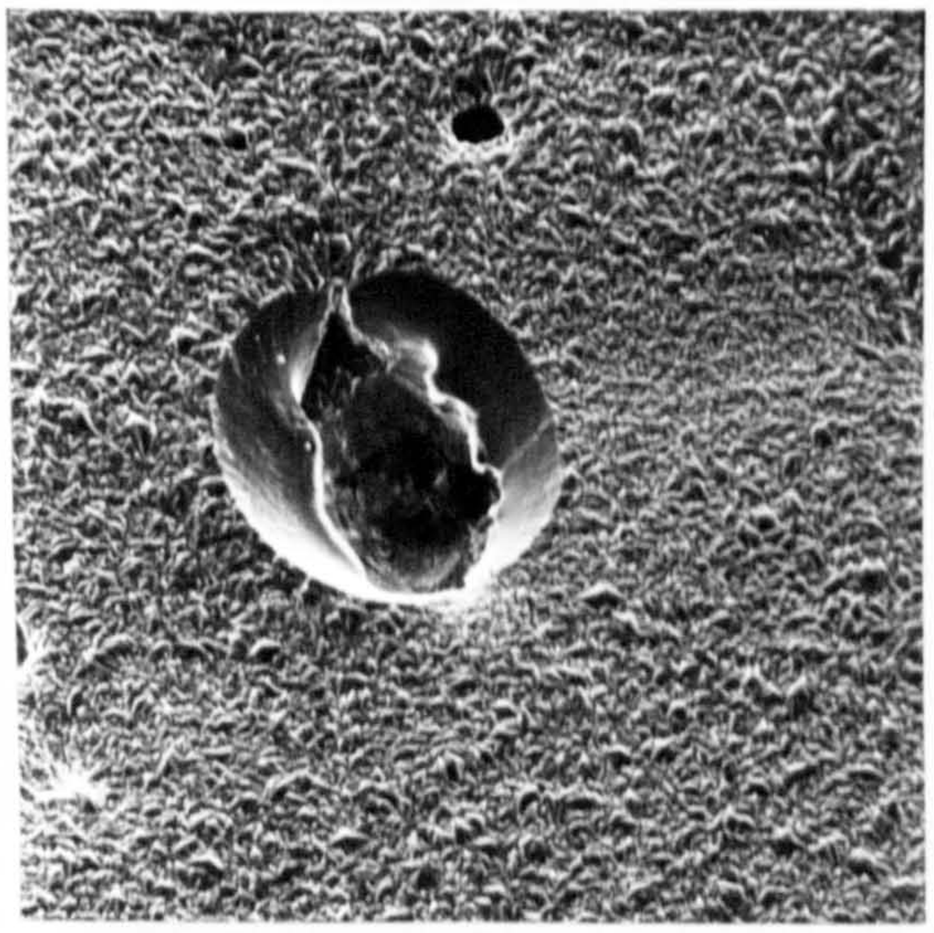

FIGURE 44P

A view of the craters seen in Figure 43P

(Magnification 500X)

FIGURE 45P

High magnification view of the PbO_2 deposit shown in Figure 43P

(Magnification 5000X)

FIGURE 46P

PbO_2 electrodeposited at 2 Adm^{-2} from a solution of 180 gl^{-1} $Pb(NO_3)_2$ plus 1 gl^{-1} Wafex at 50 ^{o}C

(Magnification 250X)

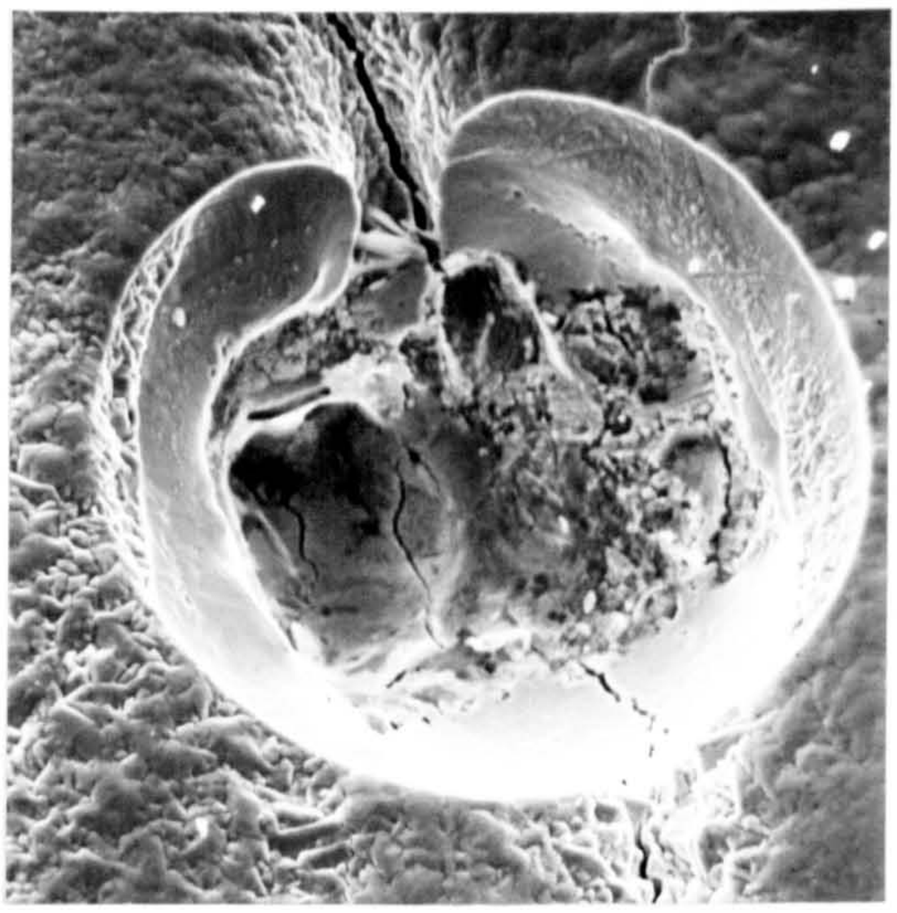

FIGURE 47P

A view of a crater seen in Figure 46P

(Magnification 1000X)

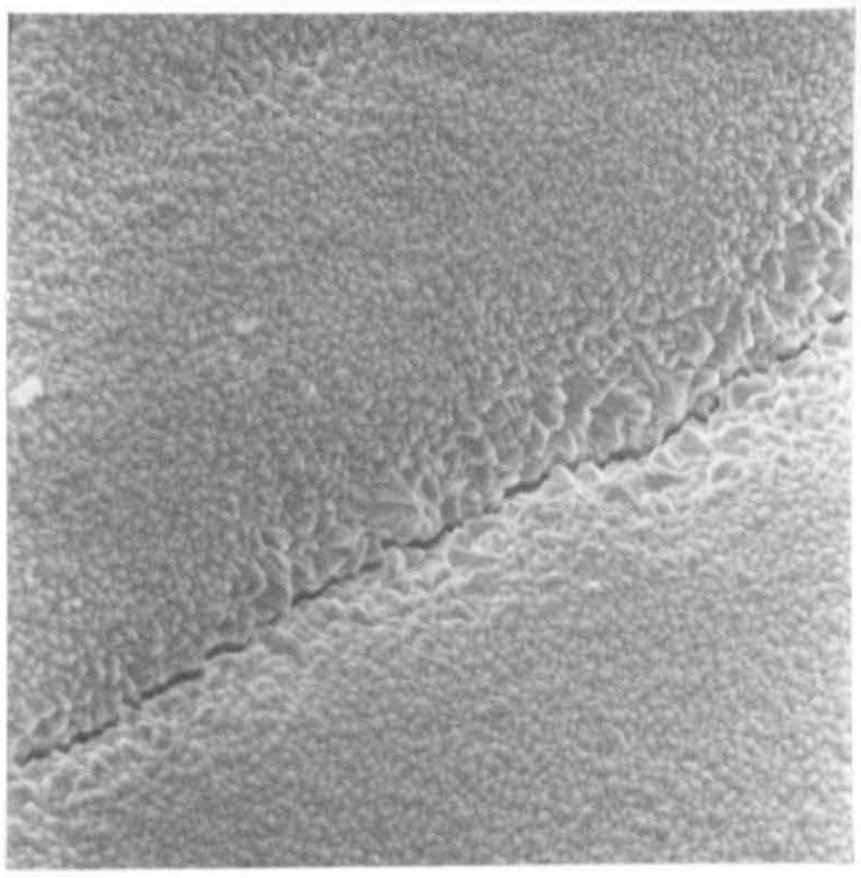

FIGURE 48P

PbO_2 electrodeposited at 1 Adm^{-2} from a solution of 180 gl^{-1} $Pb(NO_3)_2$ 1 gl^{-1} Wafex at 50 ^{o}C

(Magnification 1000X)

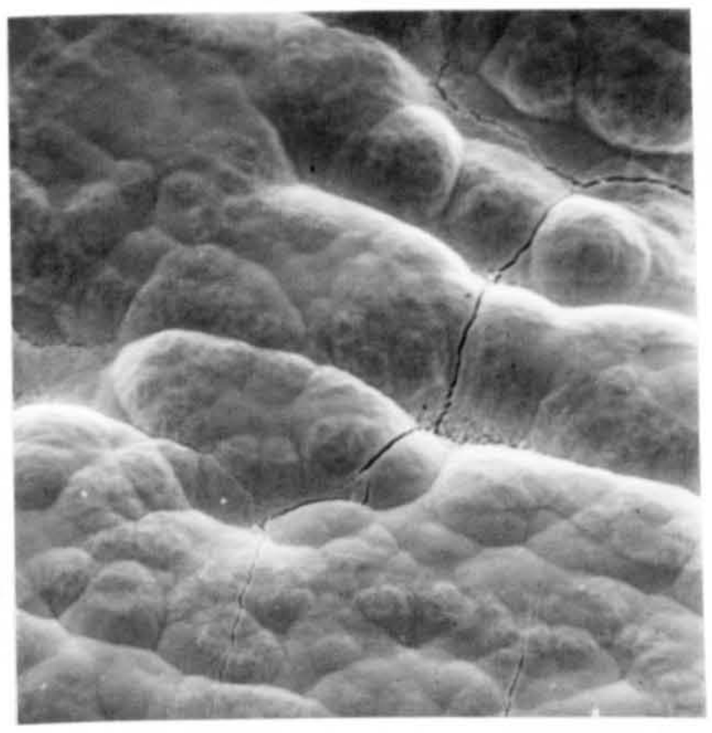

FIGURE 49P

PbO_2 electrodeposited 2 Adm^{-2} from a solution of 100 gl^{-1} $Pb(NO_3)_2$, 2 gl^{-1} Triton X100 + 0.3 gl^{-1} 1,5 napthylamine at 50 °C

(Magnification 1000X)

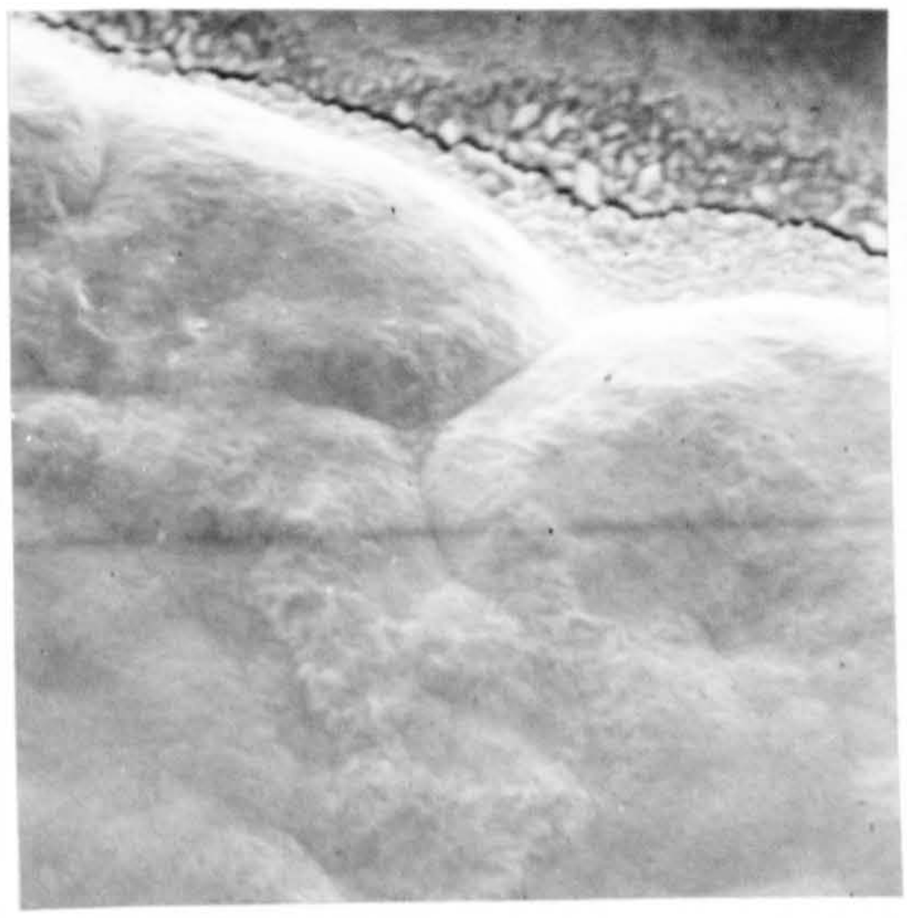

FIGURE 50P

View of crack in the PbO_2 deposit shown in Figure 49P

(Magnification 2500X)

FIGURE 51P

PbO_2 electrodeposited at 2 Adm^{-2} from a solution of 100 gl^{-1} $Pb(NO_3)_2$, 2 gl^{-1} Triton X100 + 0.5 gl^{-1} 1-nitroso napthol -3 6- disulphonic acid at 50°C.

(Magnification 1000X)

FIGURE 52P

Higher magnification view of the deposit shown in Figure 51P

(Magnification 5000X)

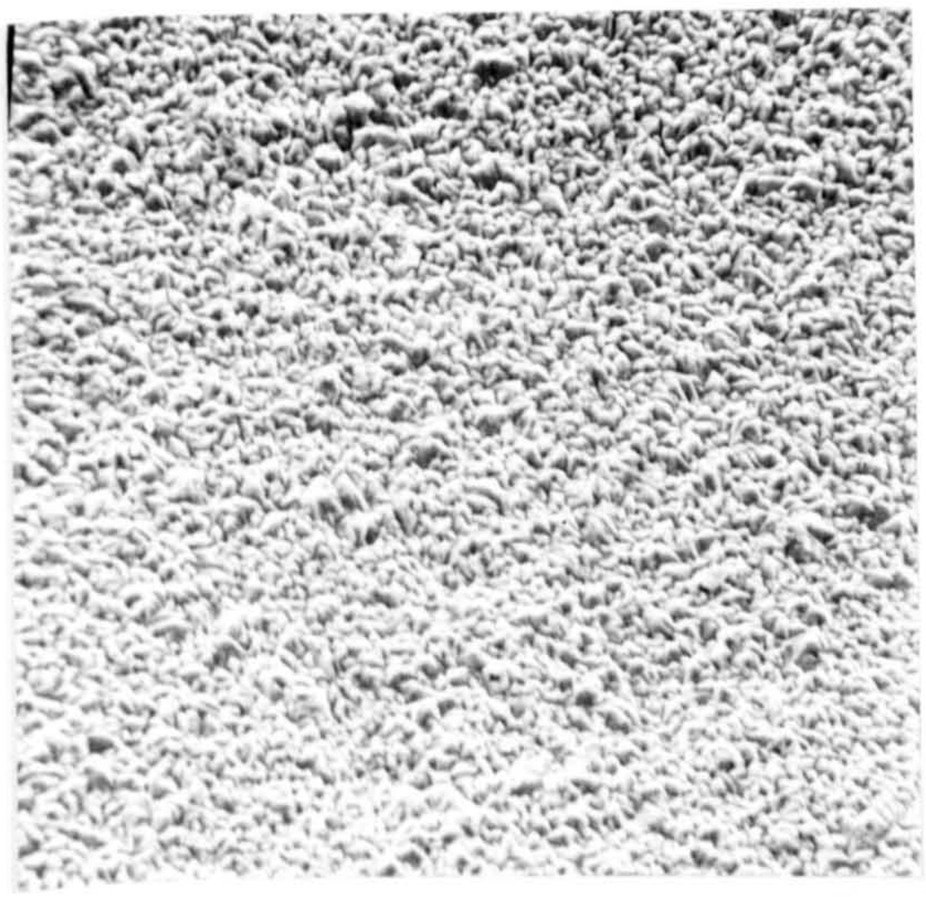

FIGURE 53P

PbO_2 electrodeposited at 2 Adm^{-2} from a solution of 100 gl^{-1} $Pb(NO_3)_2$, 2 gl^{-1} Triton X100 + 0.5 gl^{-1} 6,8 napthylamine

(Magnification 1000X)

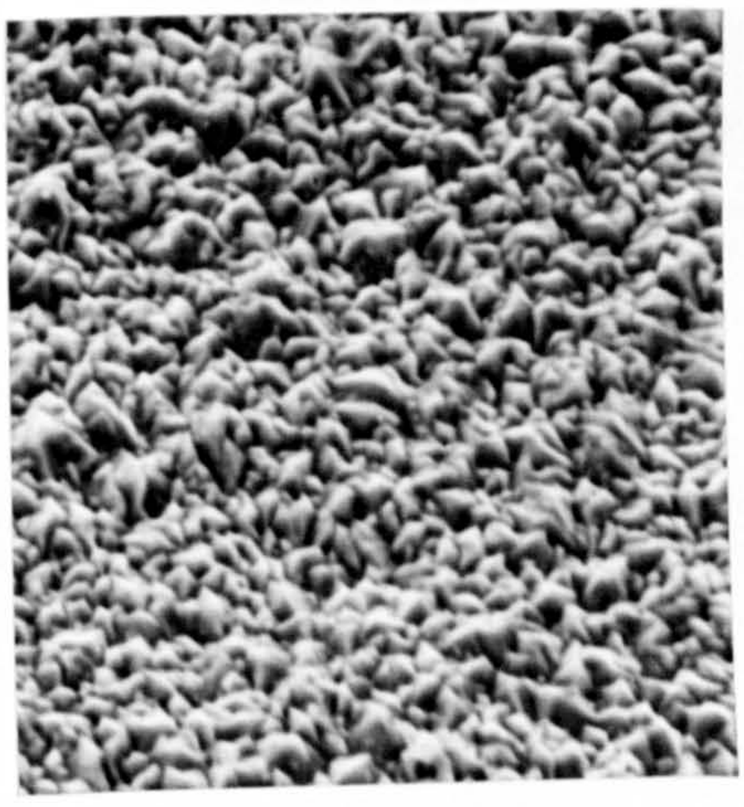

FIGURE 54P

Higher magnification view of the PbO_2 deposit shown in Figure 53P

(Magnification 2500X)

FIGURE 55P

PbO_2 electrodeposited at 2 Adm^{-2} from a solution of 100 gl^{-1} $Pb(NO_3)_2$, 2 gl^{-1} Triton X100 + 0.5 gl^{-1} 1 napthol -4 sulphonic acid at 50°c.

(Magnification 1000X)

FIGURE 56P

A higher magnification view of the PbO_2 deposit shown in Figure 55P

(Magnification 4000X)

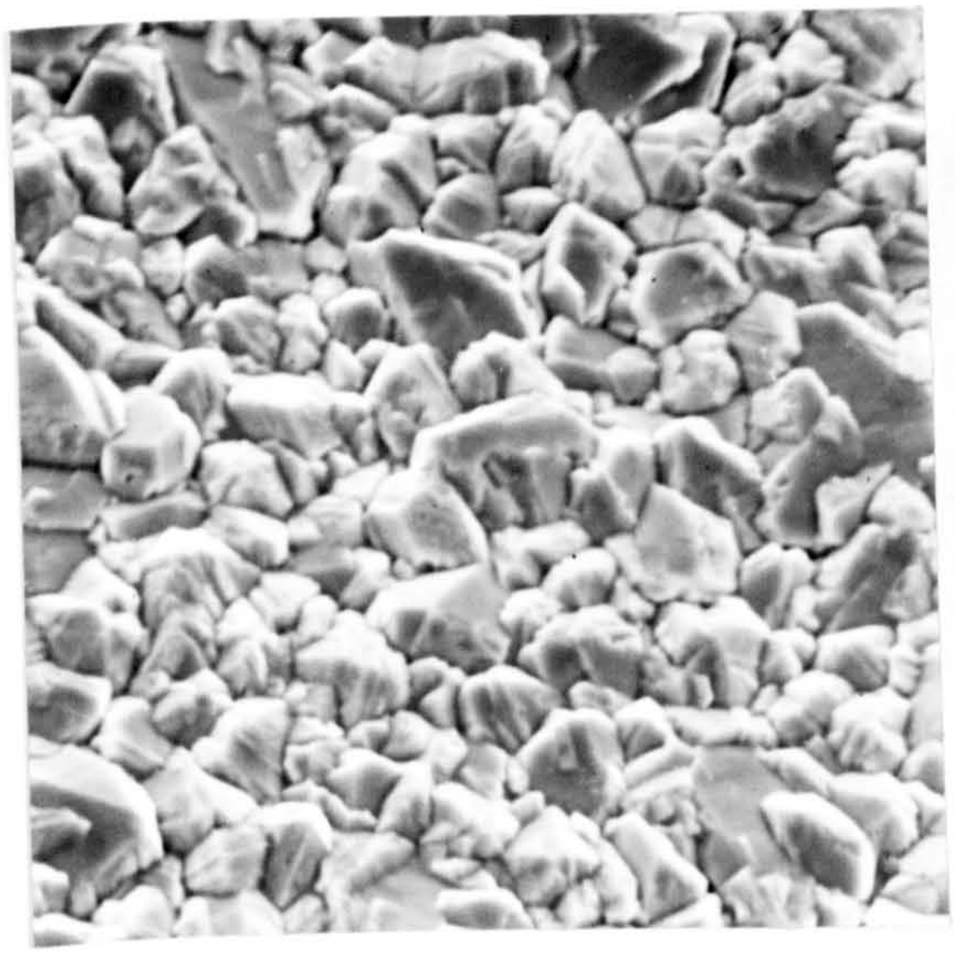

FIGURE 57P

PbO_2 electrodeposited at 2 Adm^{-2} from a solution of 100 gl^{-1} $Pb(NO_3)_2$ 2 gl^{-1} Triton X100 + 0.5 gl^{-1} napthalene -1,3,6 trisulphonic acid at 50°C.

(Magnification 2500X)

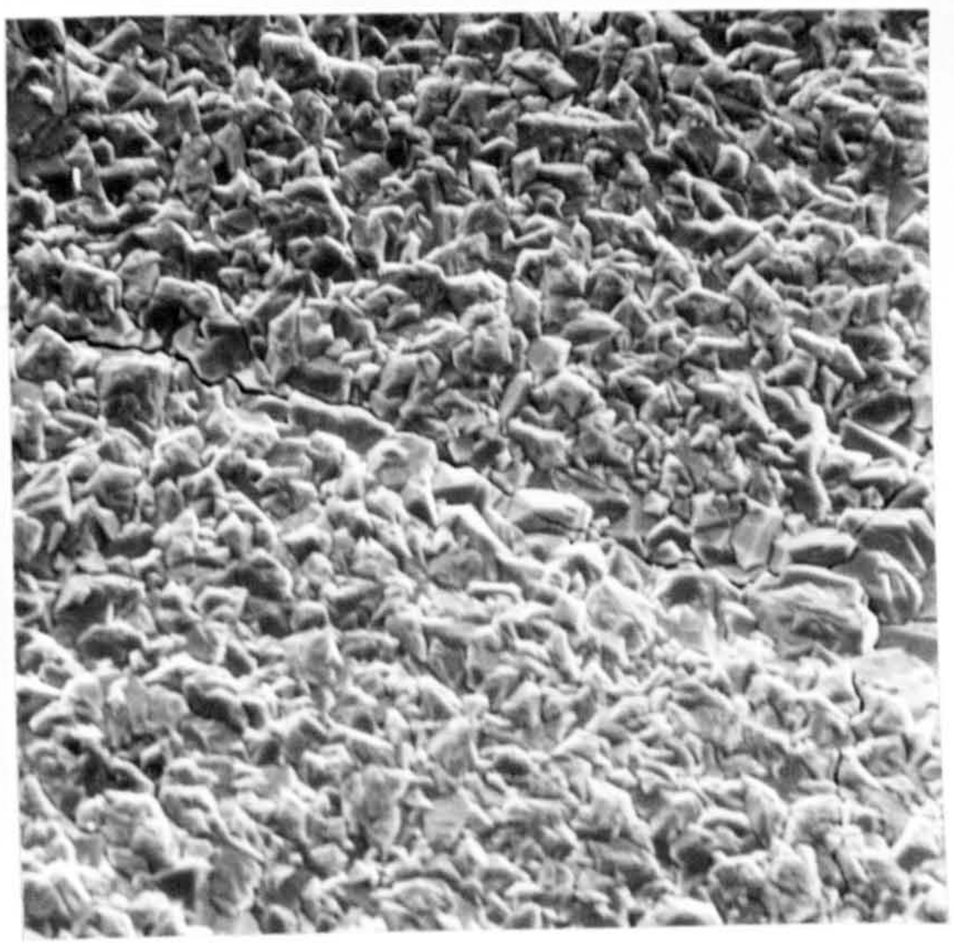

FIGURE 58P

PbO_2 electrodeposited at 2 Adm^{-2} from a solution of 100 gl^{-1} $Pb(NO_3)_2$ + 0.5 gl^{-1} gelatin at 50°C.

(Magnification 1000X)

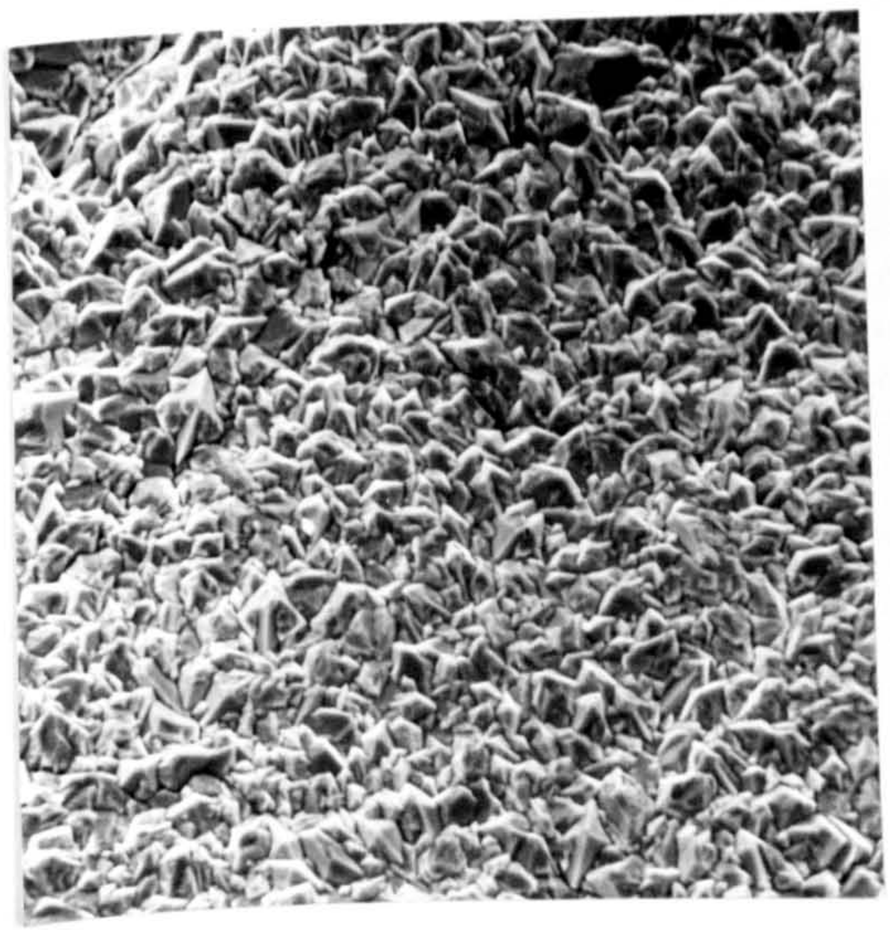

FIGURE 59P

PbO_2 electrodeposited at 2 Adm^{-2} from a solution of 360 gl^{-1} $Pb(NO_3)_2$ plus 1 gl^{-1} cetyl trimethyl ammonium bromide at 50°C.

(Magnification 1000X)

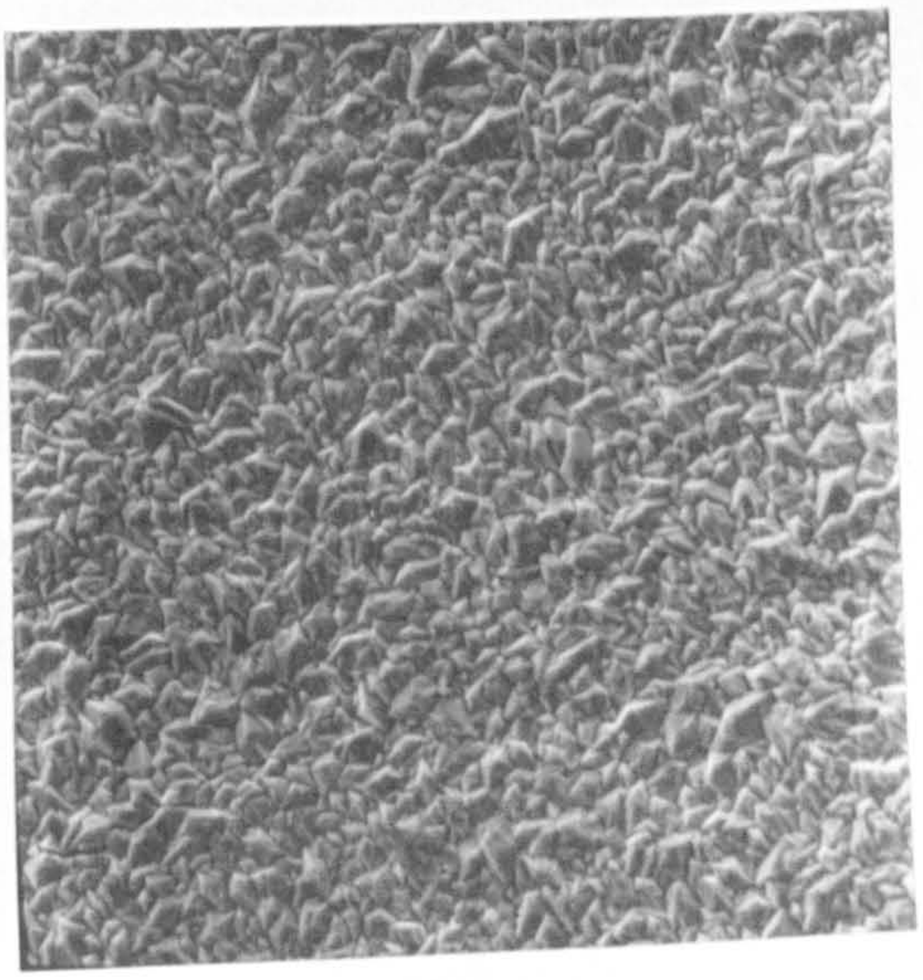

FIGURE 60P

PbO_2 electrodeposited at 1 Adm^{-2} from a solution of 180 gl^{-1} $Pb(NO_3)_2$ + 1 gl^{-1} cetyl trimethyl ammonium bromide at 50°C.

(Magnification 1000X)

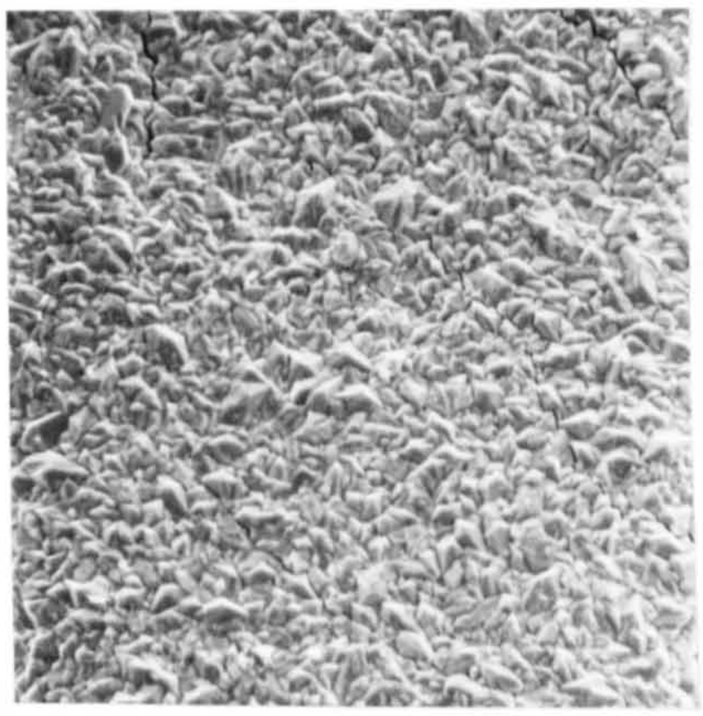

FIGURE 61P

PbO_2 electrodeposited at 4 Adm^{-2} from a solution of 100 gl^{-1} $Pb(NO_3)_2$ + 1 gl^{-1} cetyl trimethyl ammonium bromide at 50°C

(Magnification 1000X)

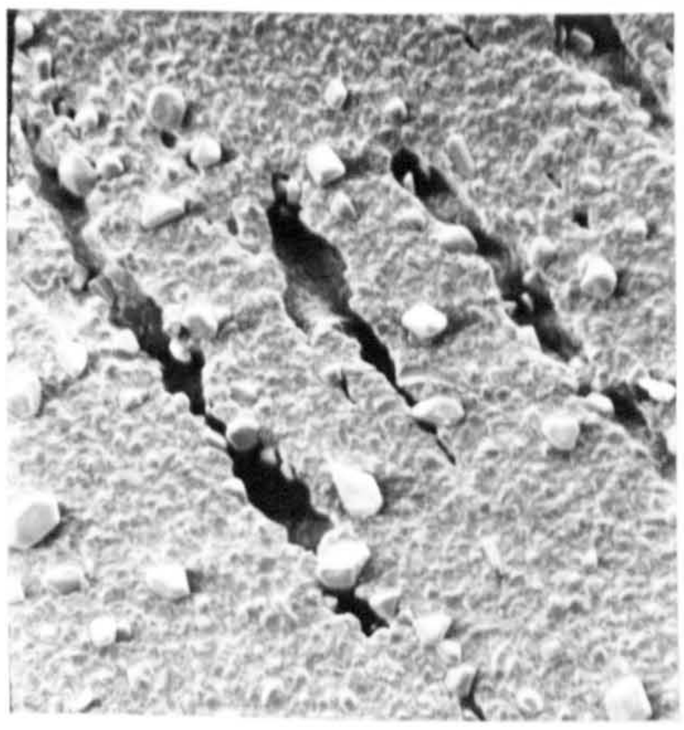

FIGURE 62P

PbO_2 electrodeposited from a solution of 20 gl^{-1} $NaCH_3COO$, 180 gl^{-1} $Pb(NO_3)_2$ at 0.5 Adm^{-2} and 50°C

(Magnification 250X)

deposit obtained from $Pb(NO_3)_2$ solutions containing CETB are shown in Figs. 59P to 61P. A reduction in grain size of the PbO_2 grains when compared to the non additive solution can be seen as can the appearance of cracks in the PbO_2 deposit but no change in the nature of the PbO_2 deposit could be detected.

Fig. 62P shows PbO_2 electrodeposited from a solution of 180 gl^{-1} $Pb(NO_3)_2$ plus 20 gl^{-1} $NaCH_3COO$, large pores in the coating together with the presence of unidentified crystals on the deposit surface can be seen.

3.1.5 X-ray diffraction studies

X-ray diffraction studies were conducted on both the Pb and PbO_2 deposits obtained from simultaneous plating solutions. The object of which was to verify the nature of the PbO_2 deposit and where possible to determine the grain size of the Pb deposit, using the technique of line broadening.

3.1.5.1 X-ray analysis of Pb electrodeposits

The X-ray diffraction patterns of Pb deposits obtained from a conventional $Pb(BF_4)_2$ plating solution (Fig. 30) and $Pb(NO_3)_2$ plating solutions containing additions of 2 gl^{-1} Triton X100 plus 0.1 gl^{-1} anthraquinone-2-monosulphonic acid or 2 gl^{-1} Triton X100 and 1.5 gl^{-1} butyne 1,4 diol are shown in Figs. 31-32 respectively. In the case of the deposit obtained from a butyne diol solution (Fig. 32) a Ni reflection peak at 2.05 A^{o} was observed and a shoulder visible on the 220 reflection at 1.75 A^{o}. These correspond to the Ni (111) reflection at 2.05 A^{o} and the (200) reflection at 1.76A^{o}.

The presence of the Ni reflection peak is thought to be due to the high porosity of the Pb deposit from this solution and was not detected on samples of Pb electrodeposited from a $Pb(BF_4)_2$ plating solution nor from a $Pb(NO_3)_2$ solution containing Triton X100 and anthraquinone-2-monosulphonic acid.

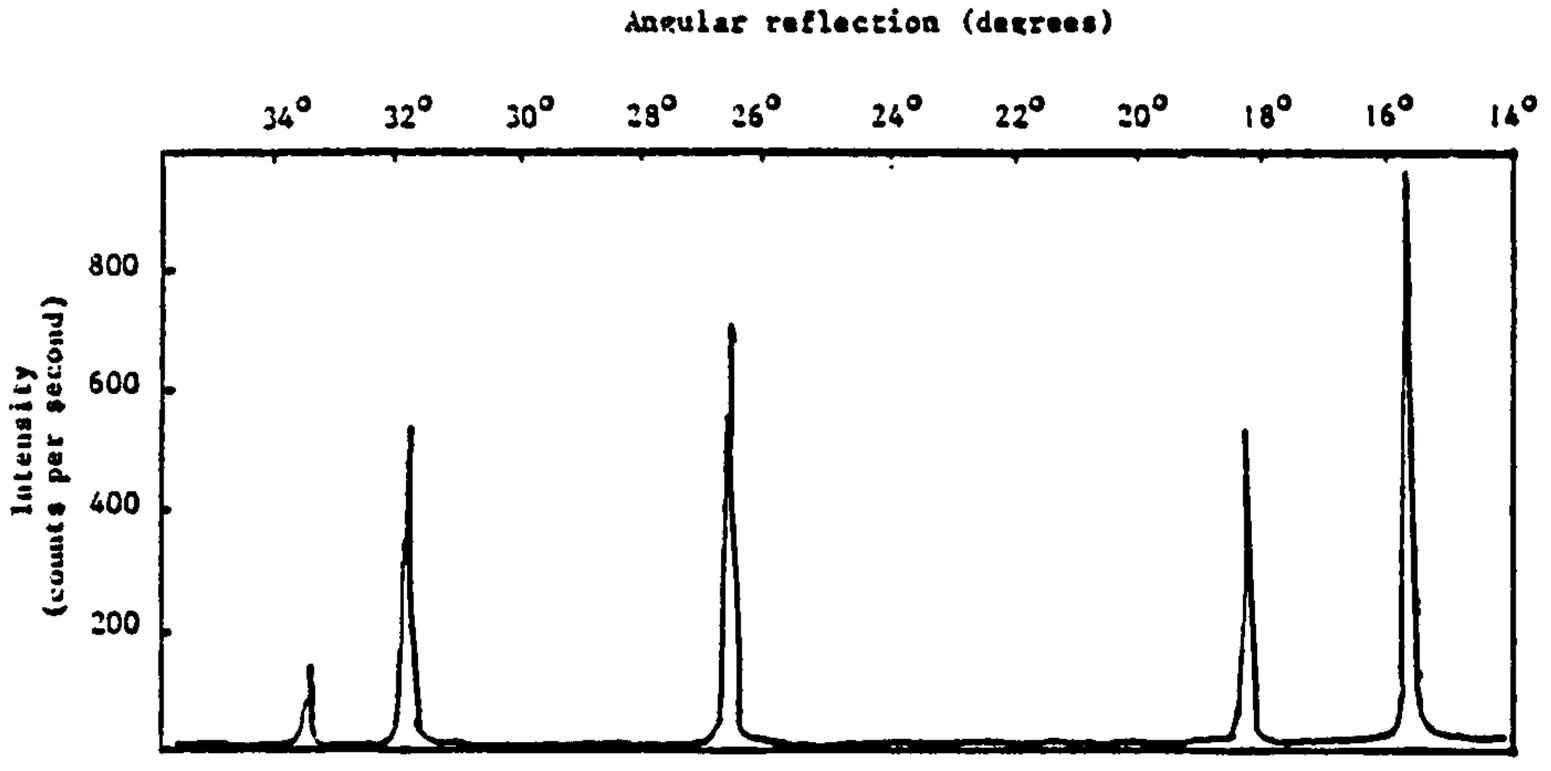

X-ray diffraction pattern for Pb electrodeposited at $2Adm^{-2}$ from a $220gl^{-1}$ $Pb(BF_4)_2$ solution for 15 minutes at room temperature.

FIGURE 30

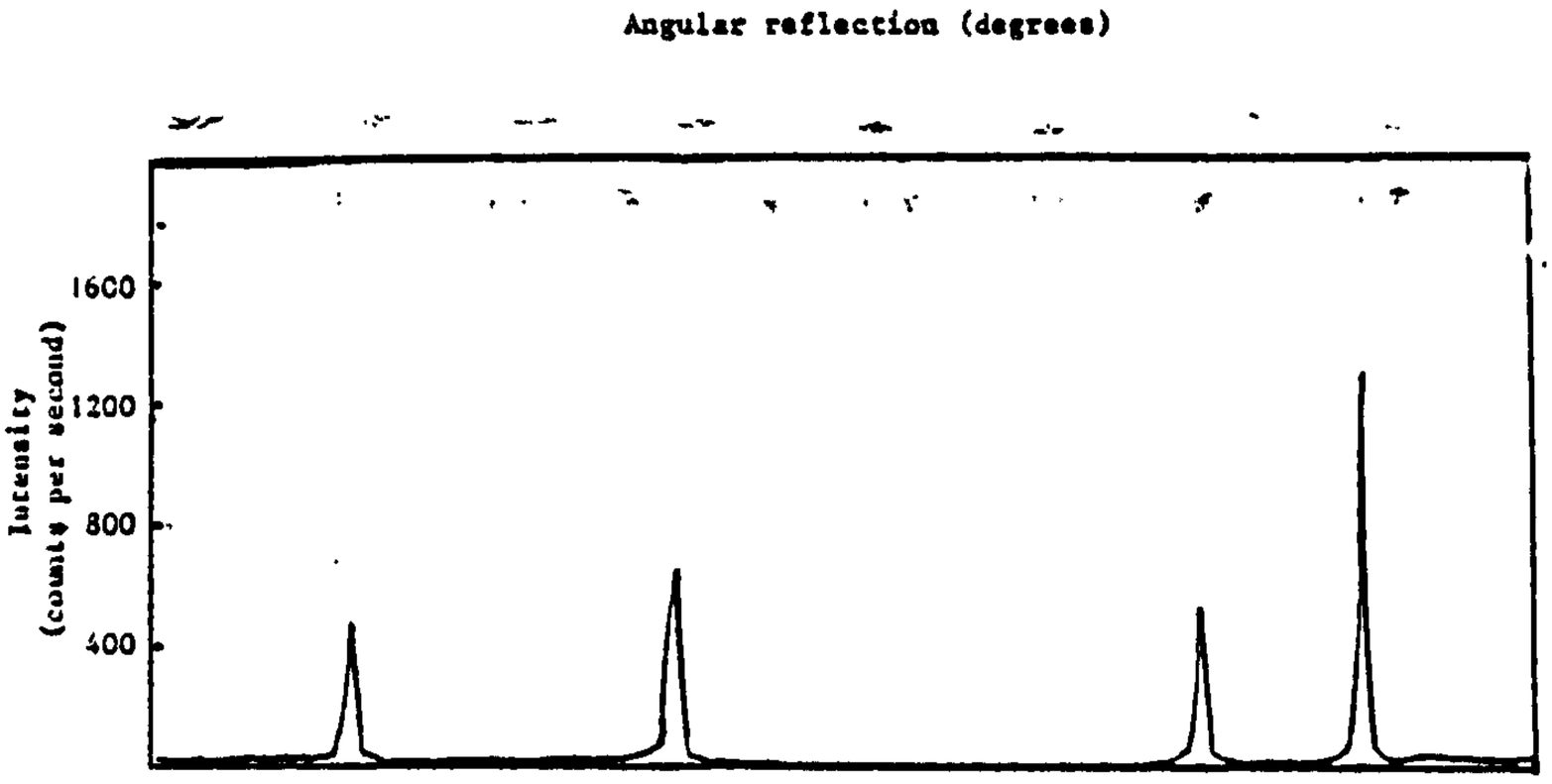

X-ray diffraction pattern for Pb electrodeposited at $2Adm^{-2}$ from a solution of $360gl^{-1}$ $Pb(NO_3)_2$ plus $2gl^{-1}$ Triton x100 and $0.1gl^{-1}$ anthraquinone-2-monosulphonic acid.

FIGURE 31

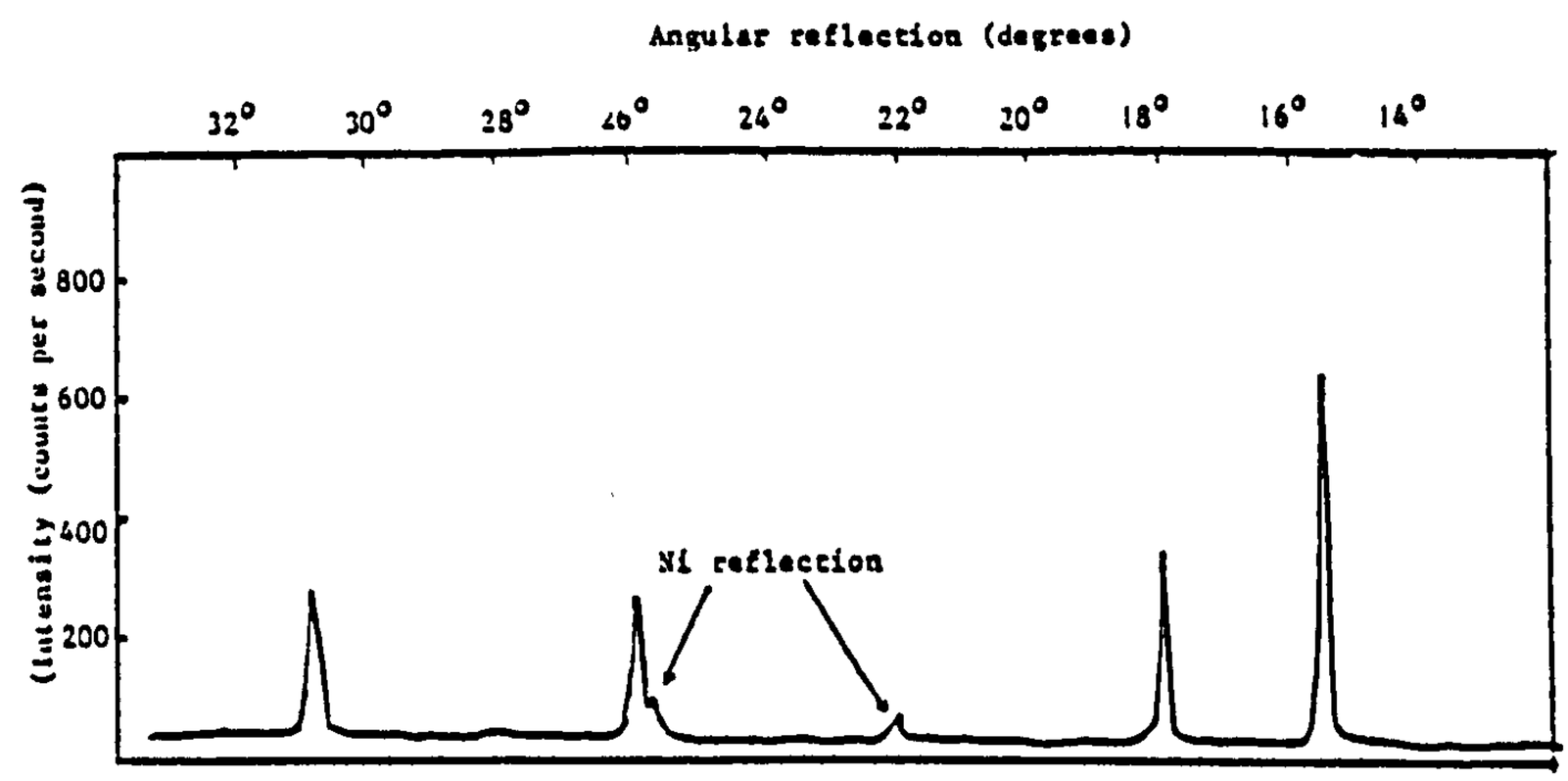

X-ray diffraction pattern for Pb electrodeposited at $2Adm^{-2}$ for 15 minutes from a $180gl^{-1}$ $Pb(NO_3)_2$ solution plus $3ml\ l^{-1}$ Triton x100 and $1.5gl^{-1}$ butyne, 1,4 diol onto a Ni substrate.

FIGURE 32

A ratio of the intensity of the (111) reflection for electro-deposited Ni foil over that for pure Ni foil measured under identical conditions gives a value of 14.1% exposed Ni for the Pb deposit obtained from a solution of 360 gl^{-1} $Pb(NO_3)_2$ + 1.5 gl^{-1} butyne 1,4 diol + 2 gl^{-1} Triton X100 and 12.0% for the Pb deposit from a solution of 180 gl^{-1} $Pb(NO_3)_2$ with the same additives.

The calculated values for the reflections obtained for the diffraction pattern for Pb deposited from a $Pb(BF_4)_2$ solution are given in Table 25, whilst details of the ASTM card index for Pb are given in the Appendix.

TABLE 25

The angular spacings and relative intensities of the diffraction peaks for Pb electrodeposited from 230 gl^{-1} $Pb(BF_4)_2$ at a c.d. of 2 Adm^{-2}

Angular Spacing (degrees)	dA°	Relative Intensity %	hkl	Listed values of dA° from the ASTM card index for Pb
15.7	2.85	100	111	2.86
18.15	2.47	51	200	2.48
26.1	1.75	70	220	1.75
31.1	1.49	52	311	1.49
32.65	1.43	13	222	1.46

The grain size for Pb electrodeposited from a conventional $Pb(BF_4)_2$ plating solution at different c.ds. was determined by measuring the extent of line broadening for a particular reflection (see Table 26). The angular width of the peak at half the peak height is related to the grain or crystallite size perpendicular to a particular reflection by the following equation.

$$D\,(hkl) = \frac{0.9\lambda}{b\ 1/2\ \cos\theta}$$

where d(hkl) = crystalite size perpendicular to given hkl plane A

λ = wavelength of radiation, A^o

b1/2 = peak width at half peak height (radians)

θ = hkl reflection angle

The larger the degree of line broadening, the smaller is the crystal size.

TABLE 26

The variation in grain size of the Pb deposit obtained from a 230 gl^{-1} $Pb(BF_4)_2$ plating solution at different c.ds.

Current density Adm^{-2}	Grain size perpendicular to 100 reflection (A^o)
1	160
2	210
4	310

The grain size of Pb deposits from other solutions was also measured using the technique of line broadening and these results are listed in Table 27.

3.1.5.2 X-ray analysis of PbO_2 electrodeposited from a $Pb(NO_3)_2$ solution

A sample of PbO_2 was electrodeposited onto a nickel substrate at 1 Adm^{-2} from a 360 gl^{-1} $Pb(NO_3)_2$ solution of pH4 at 50°C. This was then removed from the Ni substrate and ground into a fine powder and analysed on a powder diffractomter.

The diffraction pattern of the sample was recorded and compared against the existing ASTM card index for PbO_2. The diffraction pattern is shown in Fig 33 and a tabulation of the relative intensities and angular spacings given in Table 28.

The ASTM card indexes for α-PbO_2 and β-PbO_2 were used to identify the nature of the PbO_2 deposit obtained and these are shown in Appendix 2.

As can be seen from Table 27 the electrodeposited PbO_2 is essentially a mixture of both α and β-PbO_2, but is predominantly β-PbO_2.

An accurate value for the relative composition of electrodeposited PbO_2 is not possible without more detailed information for a sample of pure α-PbO_2 and β-PbO_2. Although by a simple ratio of the intensities of the major reflection peaks an approximate value of 20% α-PbO_2; 80% β-PbO_2 can be obtained. The major reflection intensity for α-PbO_2 is from the (111) plane which has a relative intensity of 34% yet the other major reflections for α-PbO_2 namely the (002) and (021) planes give values of 9% and 7% respectively. The weighted average value of these intensities indicates 19% α-PbO_2.

TABLE 28

A sample of PbO_2 electrodeposited from a 360 gl^{-1} $Pb(NO_3)_2$ solution pH4 at a current density of 1 Adm^{-2} and temperature of 50°C.

Angular reflection degrees	Relative Intensity %	dA°	Corresponding reflection plane
11.7	8	3.80	(110 α)
12.8	100	3.48	(110 β)
14.35	34	3.11	(111 α)
15.15	3	2.95	(020 α)
16.1	100	2.78	(101 β)
16.3	9	2.75	(002 α)
17.15	7	2.61	(021 α)
18.2	30	2.47	(200 β)
20.3	4	2.22	(210 β)
24.7	62	1.85	(211 β)
25.35	7	1.80	(221 α)
26.2	15	1.75	(220 β)
27.2	5	1.69	(002 β)
28.15	3	1.63	(113 α)
29.6	13	1.56	(310 β and 222 α)
30.45	16	1.52	(112 β and 331 α)
31.35	15	1.48	(301 β)
33.85	6	1.38	(202 β)
37.35	9	1.27	(321 β)
39.35	5	1.22	(222 β)

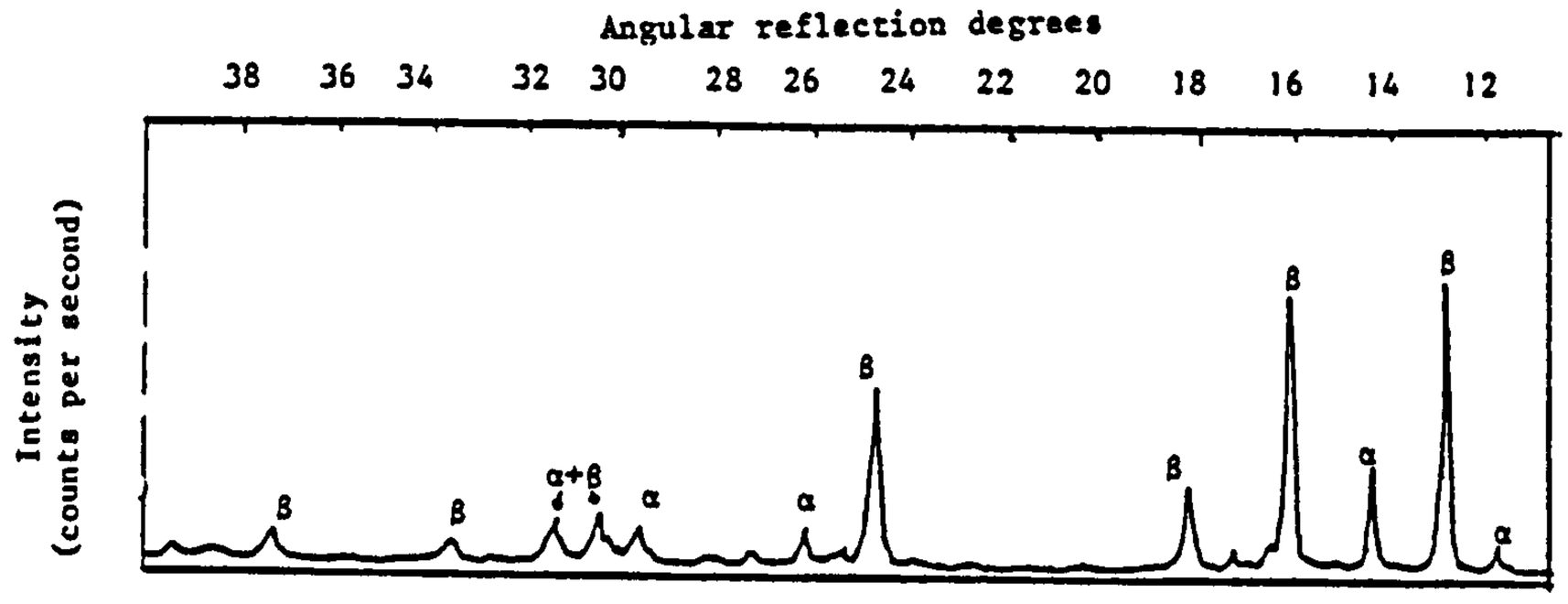

X-ray diffraction pattern for a sample of PbO_2 obtained by electrodeposition at $1Adm^{-2}$ from a solution of $360gl^{-1}$ $Pb(NO_3)_2$ pH 2.5 to 3.5 at 50°C.

FIGURE 33

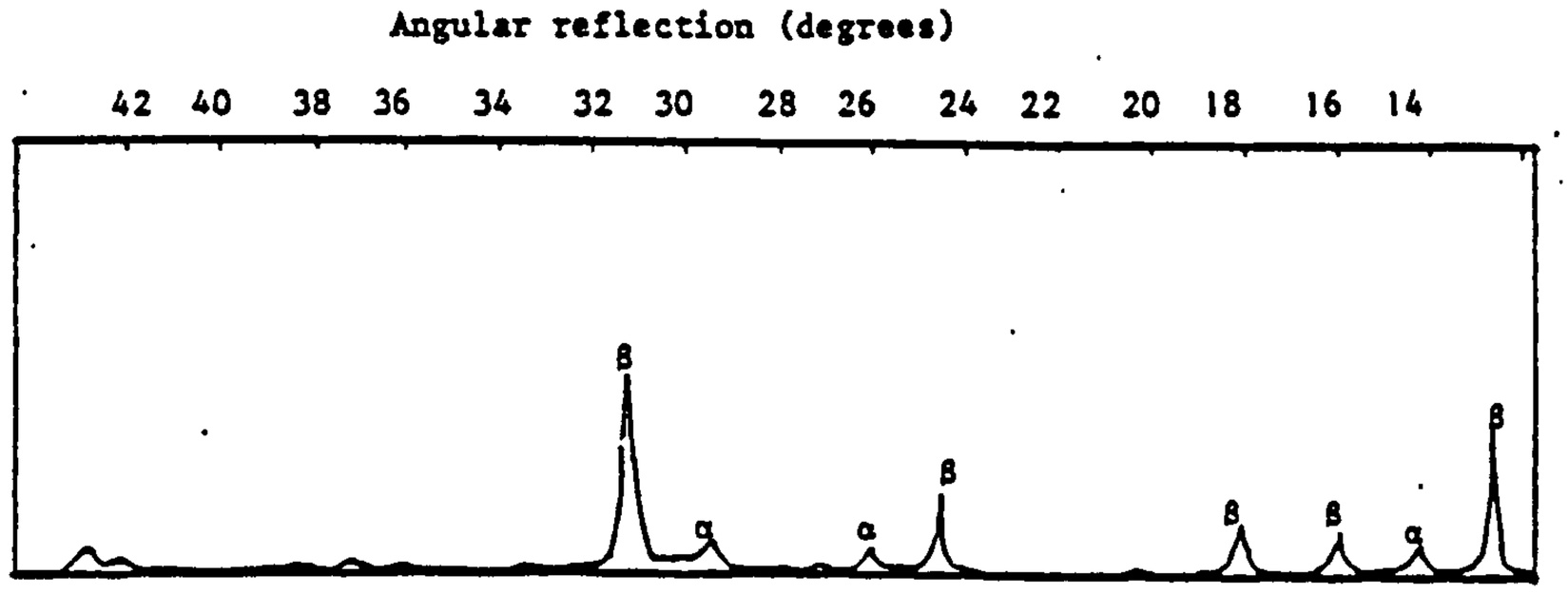

X-ray diffraction pattern for a sample of PbO_2 obtained by electro-deposition at $4Adm^{-2}$ onto a Ni foil substrate from a solution of $360gl^{-1}$ $Pb(NO_3)_2$, $3gl^{-1}$ Triton X100, $1.5gl^{-1}$ butyne 1,4 diol at 50°C.

FIGURE 34

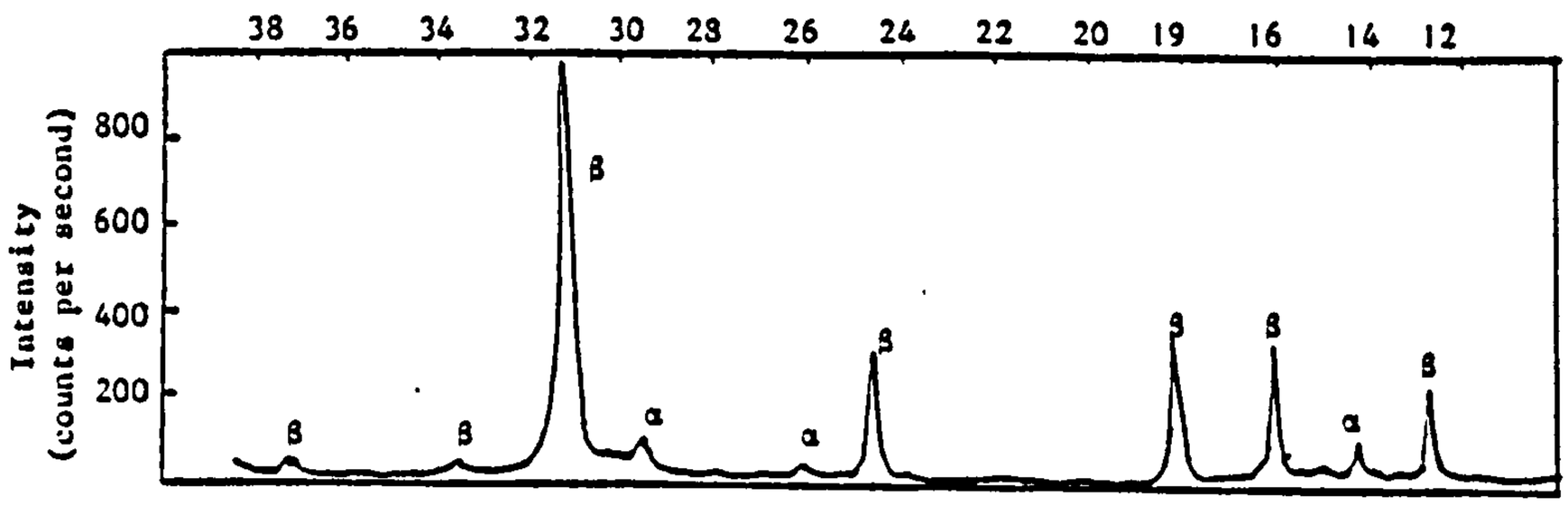

X-ray diffraction pattern for a sample of PbO_2 obtained by electrodeposition at $4Adm^{-2}$ from a solution of $360gl^{-1}$ $Pb(NO_3)_2$. onto a Ni foil substrate.

FIGURE 35

3.1.5.3 PbO_2 grain size determinations

The grain size of PbO_2 deposits was determined in the same way as for Pb deposits.

The effect of c.d. on grain size of PbO_2 deposited from a non additive solution containing 360 gl^{-1} $Pb(NO_3)_2$ at 50°C is given in Table 29.

The results given in Table 29 are the mean results of three (3) separate determinations and variations of 40A° were recorded. The effect of different solutions and deposition c.d. on the grain size of electrodeposited PbO_2 can be seen in Table 30.

3.1.5.4 X-ray analysis of PbO_2 electrodeposited from $Pb(NO_3)_2$ solutions containing selected additives

The effect of selected addition agents on the X-ray diffraction pattern of PbO_2 electrodeposited from a 360 gl^{-1} $Pb(NO_3)_2$ solution was also briefly investigated and diffraction patterns for selected additives are given in Figs. 34 - 38.

In the case of a Triton X100 and butyne 1,4 diol additive system (see Fig. 34) some preferred orientation of the deposit particularly on the (100) and (301) planes was detected, when compared to the diffraction pattern obtained for PbO_2 electrodeposited at the same c.d from a non additive containing solution (see Fig. 35). The largest intensity reflection was recorded at 1.49 A°.

TABLE 27

Variation in grain size along the 110 plane, for Pb deposited from different plating solutions at selected current densities

Plating Solution	Deposition current Density Adm^{-2}	Grain Size A^{o}
360 gl^{-1} $Pb(NO_3)_2$, 1.5 gl^{-1} butyne 1,4 diol+ 3 gl^{-1} Triton X100	2	420
360 gl^{-1} $Pb(NO_3)_2$, 0.1 gl^{-1} anthraquinone-2-sulphonic acid + 2 gl^{-1} Triton X100	1	590
	2	290
180 gl^{-1} $Pb(NO_3)_2$ + 10 gl^{-1} Na NH_2SO_3	1	510
180 gl^{-1} $Pb(NO_3)_2$ + 20 gl^{-1} Na NH_2SO_3	1	510
180 gl^{-1} $Pb(NO_3)_2$ + 40 gl^{-1} Na NH_2SO_3	1	520
	2	400
180 gl^{-1} $Pb(NO_3)_2$ + 60 gl^{-1} Na NH_2SO_3	1	460
180 gl^{-1} $Pb(NO_3)_2$ + 1 gl^{-1} tannic acid + 1 gl^{-1} Wafex	2	530
45 gl^{-1} $Pb(NO_3)_2$ + 1 gl^{-1} tannic acid + 1 gl^{-1} Wafex	1	530
	2	490
22 gl^{-1} $Pb(NO_3)_2$ + 1 gl^{-1} tannic acid + 1 gl^{-1} Wafex.	2	190

TABLE 29

The variation in grain size of PbO_2 electrodeposited from a 360 gl^{-1} $Pb(NO_3)_2$ soltuion at 50°C and at selected c.ds.

Current density Adm^{-2}	Grain size prependicular to 110 reflection A
1	305
2	290
3	240
4	215

A solution containing 1 gl^{-1} CETB gave it's second highest intensity reflection at 1.53A°, which corresponds to the (112) reflection for β-PbO_2 and the largest at 3.48 A° for the 110 β-PbO_2 plane (see Fig. 36). An α-PbO_2 reflection at 3.11A° was only barely visible.

For a solution containing 1 gl^{-1} Wafex deposited at 4 Adm^{-2} the largest intensity reflection was recorded at 1.53A°, (see Fig. 37) and a decrease in deposition c.d. reduced the grain size of the deposit as can be seen in Fig. 38. A considerable degree of preferred orientation was also observed.

The addition of $NaCH_3COO$ to a 180 gl^{-1} solution of $Pb(NO_3)_2$ also had a considerable effect on the crystallographic nature of the PbO_2 deposit obtained (see Fig. 39).

TABLE 30

Variation in grain size of electrodeposited PbO_2 obtained from different plating solutions

Solution	Deposition c.d Adm^{-2}	Grain size perpendicular to 110 reflection A°
180 gl^{-1} $Pb(NO_3)_2$	2	290
180 gl^{-1} $Pb(NO_3)_2$+	1	190
1 gl^{-1} CETB	4	270
360 gl^{-1} $Pb(NO_3)_2$+	1	240
1 gl^{-1} CETB	2	250
360 gl^{-1} $Pb(NO_3)_2$	2	280
2 gl^{-1} Triton X100 +		
0.1 gl^{-1} anthraquinone-2- monosulphonic acid		
360 gl^{-1} $Pb(NO_3)_2$ +		
3 gl^{-1} Triton X100 +	4	220
1.5 gl^{-1} butyne 1,4 diol	2	290
180 gl^{-1} $Pb(NO_3)_2$	2	95
+ 1 gl^{-1} Wafex		
180 gl^{-1} $Pb(NO_3)_2$	2	210
+ 140 gl^{-1} $NaCH_3COO$		
180 gl^{-1} $Pb(NO_3)_2$	2	185
+ 40 gl^{-1} $NaCH_3COO$		

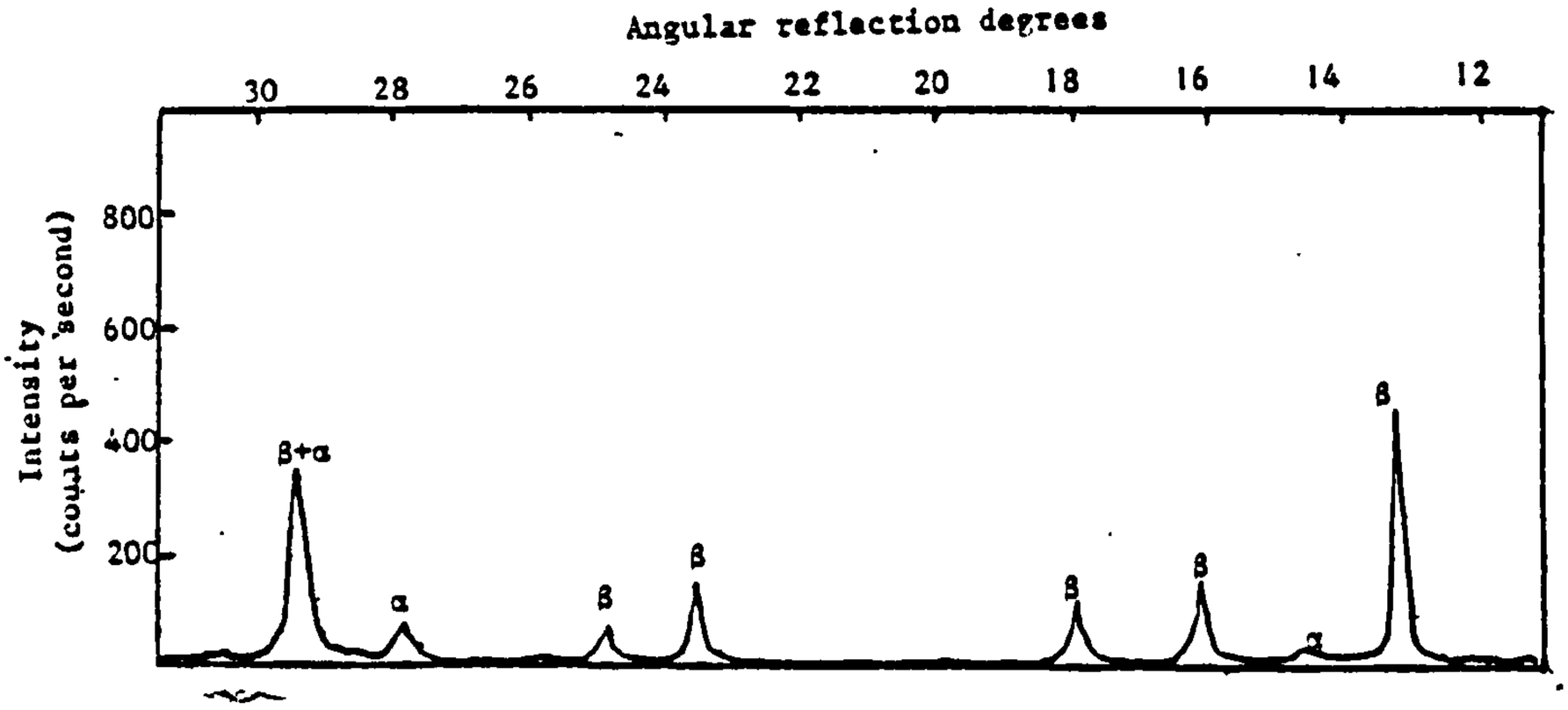

X-ray diffraction pattern for a sample of PbO_2 obtained by electrodeposition at $1Adm^{-2}$ onto a Ni foil substrate from a solution of $360gl^{-1}$ $Pb(NO_3)_2$ plus $1gl^{-1}$ cetyl trimethyl ammonium bromide.

FIGURE 36

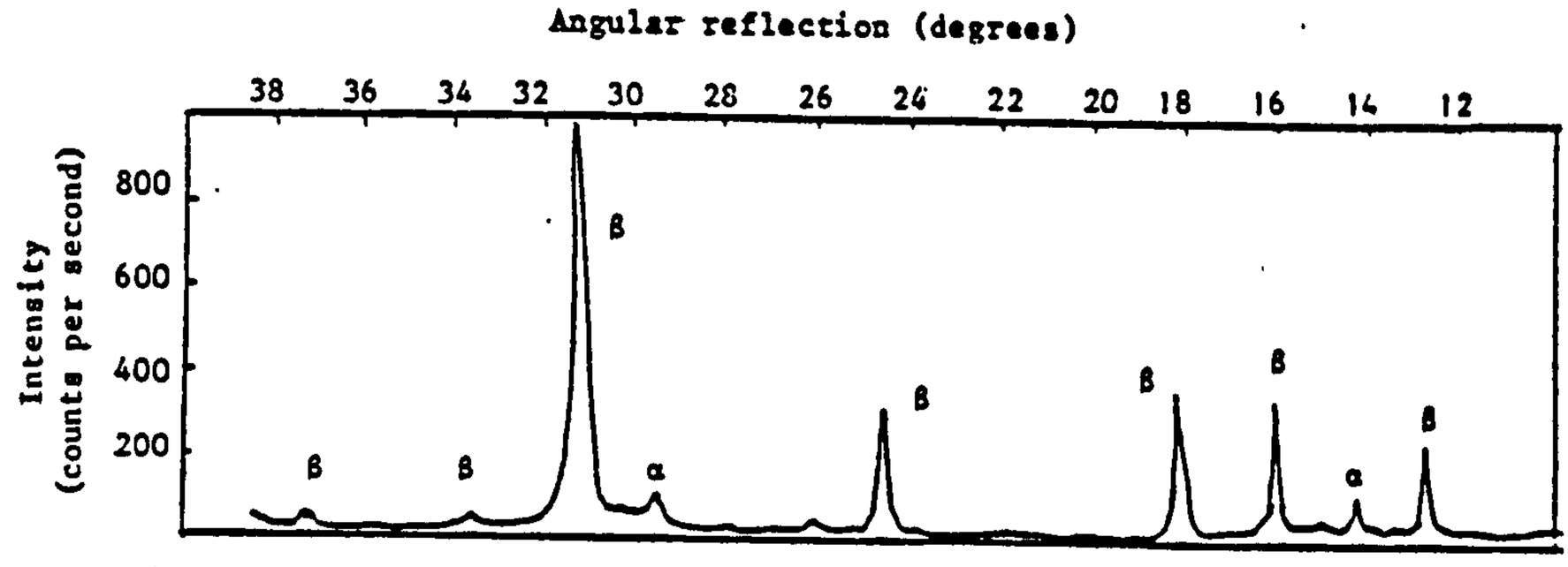

X-ray diffraction pattern for sample of PbO electrodeposited at $4Adm^{-2}$ from a solution of $360gl^{-1}$ $Pb(NO_3)_2$ plus $1gl^{-1}$ Wafex at $50^{o}C$.

FIGURE 37

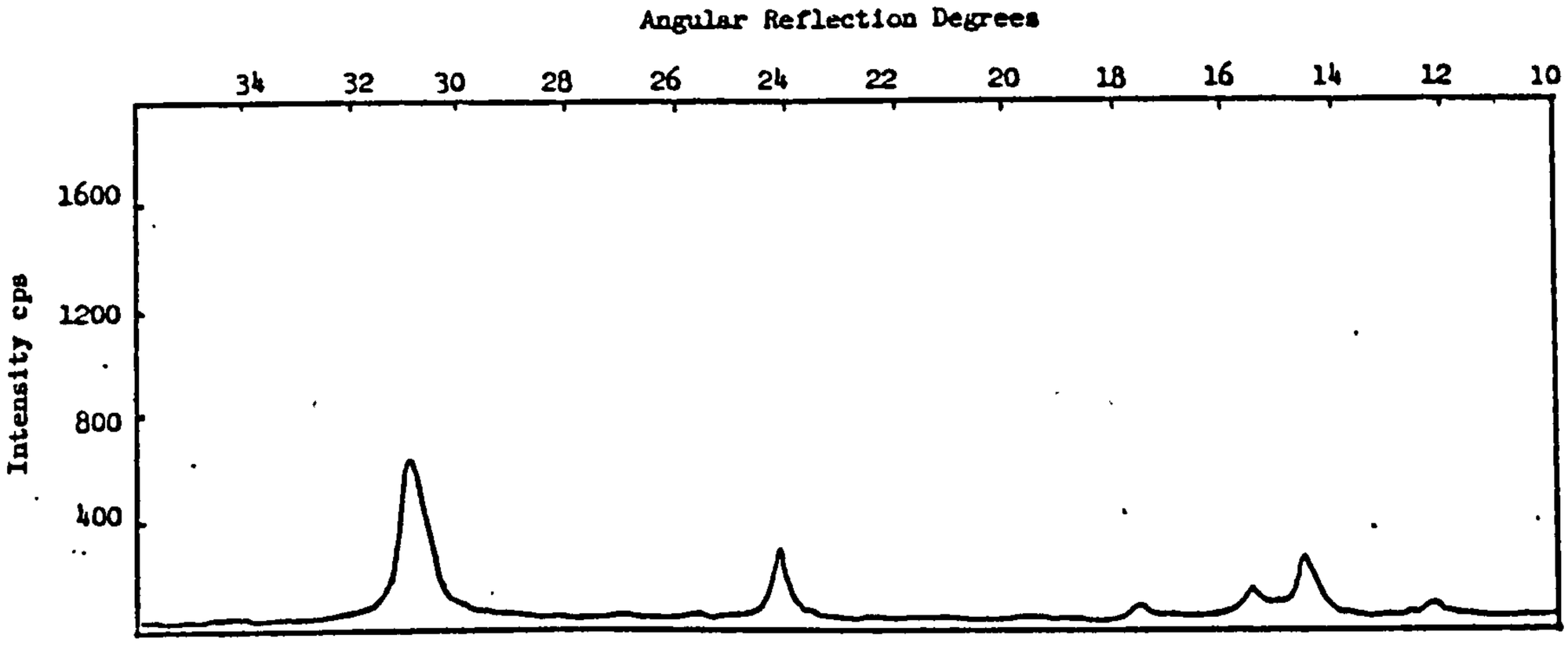

X-ray diffraction pattern for PbO electrodeposited at 2 Adm^{-2} from a solution of 360 gl^{-1} $Pb(NO_3)_2$ plus $1gl^{-1}$ Wafex

FIGURE 38

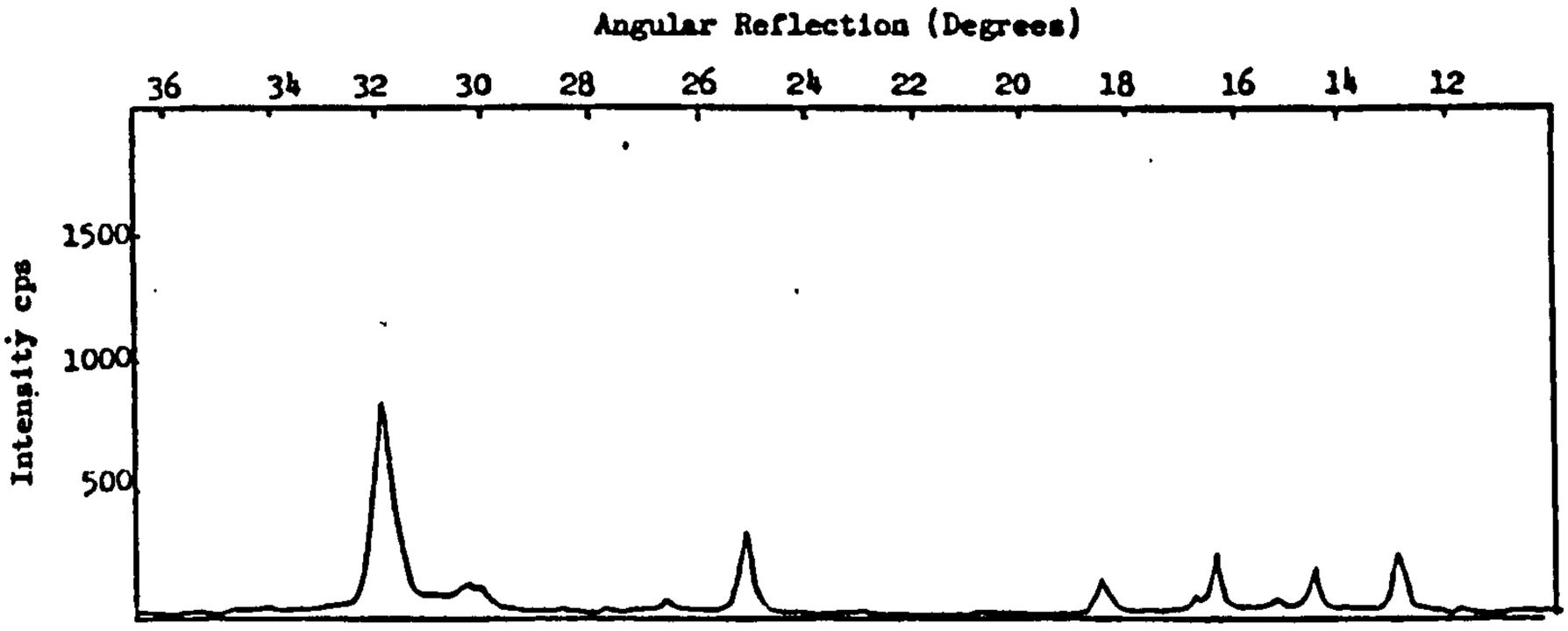

X-ray diffraction pattern for a sample of PbO_2 electrodeposited at 2 Adm^{-2} from a solution of 180 gl^{-1} $Pb(NO_3)_2$ + 10 gl^{-1} $NaCH_3COO$

FIGURE 39

3.1.6 Adhesion tests on samples of PbO_2 electrodeposited onto Ni from different plating solutions

All the PbO_2 deposits prepared by plating from a solution of 360 gl^{-1} $Pb(NO_3)_2$ at 50°C onto a Ni200 substrate gave good adhesion i.e all specimens exhibited grade 1 adhesion (see Fig. 40). Similar results were obtained from the same solution containing 2 gl^{-1} Triton X100 plus 0.1 gl^{-1} anthraquinone-2-monosulphonic acid (see Fig. 40), with the exception that one specimen was graded as being of grade 2 adhesion (moderate) whilst the other two samples shown in Fig. 40 exhibited grade 1 adhesion (good). There therefore appears to be no deleterious effect of a simultaneous plating solution containing 2 gl^{-1} Triton X100 plus 0.1 gl^{-1} anthraquinone-2-monosulphonic acid on the adhesion of PbO_2 electrodeposited from this solution onto a Ni substrate.

The results of the adhesion tests on samples of PbO_2 electrodeposited at 2 Adm^{-2} from a solution of 360 gl^{-1} $Pb(NO_3)_2$ plus 1 gl^{-1} CETB showed one grade 2 specimen but two grade 3 specimens (poor adhesion). The results from three specimens of PbO_2 deposited onto Ni200 from a solution of 360 gl^{-1} $Pb(NO_3)_2$, 3 gl^{-1} Triton X100 and 1.5 gl^{-1} butyne 1,4 diol were one grade 1 specimen, one grade 2 specimen and one grade 3 specimen (see Fig. 41).

3.1.7 Activation time of electrodeposited PbO_2

The studies on activation time were divided into three categories. First, to determine if the addition of organic compounds to the PbO_2 plating solution had any effect on the voltage rise-time; secondly, to investigate the effect of heating the PbO_2 deposit on voltage rise-time and finally to see if agitation of the $Pb(NO_3)_2$ plating solution had any effect on this parameter. The latter two subjects are covered in Section 3.4.3.

A

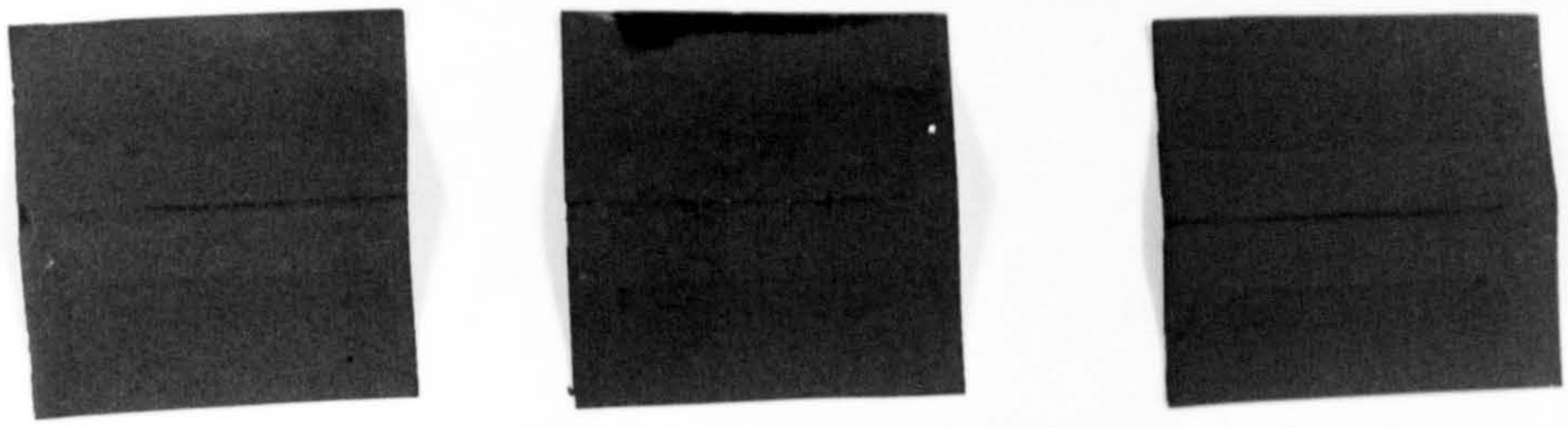

B

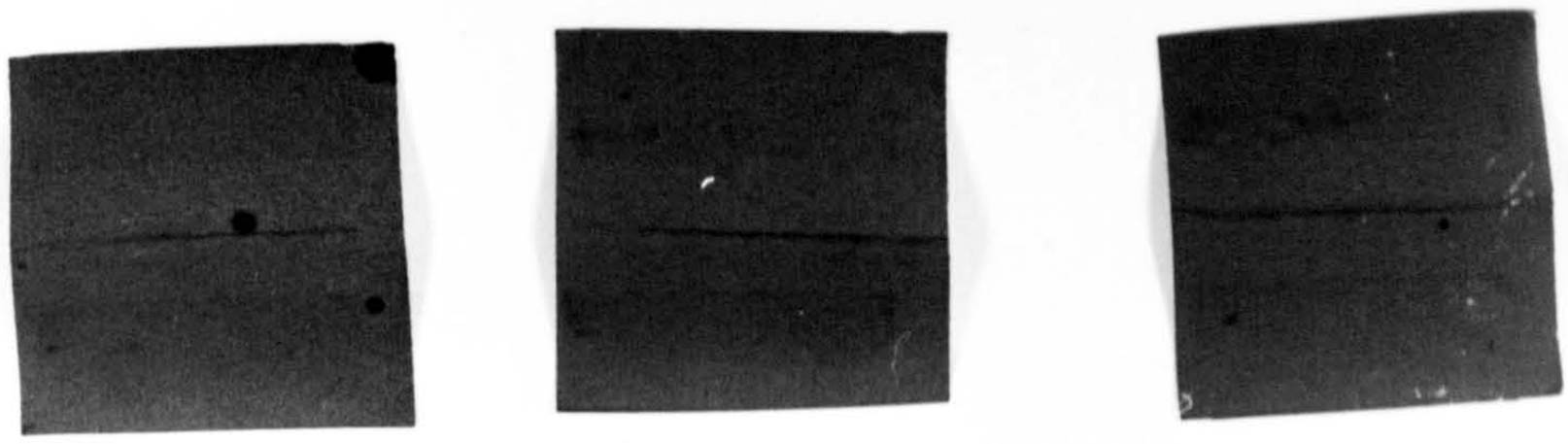

Figure 40

Samples of PbO_2 electrodeposited onto Ni200 from a solution of 360 gl^{-1} $Pb(NO_3)_2$ with and without selected addition agents at 50°C and at 2 $Adm^{-}2$ The samples subjected to the bend adhesion test.

a) 360 gl^{-1} $Pb(NO_3)_2$, + 2 gl^{-1} Triton 100 +
0.1 gl^{-1} anthraquinone -2- monosulphonic acid.

b) 360 gl^{-1} $Pb(NO_3)_2$ without addition agents.

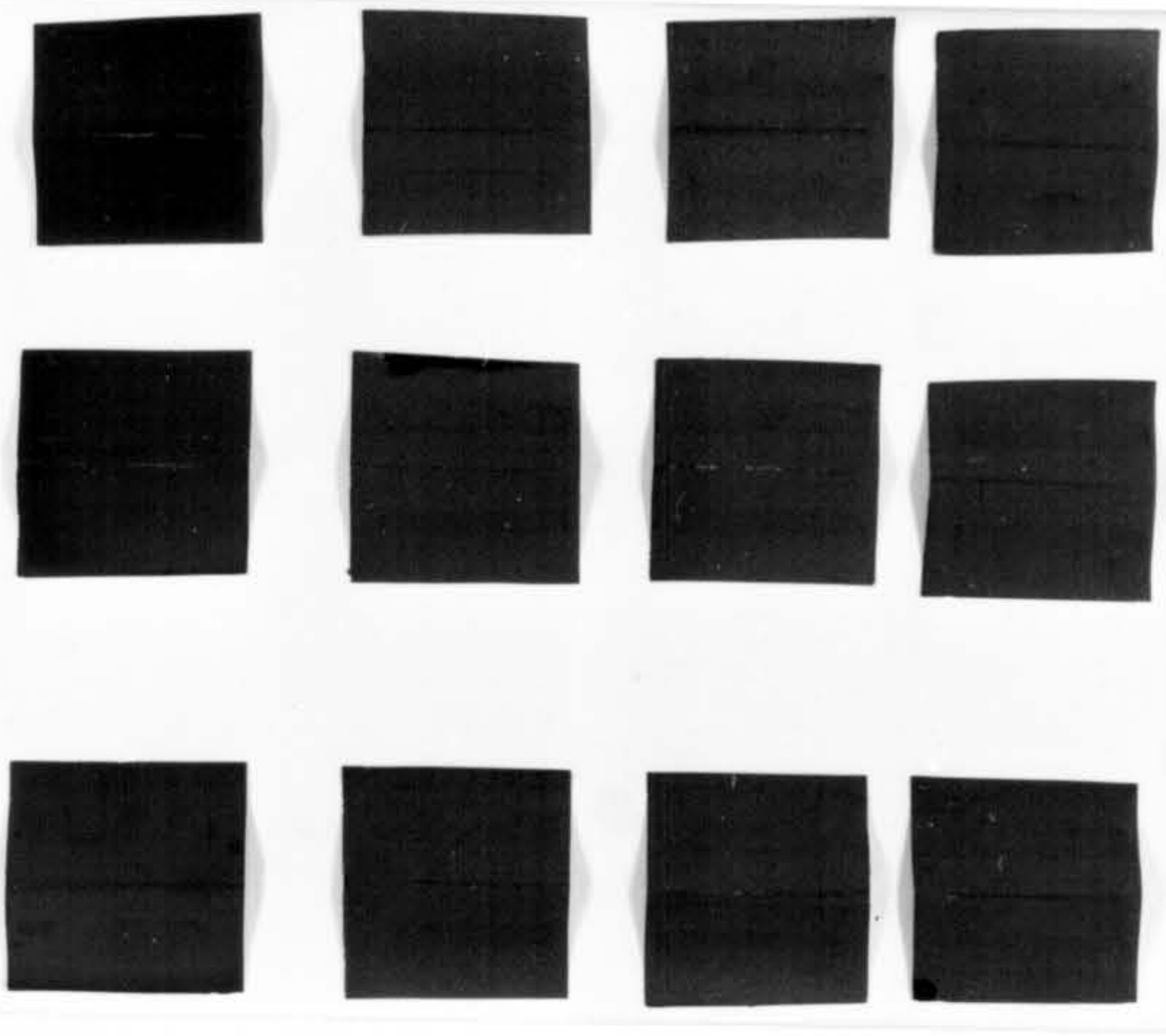

Figure 41

Samples of PbO_2 electrodeposited from a solution of 360 gl^{-1} $Pb(NO_3)_2$ containing different addition agent combination at 50°C and a current density of 2 Adm onto a Ni200 foil substrate. The samples subjected to the bend adhesion test.

a) 360 gl^{-1} $Pb(NO_3)_2$ + 1 gl^{-1} CETB

b) 360 gl^{-1} $Pb(NO_3)_2$, 2 gl^{-1} Triton X100 + 0.1 gl^{-1} anthraquinone-2-monosulphonic.

c) 360 gl^{-1} $Pb(NO_3)_2$, 3 gl^{-1} Triton X100 + 1.5 gl^{-1} butyne-1,4 diol.

d) 360 gl^{-1} $Pb(NO_3)_2$ without any additives.

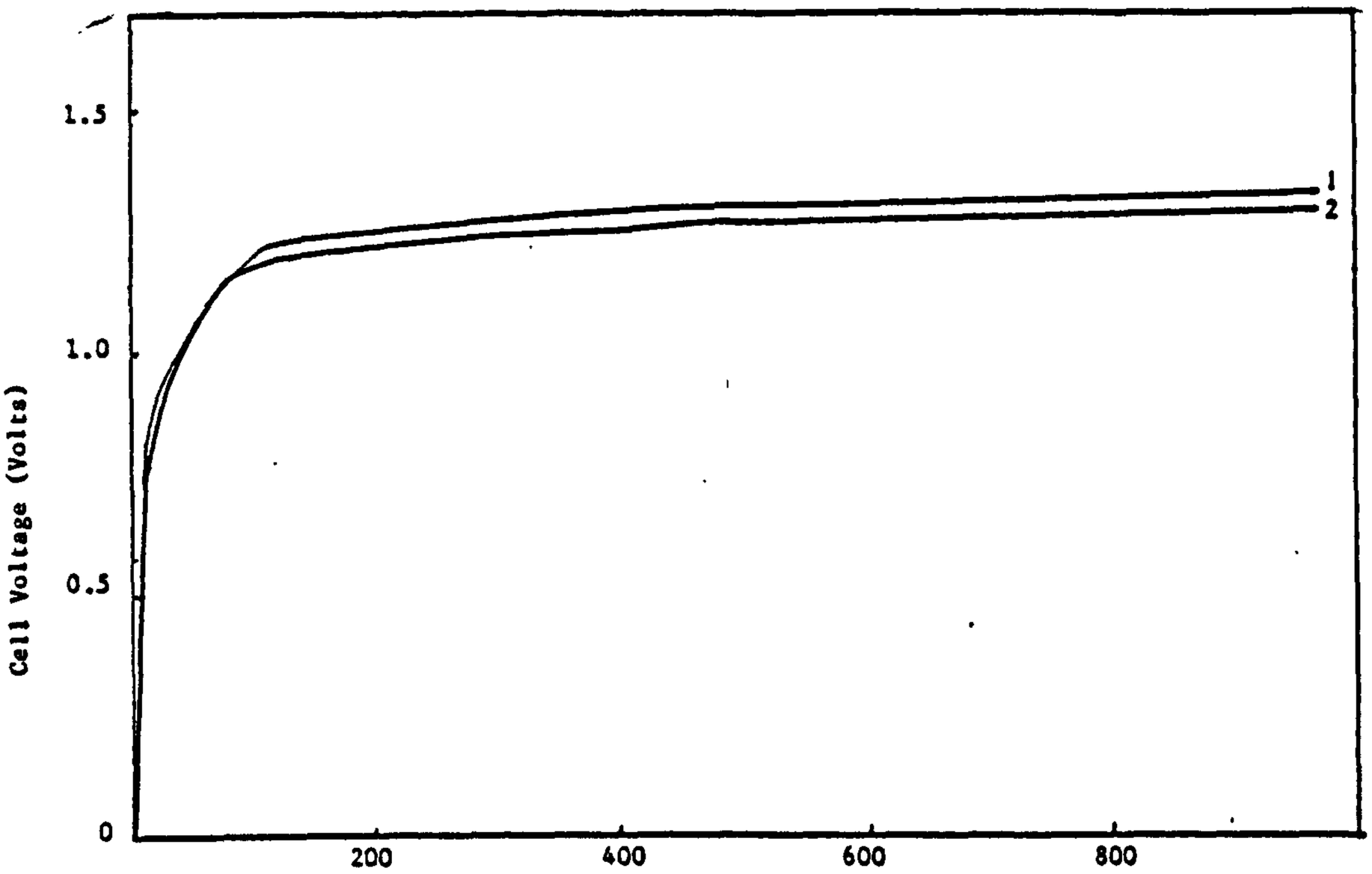

A graph of cell voltage vs time of immersion in 48% HBF_4 at -33°C for two different samples of electrodeposited βPbO_2 . The βPbO_2 electrodes obtained by electrodeposition onto a Ni foil substrate at 2 Adm^{-2} from a solution of 360 gl^{-1} $Pb(NO_3)_2$ plus 3 gl^{-1} Triton X100, 1.5 gl^{-1} butyne 1,4 diol.

FIGURE 42

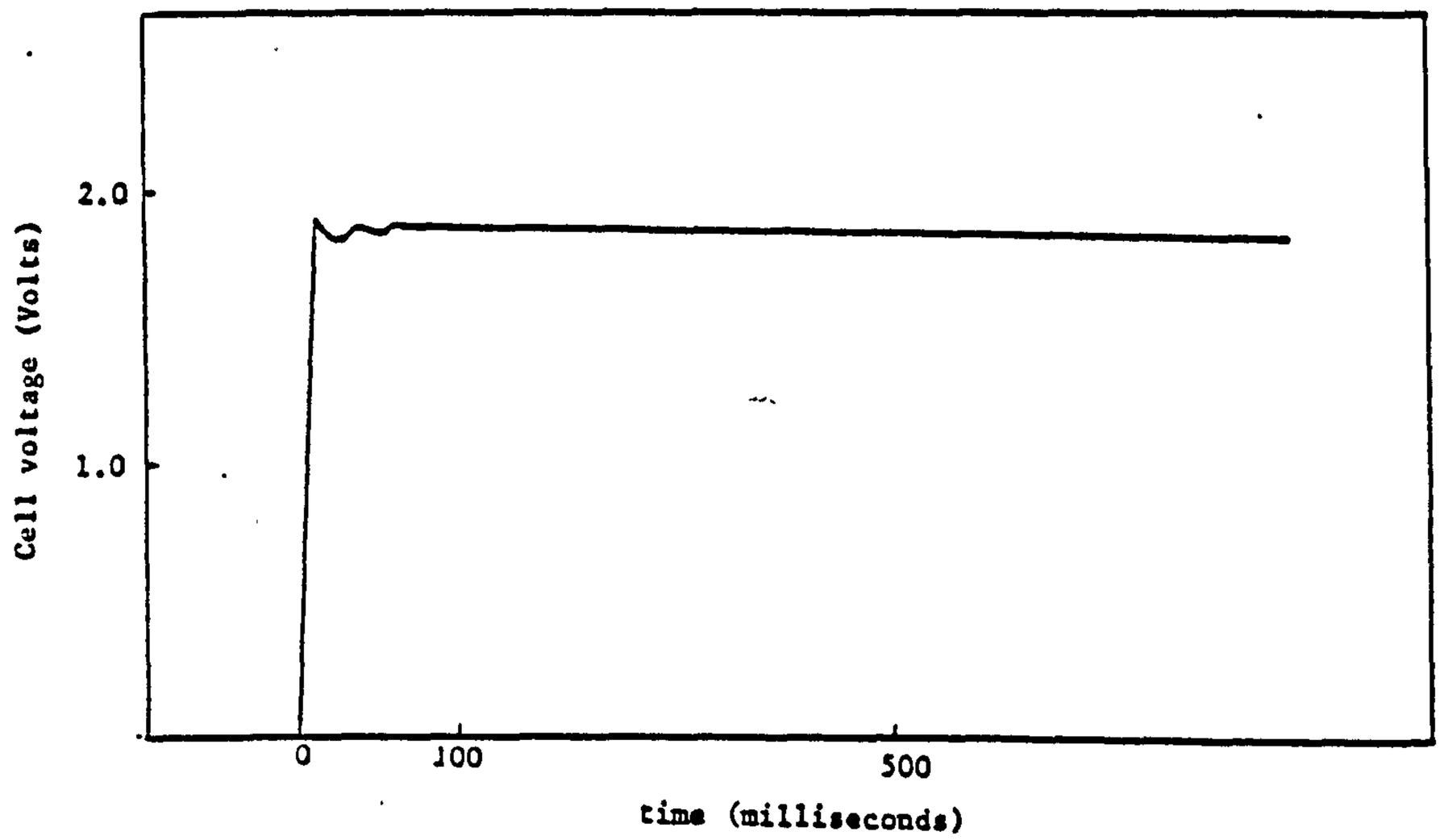

A graph of cell coltage vs time of immersion in 48% HBF_4 at -60°C for a sample of βPbO_2 electrodeposited onto a Ni foil substrate.

FIGURE 43

3.1.7.1 The effect of addition agents on the voltage rise-time for electrodeposited PbO_2

The effect of additives to the PbO_2 plating solution on the voltage rise time of the PbO_2 and Pb deposits was not found to be significant as can be seen from Fig. 42 which shows the voltage vs time curve for the Pb and PbO_2 deposit obtained from a solution containing 360 gl^{-1} $Pb(NO_3)_2$ + 1.5 gl^{-1} butyne 1,4 diol + 3 gl^{-1} Triton X100. The samples of Pb and PbO_2 obtained from this solution all satisfied the voltage rise-time requirement for $Pb/HBF_4/PbO_2$ batteries. Samples obtained from solutions containing 360 gl^{-1} $Pb(NO_3)_2$ + 0.1 gl^{-1} anthraquinone-2-monosulphonic acid + 2 gl^{-1} Triton X100 were tested, and with this solution no detrimental effect on the voltage rise times of Pb and PbO_2 deposits was also observed.

Tests carried out on samples of Pb and PbO_2 produced from the above plating solutions under plant conditions were also carried out. These showed that no detrimental effect on the voltage rise times had been produced by the additives to the $Pb(NO_3)_2$ plating solution (see also Section 3.1.8).

A typical voltage vs time curve at 60°C for a sample of PbO_2 electrodeposited from a solution containing 360 gl^{-1} $Pb(NO_3)_2$ + 0.1 gl^{-1} anthraquinone-2-monosulphonic acid + 2 gl^{-1} Triton X100 is shown in Fig. 43. All samples of Pb and PbO_2 produced from simultaneous baths and tested at elevated temperatures satisfied the initial activation time requirements although not all cells maintained the full cell voltage for the required 180 sec.

3.1.8 Plant Trials

The Pb and PbO_2 deposits obtained on the plant trials for the simultaneous electrodeposition from a solution of 360 gl^{-1} $Pb(NO_3)_2$, 1.5 gl^{-1} butyne 1,4 diol and 3 $ml\ l^{-1}$ Triton X100 were evaluated to verify that these deposits would satisfy the requirements of Specification SP3/Spec 91/71

Issue 2, and would be suitable for use as the active material in the $Pb/HBF_4/PbO_2$ primary battery. This work has been carried out by the Ionic Plating Co (Birmingham) and will only be briefly reported in this section.

A total of 20 sheets each 600 x 160 mm were plated at a c.d of 2.4 Adm^{-2} at 20 to 30°C for 30 mins. The results of the adhesion tests on Pb and PbO_2, together with the electrochemical performance tests in 48% HBF_4 at -33°C and at + 50°C and thickness measurements were all recorded. These results show that the deposits of Pb and PbO_2 from a simultaneous plating solution satisfied the specification in every respect. The mean Pb deposit thickness was 8.5 µm and that of PbO_2 was 14.8 µm.

All samples of Pb passed the adhesion test whilst 9 of the 20 PbO_2 samples exhibited Grade 1 adhesion, the remaining 11 exhibited Grade 2 adhesion. The electrochemical performance of the Pb and PbO_2 electrodes at -33°C and + 50°C is shown in Table 31.

TABLE 31

The mean values for cell e.m.f vs discharge time for a $Pb/HBF_4/PbO_2$ battery utilising Pb and PbO_2 deposits obtained by simultaneous electrodeposition from a solution of 360 gl^{-1} $Pb(NO_3)_2$, 1.5 gl^{-1} butyne 1,4 diol and 3 ml l^{-1} Triton X100, at 2.4 Adm^{-2}

	Mean Cell Voltage (Volts) for discharge at - 33°C versus time (secs)			Mean Cell Voltage (Volts) for discharge at + 50°C versus time (secs)		
Time	0.120	0.490	160	0.120	0.49	160
Voltage	1.31V	1.32V	1.38V	1.68V	1.70V	1.76V

After 1900 A-h plating at 2.4 Adm^{-2} onto Ni foils 600 x 180 mm, it was observed that the Pb deposit no longer adhered to the Ni substrate, and significant variations in deposit thickness and visual appearance were detected. The PbO_2 deposit appeared to be unaffected by the long term operation of the bath. Replenishment of the plating solution with fresh addition agents namely butyne 1,4 diol and Triton X100, was found to overcome the decline in Pb properties with time. This reduction in properties of the deposit has been shown to be due to oxidation of the addition agents at the PbO_2 anode.

Other addition agent combinations were also chosen for further trials, to determine if Pb and PbO_2 deposits from a 360 gl^{-1} $Pb(NO_3)_2$ solution containing different additives could be produced.

The additives examined were :

(a) 1.5 gl^{-1} butyne 1,4 diol + 1.5 ml l^{-1} Pluronic L64

(b) 0.2 gl^{-1} anthraquinone-2,6-disulphonic acid + 2 ml l^{-1} Triton X100

(c) 0.5 gl^{-1} anthraquinone-2,6-disulphonic acid + 2 ml l^{-1} Triton X100

(d) 0.1 gl^{-1} anthraquinone-2-monosulphonic acid + 2 ml l^{-1} Triton X100.

Pb and PbO_2 deposits from each of the above additive combinations were all found to be equally as effective as those from a butyne 1,4 diol + Triton X100 plating solution, with the deposit properties all satisfying the requirements for the $Pb/HBF_4/PbO_2$ fuse battery. Further trials would be necessary to determine the long term plating characteristics of each solution, the best additive system and to define the optimum c.d. and plating time.

3.1.9. Electrochemical studies on the anodic degradation of certain organic addition agents used in the simultaneous electrodeposition of Pb and PbO_2.

The addition agents selected for studies of their susceptibility to anodic oxidation were those that have been used in the deposition of Pb and PbO_2 from $Pb(NO_3)_2$ solutions. Since Triton X100 has been shown to be one of the most successful additives for use in the simultaneous deposition of Pb and PbO_2 the initial studies were concentrated on this particular additive.

Fig. 44 shows the effect of sweep rate on the E vs i curve for a Pt electrode, anodically polarised in a solution of 0.2M Na_2SO_4 pH2 + 2 gl^{-1} Triton X100. A current peak (i_p) was observed at + 1.65V and is attributed to the anodic oxidation of Triton X100. The potential at which this occurs (E_p) becomes more positive with increasing sweep speed. Indeed at sweep speeds greater than 100 mV sec^{-1} it is difficult to extract accurate values for both E_p and i_p.

Fig. 45 shows a typical voltammogram for the anodic polarisation of a Pt electrode in a 0.2M Na_2SO_4 solution containing 1 gl^{-1} Triton X100, and the peak (a) is due to the oxidation of Triton X100. No peak for the reduction of the oxidation products of Triton X100 was observed. The only reduction peak visible (b) is due to reduction of the thin oxide film on the Pt working electrode. The anodic oxidation of Triton X100 was found to commence at potentials greater than + 1.2 V. A similar voltammogram was obtained when Triton X114 was used as the addition agent (Fig. 46).

The higher the Trixon X100 concentration the greater the peak current (i_p) for the oxidation of Triton X100 whilst E_p becomes slightly more positive (see Fig. 47). The most interesting aspect of the addition of Triton X100 on the polarisation characteristics of a Pt electrode immersed in the test solution is the resultant increase in oxygen overvoltage. Indeed Triton X100 is not the only surfactant to exhibit this effect as can be seen from an examination of Table 39.

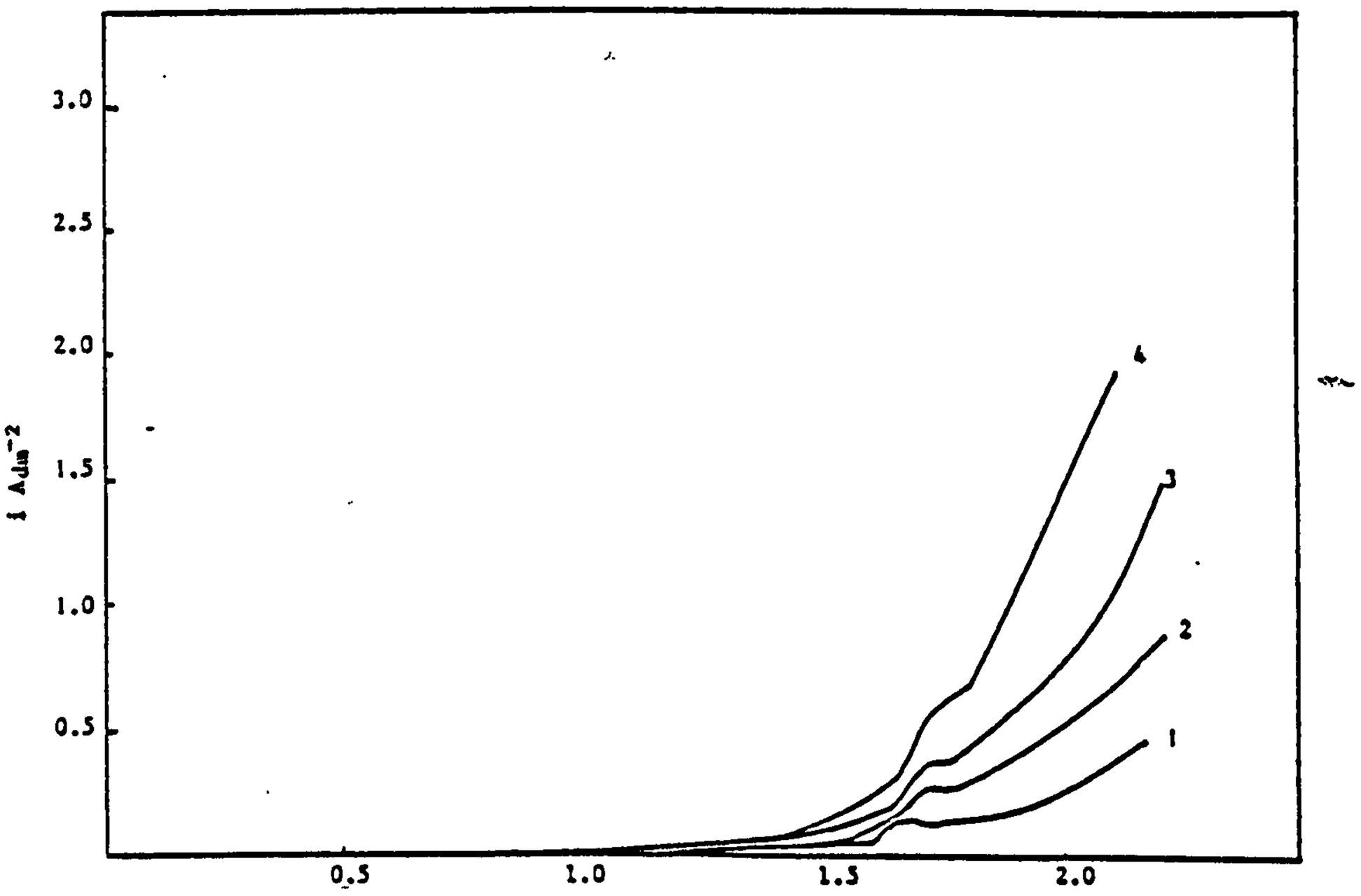

An E vs i graph for a Pt electrode anodically polarised at different sweep rates in a 0.2M Na_2SO_4 solution containing 2 gl^{-1} Triton X100.

1 = 10mV sec^{-1} 3 = 100mV sec^{-1}
2 = 50mV sec^{-1} 4 = 250mV sec^{-1}

FIGURE 44

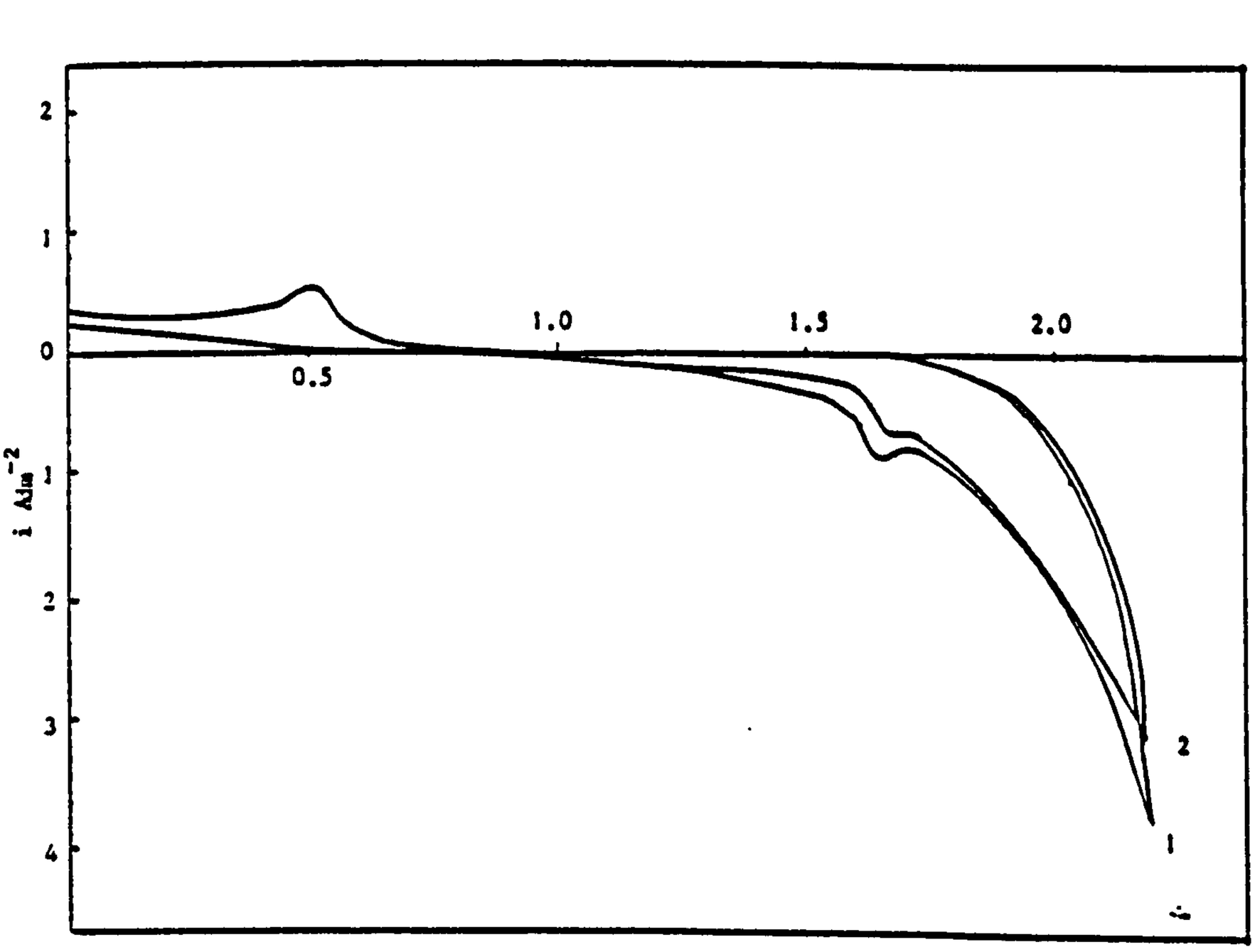

Cyclic voltammogram for a Pt electrode polarised at 10mV sec^{-1} in a 0.2M Na_2SO_4 solution containing 1 gl^{-1} Triton X100.

1 = 1st sweep 2 = 2nd sweep

FIGURE 45

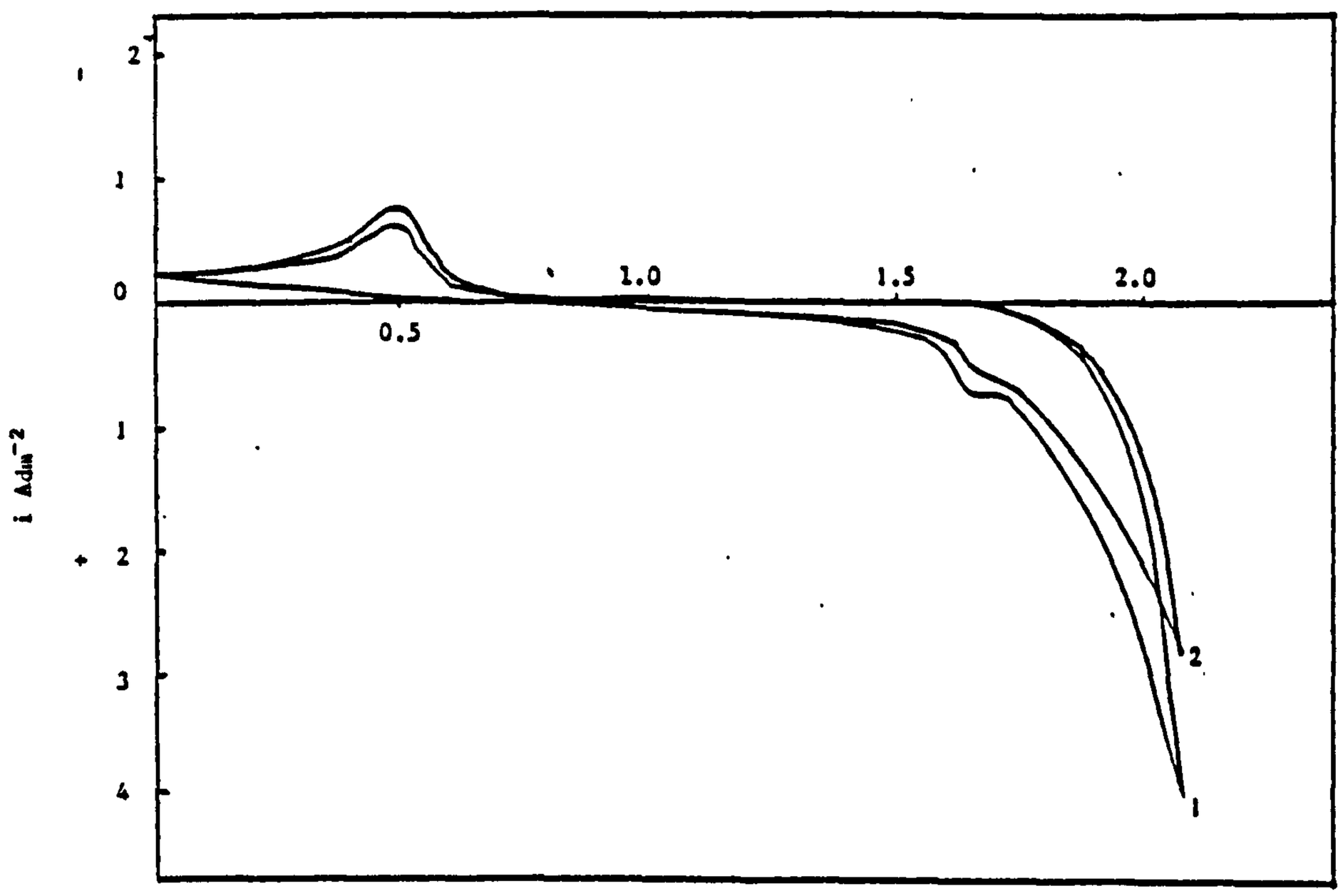

A cyclic voltammogram for a Pt electrode anodically polarised at a sweep rate of 10mV sec^{-1} in a solution of 0.2M Na_2SO_4 plus 0.5 gl^{-1} Triton X114.

1 = 1st scan 2 = 2nd scan

FIGURE 46

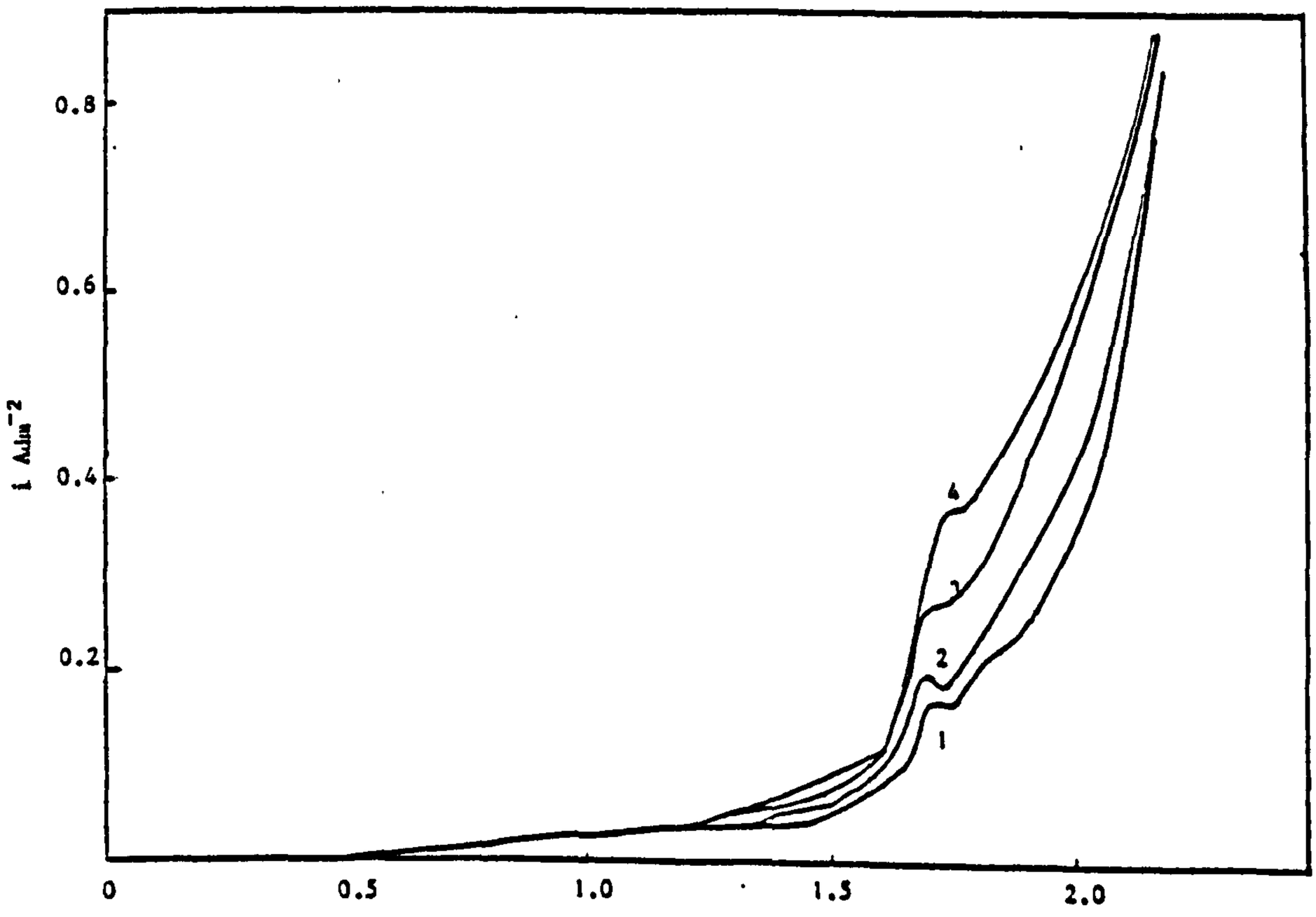

A graph showing the effect of variation in Triton X100 concentration on the anodic polarisation curve for a Pt electrode, polarised at 10mV sec^{-1}, in a 0.2M Na_2SO_4 solution.

1 = 0.5 gl^{-1} Triton X100 3 = 2 gl^{-1} Triton X100

2 = 1 gl^{-1} Triton X100 4 = 5 gl^{-1} Triton X100

FIGURE 47

Fig. 48 shows the effect of different addition agents dissolved in a 0.2M Na_2SO_4 solution on the E vs i curve, for a Pt electrode polarised at 10 mV sec^{-1} in this solution.

In the case of the addition of BRIJ35 to the 0.2M Na_2SO_4 solution no additional oxidation or reduction peaks were observed (see Fig. 49); however a slighly greater c.d. (0.076 Adm^{-2}) was observed at a given potential i.e at + 1.7V when compared to the value of 0.054 Adm^{-2} on the Pt electrode polarised at the same sweep rate in a non-additive containing solution. BRIJ35 like Triton X100 increases the oxygen over-voltage on Pt electrodes. The most noticable difference between these two additives, is that on cycling the potential of the Pt electode in solutions containing BRIJ 35 an interesting hysteresis effect is observed. Namely, the magnitude of the current for the first potential scan was higher at a given potential than for any subsequent scan (see Fig. 49). The extent of this hysteresis effect decreased with increase in BRIJ 35 concentration.

Analysis of the increase in the concentration of BRIJ35 on the potential/current relationship at a given scan rate reveals some interesting information (see Table 32). If no electrochemical reaction occured the values for the current density on the second scan would not be expected to increase, as they clearly do with increase in BRIJ 35 concentration. However, the results of the E vs i curve for the first scan do show some degree of scatter which may be associated with the reproducibility of the system. The results are indicative of degradation of this addition agent too, although this occurs at higher potentials and at a slower rate than with Triton X100.

The addition of Pluronic L64 to the test electrolyte has the effect of slightly decreasing the oxygen overvoltage on Pt, as can be seen from Fig. 48. The hysteresis effect reported for BRIJ35 was again observed with Pluornic L64, though on this occasion cycling of the potential actually resulted in the current on the second potential scan having a slightly higher value than the first at a given potential (see Table 33).

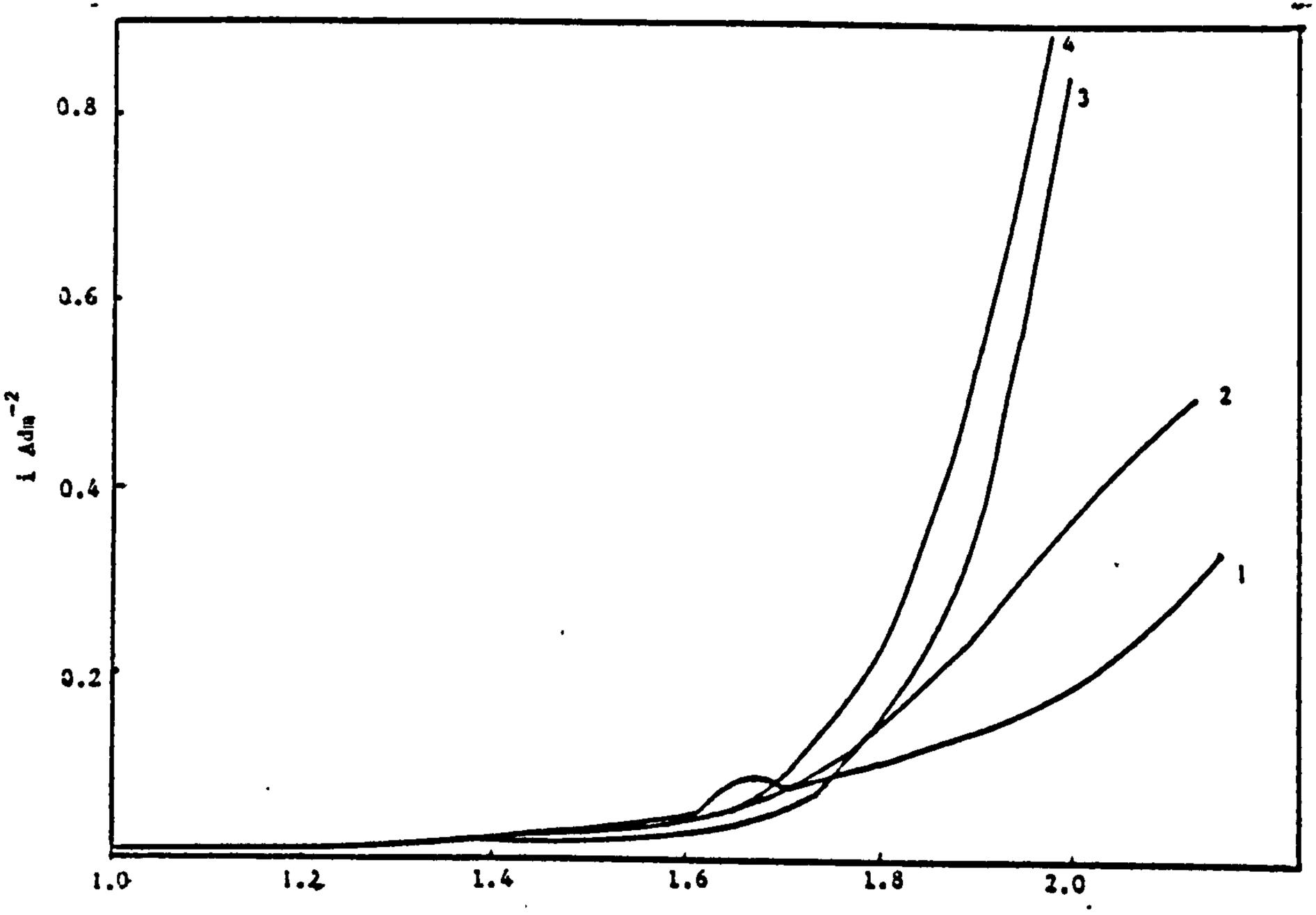

The effect of different surface active agents on the anodic polarisation curve for a Pt electrode, in a 0.2M Na_2SO_4 solution containing selected addition agents. The Pt electrode anodically polarised at a sweep rate of 10mV sec^{-1}

1 = 0.2M Na_2SO_4 + 1 gl^{-1} Triton X100 2 = 0.2M Na_2SO_4 + 1 gl^{-1} BRIJ 35

3 = 0.2M Na_2SO_4 without additives 4 = 0.2M Na_2SO_4 + 1 gl^{-1} Pluronic L64

FIGURE 48

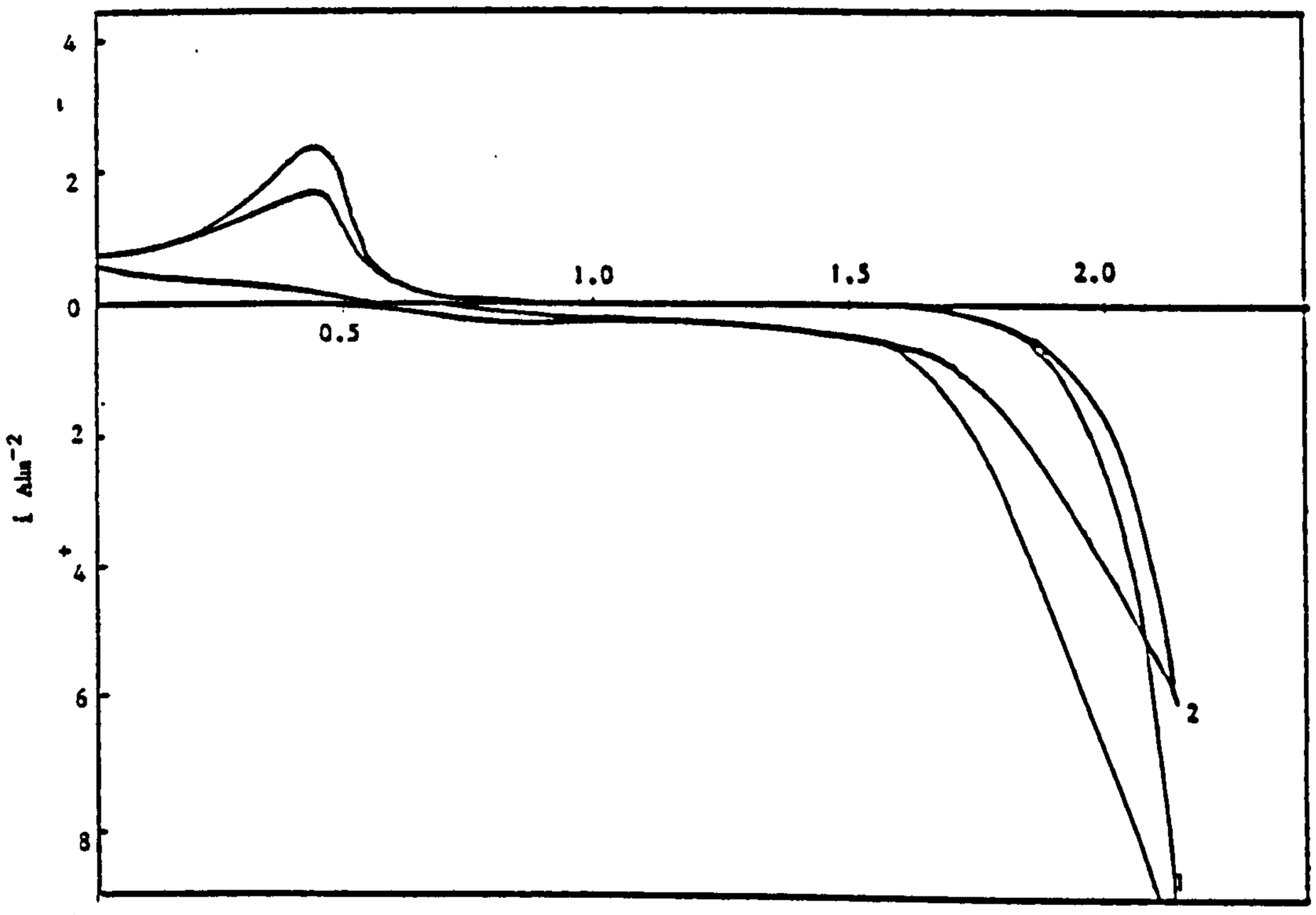

A cyclic voltammogram for a Pt electrode anodically polarised at 50mV sec^{-1} in a 0.2M Na_2SO_4 solution containing 1 gl^{-1} BRIJ 35.

1 = 1st scan 2 = 2nd scan

FIGURE 49

TABLE 32

The effect of repeated cycling of a Pt electrode in a solution of 0.2M Na_2SO_4 pH 2 containing different concentrations of BRIJ 35 on the E vs i characteristics at a sweep rate of 100 mV sec^{-1}

Concentration of BRIJ35 gl^{-1}	Current density (Adm^{-2}) at a selected potential (Volts vs SHE)				
	1.6V	1.7V	1.8V	1.9V	2.0V
0.5	0.104	0.193	0.385	0.650	0.802
	(0.088)	(0.132)	(0.225)	(0.373)	(0.57)
1	0.122	0.224	0.453	0.722	1.04
	(0.093)	(0.152)	(0.281)	(0.465)	(0.69)
5	0.120	0.192	0.453	0.634	0.922
	(0.108)	(0.191)	(0.353)	(0.569)	(0.845)

TABLE 33

The effect of repeated cycling of a Pt electrode in a solution of 0.2M Na_2SO_4 pH 2 containing different concentrations of Pluronic L64 on the E vs i characteristics at a sweep rate of 100 mV sec^{-1}

Conc Pluronic L64 gl^{-1}	Current density Adm^{-2} at a selected potential (Volts vs SHE)				
	1.6V	1.7V	1.8V	1.9V	2.0V
1	0.104	0.281	0.377	0.378	1.26
	(0.104)	(0.281)	(0.417)	(0.803)	(1.38)
2	0.092	0.16	0.297	0.577	1
	(0.092)	(0.169)	(0.396)	(0.746)	(1.26)
5	0.092	0.136	0.232	0.409	0.64
	(0.076)	(0.128)	(0.248)	(0.497)	(0.87)

Note : The figures in brackets represent current densities obtained at a given potential on a repeat potential scan on same specimen.

A graph of overpotential η vs log i for the polarisation of a Pt electrode in the test electrolyte containing 1 gl^{-1} BRIJ 35 and 1 gl^{-1} Triton X100 is shown in Fig. 50. Values of overpotential were taken, with + 1.5V as zero overvoltage and the background c.d. at this value subtracted from values of c.d. at higher overpotentials. A linear relationship between η and log i was only obtained for the non additive containing solution, where as two distinct curves were obtained for the solution containing addition agents. Values for the Tafel constant taken over the major linear portion of each graph are as follows :

a) 0.2 M Na_2SO_4, solution pH2 with no additives
240 mV $decade^{-1}$

b) 0.2 M Na_2SO_4, pH2 + 1 gl^{-1} BRIJ 35
390 mV $decade^{-1}$

c) 0.2 M Na_2SO_4, pH2 + 1 gl^{-1} Triton X100
620 mV decade

3.1.9.1 Studies on the anodic oxidation of addition agents other than BRIJ35, Triton X100 and Pluronic L64

In the case of the additive cetyltrimethylammonium bromide (CETB), two clearly defined oxidation peaks at + 1.2V and + 1.4V were observed. A typical voltammogram for a Pt electrode anodically polarised in the test solution containing CETB is shown in Fig. 51. Increase in sweep rate(v) moves E_p in a more positive direction and a linear relationship between i_p and $v^{1/2}$ was noted for each of the individual oxidation peaks. A plot of i_p vs $v^{1/2}$ is shown in Fig. 52 for the polarisation of a Pt electrode in a 0.2M Na_2SO_4 solution containing 5 gl^{-1} CETB. Lines (a) and (b) represent the relationship for the first oxidation peak shown in Fig. 51 and line (b) that for the second oxidation peak.

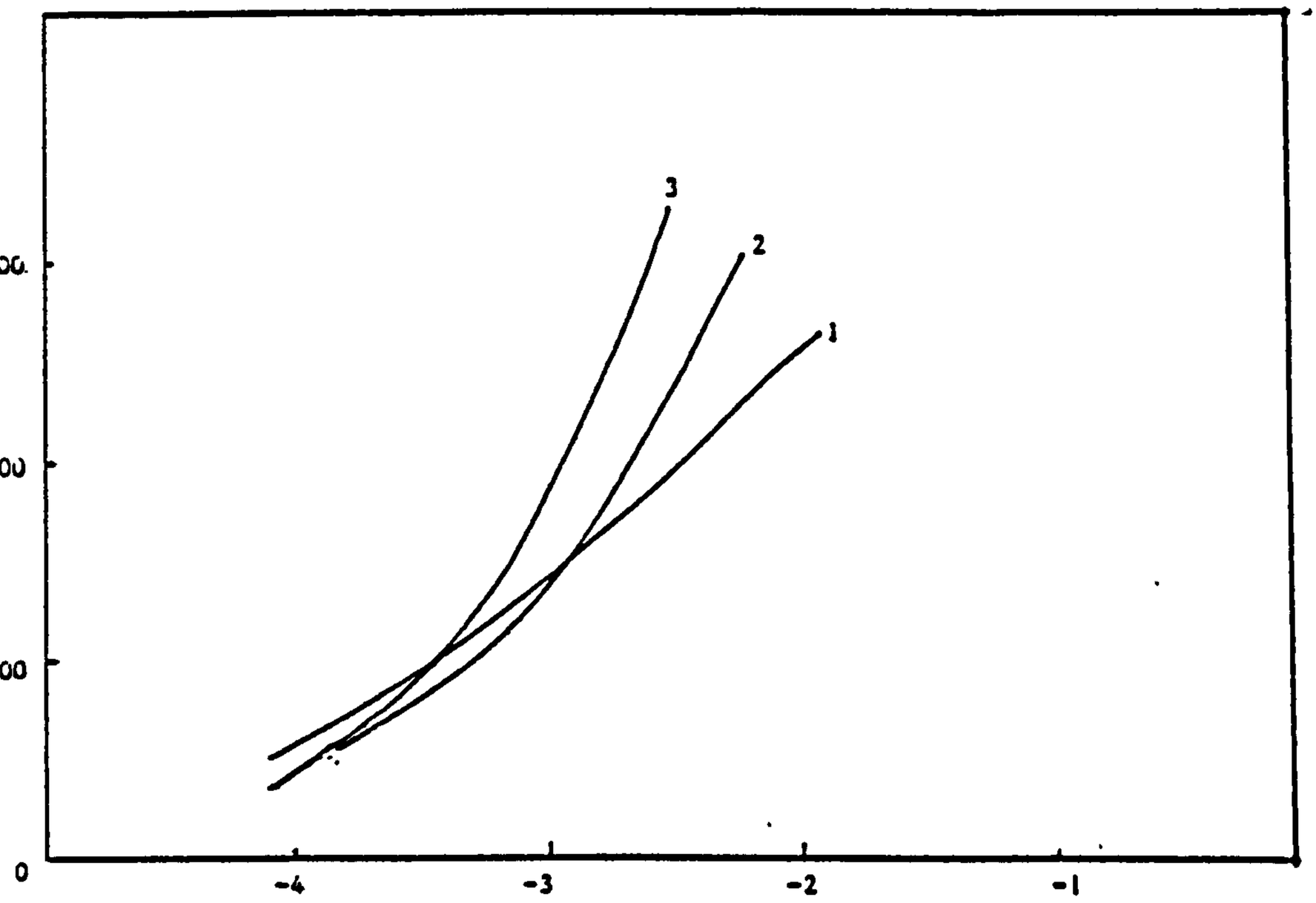

E vs log i curves for a Pt electrode anodically polarised at a sweep rate of 10mV sec^{-1} from its rest potential in a 0.2M Na_2SO_4 solution containing selected surface active agents.

1 = 0.2 M Na_2SO_4 without additives 2 = 0.2 M Na_2SO_4 + 1 gl^{-1} BRIJ 35

3 = 0.2 M Na_2SO_4 + 1 gl^{-1} Triton X100

FIGURE 50

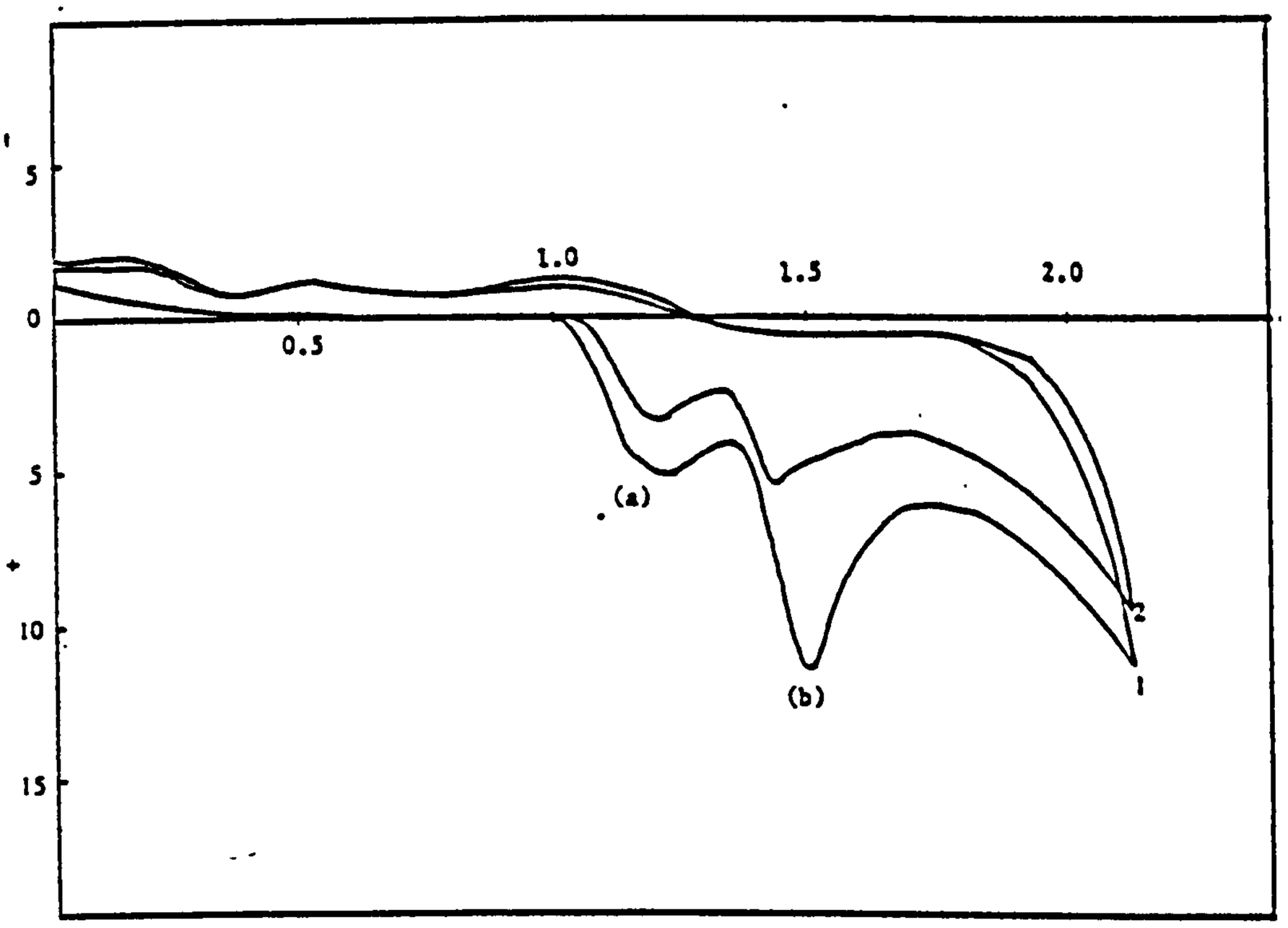

A cyclic voltammogram for a Pt electrode anodically polarised at 100mV sec^{-1} in a solution of 0.2M Na_2SO_4 plus 5 gl^{-1} cetyl trimethyl ammonium bromide.

1 = 1st scan 2 = 2nd scan

FIGURE 51

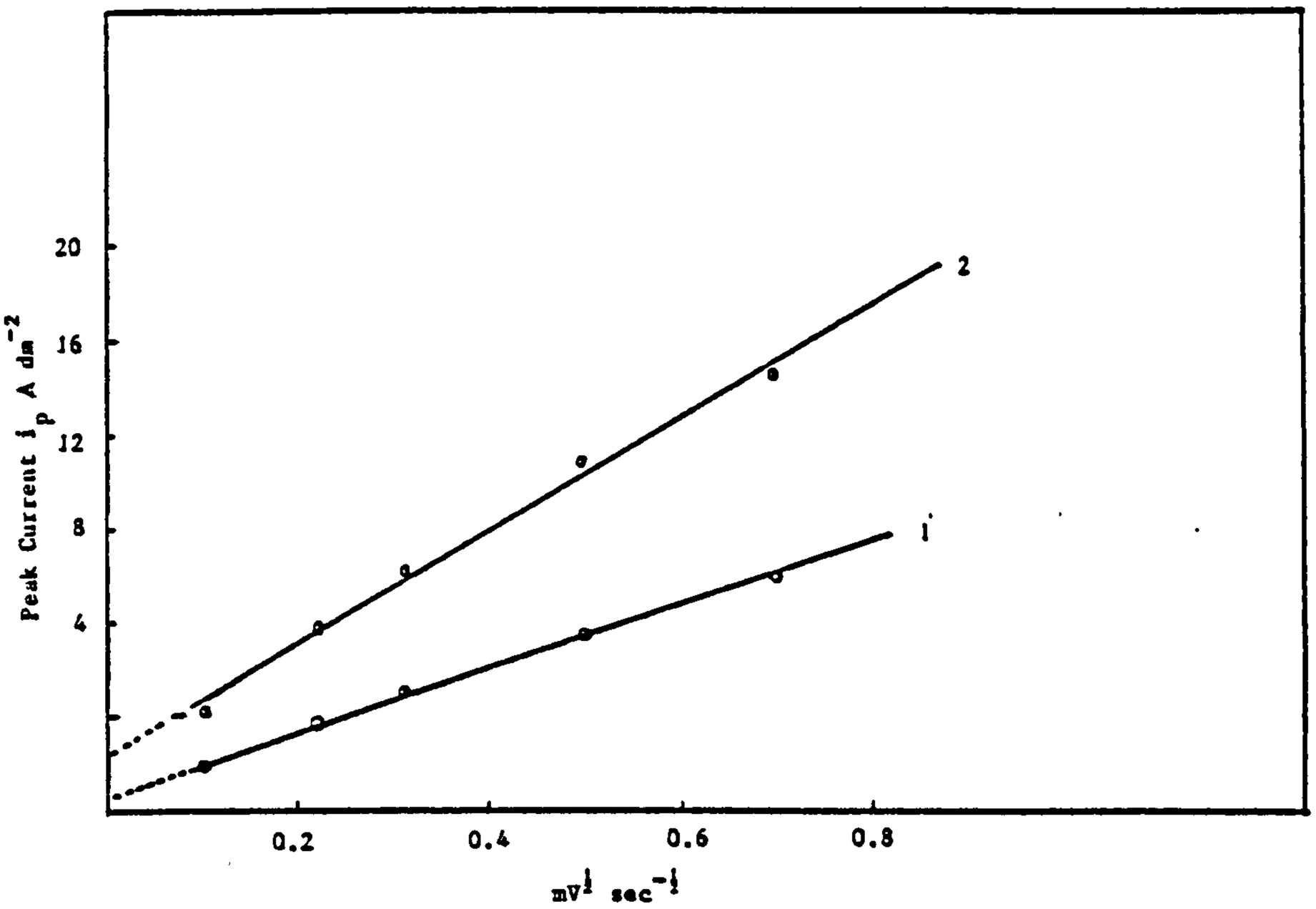

Graph of i_p vs $v^{\frac{1}{2}}$ for the anodic oxidation of 5 gl^{-1} cetyl trimethyl ammonium bromide at a Pt electrode in a 0.2M Na_2SO_4 solution.

FIGURE 52

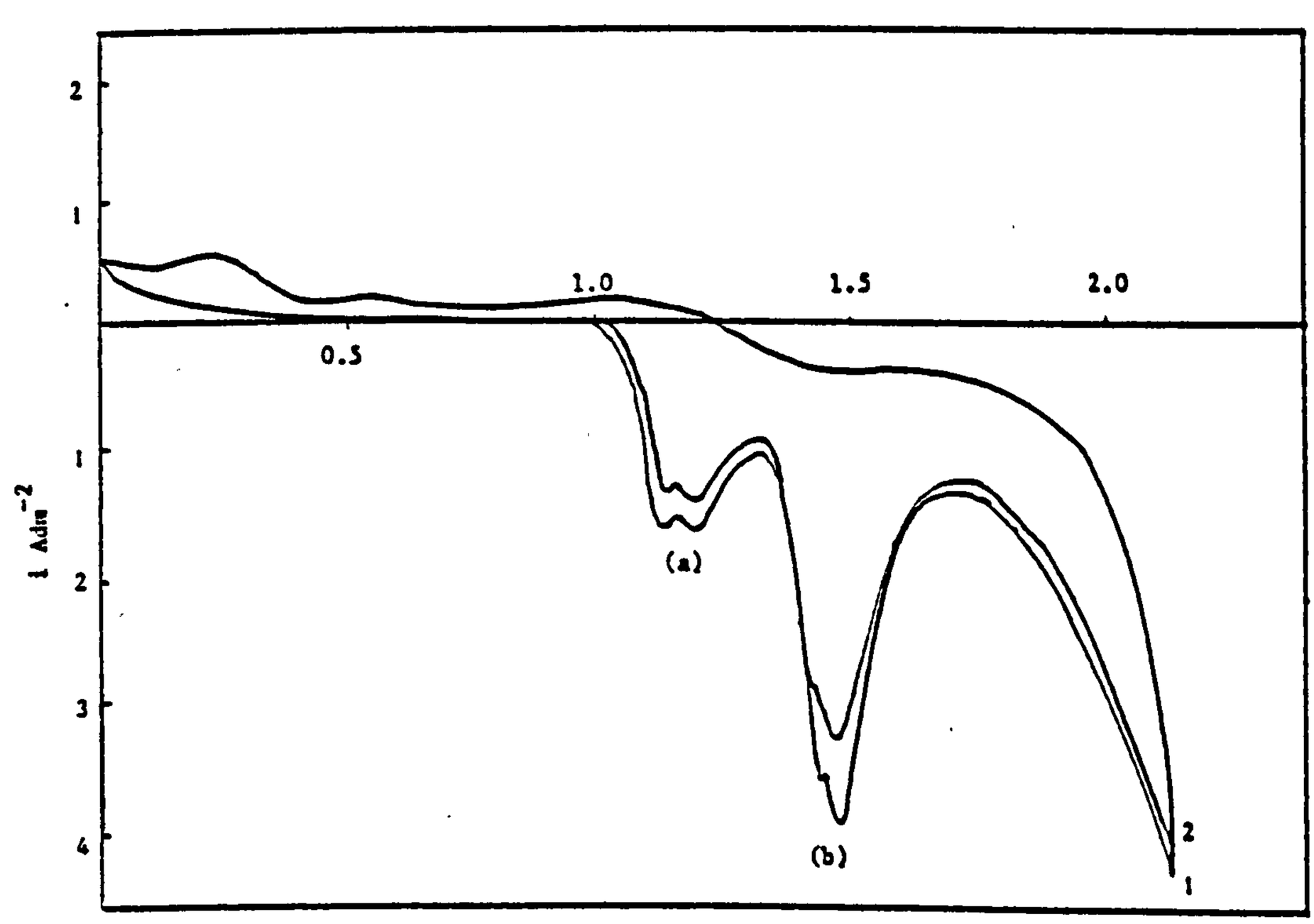

Cyclic voltammogram for a Pt electrode anodically polarised at a sweep rate of 10mV sec^{-1} in a solution of 0.2 M Na_2SO_4 + 5 gl^{-1} cetyl trimethyl ammonium bromide

1 = 1st scan 2 = 2nd scan

FIGURE 53

Three reduction peaks are visible, one due to the reduction of the Pt oxide film at about +0.25 V, and two for the reduction of the CETB oxidation products, at about +0.55 V and +1.1V. At slow sweep speeds i.e 10 mV sec^{-1}, each oxidation peak can be seen to be split into a doublet (see Fig. 53.)

'Hyamine' is the proprietary name for a quaternary ammonium compound (Di-isobutylphenoxyethyldimethylbenzyl ammonium chloride), the anodic polarisation data for this chemical dissolved in 0.2M Na_2SO_4 indicates one, if not two oxidation peaks, the first at + 1.55V and the other at about + 1.7V (see Fig. 54). The magnitude of i_p and E_p for these peaks was found to be dependent upon sweep speed and 'Hyamine' concentration. This additive also exhibited an even greater increase on the oxygen overvoltage on Pt than did Triton X100.

Anthraquinone-2-monosulphonic acid showed no additional oxidation or reduction peaks when compared to a non-additive solution of 0.2M Na_2SO_4 (see Fig. 55). The maximum solubility of this additive was only 0.5 gl^{-1}.

In the case of the additive 2-butyne-1,4-diol a possible oxidation peak was detected at + 1.1 to 1.2V (see Fig. 56). The magnitude of the current at these potentials was also found to be dependent upon butyne-diol concentration. At a concentration of 1 gl^{-1} and sweep speed of 50 mV sec^{-1}, the peak current at 1.2 V was 0.052 Adm^{-2} whilst at 5 gl^{-1} it was 0.061 Adm^{-2}. Butyne 1,4 diol also has an effect on the oxygen overvoltage on a Pt electrode, with an increase in butyne diol concentration resulting in a decrease in c.d. at + 2.0V (see Table 34).

A cyclic voltammogram for a solution of 5 gl^{-1} hydroquinone is shown in Fig. 57. This additive is readily oxidised at the Pt anode. The magnitude of the oxidation peak is dependent upon sweep rate and the concentration of additive, (see Table 35).

TABLE 34

The current density at + 2.0 V for a Pt electrode polarised at 50 mV sec^{-1} in a 0.2M Na_2SO_4 solution at pH2 containing different concentrations of butyne 1,4 diol

2,butyne-1,4-diol concentration (gl^{-1})	Current density at 2.0V (vs SHE) (Adm^{-2})
0.5	1.52
1	1.08
5	0.86

TABLE 35

The effect of hydroquinone concentration on the values of E_p (oxidation), E_p (reduction) and i_p for hydroquinone oxidation on a Pt electrode, polarised at 10 mV sec^{-1} in 0.2M Na_2SO_4 at pH2

Hydroquinone concentration gl^{-1}	i_p(oxidation) Adm^{-2}	E_p(oxidation) Volts	E_p(reduction) Volts
0.5	0.128	0.70	0.47
1	0.236	0.72	0.45
5	0.939	0.825	0.37

The current peak for the reduction of the hydroquinone oxidation products also includes current from the reduction of the Pt oxide film which occurs at the same potential. The relationship between i_p and E_p at different sweep rates for a solution containing 5 gl^{-1} hydroquinone can be seen in Table 36.

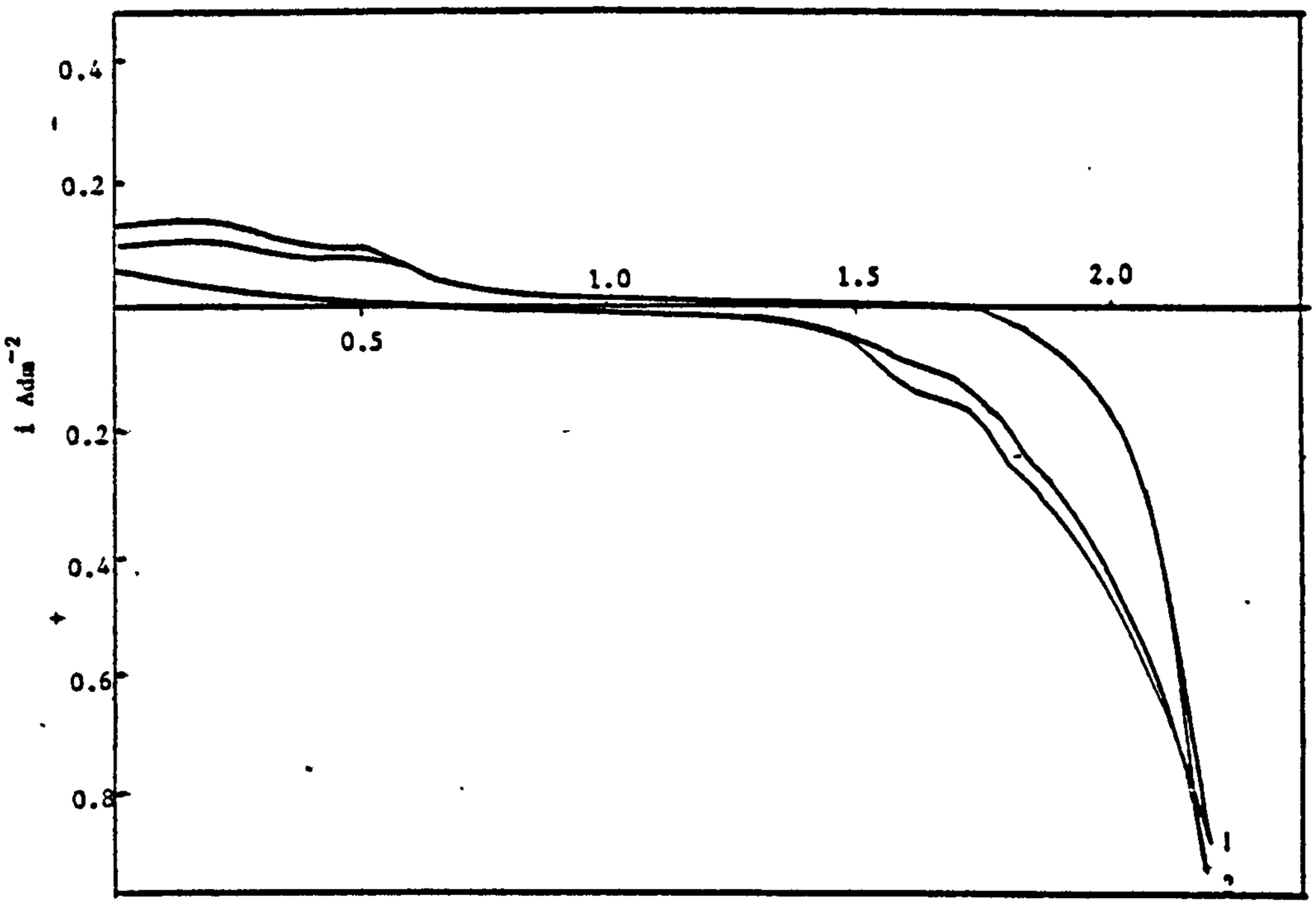

E vs SHE (Volts)

Cyclic voltammogram for the anodic oxidation of Hyamine at a Pt electrode in a solution of 0.2M Na_2SO_4 plus 5 gl^{-1} Hyamine. The Pt electrode anodically polarised at a sweep rate of 100mV sec^{-1}.

FIGURE 54

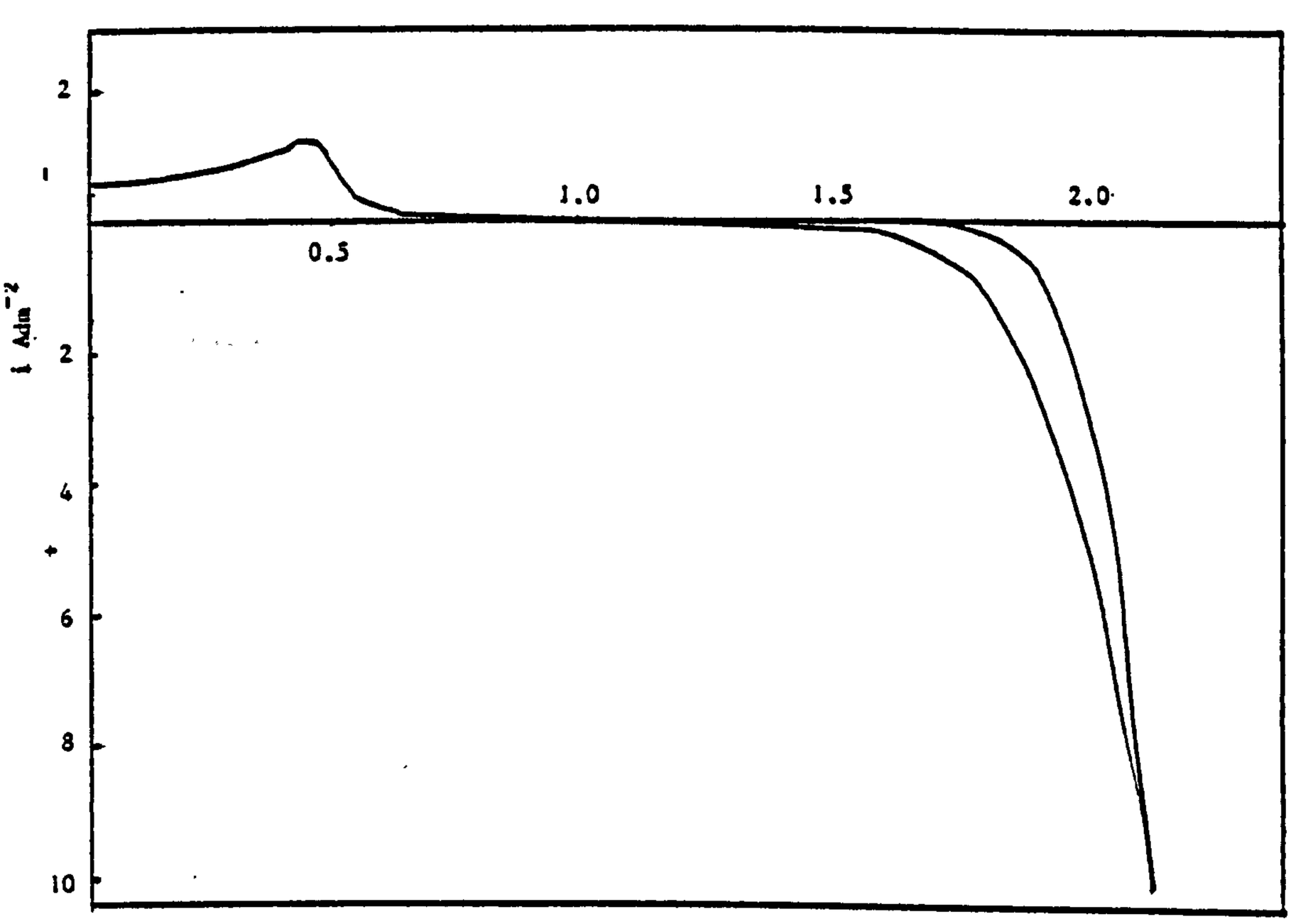

E vs SHE (Volts)

Cyclic Voltammogram for a Pt electrode anodically polarised at a sweep rate of 100 mV sec^{-1} in a 0.2 M Na_2SO_4 solution.

FIGURE 55

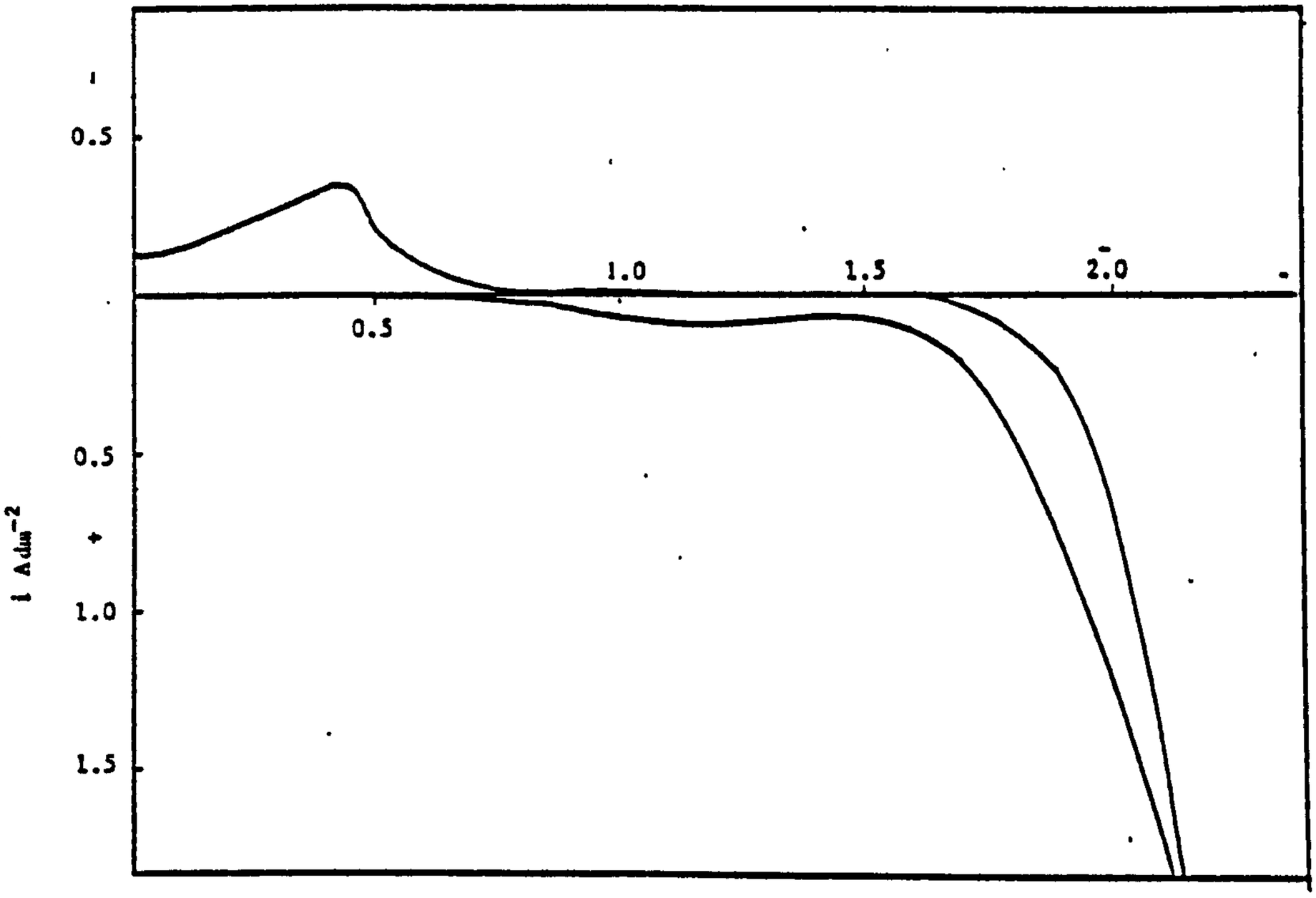

E vs SHE (Volts)

Cyclic voltammogram for a Pt electrode anodically polared at a sweep rate of 100mV sec^{-1} in a 0.2 M Na_2SO_4 solution pH2 containing 1 gl^{-1} butyne 1,4 diol.

FIGURE 56

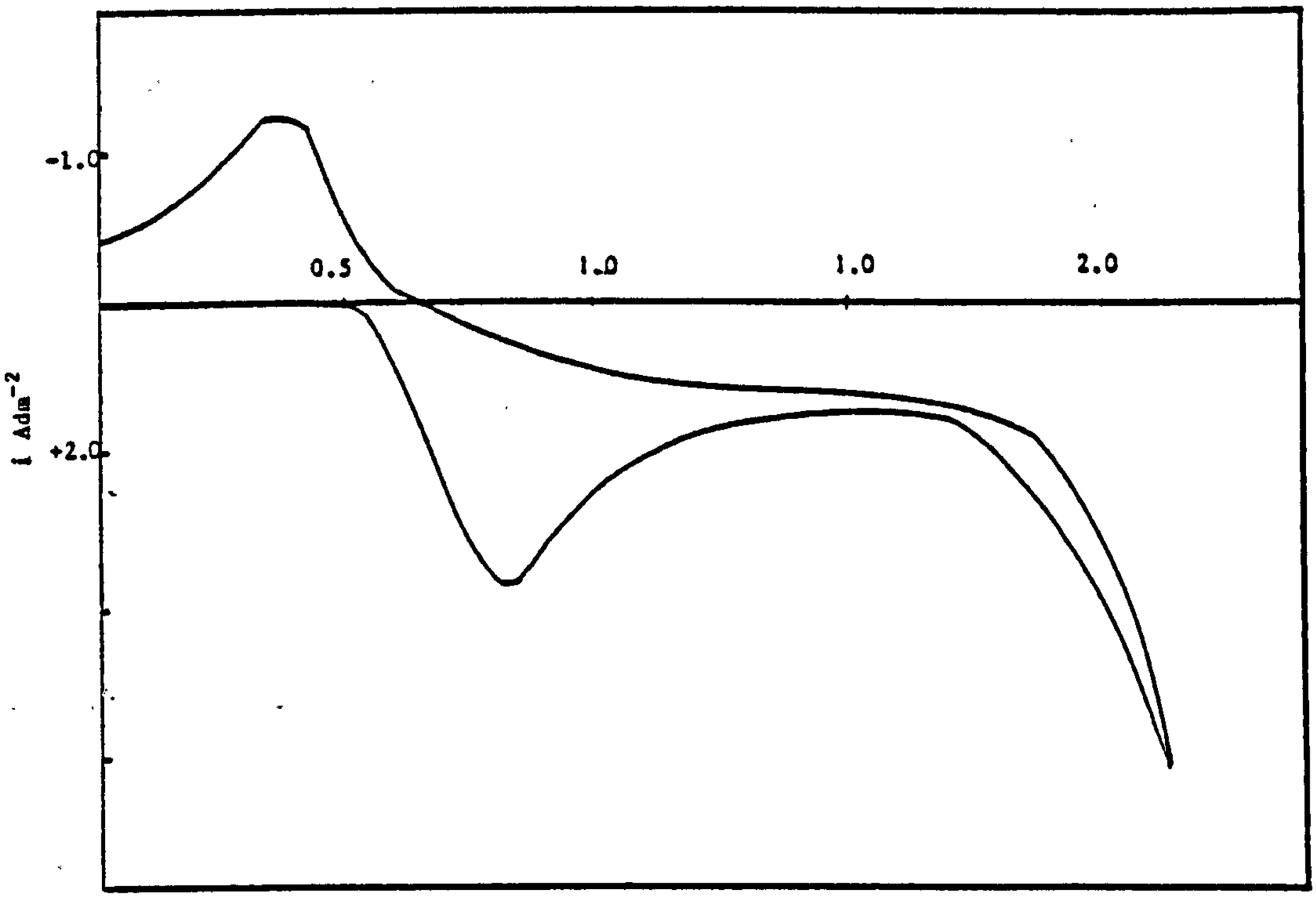

E vs SHE (Volts)

A cyclic voltammogram for a Pt electrode anodically polarised at a sweep rate of 10mV sec^{-1} in a solution of 0.2M Na_2SO_4 plus 5 gl^{-1} hydroguinone.

FIGURE 57

TABLE 36

The relationship between i_p and E_p for a Pt electrode polarised at different sweep rates in a solution of 0.2M Na_2SO_4, at pH 2 containing 5 gl^{-1} hydroquinone

E_p (Volts)	$E_{p/2}$ (Volts)	i_p Adm^{-2}	v $mV\ sec^{-1}$	$v^{1/2}$ $mV^{1/2}sec^{-1/2}$
0.825	0.675	0.937	10	0.1
0.93	0.725	1.67	50	0.141
1.0	0.75	2.17	100	0.314
1.11	0.805	2.89	250	0.500

1-napthol-4-sulphonic acid, an additive in Pb and PbO_2 deposition, was also found to be subject to oxidation at the potentials likely to be encountered in the electrodeposition of PbO_2. Fig. 58 shows a voltammogram for a Pt electrode anodically polarised in 0.2M Na_2SO_4 containing this acid. The presence of one oxidation peak is clearly visible as well as two reduction peaks, one for the reduction of the anodic oxidation products and the other for the reduction of the Pt oxide film. The effect of increasing the concentration of this additive on E_p and i_p oxidation is shown in Table 37 for a Pt electrode polarised at a sweep rate of 10 mV sec^{-1} in a supporting electrolyte of 0.2M Na_2SO_4, pH 2.

TABLE 37

Conc of 1-napthol-4-sulphonic acid gl^{-1}	E_p (Volts)	i_p (Adm^{-2})
0.5	1.05	0.024
1	1.07	0.036
5	1.1	0.096

The fact that both the oxidation and reduction peaks were concentration dependent is thought to be indicative of the fact that oxidation of 1-napthol-4-sulphonic acid is a reversible process.

Aloin and Wafex did not give any clear indication as to whether oxidation of these additives occured; a voltammogram for the anodic polarisation of Pt in a test solution containing Wafex is shown in Fig. 59.

Studies on the oxidation of tannic acid, using cyclic voltammetry reveal the presence of a possible oxidation peak at + 1.1 V (see Fig. 60), the magnitude of the current density at this potential is dependent upon the tannic acid concentration, as can be seen from Table 38.

TABLE 38

The effect of tannic acid concentration in a solution of 0.2M Na_2SO_4 pH 2 on the c.d. recorded at + 1.1 V when a Pt electrode was anodically polarised at 10 mV sec^{-1}

Tannic acid concentration gl^{-1}	Oxidation Adm^{-2}	Reduction Adm^{-2}
0.5	0.016	0.13
0.5	0.026	0.168
5	0.078	0.273

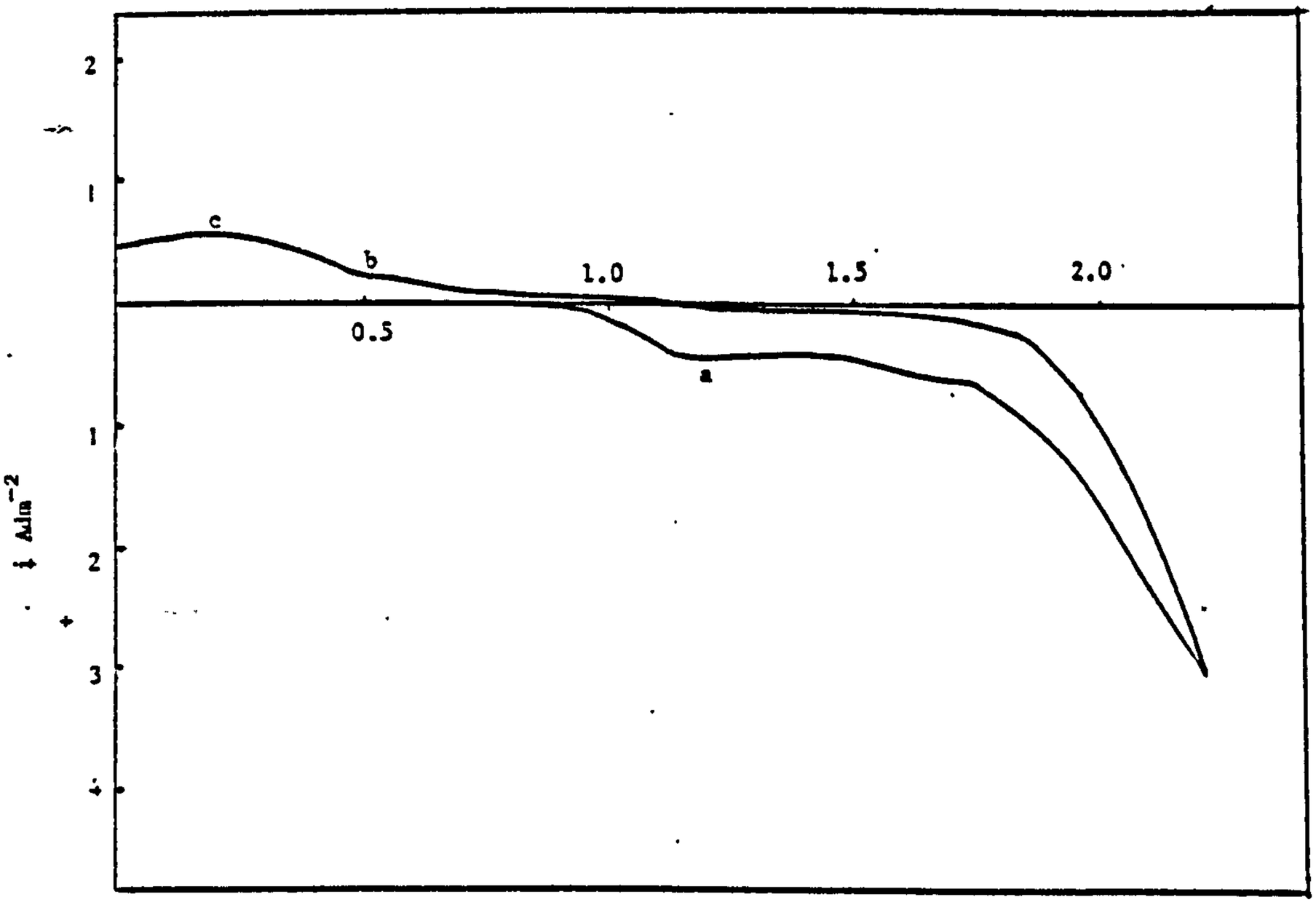

E vs SHE (Volts)

Cyclic voltammogram for a Pt electrode anodically polarised at a sweep rate of 250 mV sec^{-1} in a solution of 0.2M Na_2SO_4 plus 5 gl^{-1} 1 napthol 4 sulphonic acid.

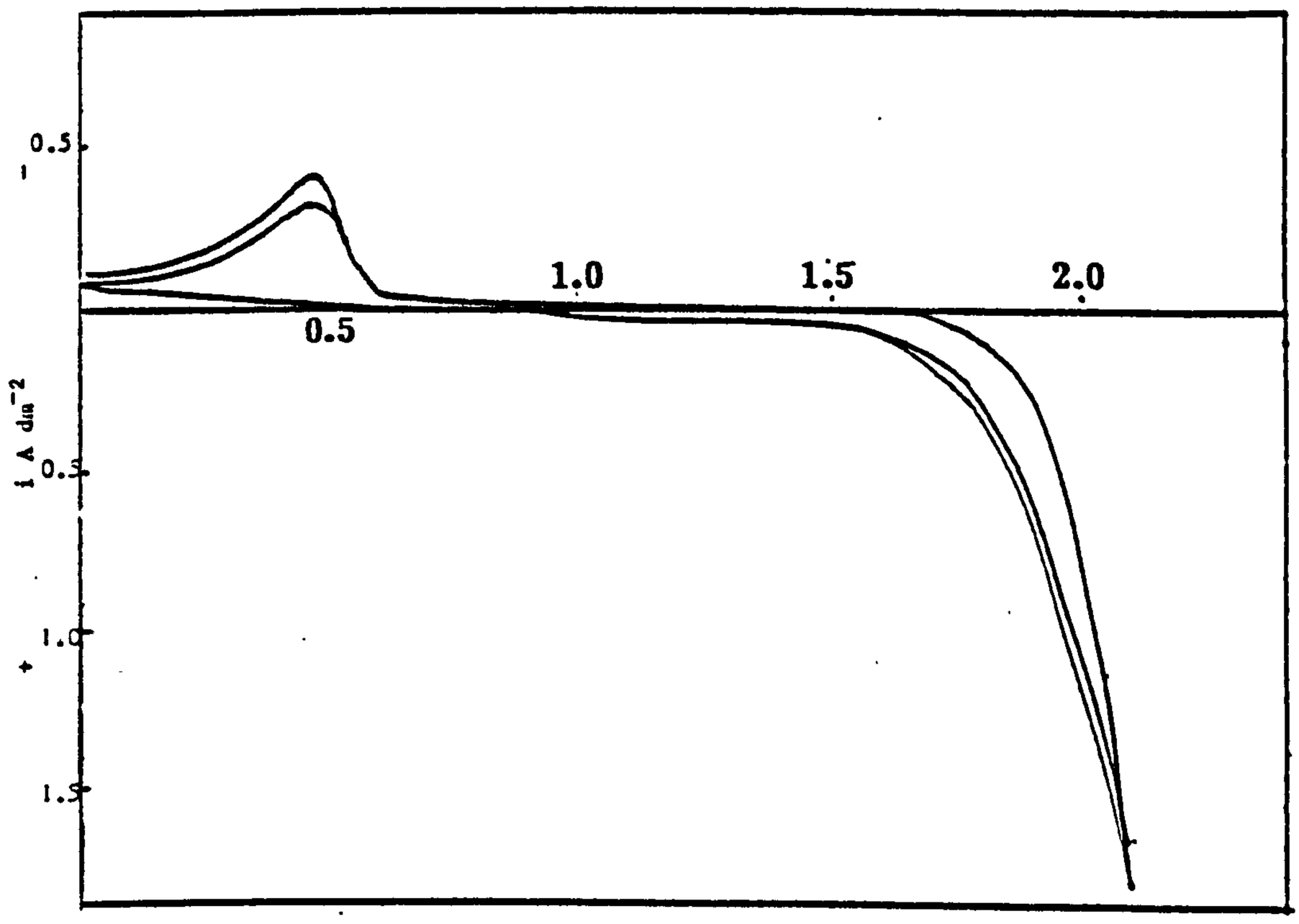

E vs SHE (Volts)

Cyclic voltammogram for a Pt electrode anodically polarised at a sweep rate of 50mV sec^{-1} in a solution of 0.2M Na_2SO_4 plus 1 gl^{-1} Wafex.

TABLE 39

The effect of different additives on the oxygen overvoltage on a Pt electrode polarised at 10 mV sec^{-1} in a solution of 0.2M Na_2SO_4, pH 2 containing different addition agents

Additive	c.d (Adm^{-2}) at selected potentials	
	+1.8V	+2.0V
1 gl^{-1} tannic acid	0.268	0.98
5 gl^{-1} tannic acid	0.268	0.98
1 gl^{-1} aloin	0.296	1.09
5 gl^{-1} aloin	0.231	0.98
1 gl^{-1} resorcinol	0.257	0.88
6 gl^{-1} resorcinol	0.353	1.09
1 gl^{-1} hydroquinone	0.35	0.96
6 gl^{-1} hydroquinone	0.53	1.02
0.5 gl^{-1} anthraquinone-2-monosulphonic acid	0.33	1.20
1 gl^{-1} butyne 1,4 diol	0.20	0.73
5 gl^{-1} butyne 1,4 diol	0.19	0.59
1 gl^{-1} Pluronic L64	0.24	1.00
5 gl^{-1} Pluronic L64	0.12	0.52
1 gl^{-1} BRIJ 35	0.152	0.37
5 gl^{-1} BRIJ 35	0.136	0.37
1 gl^{-1} Triton X100	0.10	0.19
1 gl^{-1} Triton X114	0.11	0.19
5 gl^{-1} Triton X100	0.12	0.28
1 gl^{-1} CETB	0.11	0.26
5 gl^{-1} CETB	0.16	0.30
1 gl^{-1} Hyamine	0.05	0.13
5 gl^{-1} Hyamine	0.09	0.18
0.2M Na_2SO_4 without any addition agents	0.12	0.54

3.1.9.2 Variation of Triton X100 concentration with plating time during electrodeposition of PbO_2 from a 360 gl^{-1} $Pb(NO_3)_2$ solution

The methods of analysis for Triton X100 suggested by the manufacturers were investigated.

A volumetric method using potassium ferrocyanide quoted by Schonfeld (303) was found to be unsuitable for quantitative measurements. However, a gravimetric method recommended by Barber (301) and a colorimetric method quoted by Weber (302) were both found to be suitable. Neither of these analytical procedures was found to be affected by butyne 1,4 diol present in the aqueous solution and were therefore selected for the determinations of Triton X100 dissolved in an aqueous solution.

The colorimetric method was considered to be the most accurate since there was found to be some degree of variation in the weight readings obtained using the gravimetric method. This variation in weight was a genuine phenomenon since Barber reported a 1.6% variation in weight at a Triton X100 concentration level of approximately 3 gl^{-1}. The values obtained in the present studies however showed an 8% variation which was considered to be too great to enable accurate determinations of the Triton X100 content to be made. The results of the variation in concentration of Triton X100 in a stock solution of 360 gl^{-1} $Pb(NO_3)_2$ and 1.5 gl^{-1} butyne 1,4 diol with plating time at a c.d. 2.4 Adm^{-2} and 35°C are given in Table 40.

As can be seen the values obtained with the gravimetric method were slightly higher than those obtained using the colorimetric method. However, both methods show that the Triton X100 concentration falls rapidly during the first 250 A-h plating, then attains a steady value. No suitable method of analysis for butyne 1,4 diol was found as the few methods considered, were found to be sensitive to Triton X100, present in the solution.

TABLE 40

Variation of Triton X100 concentration with plating time for a 450 litre solution of 360 gl^{-1} $Pb(NO_3)_2$ using both gravimetric and colorimetric methods of determination.

Charge passed at a c.d of 2.4 Adm^{-2} A-h	Triton X100 concentration (gl^{-1}) Colorimetric Method	Gravimetric Method
0	2.7	2.8
250	1.5	1.6
500	1.3	1.7
700	1.5	1.4
1000	1.4	1.5
1250	1.4	1.7
1900	1.3	1.7

Butyne 1,4 diol was attacked by both bromine water and $KMnO_4$, as was Triton X100. It was therefore decided to determine the total quantity of oxidisable material in a given solution and use this as a method of calculating the butyne diol concentration.

The oxidation of both additives by $KMnO_4$ was chosen as the method to use, since from a knowledge of the total amount of oxidisable material and the Triton X100 concentration (determined by a separate method)it was possible to calculate the butyne 1,4 diol concentration.

This method was found difficult to use since it involved a back titration, the end point for which was not clearly defined. Nevertheless approximate values for the butyne diol content obtained using this method were obtained and are given in Table 41.

TABLE 41

The variation of butyne 1,4 diol concentration with plating time for a 450 litre solution of 360 gl^{-1} $Pb(NO_3)_2$

Amp hours plating at 2.4 Adm^{-2}	Butyne 1,4 diol content gl^{-1}
0	1.9
250	1.3
500	1.0
750	0.4
1250	0.6
1900	0.6

3.1.9.3 Determination of the breakdown products resulting from the anodic oxidation of certain addition agents.

Preliminary experiments were conducted to investigate the rate of electrochemical degradation of certain organic addition agents on a Pt anode in a sulphuric acid electrolyte and where possible to identify the degradation products formed.

The first method chosen was the addition of 3 gl^{-1} of the surfactant under investigation to a 2M H_2SO_4 solution. The solution was then electrolysed using a Pt anode and cathode, at 2 Adm^{-2} for a fixed period. Samples of the solution were removed after certain periods of time, and analysed on a Pye Unicam U.V spectrophotometer.